Synthesis of Biobased Polyethers, Polyesters and Polyamides from Canola Oil Derived Monomers Using Microwave Irradiation

by

Reza Ahmadi

A thesis submitted in partial fulfillment of the requirements for the degree of

Doctor of Philosophy

in

Bioresource and Food Engineering

Department of Agricultural, Food and Nutritional Science

University of Alberta

ABSTRACT

Polymers are essential in modern life's sustainable growth with their diverse applications in packaging, construction, automotive, electronic industries, etc. Nowadays, polymer industry mainly depends on petroleum resources as feedstock and energy source. Increased environmental concerns and limited petroleum resources have impelled industry and researchers to look for renewable feedstocks and alternative methods of polymer synthesis. Plant oils have been considered as prospective feedstocks for the polymer industry due to their worldwide availability and structural similarity to petroleum resources. Microwave irradiation has also emerged as an alternative heating technique for polymer synthesis. This thesis investigated the synthesis and characterization of different polymers from canola oil-derived monomers under conventional heating and microwave irradiation.

In the first study, α-olefin (1-decene) was polymerized to biopolyethers after chemical modification. 1-decene was first converted to 1,2-epoxydecane using m-chloroperoxybenzoic acid, and then subjected to ring-opening polymerization (ROP). Microwave-assisted epoxidation of 1-decene was optimized at 5 min (67% yield), whereas, the conventional epoxidation was completed at 60 min (> 93% yield). ROP of 1,2-epoxydecane was carried out using modified methyl aluminoxane (MMAO) catalyst and resulted in the production of high-molecular weight biopolyethers ($\overline{M}_w$> 2 × 10^6 g/ mol). A three-factor, three-level Box-Behnken response surface design was employed to investigate the effect of process parameters such as time, temperature, and the solvent-monomer ratio on the yield of microwave ring-opening polymerization. Although elevating all test parameters enhanced polymerization yield, the temperature was more effective than other variables. The optimal predicted parameters of reaction time 9.97 min, temperature 99.69 °C, and solvent to monomer ratio of 5.27:5 resulted in the maximum polyether yield of

82.51%. The microwave-assisted ROP improved the polymerization yield (about 9.8%) and reduced the required amount of solvent by 30% compared to the conventional reaction. Thermal stability of biopolyethers produced under both heating methods was comparable, with the melting temperature of 89°C and decomposition temperature in the range of 325- 418 °C. The microwave irradiation yielded a biopolyether with lower glass transition (T_g) compared to the conventional heating, which was explained by the microwave's effect on the polymer's tacticity.

The second and third studies investigated synthesis and characterization of two long-chain, unsaturated polyamides, PA (DMOD-PXDA) and PA (DMOD-DETA), from dimethyl 9-octadecenedioate (DMOD) and two different amines (*p*-Xylylenediamine and diethylenetriamine) under conventional heating and microwave irradiation. The melting temperature of polyamides was around 190 °C with higher values for the conventionally polycondensed ones. Polyamides' films were also prepared, and their characteristics were evaluated. PA (DMOD-PXDA) films had tensile strengths of about 20 Mpa. The percent elongation at break of the film from conventionally polymerized PA (DMOD-PXDA) was 3 times higher than its microwave polymerized counterpart. Regarding PA (DMOD-DETA) films, the film from conventionally polymerized PA (DMOD-DETA) showed higher tensile strength but lower percent elongation at break compared to its microwave counterpart. In the last study, a one-pot synthesis approach for producing a novel long-chain, unsaturated bio-based polyester using three canola oil-based monomers including dimethyl 9-octadecenedioate, its acid (9-octadecenedioic acid), and 1,2-epoxydecane was developed. The one-pot polymerization was carried out in two sequential steps, the addition of 9-octadecenedioic acid to 1,2-epoxydecane followed by polycondensation of the resulting biodiol (bis(2-hydroxydecyl) octadec-9-enedioate (BHOD)) with dimethyl 9-octadecenedioate. The first step of the reaction (acid-epoxy addition) was successfully performed without using any solvent or

catalysts under both conventional and microwave heating. The microwave acid-epoxy addition resulted in a 6-fold decrease in reaction time (30 min) compared to conventional heating (3 hrs). The second step to produce the long-chain, unsaturated biopolyester was carried out using $SnCl_2$ catalyst in a solvent-free media and a high vacuum under conventional heating. Interestingly, the synthesized biopolyester was a thermally stable long-chain polymer with a decomposition temperature of > 329 °C and a melting temperature of > 276 °C. The biopolyester's thermal properties were comparable to the commonly used commercial polyesters such as polyethylene terephthalate (PET) and polybutylene terephthalate (PBT).

Overall, this work developed synthesis approaches and rapid processes for synthesizing high molecular weight biopolyethers and long-chain biopolyester and polyamides with unsaturated motifs which are highly attractive from both industrial and academic points of view.

PREFACE

This thesis contains original work done by Mr. Reza Ahmadi and has been written according to the guidelines for a paper format thesis of the Faculty of Graduate Studies and Research at the University of Alberta. This thesis's concept originated from my supervisor Dr. Aman Ullah and me, and the research was funded by grants from Alberta Innovates and Alberta Canola Producers Commission.

The thesis consisted of six chapters: Chapter 1 provides a general introduction to the context and the objectives of the thesis; Chapter 2 is a literature review on several topics relevant to this thesis, and a version of chapter 2 will be submitted to *Angewandte Chemi Internation Edition* as a review article; Chapter 3 has been published as "Microwave-Assisted Rapid Synthesis of Polyether from Plant Oil Derived Monomer and its optimization by Box-Behnken Design" by Reza Ahmadi and Aman Ullah in the *Journal of RSC Advances.* 7: 27946–27959 (2017); In this chapter, Reza Ahmadi was responsible for the experimental design and conducting the experiments, data analysis and writing the first draft of the manuscript. Dr. Aman Ullah is the corresponding author and was responsible for the experimental design, data interpretation, correction and submission of the manuscript. Chapter 4 has been published as "Synthesis and Characterization of Unsaturated Biobased-Polyamides from Plant Oil" by Reza Ahmadi and Aman Ullah in *ACS Sustainable Chemistry & engineering.* 8, 8049-8058 (2020); In this chapter, Reza Ahmadi was responsible for designing and conducting the experiments, data analysis and writing the first draft of the manuscript. Dr. Ullah is corresponding authors and was responsible for the experimental design, data interpretation, correction and submission of the manuscript. Chapter 5 is to be submitted to the *green chemistry* for consideration for publication as Reza Ahmadi and Aman Ullah, "One-pot Synthesis of a Long-chain, Unsaturated Biopolyester from Plant oil-derived Monomers". In this

chapter, Reza Ahmadi was responsible for designing and conducting experiments, data analysis and writing the first draft of the manuscript. Dr. Ullah is the corresponding author and was responsible for the experimental design, data interpretation, correction and submission of the manuscript. The last Chapter 6 gives the discussion on chapters of the thesis and concluding remarks with further discussion for future research directions.

DEDICATION

This thesis is dedicated to my beloved family

ACKNOWLEDGMENTS

Finally, I would like to gratefully express my gratitude to my late father Mr. Golamhassan Ahmadi who, although is no longer with us, continues to inspire and encourage me by his strong belief in me. I would also like to sincerely thank my mother, Mrs. Zinat Ghafari and my siblings without whom I could not have completed my research work. I have no words to thank them for being by my side, for their emotional and spiritual support, understanding, and encouragement through these years.

My last, but not least, appreciation goes to my beloved wife, Dr. Forough Jahandideh, whose love, patience, and support are always with me. You have always been a source of unwavering passion and encouragement in my life. Thank you, my cute little daughter, Adrina, and my newborn baby, Ryan, for being good kids with your mom when I was finishing my Ph.D. at School.

TABLE OF CONTENTS

LIST OF TABLES

LIST OF SCHEMES

xiv

LIST OF FIGURES

LIST OF ABBREVIATIONS

AFM -Atomic force microscopy

ATR-FTIR- Attenuated total reflectance - Fourier transform infrared spectroscopy

ANOVA- Analysis of variance

BBD-Box–Behnken Design

BHOD- bis(2-hydroxydecyl) octadec-9-enedioate

BPs (DMOD-BOHOD)- Biopolyester from dimethyl 9-ocatdecenedioate and bis(2-hydroxydecyl) octadec-9-enedioate

$CDCl_3$- Deuterated chloroform

C NMR- Solid-state carbon nuclear magnetic resonance spectroscopy

CO_2- Carbon dioxide

CH- Conventional heating

DCM- Dichloromethane

DETA- Diethylenetriamine

DMA- Dynamic mechanical analysis

DMF- Dimethyl formamide

DMOD- Dimethyl 9-Ocatdecenedioate

DSC- Differential scanning calorimetry

ATR-FTIR- Attenuated total reflectance - Fourier transform infrared spectroscopy

GC-FID- Gas chromatography-flame ionization detector

GC-MS- Gas chromatography-mass spectrometry

GPC- Gel permeation chromatography

HCL- Hydrochloric acid

HFIP- 1,1,1,3,3,3-hexafluoro-2-propanol

H NMR- Proton nuclear magnetic spectroscopy

KOH Potassium hydroxide

Microwave- MW

Microwave heating- MH

MMAO-12- Modified methyl aluminoxane

m-CPBA- 3-chloroperoxybenzoic acid

$\overline{M_n}$- Average molecular number

$\overline{M_w}$- Average molecular weight

NaOH- Sodium hydroxide

N_2- Nitrogen

PA- Polyamide

PD- Polydispersity index

PXDA- p-Xylelenediamine

PY- Polymerization yield

RSM- Response surface methodology

SEC- Size exclusion chromatography

SEM- Scanning electron microscopy

$SnCl_2$- Tin (II) chloride (

TBD- 1,5,7-triazabicyclo[4.4.0]dec-5-ene

TFAA- trifluoroacetic anhydride

TG- Triacylglycerol

TGA- Thermogravimetric analysis

THF- Tetrahydrofuran

TLC- Thin layer chromatography

XPS- X-ray photoelectron spectroscopy   WAXD- Wide-angle X-ray diffraction

CHAPTER 1; GENERAL INTRODUCTION AND THESIS OBJECTIVES

1. General Introduction

1.1. Polymer industry; challenges and opportunities

Hermann Staudinger defined the term polymer in 1920 as a chemical compound with identical small molecules linking together by strong chemical bonds to make long chains of repeating units (Peplow, 2016) . Synthetic organic polymers were first created from petroleum resources in the early 20th century. Since then, they have become one of the most versatile materials inspiring innovations with a notable contribution to our modern life (Braun et al., 2013). The worldwide polymer production has had an average annual growth rate of 5% per year since 1950, with the total annual plastic usage exceeding 350 million metric tons in 2018 (Garside, 2020). Polymers have attracted more attention compared to other materials owing to their superior properties such as easy processability, tunability, chemical resistance, low cost, and high strength/density ratios, to name a few. Synthetic polymers have a wide range of applications in different industries, from clothing, packaging, paint, and coatings to sports equipment and construction. They have also been used in more sophisticated industries such as electronics, medicine, automotive, aerospace, etc. (Zhang et al., 2017); (Du et al., 2012); (Guo et al., 2013).

Nevertheless, the polymer industry has received both admiration and criticism since the appearance of polymeric materials in the market. The polymer industry has been appreciated due to its involvement in comfort and facilitation of human life and creating thousands of job opportunities. However, the criticisms have escalated over the polymer industry due to the environmental, health, and safety concerns attributed to its energy source, feedstock, and products

(Van Der Ploeg, 2011); (Jambeck et al., 2015). Extraction and exploitation of crude oil are associated with environmental risks and irreversible impact on climate. Moreover, due to their non-degradable nature, durable plastic fragments remain in landfills, dumps, and oceans, causing more environmental concerns. Nonetheless, crude oil's limited resources are another obstacle threatening the polymer industry's survival and human sustainable community development (Chikkali and Mecking, 2012).

1.2. **Prospective solutions to overcome the challenges of the polymer industry**

1.2.1. **Replacement of petroleum-based feedstock with renewable resources**

Although there is no fast and straightforward solution to solve the polymer industry's complex problems, production of sustainable polymers from renewable resources has been considered as one viable option. Therefore, research has mainly focused on reducing the polymer industry's reliance on petroleum resources (Zhu et al., 2016). In this context, a feasible strategy is replacing the polymer industry's feedstock with renewable ones.

Apart from all the imagined perspectives and supports for the innovation in sustainable polymers, the transformation to a sustainable, resilient, and climate-safe polymer industry is not happening fast enough to keep pace with petroleum-based polymers' global production. Currently, only about 1% of the annual plastic market is shared with the bioplastic industry ("Dynamic growth: global production capacities of bioplastics 2019-2024 Bioplastics," 2019). There are different reasons behind this slow progress towards sustainable polymers including the tedious synthesis processes of bio-derived platform chemicals and polymers and their costly production. Moreover, bioplastics lack the high-performance, characteristics of synthetic polymers, hence impeding the transformation of the traditional plastics industry to the bio-derived plastic industry (Lligadas et al., 2013). Further, the produced sustainable polymers usually exhibit inferior thermal resistance,

mechanical strength, processability, and compatibility compared with their petroleum-based counterparts (Peplow, 2016). These shortcomings need to be overcome before a substantial change could occur in the contribution of sustainable polymers in the market share. Consequently, researchers have adapted two general approaches to overcome the obstacles and produce novel sustainable polymers; 1) producing known monomers or polymers such as polyethylene and polyethylene terephthalate from biomass , and 2) production of polymers with new sustainable structures such as polylactide from renewable raw materials (Zhu et al., 2016).

Proteins and carbohydrates, as renewable raw materials, are not considered good choices to replace petroleum feedstock. Protein and carbohydrate-based polymers are usually moisture sensitive, difficult to process, and brittle, especially in the absence of plasticizers. Plant oils, on the other hand, are promising feedstocks for producing sustainable polymers. Having similar hydrocarbon structure to petroleum oil with hydrophobic properties, environmentally friendly nature, economic benefits, and worldwide availability are some of the advantages making plant oils attractive feedstocks for the industry. Nature also has a very high potential for producing this renewable feedstock (De Espinosa and Meier, 2011). The global production of plant oils exceeded 207 million metric tons in the 2019/2020 crop year (Shahbandeh, 2020). While many chemical procedures can be employed to synthesize various monomers and polymers from plant oils, minor modifying reactions might be necessary to convert the plant oil-derived monomers to suitable platform chemicals for polymerization (Nayak, 2000). Polymers produced from renewable resources based on plant oils are often called bio-derived or plant oil-derived polymers.

1.2.2. **Replacement of conventional heating source with microwave irradiation**

Polymers synthesis requires energy (heating) like other chemical reactions. Polymer industry uses fossil fuels as the primary energy source of heating to synthesize polymers. Apart from the

environmental concerns regarding this energy source, the polymer industry has also faced some limitations in heating polymerization media using conventional methods. Conducting polymerization reactions using conventional heating methods is time-consuming and involves side reactions (Lidstrom et al., 2001). Solvents are also necessary for different steps of monomer production and polymerization reactions. The use of high amounts of solvents and low polymerization yield are some other challenges of the polymer industry (Hoogenboom and Schubert, 2007). Besides, slow catalyst-monomer interaction and low heating flow through conduction/convection in conventional heating methods leads to generation of a heterogeneous reaction media and limits the control activation parameters (Sinnwell and Ritter, 2007). Therefore, researchers have focused on finding alternatives to conventional heating methods in order to reduce the polymer industry's dependence on petroleum resources on one hand, and increase the efficiency of polymerization reactions, on the other hand. In this regard, microwave irradiation has attracted researchers' attention as an alternative heating technique for polymer synthesis in recent decade.

Microwave irradiation is a highly specific heating method that intrinsically excites dipolar oscillation and induces ionic conduction due to its specific wavelength (Bogdal et al., 2003). As an environmentally sustainable heating method, microwave irradiation deals with shorter reaction times and halogen-free solvents or even solvent-free (green chemistry) polymerization and generates polymers with higher yields and purity (Kempe et al., 2011); (Wiesbrock et al., 2004); (Falciglia et al., 2018). Microwave irradiation could be technically superior to conventional heating due to its instantaneous, rapid, and uniform heating of the reaction media as well as the non-contact heating style, which prevents the decomposition of molecules close to the reaction vessel's walls.

4

2.   Hypotheses and objectives

Based on the stated issues and prospective solutions, we hypothesized that canola oil could be exploited to produce platform biochemicals and biobased polymers, including polyether, polyamide, polyester, and polyolefins. Moreover, as an alternative-heating source, microwave irradiation has the potential to develop biopolymers in minimal solvent usage or solvent-free conditions with shorter reaction times compared to the conventional heating method.

The proposed research's overall objective was to produce different kinds of biobased polymers from canola oil-derived monomers, including 1-decene and dimethyl 9-octadecenedioate using both microwave and conventional heating methods. Each step of the reactions and the purity of the resulted products were monitored using proton nuclear magnetic resonance spectroscopy (^{1}H NMR) and attenuated total reflectance Fourier transform infrared spectroscopy (ATR-FTIR). The resulting polymers were characterized using size exclusion chromatography (SEC), differential scanning calorimetry (DSC), thermal gravimetric analysis (TGA), dynamic mechanical analysis (DMA), Wide-angle X-ray scattering (WAXD), X-ray photoelectron spectroscopy (XPS), and universal tensile testing machine.

The specific objectives of this study included:

1) Production of a fully biobased polyether from 1-decene through its epoxidation into 1,2-epoxydecane and polymerization through the ring-opening polymerization procedure.

2) Synthesis of a semi-aromatic and unsaturated polyamide from dimethyl 9-octadecenedioate through its reaction with an aromatic diamine called *p*-Xylylenediamine.

3) Preparation of a linear unsaturated polyamide from dimethyl 9-octadecenedioate through its reaction with diethylenetriamine.

4) Synthesis of a long-chain biopolyester from dimethyl 9-octadecenedioate, its acid and 1-decene through a one-pot polymerization approach.

References

Bogdal, D., Penczek, P., Pielichowski, J., Prociak, A., 2003. Microwave assisted synthesis, crosslinking, and processing of polymeric materials. Adv. Polym. Sci. 163, 193–263. https://doi.org/10.1007/b11051

Braun, D., Cherdron, H., Rehahn, M., Ritter, H., Brigitte, V., 2013. Polymer Synthesis: Theory and Practice, 5th ed, Trabajo Infantil. Springer-Verlag Berlin Heidelberg. https://doi.org/10.1017/CBO9781107415324.004

Chikkali, S., Mecking, S., 2012. Refining of plant oils to chemicals by olefin metathesis. Angew. Chemie - Int. Ed. 51, 5802–5808. https://doi.org/10.1002/anie.201107645

De Espinosa, L.M., Meier, M.A.R., 2011. Plant oils: The perfect renewable resource for polymer science?! Eur. Polym. J. 47, 837–852. https://doi.org/10.1016/j.eurpolymj.2010.11.020

Du, Y., Shen, S.Z., Cai, K., Casey, P.S., 2012. Research progress on polymer-inorganic thermoelectric nanocomposite materials. Prog. Polym. Sci. 37, 820–841. https://doi.org/10.1016/j.progpolymsci.2011.11.003

Dynamic growth: global production capacities of bioplastics 2019-2024 Bioplastics [WWW Document], 2019. . Eur. Bioplastics. URL https://www.european-bioplastics.org/wp-content/uploads/2019/11/Report_Bioplastics-Market-Data_2019_short_version.pdf

Falciglia, P.P., Roccaro, P., Bonanno, L., De Guidi, G., Vagliasindi, F.G.A., Romano, S., 2018. A review on the microwave heating as a sustainable technique for environmental remediation/detoxification applications. Renew. Sustain. Energy Rev. 95, 147–170. https://doi.org/10.1016/j.rser.2018.07.031

Garside, M., 2020. Global plastic production 1950-2018 [WWW Document]. Statistica. URL https://www.statista.com/statistics/282732/global-production-of-plastics-since-1950/

Guo, B., Glavas, L., Albertsson, A.C., 2013. Biodegradable and electrically conducting polymers for biomedical applications. Prog. Polym. Sci. 38, 1263–1286. https://doi.org/10.1016/j.progpolymsci.2013.06.003

Hoogenboom, R., Schubert, U.S., 2007. Microwave-assisted polymer synthesis: Recent developments in a rapidly expanding field of research. Macromol. Rapid Commun. 28, 368–386. https://doi.org/10.1002/marc.200600749

Jambeck, J., Geyer, R., Wilcox, C., Siegler, T.R., Perryman, M., Andrady, A., Narayan, R., Law, K.L., 2015. Plastic waste inputs from land into the ocean 347, 3–6. https://doi.org/10.1126/science.1260352

Kempe, K., Becer, C.R., Schubert, U.S., 2011. Microwave-assisted polymerizations: Recent status and future perspectives. Macromolecules 44, 5825–5842. https://doi.org/10.1021/ma2004794

Lidstrom, P., Tierney, J., Wathey, B., Westman Jacob, 2001. Microwave-assisted green organic synthesis-a review. Tetrahedron 57, 9225–9283.

Lligadas, G., Ronda, J.C., Galià, M., Cádiz, V., 2013. Renewable polymeric materials from vegetable oils: A perspective. Mater. Today 16, 337–343. https://doi.org/10.1016/j.mattod.2013.08.016

Nayak, P.L., 2000. Natural oil-based polymers: Opportunities and challenges. J. Macromol. Sci. - Polym. Rev. 40, 1–21. https://doi.org/10.1081/MC-100100576

Peplow, M., 2016. The plastics revolution: how chemists are pushing polymers to new limits. Nature 536, 266–268.

Shahbandeh, M., 2020. Vegetable oils: production worldwide 2012/13-2019/20, by type [WWW

Document]. Statistica. URL https://www.statista.com/statistics/263933/production-of-vegetable-oils-worldwide-since-2000/

Sinnwell, S., Ritter, H., 2007. Recent advances in microwave-assisted polymer synthesis. Aust. J. Chem. 60, 729–743. https://doi.org/10.1071/CH07219

Van Der Ploeg, F., 2011. Natural resources: Curse or blessing? J. Econ. Lit. 49, 366–420. https://doi.org/10.1257/jel.49.2.366

Wiesbrock, F., Hoogenboom, R., Schubert, U.S., 2004. Microwave-assisted polymer synthesis: State-of-the-art and future perspectives. Macromol. Rapid Commun. 25, 1739–1764. https://doi.org/10.1002/marc.200400313

Zhang, C., Garrison, T.F., Madbouly, S.A., Kessler, M.R., 2017. Recent advances in vegetable oil-based polymers and their composites. Prog. Polym. Sci. 71, 91–143. https://doi.org/10.1016/j.progpolymsci.2016.12.009

Zhu, Y., Romain, C., Williams, C.K., 2016. Sustainable polymers from renewable resources. Nature 540, 354–362. https://doi.org/10.1038/nature21001

CHAPTER 2: LITERATURE REVIEW

2.1. **Plant oils' triglycerides as a sustainable feedstock for the polymer industry**

While a wide range of oil plants exist in nature, palm, soybean, rapeseed, and sunflower are the major oil plants cultivated in the 2019/2020 crop year with the harvested amount of 75.7, 56.7, 27.0, and 20.7 million metric tons, respectively (Shahbandeh, 2020). Plant oils are extracted mechanically and chemically (using solvents), usually from plant seeds such as soybean, or less often, from plant fruits like the palm. Triacylglycerols (TGs) are the main components of plant oils, consisting of a glycerol molecule linked with three saturated and/or unsaturated fatty acids (FAs) (Scheme 2. 1). Since FAs constitute most of the TGs total weight (~95%), the composition of FAs dictates plant oils' characteristics (Table 2. 1 & 2. 2). The high functionality of TGs makes them suitable precursors for synthesizing polymers. TGs functional groups can be carbon-carbon double bonds (C=C bonds) presenting in all unsaturated fatty acids (UFAs) or other groups such as allylic carbons (methylene moieties next to a C=C bond), ester groups, alpha-carbons (methylene sites next to ester bonds), and, to a lesser extent, terminal methyl groups (omega carbons) (Scheme 2. 1) (Gandini and Lacerda, 2019). In addition to these general functional groups, TGs of some specific plant oils possess some unusual functional groups on certain fatty acids such as hydroxyls (Ricinoleic acid in TGs of castor oil and Lesquerella oil) or epoxies (Vernolic acid in TG of vernonia oil), too (Table 2. 2) (Zhang et al., 2017a). Two main approaches for synthesizing polymers from TGs include 1) direct production of crosslinked polymers from TGs; 2) creating desired polymers through the TGs' derived monomers. Direct production of polymers from TGs is based on manipulating functional groups of FAs in TGs such as internal double bonds, hydroxyls, or epoxides through two different strategies. The first strategy involves direct polymerization of TGs' functional groups through different polymerization methods, while

the second strategy deals with polymerization of chemically modified functional groups of TGs. However, the second approach of creating polymers from the TGs' derived monomers is based on the refining of TGs to different platform chemicals and their future polymerization. The refining process usually starts with hydrolyzing triglycerides to glycerol and a mixture of FAs (Scheme 2. 1). The glycerol, as a safe organic building block for polymer chemistry, is widely used to synthesize polyesters, polyurethanes, or telomers (Kempe et al., 2011). Despite the drawback of increasing polymerization steps, this strategy allows the conversion of naturally occurring functional groups with low reactivity and diversity (mostly double bonds) to more active functional groups, thus broadening polymer synthesis possibilities (Chikkali and Mecking, 2012).

1- Ester group, 2-Double bond, 3- Monoallylic position, 4- Bisallylic position, 5- Alpha position
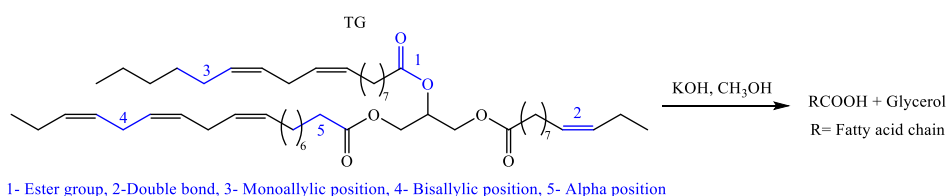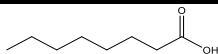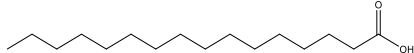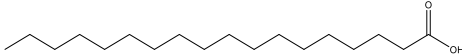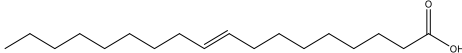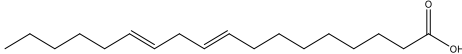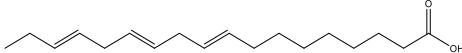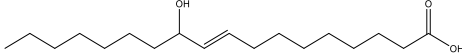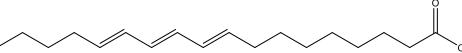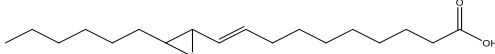
Scheme 2. 1) Triglyceride structure, its reactive sites, and transesterification reaction (Miao et al., 2014).

Table 2. 1) Composition of common Plant oils (Zhang et al., 2017b).

Plant oils	Fatty acid (%)				
	C16:0	C18:0	C18:1	C18:2	C18:3
Canola	4.0	1.8	60.9	21.0	8.8
Palm	44.4	4.1	39.3	10.0	0.4
Soybean oil	10.6	4.0	23.3	53.7	7.6
Rapeseed	3.8	1.2	18.5	14.5	11.0
Sunflower	7.0	4.5	18.7	67.5	0.8
Castor	2.0	1.0	7.0	3.0	0.5
Corn	10.9	2.0	25.4	59.6	1.2
Linseed	6.0	4.0	22.0	16.0	52.0
Olive	9.0	2.7	80.3	6.3	0.7
Cottonseed	21.6	2.6	18.6	54.4	0.7

Table 2. 2) Common fatty acids in plant oils (Adekunle, 2015).

Fatty acids	Structure	Formula
Caprylic		$C_8H_{16}O_2$
Palmitic		$C_{16}H_{32}O_2$
Stearic		$C_{18}H_{36}O_2$
Oleic		$C_{18}H_{34}O_2$
Linoleic		$C_{18}H_{32}O_2$
Linolenic		$C_{18}H_{30}O_2$
Ricinoleic		$C_{18}H_{34}O_3$
α-Eleostearic		$C_{18}H_{30}O_2$
Vernolic		$C_{18}H_{32}O_3$

2.1.1. Sustainable Polymers based on TGs

Crosslinked polymers from TGs

The functional groups in the FAs of TGs are directly exploited to make the crosslinked polymer. The production of crosslinked polymers from TGs has been discussed extensively in the literature (Xia and Larock, 2012); (Lu and Larock, 2009); (Gandini and Lacerda, 2019); (Mosiewicki and Aranguren, 2013); (Wool, 2005). Although being straightforward, this strategy is limited due to the low active functional groups of TGs. Therefore, TGs, despite having straightforward polymethylene chains, are not attractive feedstock for the polymer industry without appropriate modifications. Anyway, crosslinked polymers' production by treating their unsaturated motifs directly or after chemical modification will be discussed here.

Direct polymerization of TGs through their unsaturated motifs

The main polymerization methods compatible with the unsaturated motifs of TGs are radical and cationic polymerization.

Free radical polymerization of TGs

Although the free radical polymerization method can be employed to polymerize TGs through their unsaturated motifs, this method has attracted relatively little attention. The occurrence of chain transfer on the allylic positions of FAs is the fundamental reason that makes polymerization slow and reduces the yield of macromolecular structures (Lu and Larock, 2009). Nonetheless, this method has been employed to produce some crosslinked polymeric materials through oxido-polymerization of TGs from drying oils such as tung oil and linseed oil (Gandini and Lacerda, 2019). TGs are oxidized by atmospheric oxygen, which results in hydrogen abstraction from a bis-allylic methylene group between two double bonds. The next polymerization steps are peroxidation, perepoxidation, hydroperoxidation, epoxidation, and crosslinking through radical recombination to reach a polymeric peroxide with network structure (Scheme 2. 2) (Gandini and Lacerda, 2019); (Çakmakli et al., 2005). Cobalt dryers, such as cobalt 2-ethyl hexanoate, are capable of accelerating all reactions involved in the oxidative polymerization of linseed TGs (Mallégol et al., 2000). Alkyd resins and linoleum floor covers are the common products generated by this method.

It is reported that the oxido-polymerization of soybean TGs results in the creation of a product with two parts: a crosslinked and a waxy soluble polymeric part. The waxy soluble polymeric soy TGs can be used as macroinitiators to progress the free radical polymerization of different vinyl monomers. The initiation of comonomers of methyl methacrylate (MMA), styrene (ST), and *n*-butyl methacrylate (nBMA) with the soluble polymeric soy TGs resulted in biodegradable and

biocompatible grafted copolymers (Çakmakli et al., 2005). The polymeric linseed TGs were also grafted with MMA and ST to generate their graft copolymers with high yields and the molecular weights varying between 37 to 470 kDa (Cakmakli et al., 2004). The grafted copolymers from soybean and linseed TGs showed good potential to be used in tissue engineering due to their cell adhesion.
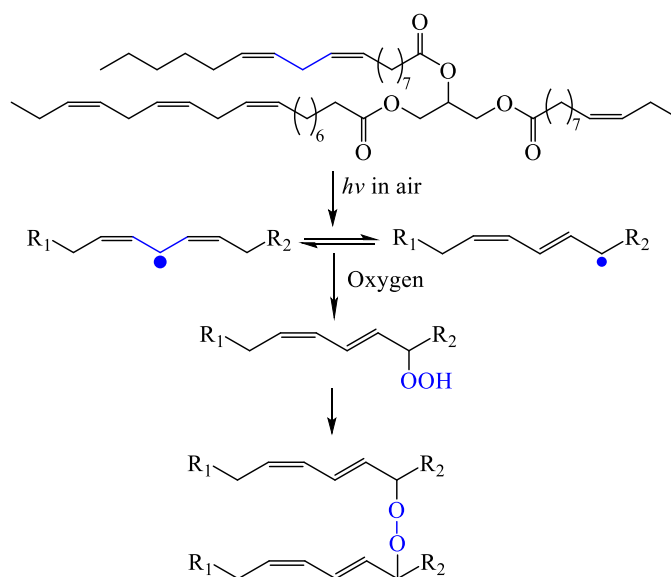
Scheme 2. 2) Oxido-polymerization of drying TGs. R_1 and R_2 are the rest of the TG structure around the nonconjugated double bonds. (Gandini and Lacerda, 2019); (Mallégol et al., 2000).

When TGs have the conjugated C=C bonds, they can be attacked more easily by free radicals than unconjugated ones (Gandini and Lacerda, 2019). In this context, tung oil's TGs, with around 84% α-eleostearic fatty acid (cis-9, trans-11, trans-13-octadecatrienoic acid), is natural conjugated candidate which has been copolymerized with styrene and divinylbenzene (DVB) (Madbouly et al., 2014). Their thermal copolymerization was carried out at 85-160 °C, and the resulted copolymers were transparent thermosets with light yellow color and contained 30-70 wt% tung oil (Scheme 2. 3) (Li and Larock, 2003a). These copolymers were thermally stable below 300 °C with a maximum degradation rate at 493-506 °C and glass transition temperatures of -2 °C to +116 °C.

The thermoset copolymers prepared by thermal free-radical polymerization of conjugated linseed TGs, styrene, and DVB also showed similar properties (Kundu and Larock, 2005).
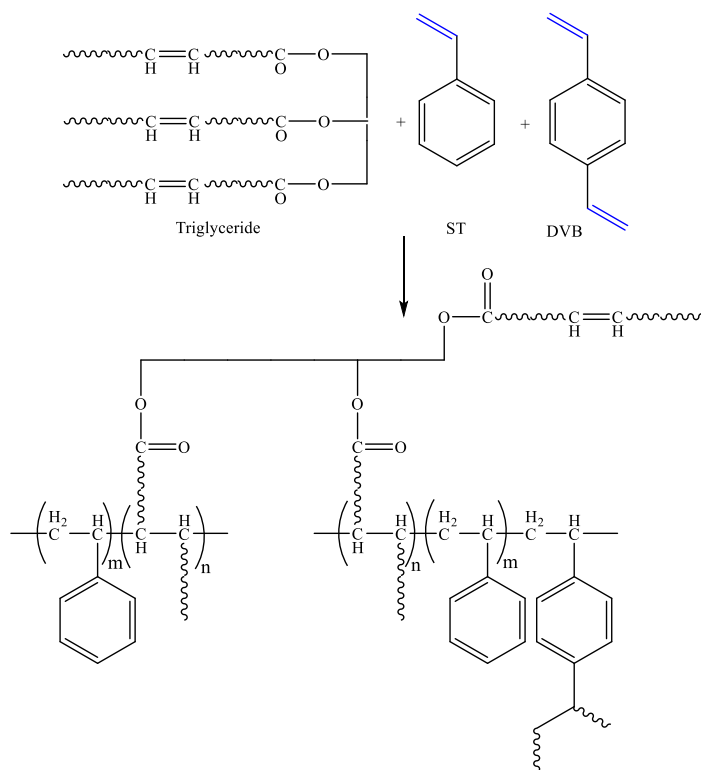
Scheme 2. 3) Copolymerized TGs of tung oil with styrene (ST) and divinylbenzene (DVB).

Soybean TGs have been reported to be highly isomerized to conjugated counterparts using rhodium catalysts under mild reaction conditions (Larock et al., 2001). Both conjugated soybean and linseed TGs were polymerized by benzoyl peroxide, tert-butyl hydroperoxide (TBHP), and their combination as the initiator. The polymerization, however, just increased the viscosity of conjugated TGs (Gandini and Lacerda, 2019). Copolymerization of these TGs with different comonomers was further studied to develop biobased materials with enhanced properties. Polymerization of conjugated TGs with acrylonitrile (AN) and DVB initiated by azobisisobutyronitrile (AIBN) generated transparent yellow thermosets bearing mechanical

characteristics from hard and brittle to soft and rubbery (Valverde et al., 2008); (Henna et al., 2007).

Ghosh et al. also employed an atom transfer radical polymerization (ATRP) method to produce a homopolymer from soybean TGs and its copolymers with methyl acrylate (MA) and methyl methacrylate (MMA). The ATRP was accomplished at 90 °C under microwave irradiation using anhydrous Iron (III) chloride ($FeCl_3$) as the catalyst, diethylenetriamine (DETA) as the ligand, AIBN as the initiator, toluene as the solvent, and metallic iron (Fe) as the reducing agent. The resulted copolymers were used as biodegradable multifunctional additives in mineral base stocks (Karmakar and Ghosh, 2016).

Cationic polymerization of TGs

The unsaturated motifs of TGs are susceptible to cationic polymerization even more than ethylene and propylene due to their slightly more nucleophilic characteristics. Therefore, TGs are considered cationically polymerizable monomers or "cationic monomers" from a thermodynamic perspective (Kennedy and Marechal, 1982). While the cationic polymerization of TGs can be proceeded using initiators such as Protic acids and Lewis acids ($BF_3 \cdot OEt_2$, $TiCl_4$, $ZnCl_2$, $AlCl_3$, and $SnCl_4$), the boron trifluoride etherate ($BF_3 \cdot OEt_2$) is considered the most efficient cationic initiator for this purpose (Scheme 2. 4) (Marks et al., 2001). The TGs' cationic copolymerization with classical reactive monomers, such as ST, DVB, norbornadiene (NBD), or dicyclopentadiene (DCPD), could tackle this limitation and result in the hard plastics' production (Marks et al., 2001); (Andjelkovic et al., 2005); (Li et al., 2003). The cationic copolymerization of a range of TGs from different sources (olive, peanut, sesame, canola, corn, soybean, grapeseed, sunflower, low saturation soy, safflower, walnut, and linseed oils) with DVB or a combination of ST and DVB comonomers was investigated by Larock and coworkers (Andjelkovic et al., 2005). The

unsaturated fatty acid content of TGs from oils determines their degree of unsaturation and reactivity. Interestingly, Larock and coworkers found that all copolymers' characteristics (thermal, mechanical, and crosslink densities) gradually increase with respect to the reactivity of TGs except the copolymers' gelation time. All their resulted copolymers were thermosets with densely crosslinked structures and thermally stable at temperatures below 200 °C. The final copolymers showed diverse characteristics in terms of mechanical properties, from hard and brittle to relatively soft and ductile plastics. Typically, linseed TGs provided copolymers with better mechanical properties than other TGs (Andjelkovic et al., 2005).

Initiation:

$$BF_3 \cdot OEt_2 \; + \; H_2O \; \rightleftharpoons \; BF_3 \cdot OH_2 \; + \; Et_2O$$

$$BF_3 \cdot OH_2 \; + \; CH_2{=}CHR \; \rightleftharpoons \; CH_3{-}\overset{R}{\underset{H}{C}}{+} \; (BF_3\,OH)^-$$

Propagation:

$$CH_3{-}\overset{R}{\underset{H}{C}}{+} \; (BF_3\,OH)^- \; + \; n \; H_2C{=}CHR \; \rightleftharpoons \; H{\left(\!\!\overset{R}{\diagup}\!\!\right)}_n\overset{R}{\underset{H}{C}}{^+} \; (BF_3OH)^-$$
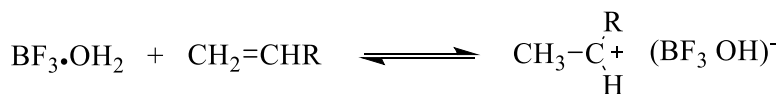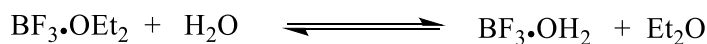
Scheme 2. 4) Initiation mechanism of $BF_3 \cdot OEt_2$ (Marks et al., 2001).

Li and Larock extensively studied the cationic copolymerization of TGs, from different kinds of soybean oil (regular, low saturation, and conjugated low-saturation), with ST and/or DVB initiated by $BF_3 \cdot OEt_2$ or related modified initiators (Li and Larock, 2000); (Li and Larock, 2001a); (Li and Larock, 2001b); (Li and Larock, 2002a); (Li and Larock, 2002b); (Li and Larock, 2003b); (Li et al., 2001). Poor miscibility between TGs and $BF_3 \cdot OEt_2$ and the large differences between TGs and DVB's reactivity resulted in heterogeneous reactions with the generation of solid white particles at the early stages of copolymerization and phase-separation. This issue was resolved by modifying $BF_3 \cdot OEt_2$ with Norway fish oil ethyl ester (NFO). This modified $BF_3 \cdot OEt_2$ initiator has high

16

miscibility with both TGs and DVB. Therefore, it facilitated the homogeneous copolymerization of the monomers. The crosslinking yield of copolymers (crosslinks from 80 to 92%, or crosslinking densities from 74 to 4×10^4 mol/m^3) was attributed to both reactivity of TGs and concentration of crosslinking agents, especially DVB compared to norbornadiene or dicyclopentadiene. Thermogravimetric analysis (TGA) of copolymers revealed that all copolymers were thermally stable at temperatures below 200 °C. Indeed, copolymers' thermal stability depended on the amount of unreacted TGs in the bulk polymer. Moreover, the room-temperature storage moduli of the produced copolymers ranged from 6×10^6 to 2×10^9 Pa, and their glass-transition temperatures (T_g) were comparable to those of commercially available rubbery materials and conventional plastics in a range of 0 °C to 105 °C. The copolymers exhibited the characteristics of materials ranging from soft rubbers to ductile plastics to relatively brittle plastics. In summary, copolymers generated from the conjugated low-saturated soybean TG had the highest thermal, thermomechanical, and mechanical properties.

Cationic polymerization of soybean TG and its copolymers with ST and DVB has also been investigated under conventional and microwave heating when the BF$_3$·OEt$_2$ initiator was modified with methyl oleate (Sacristán et al., 2010). Microwave heating reduced the reaction time from more than 24 h to about 1 hour. Besides, microwave reduced the temperature from 140 °C to 110 °C without any effect on the polymerized TGs' unsaturation degree.

A high molecular weight (118,300 g/mol) soybean-based polymer was created through the cationic polymerization of soybean TG in the supercritical carbon dioxide medium initiated by unmodified BF$_3$·OEt$_2$ (Liu and Erhan, 2010). The polymerization occurred at 140 °C and was completed after 3 hours. The comparison between gel permeation chromatography (GPC) of soybean oil and its

polymer showed a stepwise soy TG polymerization process. The Lewis acid firstly catalyzed a slow Diels-Alder intermolecular and/or an intramolecular cycloaddition reaction of TG molecules to create dimers and trimers. The generated oligomers then polymerized quickly to yield a high molecular weight soybean-based polymer (Liu and Erhan, 2010).

Different compositions of tung TG with DVB and ST/DVB were also cationically polymerized using modified $BF_3 \cdot OEt_2$ with tetrahydrofuran under a stepwise heating procedure (Meiorin et al., 2012). The mechanical, thermomechanical of copolymers was tuned using different compositions of monomers. Tung copolymers with higher DVB concentration exhibited higher T_g (> 140 °C) and elastic modulus and lower resistance. It was due to an improvement in copolymers' crosslinking density and rigidity with increasing DVB concentration in copolymers (Meiorin et al., 2012).

Polymerization of TGs after structural modifications

This section focuses on modifying TGs' C=C bonds, the most popular functional group in TGs, to polymerize the TGs molecules. The addition of a functional group on the acyl chains through C=C bonds has been accepted as a viable approach to increase TGs reactivity for polymerization into new materials. Introducing reactive OH groups into acyl chains is one of the common modification procedures (Scheme 2. 5). Epoxidation of TGs' C=C bonds followed by opening the resulting epoxy ring using proton donors makes TGs appropriate alcoholic platforms for polymerization. Peracid, generated *in situ* from hydrogen peroxide and acetic or formic acid, is capable of epoxidizing TGs' C=C bonds with 75-90% (Omonov et al., 2016). TGs' chemo-enzymatic epoxidation has also introduced more efficient epoxidation procedures. This method can also suppress undesirable ring-opening of epoxides (Rüsch and Warwel, 1999). On the other hand,

hydrogen halides, including HCl and HBr, water (H_2O), hydrogen (H_2), and carboxylic acids (RCO_2H), are the desirable proton donors for the opening of epoxy rings (Scheme 2. 5. B.2).
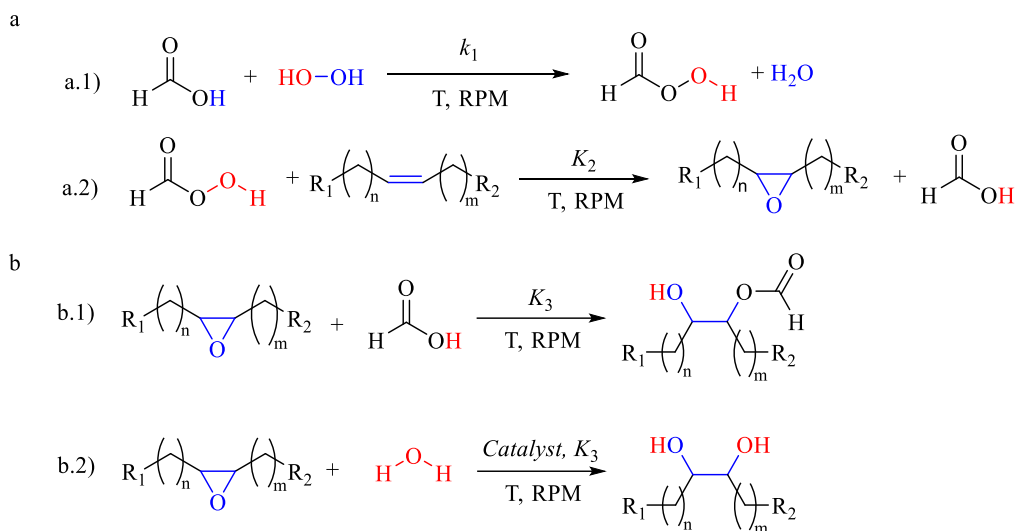
Scheme 2. 5) Introduction of reactive OH group into acyl chains: the first step (a) includes peracid formation (a.1) followed by epoxidation of TGs double bonds (a.2), and the second steps (b) possible epoxy ring-opening with formic acid (b.1), and water as a nucleophile (b.2) (Omonov et al., 2016).

Among the mentioned proton donors, alcohols (ROH) are the most suitable for producing high functionality platforms (Ionescu et al., 2008). Ring-opening of the epoxidized soy TGs was performed using different alcohols, including methanol, 1,2-ethanediol, and 1,2-propanediol in the presence of tetrafluoroboric acid as the catalyst (Wang et al., 2009); (Dai et al., 2009). The resulted products were then polymerized with 2,4-toluene diisocyanate to produce soy-based polyurethane. Interestingly, the alcohols with a higher number of OH groups, such as 1,2-propanediol, provided alcoholic platforms with more hydroxyl groups per oxirane. They are consequently producing polyurethanes with high crosslinking density and superior mechanical properties (Wang et al., 2009); (Dai et al., 2009). Primary hydroxyl groups are usually more reactive than the secondary hydroxyl groups towards aromatic isocyanates. Soy polyols from the reaction of epoxidized soy

19

TGs with methanol were also ethoxylated with ethylene oxide. The ethoxylation resulted in the soy polyols with both primary and secondary hydroxyl groups before polymerization with 2,4-toluene diisocyanate (Scheme 2. 6) (Ionescu et al., 2008).
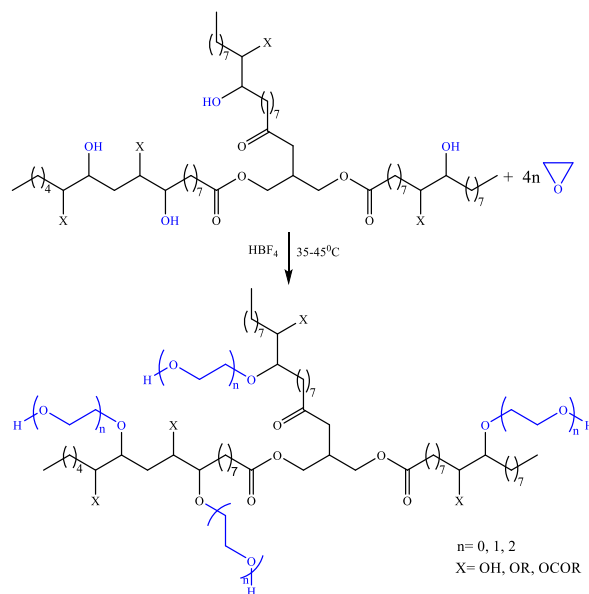
Scheme 2. 6) Ethylene oxide reaction for the formation of soybean polyols with primary and secondary hydroxyl groups (Ionescu et al., 2008).

Lactic acid (LA) has also been used for the ring-opening of epoxidized soy TGs (Scheme 2. 7). Temperature exhibited a positive effect on the production of polyols with higher functionality using LA. In addition, the equivalent amount of lactic acid in the reaction with epoxidized soy TGs can affect the ring-opening yield of epoxidized TGs. Indeed, higher yields (> 80%) for the ring-opening reaction were achieved only when the lactic acid equivalent values were more than 0.4. The resulting polyol was polymerized with a polymeric diphenylmethane diisocyanate and yielded a rigid polyurethane foam (Herrán et al., 2019). Production of soy-based polyurethanes in one step and minimum time was investigated in other studies (Pechar et al., 2007); (Monteavaro et al., 2005). For this purpose, the conversion of soy TG to polyols was directly performed in one-pot with hydrogen peroxide and formic or acetic acid. The excessive heating of created epoxidized soy

TGs in the presence of acids led to the opening of epoxides and polyols' production. The cost-effectiveness and simplicity of this procedure were interesting despite the low functionality of resulting polyols.
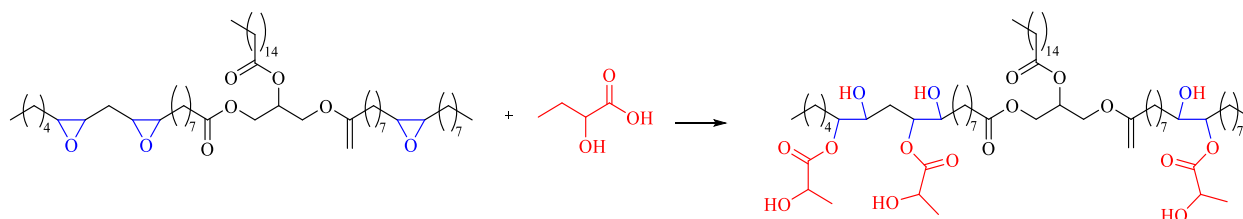
Scheme 2. 7) Ring-opening reaction between epoxidized soybean TG and LA (Herrán et al., 2019); (Li et al., 2015).

A novel photocurable platform chemical from acrylated soy TG has been chemically produced through two steps, as shown in Scheme 2. 8 (Pelletier et al., 2006). The first step involved the reaction of acrylic acid with epoxidized soy TG, and the second step was photo-crosslinking of acrylated soy TGs promoted with Darocure 1173 (2-hydroxy-2-methyl-1-phenyl-propane-1-One) as a photoinitiator under UV irradiation ($\lambda > 280$ nm). An average of five acrylic moieties per TG molecule made the acrylated soy TG, a profitable UV-induced free radical polymerization platform chemical. Acrylated soy TGs had a great potential to convert into polymers with high crosslinking, gel content, and tolerance to the atmospheric oxygen within a few seconds (Pelletier et al., 2006). These characteristics are suitable for producing UV inks and other film coatings. The epoxidized soy TG was also reacted with another platform chemical created from acryloyl chloride reaction with betulin (a biomolecule from the bark of white birch). Compared to the acrylated soy TGs, the new soy-based platform chemical's photocuring took more time with much more photoinitiator (Auclair et al., 2015); (Auclai et al., 2016).
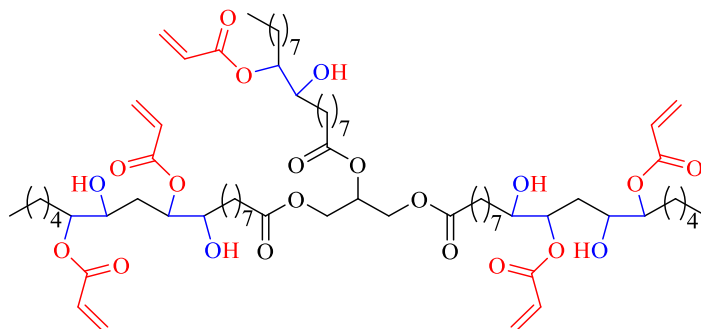
Scheme 2. 8) The acrylated soybean oil structure (Pelletier et al., 2006).

An environmentally friendly, solvent, and catalyst-free method for producing polyols has been studied recently (Zhang et al., 2013). This study resulted in the creation of polyols from epoxidized soy TG and castor oil fatty acid bearing OH group (ricinoleic acid) (Scheme 2. 9).
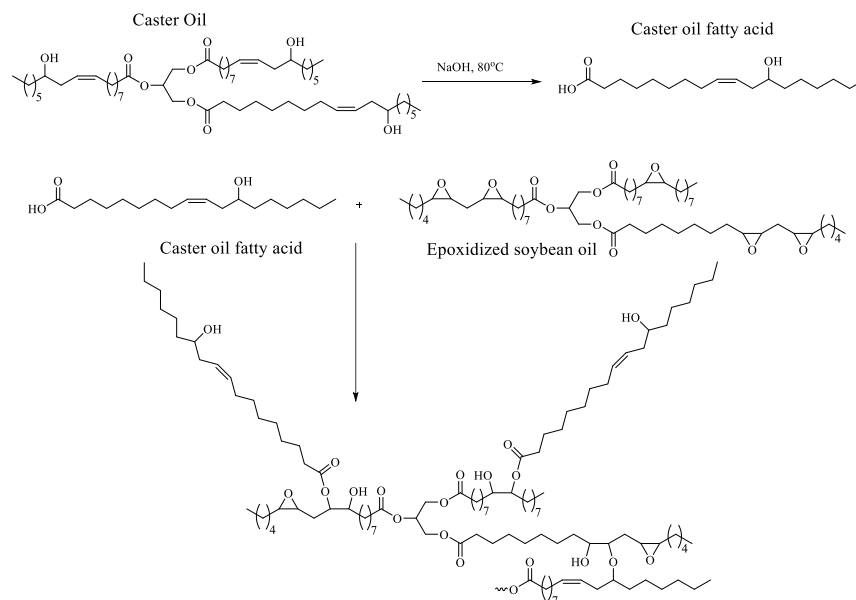
Scheme 2. 9) Polyols from epoxidized soy TG and castor oil fatty acid (Zhang et al., 2013).

The optimum ratio of carboxyl to epoxy groups was 0.5:1 for the complete ring opening of epoxidized soy TG. The epoxidized soy TG was used to prepare polyols for producing highly crosslinked polyurethanes. The resulting polyol was also reacted with isophorone diisocyanate

(IPDI) to introduce a polyurethane with a molecular weight of more than 3000 g mol^{-1}, a T_g of less than 30 °C, and an initial decomposition temperature of more than 250 °C (Scheme 2. 10).
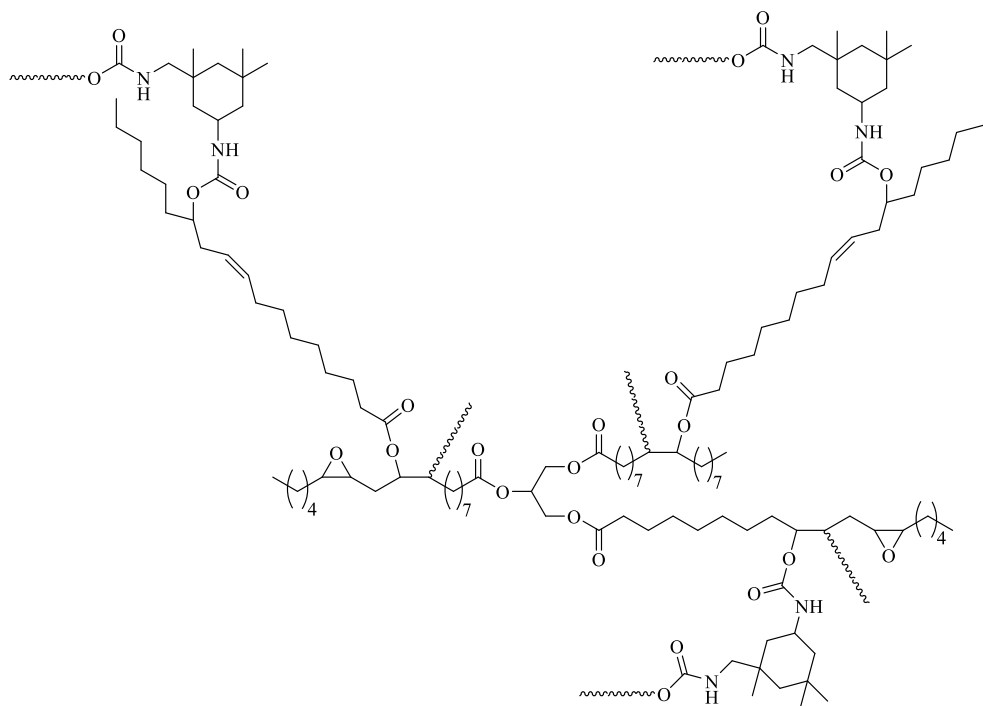
Scheme 2. 10) Polyurethane from polyols derived from epoxidized soy TG and castor oil fatty acid (Zhang et al., 2013).

Mechanical analysis of this product showed a tensile strength of around 12 MPa and the percent elongation at break of > 200% (Zhang et al., 2013). Epoxidized soy TG was also cured with different dicarboxylic-terminated 1010 oligomers of polyamide (M_n of 1149 g mol^{-1}) to produce fully biobased epoxy thermosets (Scheme 2. 11). Higher oligomer contents increased crosslink density and crystallization of the epoxy thermosets, leading to improved stiffness and heat resistance (Wang et al., 2019).
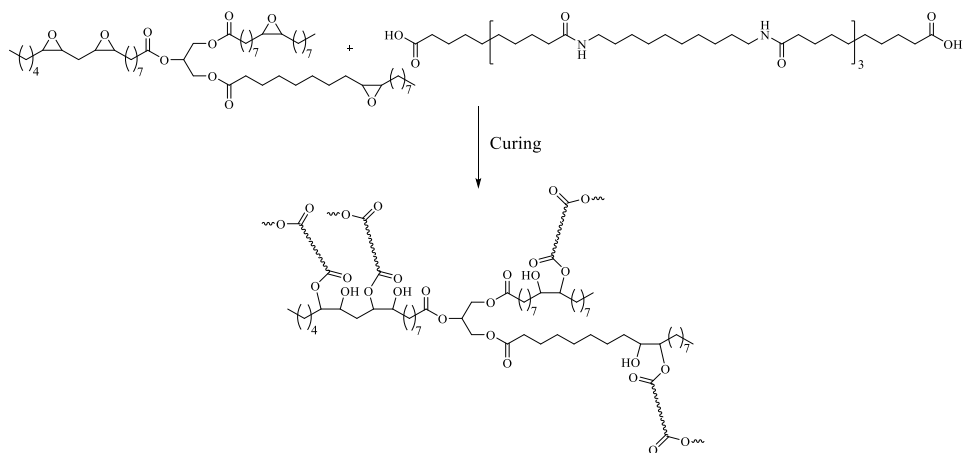
Scheme 2. 11) Curing of epoxidized soybean TG with polyamide 1010 oligomer (Wang et al., 2019).

2.1.2. **Sustainable polymers based on the synthesized platform chemicals from TGs**

The plant oil-based platform chemicals are typically synthesized via transesterification of TGs, firstly proposed by E. Duffy and J. Patrick in 1853 (Santhoshkumar et al., 2019). The transesterification of TGs can be usually facilitated by acid or base methanolic solutions as well as enzymatic methanolic solution. The primary TGs' transesterification methods in most commercial processes are based on the base methanolic solutions of sodium hydroxide (NaOH) and potassium hydroxide (KOH), as well as their carbonates and metal alkoxides. Their economic advantages, their ability to provide a fast rate reaction with high conversion yield, and their less corrosive nature than acidic compounds made them suitable for the industry (Schuchardt et al., 1998).

The base-catalyzed transesterification of TGs converts natural TGs of plant oils into their fatty acid methyl esters (FAMEs) and glycerol through four different steps (Scheme 2. 12). First, the base (catalyst) reacts with the alcohol and produces an alkoxide and a protonated catalyst. Second, the alkoxide attacks nucleophilically to the carbonyl groups of TG and generates a tetrahedral intermediate. It converts to FAMEs and the corresponding anion of diglyceride at the third step.

Fourth, the anion deprotonates the catalyst leading to the regeneration of the catalyst and repeating the steps to reach a mixture of different FAMEs and glycerol as final products (Schuchardt et al., 1998). Although glycerol can be used as a platform chemical for making polymers, FAMEs have been mainly considered as the attractive substrates for producing novel polymers (Xia and Larock, 2012); (Biermann et al., 2011). FAMEs have the superior characteristics of lipophilicity due to their long hydrocarbon chain compared to carbohydrates and most other biomass-derived feedstocks.
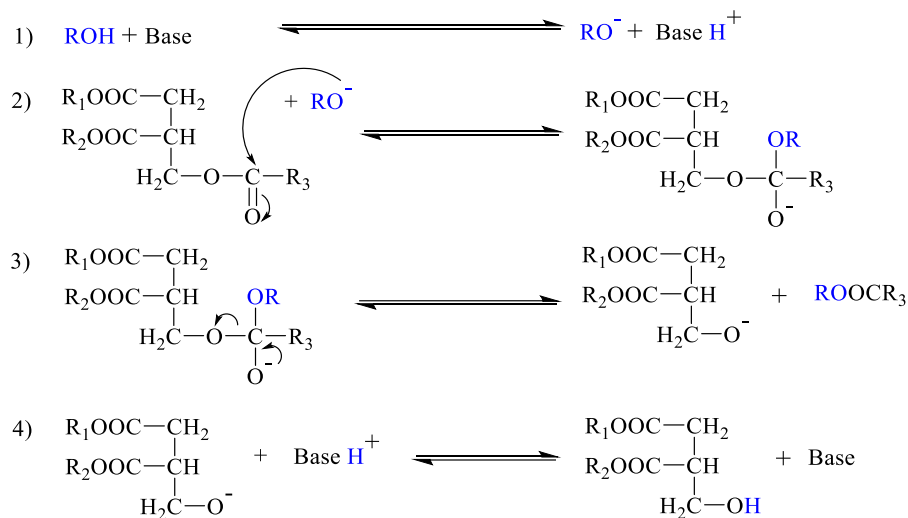
Scheme 2. 12) Base-catalyzed transesterification of TGs (Schuchardt et al., 1998).

In comparison with TGs, FAMEs have carboxylic polar head groups in addition to other functional groups that make them more desirable substrates for synthesizing different platform chemicals and a wider range of polymers. However, C=C bonds still have an outstanding contribution in creating new platform chemicals and polymers from unsaturated FAMEs. FAMEs can be used solely as platform chemical for making polymers through epoxidation of C=C bonds, and then their ring-opening polymerization (Kollbe Ahn et al., 2012) or polymerization of modified epoxy rings (Kollbe Ahn et al., 2011). FAMEs can also be used to create different platform chemicals through

cleavage reactions on C=C bonds. This approach broadens the application of FAMEs for designing a variety of novel biobased polymers by producing monomers with two external active sites and by-products carrying one external active site. The cleavage reactions of FAMEs are ozonolysis or catalytic oxidation of their C=C bonds. They usually yield α,ω-dicarboxylic acids, and derivatives with medium chain length and monofunctional oxygenates (Omonov et al., 2014); (Enferadi Kerenkan et al., 2016). Pyrolysis and alkali fusion of ricinoleic acid, the major free fatty acid (FFA) of castor oil, has been performed to cleave its structure and produce new platform chemicals (Mutlu and Meier, 2010). While the ricinoleic acid's pyrolysis forms 10-undecenoic acid and heptanal (a stoichiometric by-product), the ricinoleic acid's alkali fusion affords sebacic acid and octan-2-ol. The 10-undecenoic acid and sebacic acid are the commercially favorable chemicals for the production of nylon-11 and nylon-6,10, respectively (Rulkens and Koning, 2012). Fatty acids are industrially attractive substrates to be transformed by other reactions including hydrogenation, isomerization, and fermentative ω-oxidation to yield linear dicarboxylic acids, and dimerized to yield branched products (Biermann et al., 2011); (Xia and Larock, 2012); (Anneken et al., 2012). The catalytic C=C cleavage reactions could potentially enhance this portfolio of approaches for introducing novel chemical platforms. In this respect, catalytic olefin metathesis as a ground-breaking advance in chemical synthesis has attracted the attention of both academia and industry (Grubbs, 2006); (Schrock, 2006); (Chauvin, 2006).

Platform chemicals from metathesis of unsaturated FAMEs or FFA

Catalytic olefin metathesis firstly forms a four-membered ring intermediate by recognizing two olefins (alkenes) substrates' unsaturated motifs. Then four-membered ring intermediate rearranges to create two new carbon-carbon double bonds and encourage unique skeletal rearrangements. The large scale catalytic olefin metathesis has been practiced from almost 60 years ago when propylene

was targeted to convert into ethylene and butene in the Phillips Triolefin Process (a reverse procedure of the way round today) (Alperowicz, 2002); (Mol, 2004). The accessibility of a catalyst to different olefins is significantly different. The challenge elevates when the C=C is an internal bond or disubstituted, tri- or tetrasubstituted. These structures escalate steric hindrance levels and complicate *cis* and *trans* (or *E* and *Z*) selectivity control and consequently limit the catalyst's accessibility. Olefin metathesis catalysts have significantly powered the synthesis of platform chemicals from alkenes such as FAMEs or FFAs. They overcame the cumbersome alkenes' accessibility challenges and enhanced the efficiency and stereoselective synthesis of the more substituted olefins. In addition, olefin metathesis reactions prevent the generation of by-products or only generate volatile by-products such as ethylene which is easily removable. Microwave-assisted olefin metathesis has also provided a remarkably-efficient and solvent-free approach for converting olefins (Ullah and Arshad, 2017); (Ullah and Arshad, 2018); (Pradhan et al., 2020). Finally, both feedstock and products of this reaction are reasonably stable and active to be used sufficiently in a wide range of transformations through their π-bond even after extended storage times.

The catalytic metathesis reaction has been performed using both heterogeneous and homogenous metal-based catalysts such as tungsten (Van Dam et al., 1972); (Dam et al., 1974); rhenium (Morrison et al., 2014), molybdenum (Malcolmson et al., 2008), and ruthenium (Ullah and Arshad, 2017). The basic metathesis catalytic systems are cheap and easy to prepare. However, they are of inferior quality to tolerate most untargeted functional groups on the molecule. Therefore, a high load of them requires to reach a good conversion of olefins (Trnka and Grubbs, 2001). Importantly, impurities such as water and peroxides, which are part of plant oil feedstock, also negatively affect these catalytic systems. However, advances in the development of metathesis catalysts have,

fortunately, generated the modern heterogeneous Grubbs' first generation (G1) and second-generation (G2) catalysts, as well as Hoveyda-Grubbs second generation (HG2) catalyst to tackle those problems (Scheme 2. 13). These catalysts are efficient, compatible with untargeted functional groups, insensitive to oxygen, active in water (with the modifications to the ligand system), and work remarkably efficient under microwave irradiation (Trnka and Grubbs, 2001); (Lipshutz and Ghorai, 2012); (Ullah and Arshad, 2017); (Pradhan et al., 2020).
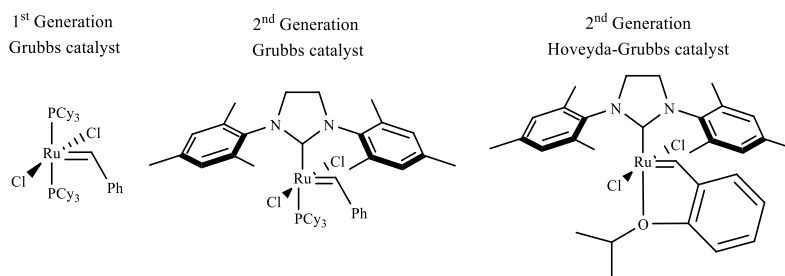
Scheme 2. 13) Grubbs and Hoveyda-Grubbs catalysts.

The catalytic olefin metathesis is a versatile chemical reaction due to its abilities to accomplish different approaches such as self-metathesis (SM), cross-metathesis (CM), ring-closing metathesis (RCM), ring-opening metathesis (ROM), ring-opening metathesis polymerization (ROMP), and acyclic diene metathesis (ADMET) polymerization. The most frequent metathesis approaches applied on the FAMEs or FFAs to produce suitable polymerization platforms are self-metathesis or cross-metathesis (Ngo et al., 2006). The FAMEs' or FFAs' cross-metathesis is usually performed by functionalized olefins like acrylates, acrylonitrile, and allyl chloride (Miao et al., 2011); (Miao et al., 2010) and simple alkenes like ethylene, 1-butene, 2-butene or 1,5-hexene (Ullah and Arshad, 2017); (Pradhan et al., 2020); (Patel et al., 2006); (Marx et al., 2015).

Most studies on the metathesis of FAMEs to create novel chemical platforms have focused on methyl oleate (methyl cis-9-octadecenoate). The SM of methyl oleate led to linear

monounsaturated α,ω-diesters of dimethyl 9-octadecenedioate (DMOD) as suitable chemical platforms for polymer industry (Scheme 2. 14) (Zelin et al., 2013); (Marx et al., 2015). The CM of methyl oleate with ethene (ethenolysis) introduced methyl 9-decenoate and 1-decene, two platform chemicals which can be used for producing a variety of polymers and copolymers (Scheme 2. 14) (Nieres et al., 2016). CM of methyl oleate has also been reported with 2-butene, 2-pentene, and a mixture of 2-hexene and 3-hexene (Biermann et al., 2011). The factors affecting the efficiency and selectivity of the CM reaction of methyl oleate were studied in a series of reactions with different terminal and internal olefins. It was revealed that the type of ruthenium catalysts has an important effect on side reactions such as isomerization, additions, and even catalyst selectivity. It was also reported that molar ratio and nature of substituent in the olefins could highly affect the conversion of methyl oleate and the selectivity of the CM for making desired platform chemicals (Awang et al., 2016). The same results were confirmed in the study of CM reactions of methyl oleate and two other methyl esters with eugenol using the ruthenium-carbene catalyst (G2) in isopropanol or ethanol at 50 °C (Le et al., 2018).
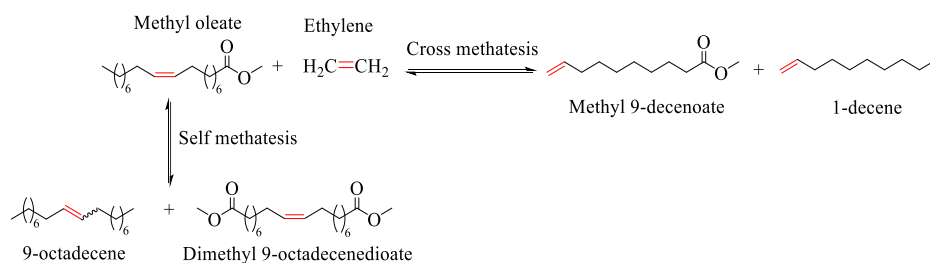
Scheme 2. 14) Self- and cross-metathesis of methyl oleate (Nieres et al., 2016).

The metathesis reaction of other FAMEs from different plant sources to create novel platform chemicals has also been extensively investigated. The SM of long-chain unsaturated FAMEs of methyl palmitoleate, methyl vaccinate, methyl erucate (major fatty acid of high erucic rapeseed oil and crambe oil), methyl elaidate, methyl 11-eicosenoate, methyl petroselenate (major fatty acid of

coriander oil), methyl 5-eicosenoate (methyl gadoleate, major fatty acid of meadow foam oil), methyl ricinoleate (major fatty acid of castor oil), and methyl undecenoate (second-generation product of castor oil) has been reported in the literature (De Espinosa and Meier, 2011). Polyenes, monoesters, diesters, and cyclopolyenes are different intermediate products from these sources.

α-eleostearic acid ((9Z,11E,13E)-octadeca-9,11,13- trienoic acid) methyl ester

1-5 mol%
Toluene or neat
100oC or RT= 2 or 24 hr *cis*-1,4-diacetoxy-2-butene

Methyl 11-acetoxyundec-9-enoate + 2 Hexa-2,4-diene-1,6-diyl diacetate + Hept-2-en-1-yl acetate

10% Pd/C
16h
RT, atm [H]

hexa-1,3,5-triene-1,6-diyl diacetate Octane-1,8-diyl diacetate

99% of 11- acetoxy-undecanoate + 2 53% of 1,6-hex- andiol diacetate + 94% of Heptyl acetate

Hydrolysis + H₂O
- HO

11-hydroxynonanoic acid for polyesters + 1,6-hexanediol for polyurethans + 1-Heptanol for comsmetics

Scheme 2. 15) Synthesis of Polyester and Polyurethane Monomers via Cross Metathesis (CM).

Ricinoleic acid methyl ester (a hydroxyl fatty acid methyl ester in castor oil) was also ethenolized using a homogeneous ruthenium catalyst resulted in methyl 9-decenoate and 1-decene-4-ol (Behr et al., 2012). Interestingly, the same products were also produced through the ethenolysis of ricinoleic acid and castor oil in the same conditions (Behr et al., 2012). CM reaction of α-eleostearic acid ((9Z,11E,13E)-octadeca-9,11,13-trienoic acid) methyl ester from tung oil with *cis*-

1,4-diacetoxy-2-butene along with a palladium on carbon (Pd/C)-catalyzed hydrogenation produced a mixture of methyl 11-acetoxyundecanoate (polyester raw material), 1,6-diacetoxy-hexane (precursor of 1,6-hexanediol polyurethane monomer), and heptyl acetate (fragrance) (Scheme 2. 15) (Kovács et al., 2017).
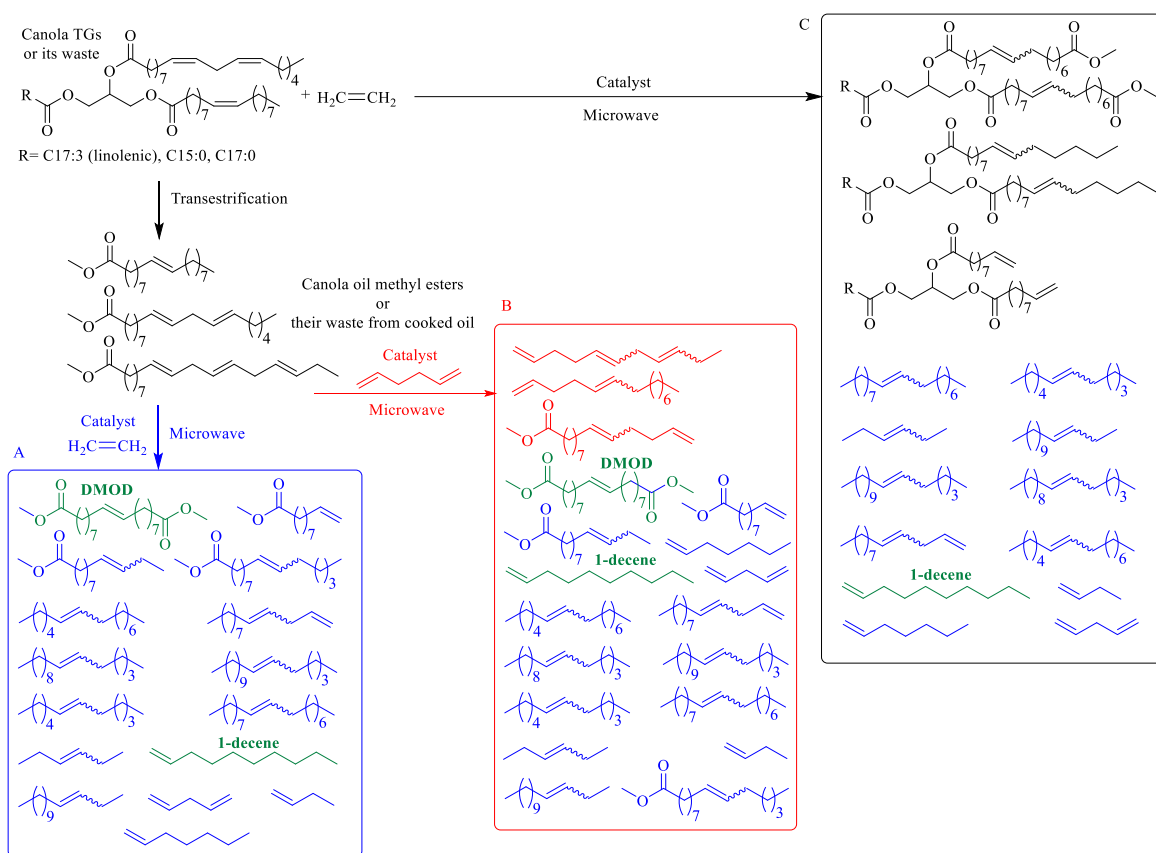
Scheme 2. 16) Ethenolysis (A) and alkenolysis (B) of canola oil methyl esters and canola oil cooking waste, and direct ethenolysis of canola TGs (C) under microwave conditions (Ullah and Arshad, 2017).

Our group has recently reported a remarkably efficient and green procedure for ethenolysis and alkenolysis (using 1,5-hexadiene) of canola TGs and its methyl esters, as well as TGs of canola waste/recycled cooking oils using microwave technology in a solvent-free media (Scheme 2. 16). These reactions with very good yield and selectivity resulted in producing a range of different

mono- and poly-unsaturated olefins, monoesters, and a diester (DMOD). The reaction time was reduced to less than 1 min using 2nd generation Hoveyda-Grubbs catalyst (0.002-0.1 mol%) (Ullah and Arshad, 2017); (Ullah and Arshad, 2018).

Polymers from the platform bio-chemicals derived from TGs

The most prominent petroleum-based polymers that possess aliphatic backbones are polyolefins. Their aliphatic polycondensates such as polyamides, polyesters, and polyethers provide unique properties such as degradability, compostability, and biocompatibility due to their polar groups. These polar groups usually determine the physical properties of petroleum-based aliphatic polycondensates because of their short linear carbon per repeating unit ($\leq$6C). For example, the high density of amide groups in polyamide 6 provides excellent thermal and mechanical properties to this polymer. However, these amide groups demand high processing temperatures and weaken the water-resistance properties of polyamide. Therefore, the development of long-chain aliphatic polyesters, polyamides, and polyurethanes to bridge the gap between conventional polyolefins and polycondensates is of great importance. The major approach for making this class of polymers is based on the linear α,ω-difunctional monomers. In this regard, platform bio-chemicals derived from TGs are one of the most promising monomers to make long-chain aliphatic polyesters and polyamides. Here, we have discussed some of the procedures for preparing long-chain aliphatic polycondensates with promising characteristics. Methyl 10-undecenoate, one of the linear α,ω-difunctional monomers derived from TGs, has been used to produce long-chain aliphatic polycondensates. A straightforward and efficient method to prepare long-chain polyamide and copolyamide from methyl 10-undecenoate was reported by Meier et al. (Türünç et al., 2012). First, thiol-ene addition reaction was employed to make methyl 11-(2-aminoethylthio) undecanoate from methyl 10-undecenoate and cysteamine hydrochloride (Scheme 2. 17). Then, they

homopolymerized it and even copolymerized it with adipic acid and 1,6-hexamethylene diamine. The study revealed that renewable monomers have an excellent potential to synthesize polyamides and even copolyamides with adjustable thermal and solubility properties. It was also reported that the percentage increase of adipic acid and 1,6-hexamethylene diamine could potentially restrict macromolecular diffusion and result in polyamides with low molecular weights due to the strong intermolecular interactions. Finally, the study suggested that using a high-boiling solvent during polymerization, which acts as a plasticizer, is necessary to reach higher molecular weight polymers.
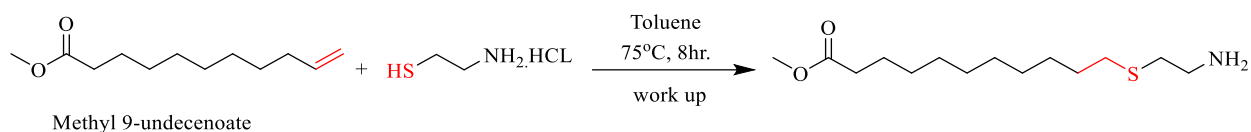
Scheme 2. 17) Synthesis of methyl 11-(2-aminoethylthio) undecanoate from methyl 10-undecenoate and cysteamine hydrochloride.

Ultra-strong polyamide elastomers from methyl 10-undecenoate have recently been created through a unidirectional processing method (Scheme 2. 18) (Song et al., 2019). First, an α, ω-diene amide monomer consisting of twenty linear carbons and two amides with hydroxyl side group (N,N'-(2-hydroxypropane-1,3-diyl)bis(undec-10-enamide), UDA) was produced through amidation of methyl 10-undecenoate with 1,3-diamino-2-propanol. Then, thiol-ene addition polymerization was carried out between the resultant monomer and 2,2'-(Ethylenedioxy)diethanethiol. The additional hydroxyl group in the diene monomer was also employed to control polyamide crystallinity, which can tune mechanical properties. For this purpose, UDA was reacted with butyric anhydride to produce 1,3-di(undec-10-enamido)propan-2-yl butyrate (BUDA). This reaction introduced a larger pendant group on UDA to produce BUDA

that could later inhibit its polymer's crystallization. The obtained polyamides had an ultimate

tensile strength of ~200 MPa and maintained good elasticity.
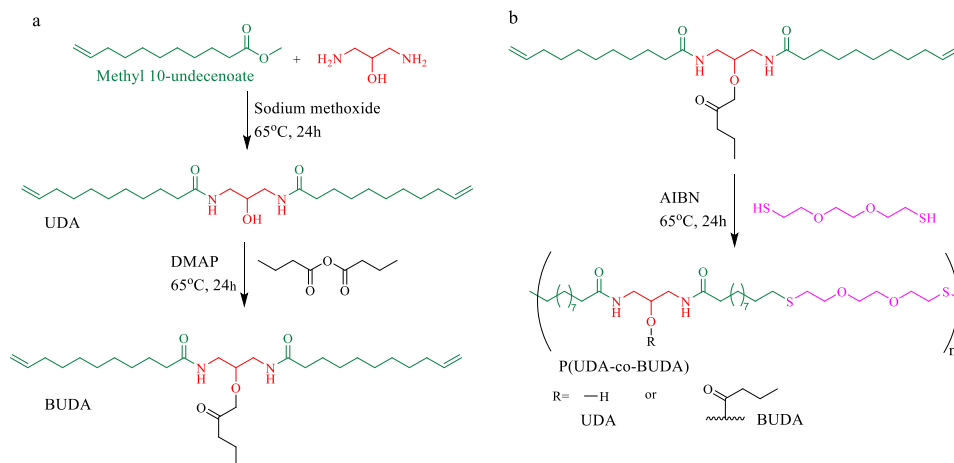
Scheme 2. 18) Synthesis of diene monomers from a methyl 10-undecenoate (a); thiol-ene addition polymerization of the synthesized monomers to produce polyamides (b) (Song et al., 2019).
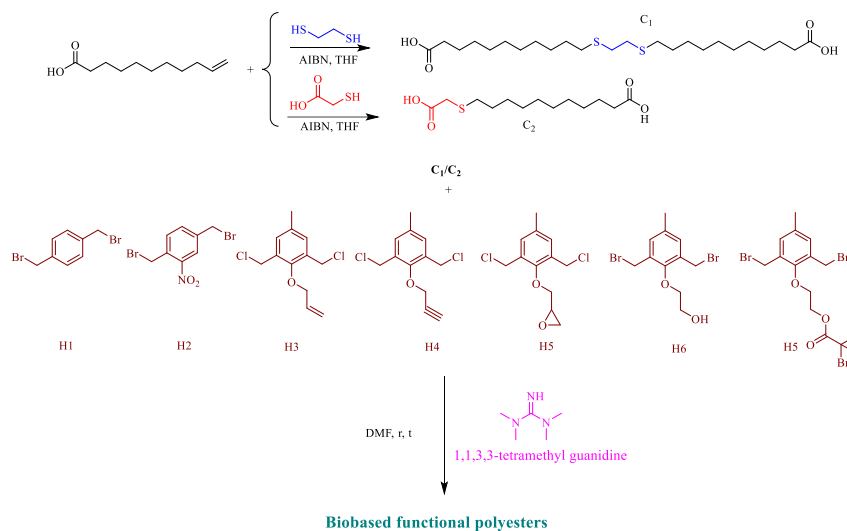
Scheme 2. 19) Synthesis of functional polyesters with different side groups (Li et al., 2014).

10-undecenoic acid has also been used to produce a biobased functional polyester with active side

groups (Li et al., 2014). 10-undecenoic acid was first converted to two different diacid monomers

of 11,11'-(ethane-1,2-diylbis(sulfanediyl))diundecanoic acid (C1) and 11-

((carboxymethyl)thio)undecanoic acid (C2) via thiol-ene addition reaction of the acid with 1,2-dithiol and 2-mercaptoacetic acid, respectively (Scheme 2. 19). The resultant monomers were then polymerized with different dihalide monomers through a facile and efficient strategy to synthesize functional polyesters. The polymerization reaction was performed at room temperature using 1,1,3,3-tetramethyl guanidine as a promoter. Different dihalide monomers produced functional polyesters with distinct side groups (Li et al., 2014).
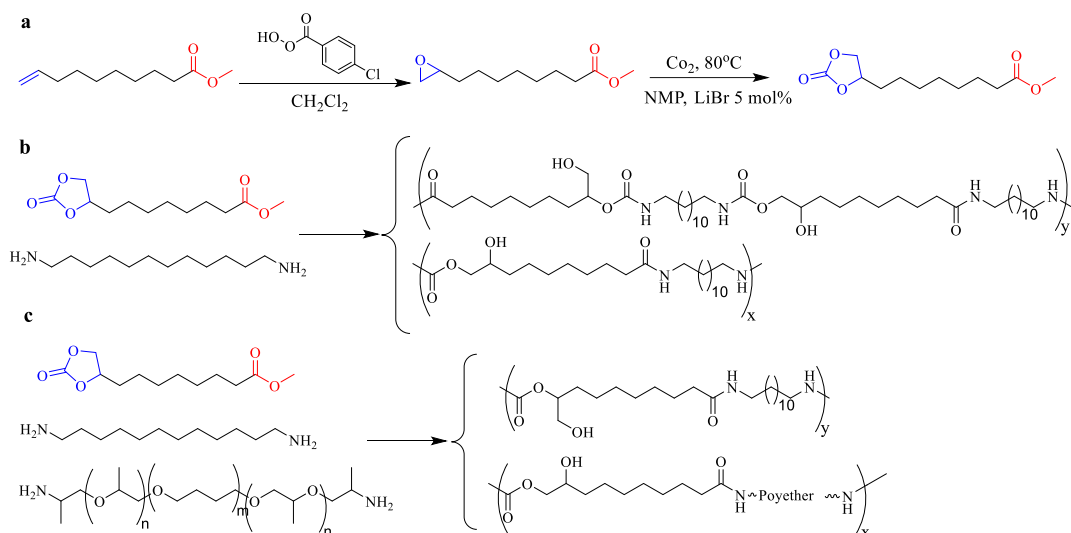
Scheme 2. 20) a) Synthesis of cyclic carbonate-methyl ester (CC-ME) monomers. b) Synthesis of nonsegmented poly(amide-hydroxyurethane) (PA$_{12}$HU) copolymers. c) One-pot melt polymerization of segmented poly(amide-hydroxyurethane) with PTMO-based polyether 1 kDa soft segment (PA$_{12}$HU-PTMO) (Zhang et al., 2016).

Production of biobased polymers from methyl 9-decenoate, as another platform bio-chemical derived from TGs, has also been studied. Zhang et al., synthesized non-isocyanate poly(amide-hydroxyurethane)s from methyl 9-decenoate (Scheme 2. 20) (Zhang et al., 2016). A hetero-functional AB monomer with cyclic carbonate and methyl ester (CC-ME) was first synthesized from methyl 9-decenoate and CO_2 through a two-step procedure of epoxidation and carbonation. The CC-ME monomer was then polymerized using a one-pot synthetic platform with 1,12-

diaminododecane and poly(tetramethylene oxide) (PTMO)-based polyether diamine. This procedure allowed synthesizing both non-segmented poly(amide-hydroxyurethane) (PA$_{12}$HU) and segmented PA$_{12}$HU-PTMOs with varying polyether contents. The PA$_{12}$HU showed characteristics of a semi-crystalline copolymer while incorporating a low T_g 1 kDa polyether diamine added flexibility to segmented PA$_{12}$HU-PTMOs and reduced its crystallinity and melting point due to shorter and fewer hard segments. The resulting segmented PA$_{12}$HU-PTMOs represent the first examples of film-forming, linear isocyanate-free polyurethane with mechanical integrity and processability. Compared to conventional segmented polyurethanes, PA$_{12}$HU-PTMOs showed similar thermal degradation temperature, slightly higher water uptake, lower tensile strength due to their phase-mixed morphologies, and potentially lower molecular weights.

2.2. Microwave technology as an alternative heating source for the polymer industry

2.2.1. Microwave Irradiation

Microwaves are the electromagnetic waves with wavelengths longer than 1 mm and less than 1 m and frequencies of 300 GHz to 300 MHz between infrared radiation and radio frequencies (Figure 2. 1). Microwaves have extensive application in the field of telecommunication. For example, mobile phones, radar, and radio line transmissions are based on the wavelengths between 1 and 25 cm. Only specific frequencies have been used for industrial, scientific, or medical applications. Currently, the allocated wavelengths for household and industrial microwave ovens (applicators) are usually at either 12.2 cm (2.45 GHz) or 33.3 cm (900 MHz) to avoid interferences with telecommunication devices (Chia et al., 1995). Like common microwave ovens, microwave reactors designed for chemical reactions also utilize the frequency of 2.45 GHz. Microwaves contain both electric (E) and magnetic (B) fields with their vectors always being perpendicular to one another. They are also perpendicular to the propagation direction of the wave (Fig 2. 2). During

MW irradiation, the irradiated medium partially absorbs the electric power and converts it into heat according to the law of Lambert and Beer.
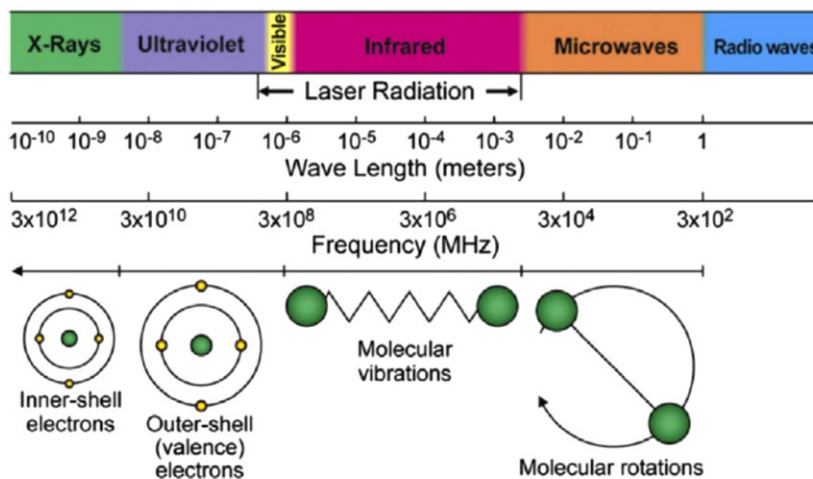
Figure 2. 1) Electromagnetic spectrum (Falciglia et al., 2018).
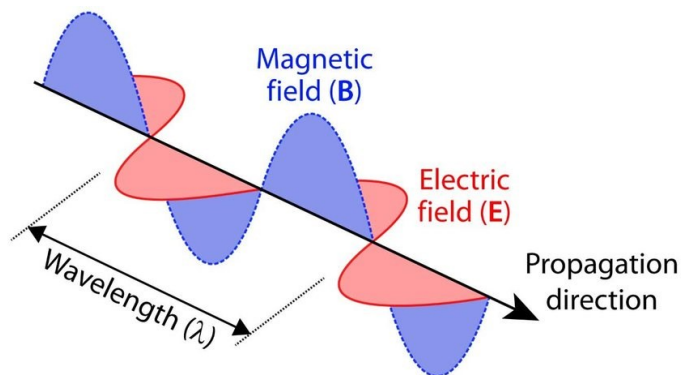
Figure 2. 2) An electromagnetic microwave consisting of electric (E) and magnetic (B) fields.

Microwave irradiation facilitates the chemical reactions through direct interaction with material leading to the thermal effect, which might be easily estimated by temperature measurements. Besides, microwave irradiation applies a specific (non-thermal) effect on the material, too. Indeed, a contribution of these two effects can be responsible for the microwave's observed effect (de la Hoz et al., 2007).

Table 2. 3) Differences between microwave and conventional heating.

Microwave irradiation	Conventional heating
Energetic coupling	Conduction/ convection
Coupling at the molecular level	Superficial Heating
Rapid	Slow
Volumetric	Superficial
Selective	Nonselective
Dependent of the properties of the material	Less dependent

The microwave's thermal effects on the chemical reactions are inherently different from conventional heating. The differences are summarized in table 2. 3. The microwave's thermal effects are a consequence of:

1) The inverted heat transfer: The energy in conventional heating is transferred from the surface of an external heat source by conduction, convection, or radiation and is then transferred towards the colder interior regions by thermal conduction and convection. The energy transfer in microwave heating, on the other hand, is the reverse of that in conventional heating (Fig 2. 3). The energy is directly deposited in the material after microwave penetration. Then, heat is produced throughout the volume of the material as opposed to the heat transfer in conventional heating (Motasemi and Afzal, 2013). This unique inverse heat transfer advances a uniform material heating, increases energy transfer efficiency, and reduces heating time compared to the conventional method.
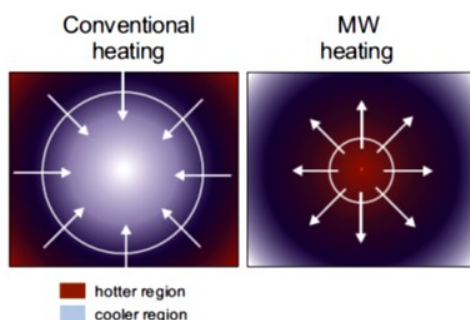
Fig 2. 3) Direction of heat transfer and temperature distribution in conventional and microwave heating (Falciglia et al., 2018).

2) Overheating of polar liquids: Rapid internal heating of the reaction mixture occurs due to the direct interaction of the electromagnetic irradiation (microwave energy) with the molecules when the microwave is used for chemical syntheses. If the reaction components have a low absorbing capacity, the addition of polar additives, such as ionic liquids, can accelerate the chemical reaction. In fact, the presence of monomers or other polar components in solvents can shorten the reaction time under microwave heating compared to other heating methods. In modern microwaves, the possibility of running chemical reactions in closed/sealed vessel mode enables employment of temperatures higher than the solvent's boiling point, which is a limitation for conducting reactions under reflux conditions when the same solvent is used (Kempe et al., 2011).

3) Hot spots (Inhomogeneities): Hot spots in microwave heating are a consequence of the applied field's inhomogeneity. The inhomogeneity causes a much greater temperature than the macroscopic temperature in specific zones within the sample. These zones cannot represent the reaction conditions as a whole (de la Hoz et al., 2007).

4) Selective heating: Microwave irradiation is a selective mode of heating. Characteristically, microwaves generate rapid, intense heating of polar substances while apolar substances do not absorb the radiation and are not heated. The agitation of polar molecules/ions under an oscillating electric or magnetic field is the fundamental mechanism of heating using microwave technology (Mutyala et al., 2010). The presence of an oscillating field compels polar molecules/ions to orient themselves in phase with the electric field. However, resisting forces (inter-particle and inter-molecular interaction and resistance) restrict the induced molecular motions causing random motion and heat production. Therefore, microwave facilitates chemical syntheses through rotation, friction, and the collision of

molecules. Selective heating has been used in solvents, catalysts, and reagents. These effects can be employed efficiently to improve processes, modify selectivities, or even to perform reactions that do not occur under classical conditions (de la Hoz et al., 2007).

Regarding the microwave's non-thermal or specific effects, they are still ongoing debates on them (Gawande et al., 2014). It is also reported that the separation of thermal and non-thermal effects is difficult and not specified. However, the non-thermal effects of microwave irradiation, such as molecular mobility and stabilization effects, are still considered, especially in the reactions that the results cannot be explained solely by a thermal effect (de la Hoz et al., 2007).

2.2.2. Microwave reactors

Domestic microwave ovens (Figure 2. 4.a) are frequently employed in chemical reactions of materials that highly absorb microwave radiations at high temperatures and short times. In modern microwave reactors, a protected cavity is designed to minimize the explosion risk and improve heat transfer to the chemical medium. Automatic microwave reactors with the capacity to perform several reactions sequentially are equipped with a robotic arm to move the vials in and out of the cavity in an automated manner (Figure 2. 4.b). Microwave reactors with flexible platforms (Figure 2. 4.c) enable scientists to perform chemical reactions in different modes to meet the research needs; in a continuous flow, in a large batch vial with a stirrer, or a round-bottom flask with a reflux condenser on top. The unattended automated microwaves (Figure 2. 4.d) are new types of microwave reactors that can automatically prepare the reaction vials by taking the material from stock solutions or samples from vials following the reactions (Kempe et al., 2011).

Figure 2. 4) Selected examples for microwave chemical reactors: a) a domestic microwave oven, b) Initiator Eight (Biotage, Sweden, www.biotage.com), c) CEM Discover (CEM, https://www.indiamart.com), and d) Chemspeed Swave automated microwave synthesizer (Chemspeed, Switzerland, https://www.chemspeed.com).

2.2.3. Microwave-assisted polymerization

Microwave has been used extensively in food processing, drying, chemical, and polymer industries since the 1950s after its first application by Percy Spencer to heat foodstuffs. Although it was employed in organic chemistry before the mid-1980s (Kumar et al., 2020), The first reports on microwave irradiation's effect on the organic reactions' acceleration were published (Gedye et al., 1986); (Giguere et al., 1986) in 1986. In this context, microwave-assisted polymerization has been employed to create different kinds of polymers as reviewed elsewhere (Kempe et al., 2011); (Wiesbrock et al., 2004); (Komorowska-Durka et al., 2015); (Hoogenboom and Schubert, 2007); (Sinnwell and Ritter, 2007); (Zhang et al., 2007). This thesis's focus is on microwave-assisted ring-opening and polycondensation polymerization reactions being discussed in the following sections.

Microwave-assisted ring-opening polymerization

Ring-opening polymerization (ROP) is a chain-growth polymerization technique in which cyclic monomers are added to one end of the polymer chain carrying a reactive center. The resulting polymer's end groups depend on the applied initiator and occurring termination reactions (Cama et al., 2017). The reactive center on the polymer chain's terminal end can be ionic, cationic, or

41

radical. The cyclic monomers' driving force for contributing to ROP is the ring's steric repulsions or bond-angle strain. These cyclic monomers usually contain alkenes, alkanes, or heteroatoms in the ring (Nuyken and Pask, 2013). The polymerization's ability and the corresponding driving force vary depending on the ring structure's type and size. Ring-opening polymerization has already been used to produce many commercially available polymers, including polyesters from cyclic ester (lactones), polysiloxanes from cyclic siloxanes, and PAs from cyclic amides (lactams) (Deb et al., 2018). The initial step in ROP is opening the monomer's ring, followed by the polymer's subsequent chain-growth. Monomer's ring opening can be achieved by adding metal catalysts or a small amount of a nucleophilic reagent (Lewis base) or an electrophilic reagent (Lewis acid) as the initiator. When the initiator is a nucleophilic reagent, the reaction is called anionic ROP. In the case of using an electrophilic reagent as the initiator, the reaction is called cationic ROP. The microwave heating benefits ROP by providing good control over the polymerization process and accelerating polymerization rates (Kempe et al., 2011). Regarding the microwave-assisted ROP, the main focus has been placed on the ring-opening polymerization of cyclic esters as well as the living cationic ring-opening polymerization of 2-oxazolines.

The biodegradable aliphatic polyesters can be produced through the ROP of the cyclic esters like lactones and lactides. The resulting polyesters can be used in drug-delivery systems or fabrication of scaffolds in tissue engineering. Among different cyclic esters, the primary research has been conducted on the production of lactides or ε-caprolactone through microwave-assisted ROP.

The enzyme-catalyzed (Novozymes 435) polymerization of ε-caprolactone has been investigated under reflux conditions in different solvents (toluene, benzene, and diethyl ether) using both conventional and microwave heating (Kerep and Ritter, 2006). The solvent selection had a major effect on the ROP of monomer. While diethyl ether had a positive effect on polymerization

acceleration under microwave irradiation, toluene and benzene showed a negative effect and decelerated the ROP. The authors reported that the boiling point, rather than the solvent's nature (all apolar), was responsible for this study's observed effects. The microwave-assisted ROP of ε-caprolactone with other monomers to produce a poly (ε-caprolactone)-block-poly(ethylene glycol)-block-poly(ε-caprolactone) copolymer has also been studied. Irradiation time, microwave power, length, and amount of added polyethylene glycol were effective in monomer conversion and the polymers' molecular weight (Yu and Liu, 2005). The microwave-assisted ROP of ε-caprolactone has been investigated recently using a novel catalytic/initiating system created from layered double hydroxides (LDH) functionalized with ionic liquid (IL) (Fig 2. 5) (Bujok et al., 2020).

The effects of the modified LDH on the anionic mechanism of microwave-assisted ROP of ε-caprolactone were then investigated. Microwave heating significantly accelerated the polymerization reaction by making the catalytic sites (IL-anions) more accessible for the ε-caprolactone molecules. Microwave-induced molecular rotations of the intercalated IL-anions lead to LDH delamination and exfoliation into individual nanosheets. Moreover, microwave irradiation releases decanoate anions that easily catalyze further polymerization. Compared to the conventional heating, microwave-assisted ROP increased the reaction's rate of ε-caprolactone 4.6 times through a synergistic effect between the intercalated organic species and the microwaves. Indeed, this study reported an easy, environmental-friendly (solvent-free), and practical route for synthesizing organometallic catalyst-free PCL with terminal OH and COOH groups (Bujok et al., 2020).
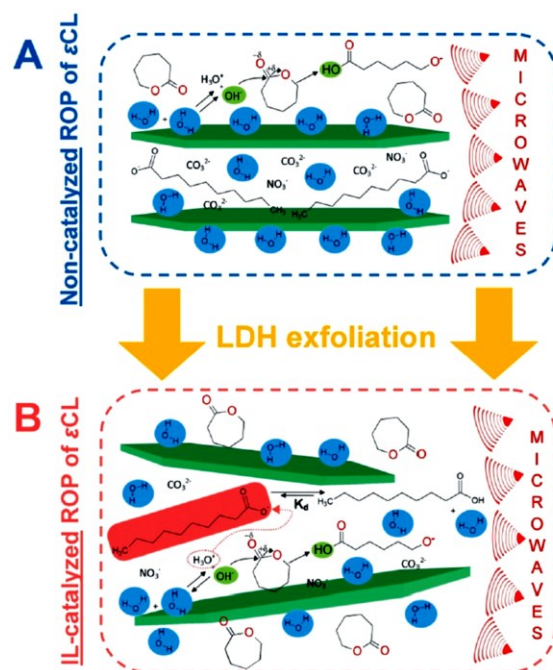
Fig. 2. 5) Initiation scheme of microwave-assisted ROP of ε-caprolactone in the presence of modified LDH: non-catalyzed (A) and IL-catalyzed (B) path (Bujok et al., 2020).

Microwave-assisted polycondensation

The polymer industry has benefited greatly from polycondensation reactions as a form of step-growth polymerization reaction to create polyesters, polyamides, and certain resins and silicones. Polycondensation reactions usually suffer from the release of various low molecular by-products such as water, alcohol, and salt. Effective removal of these by-products from the reaction media is essential to ensure a high reaction rate, conversion, and molecular weight of the final product. Production of polyesters from diols and diacids and polyamides from diamine and diacids are some examples of step-growth polymerization (Scheme 2. 21).

Poly(lactic acid) (PLA) is the most popular bioplastic with ideal industrial characteristics of low weight, low processing temperature (compared to metal and glass), no environmental pollution, good printability, and ease of conversion into different forms (Lim et al., 2008). Takeuchi et al. studied the direct microwave-assisted polycondensation of lactic acid to a high molecular weight

PLA (>10,000 g.mol^{-1}) (scheme 2. 22), which was not reported before (Nagahata et al., 2007). They observed that microwave strikingly accelerated the polymerization rate of lactic acid compared to conventional heating and resulted in PLA's formation with a molecular weight of 16,000 g.mol^{-1} within 30 min. They also investigated the effect of different catalysts in this process and pointed out the enhanced catalytic activity of binary catalysts such as SnCl$_2$/p-TsOH.
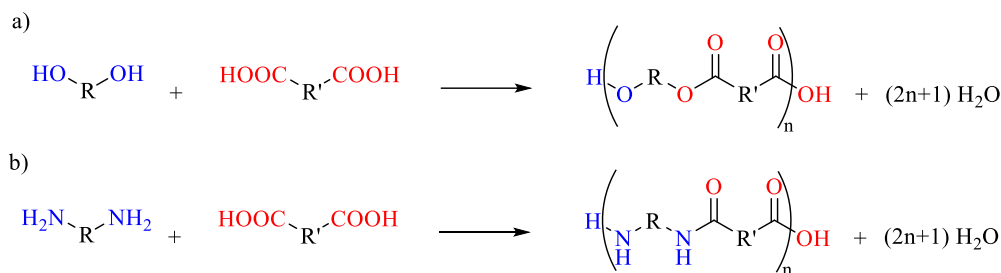
Scheme 2. 21) step-growth polycondensation of a) polyesters b) polyamides.
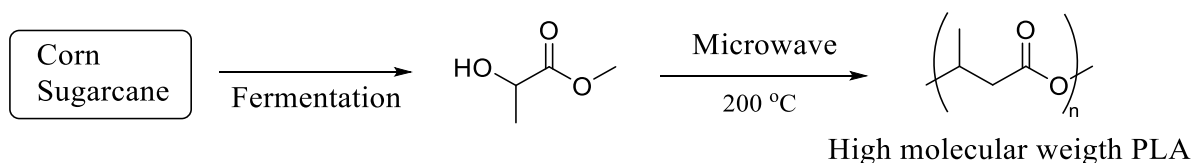
Scheme 2. 22) The PLA synthesis.

The synthesis of Poly(L-lactic acid) (PLLA) under microwave irradiation was also investigated using a special microwave equipped with an external cooling system to provide an isothermal condition throughout the polymerization process. This system provided simultaneous cooling of the reaction vessel with *o*-xylene to generate a constant and continuous microwave power in the reactor at isothermal condition during the polymerization (Temur Ergan and Bayramoğlu, 2018). The produced PLLA polymer had a higher polymerization rate, polymer yield, average-molecular weight, dispersity, and thermal properties than those generated under conventional heating. Crystalline measurements of the products revealed that microwave affected the polymers' optical

purity (L or D). Additionally, the energy-saving using microwave technology was approximately 73.1% in this study.

Microwave has also been employed to synthesize poly(butylene succinate) (PBS). Microwave-assisted activation of reactants (1,4- butanediol (BD) and succinic acid (SA)), as well as the effect of water, produced as a by-product during the polycondensation, on the reaction acceleration rate, was investigated in this study. Microwave heating was reported to selectively activate the reactants and remove water from the reaction solution more rapidly and to a greater extent than oil bath heating under identical conditions (i.e., time and temperature). They also showed that the accelerated removal of the water by-product is the principal effect of microwave irradiation in PBS synthesis (scheme 2. 23) (Nagahata et al., 2018).
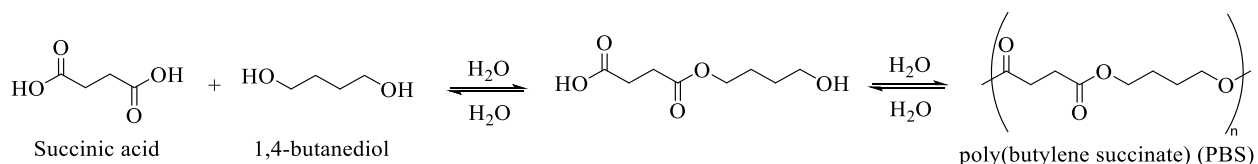
Scheme 2. 23) the synthesis of poly(butylene succinate) through polycondensation of succinic acid and 1,4- butanediol.

References

Adekunle, K.F., 2015. A review of vegetable oil-based polymers: synthesis and applications. Open J. Polym. Chem. 05, 34–40. https://doi.org/10.4236/ojpchem.2015.53004

Alperowicz, N., 2002. PCS studies propylene expansion using olefin conversion process. Chem. Week, Mar 6 164, 16.

Andjelkovic, D.D., Valverde, M., Henna, P., Li, F., Larock, R.C., 2005. Novel thermosets prepared by cationic copolymerization of various vegetable oils - Synthesis and their structure-property relationships. Polymer (Guildf). 46, 9674–9685. https://doi.org/10.1016/j.polymer.2005.08.022

Anneken, D.J., Both, S., Christoph, R., Fieg, G., Steinberner, U., Westfechtel, A., 2012. Fatty Acids. Ullmann's Encycl. Ind. Chem. https://doi.org/10.1002/14356007.a10

Auclai, N., Kaboorani, A., Riedl, B., Landry, V., 2016. Acrylated betulin as a comonomer for bio-based coatings. Part II: Mechanical and optical properties. Ind. Crops Prod. 82, 118–126. https://doi.org/10.1016/j.indcrop.2015.11.081

Auclair, N., Kaboorani, A., Riedl, B., Landry, V., 2015. Acrylated betulin as a comonomer for bio-based coatings. Part I: Characterization, photo-polymerization behavior and thermal stability. Ind. Crops Prod. 76, 530–537. https://doi.org/10.1016/j.indcrop.2015.07.020

Awang, N.W., Tsutsumi, K., Huštáková, B., Yusoff, S.F.M., Nomura, K., Yamin, B.M., 2016. Cross metathesis of methyl oleate (MO) with terminal, internal olefins by ruthenium catalysts: Factors affecting the efficient MO conversion and the selectivity. RSC Adv. 6, 100925–100930. https://doi.org/10.1039/c6ra24200f

Behr, A., Krema, S., Kampar, A., 2012. Ethenolysis of ricinoleic acid methyl ester – an efficient way to the oleochemical key substance methyl dec-9-enoate. RSC Adv. 2, 12775–12781. https://doi.org/10.1039/c2ra22499b

Biermann, U., Bornscheuer, U., Meier, M.A.R., Metzger, J.O., Schäfer, H.J., 2011. Oils and fats as renewable raw materials in chemistry. Angew. Chemie - Int. Ed. 50, 3854–3871. https://doi.org/10.1002/anie.201002767

Bujok, S., Konefał, M., Abbrent, S., Pavlova, E., Svoboda, J., Trhlíková, O., Walterová, Z., Beneš, H., 2020. Ionic liquid-functionalized LDH as catalytic-initiating nanoparticles for microwave-activated ring opening polymerization of ϵ-caprolactone. React. Chem. Eng. 5, 506–518. https://doi.org/10.1039/c9re00399a

Çakmakli, B., Hazer, B., Tekin, I.Ö., Cömert, F.B., 2005. Synthesis and characterization of

polymeric soybean oil-g-methyl methacrylate (and n-butyl methacrylate) graft copolymers: Biocompatibility and bacterial adhesion. Biomacromolecules 6, 1750–1758. https://doi.org/10.1021/bm050063f

Cakmakli, B., Hazer, B., Tekin, I.O., Kizgut, S., Koksal, M., Menceloglu, Y., 2004. Synthesis and characterization of polymeric linseed oil grafted methyl methacrylate or styrene. Macromol. Biosci. 4, 649–655. https://doi.org/10.1002/mabi.200300117

Cama, G., Mogosanu, D.E., Houben, A., Dubruel, P., 2017. Synthetic biodegradable medical polyesters: poly-ε-caprolactone, in: Zhang, X. (Ed.), Science and Principles of Biodegradable and Bioresorbable Medical Polymers. Elsevier Ltd. https://doi.org/https://doi.org/10.1016/B978-0-08-100372-5.00003-9

Chauvin, Y., 2006. Olefin metathesis: The early days (nobel lecture). Angew. Chemie - Int. Ed. 45, 3740–3747. https://doi.org/10.1002/anie.200601234

Chia, L.H.L., Boey, F.Y.C., Jacob, J., 1995. Review Thermal and non-thermal interaction of microwave radiation with materials. J. Mater. Sci. 30, 5321–5327.

Chikkali, S., Mecking, S., 2012. Refining of plant oils to chemicals by olefin metathesis. Angew. Chemie - Int. Ed. 51, 5802–5808. https://doi.org/10.1002/anie.201107645

Dai, H., Yang, L., Lin, B., Wang, C., Shi, G., 2009. Synthesis and characterization of the different soy-based polyols by ring opening of epoxidized soybean oil with methanol, 1,2-ethanediol and 1,2-propanediol. JAOCS, J. Am. Oil Chem. Soc. 86, 261–267. https://doi.org/10.1007/s11746-008-1342-7

Dam, V.P.B., Mittelmeijer, C., M., C., B., 1974. Homogeneous catalytic metathesis of unsaturated fatty esters: New synthetic method for preparation of unsaturated mono-and dicarboxylic acids. J. Am. Oil Chem. Soc. 51, 389–392. https://doi.org/10.1007/BF02635013

De Espinosa, L.M., Meier, M.A.R., 2011. Plant oils: The perfect renewable resource for polymer science?! Eur. Polym. J. 47, 837–852. https://doi.org/10.1016/j.eurpolymj.2010.11.020

de la Hoz, A., Díaz-Ortiz, A., Moreno, A., 2007. Review on non-thermal effects of microwave irradiation in organic synthesis. J. Microw. Power Electromagn. Energy 41, 44–64. https://doi.org/10.1080/08327823.2006.11688549

Deb, P.K., Kokaz, S.F., Abed, S.N., Paradkar, A., Tekade, R.K., 2018. Pharmaceutical and biomedical applications of polymers, in: Basic Fundamentals of Drug Delivery. pp. 203–267. https://doi.org/10.1016/B978-0-12-817909-3.00006-6

Enferadi Kerenkan, A., Béland, F., Do, T.O., 2016. Chemically catalyzed oxidative cleavage of unsaturated fatty acids and their derivatives into valuable products for industrial applications: A review and perspective. Catal. Sci. Technol. 6, 971–987. https://doi.org/10.1039/c5cy01118c

Falciglia, P.P., Roccaro, P., Bonanno, L., De Guidi, G., Vagliasindi, F.G.A., Romano, S., 2018. A review on the microwave heating as a sustainable technique for environmental remediation/detoxification applications. Renew. Sustain. Energy Rev. 95, 147–170. https://doi.org/10.1016/j.rser.2018.07.031

Gandini, A., Lacerda, T.M., 2019. Polymers from Plant Oils, 2nd ed. John Wiley & Sons, Inc.

Gawande, M.B., Shelke, S.N., Zboril, R., Varma, R.S., 2014. Microwave-assisted chemistry: Synthetic applications for rapid assembly of nanomaterials and organics. Acc. Chem. Res. 47, 1338–1348. https://doi.org/10.1021/ar400309b

Gedye, R., Smith, F., Westaway, K., Ali, H., Baldisera, L., Laberge, L., Rousell, J., 1986. The use of microwave ovens for rapid organic synthesis. Tetrahedron Lett. 27, 279–282. https://doi.org/10.1016/S0040-4039(00)83996-9

Giguere, R.J., Bray, T.L., Duncan, S.M., Majetich, G., 1986. Application of commercial microwave ovens to organic synthesis. Tetrahedron Lett. 27, 4945–4948. https://doi.org/10.1016/S0040-4039(00)85103-5

Grubbs, R.H., 2006. Olefin-metathesis catalysts for the preparation of molecules and materials (Nobel lecture). Angew. Chemie - Int. Ed. 45, 3760–3765. https://doi.org/10.1002/anie.200600680

Henna, P.H., Andjelkovic, D.D., Kundu, P.P., Larock, R.C., 2007. Biobased Thermosets from the Free-Radical Copolymerization of Conjugated Linseed Oil Phillip. J. Appl. Polym. Sci. 104, 979–985.

Herrán, R., Amalvy, J.I., Chiacchiarelli, L.M., 2019. Highly functional lactic acid ring-opened soybean polyols applied to rigid polyurethane foams. J. Appl. Polym. Sci. 136, 47959 (1–13). https://doi.org/10.1002/app.47959

Hoogenboom, R., Schubert, U.S., 2007. Microwave-assisted polymer synthesis: Recent developments in a rapidly expanding field of research. Macromol. Rapid Commun. 28, 368–386. https://doi.org/10.1002/marc.200600749

Ionescu, M., Petrović, Z.S., Wan, X., 2008. Primary hydroxyl content of soybean polyols. J. Am. Oil Chem. Soc. 85, 465–473. https://doi.org/10.1007/s11746-008-1210-5

Karmakar, G., Ghosh, P., 2016. Atom Transfer Radical Polymerization of Soybean Oil and Its Evaluation as a Biodegradable Multifunctional Additive in the Formulation of Eco-Friendly Lubricant. ACS Sustain. Chem. Eng. 4, 775–781. https://doi.org/10.1021/acssuschemeng.5b00746

Kempe, K., Becer, C.R., Schubert, U.S., 2011. Microwave-assisted polymerizations: Recent status and future perspectives. Macromolecules 44, 5825–5842. https://doi.org/10.1021/ma2004794

Kennedy, J.P., Marechal, E., 1982. Carbocationic Polymerization. John Wiley & Sons, New York.

Kerep, P., Ritter, H., 2006. Influence of microwave irradiation on the lipase-catalyzed ring-opening polymerization of e-caprolactone. Macromol. Rapid Commun. 27, 707–710. https://doi.org/10.1002/marc.200500781

Kollbe Ahn, B., Wang, H., Robinson, S., Shrestha, T.B., Troyer, D.L., Bossmann, S.H., Sun, X.S., 2012. Ring opening of epoxidized methyl oleate using a novel acid-functionalized iron nanoparticle catalyst. Green Chem. 14, 136–142. https://doi.org/10.1039/c1gc16043e

Kollbe Ahn, B.J., Kraft, S., Sun, X.S., 2011. Chemical pathways of epoxidized and hydroxylated fatty acid methyl esters and triglycerides with phosphoric acid. J. Mater. Chem. 21, 9498–9505. https://doi.org/10.1039/c1jm10921a

Komorowska-Durka, M., Dimitrakis, G., Bogdał, D., Stankiewicz, A.I., Stefanidis, G.D., 2015. A concise review on microwave-assisted polycondensation reactions and curing of polycondensation polymers with focus on the effect of process conditions. Chem. Eng. J. 264, 633–644. https://doi.org/10.1016/j.cej.2014.11.087

Kovács, E., Turczel, G., Szabó, L., Varga, R., Tóth, I., Anastas, P.T., Tuba, R., 2017. Synthesis of 1,6-hexandiol, polyurethane monomer derivatives via isomerization metathesis of methyl linolenate. ACS Sustain. Chem. Eng. 5, 11215–11220. https://doi.org/10.1021/acssuschemeng.7b03309

Kumar, A., Kuang, Y., Liang, Z., Sun, X., 2020. Microwave chemistry, recent advancements, and eco-friendly microwave-assisted synthesis of nanoarchitectures and their applications: a review. Mater. Today Nano 11, 100076. https://doi.org/10.1016/j.mtnano.2020.100076

Kundu, P.P., Larock, R.C., 2005. Novel conjugated linseed oil-styrene-divinylbenzene copolymers prepared by thermal polymerization. 1. Effect of monomer concentration on the structure and

properties. Biomacromolecules 6, 797–806. https://doi.org/10.1021/bm049429z

Larock, R.C., Dong, X., Chung, S., Reddy, C.K., Ehlers, L.E., 2001. Preparation of conjugated soybean oil and other natural oils and fatty acids by homogeneous transition metal catalysis. JAOCS, J. Am. Oil Chem. Soc. 78, 447–453. https://doi.org/10.1007/s11746-001-0284-1

Le, D., Samart, C., Tsutsumi, K., Nomura, K., Kongparakul, S., 2018. Efficient conversion of renewable unsaturated fatty acid methyl esters by cross-metathesis with eugenol. ACS Omega 3, 11041–11049. https://doi.org/10.1021/acsomega.8b01695

Li, F., Hasjim, J., Larock, R.C., 2003. Synthesis, structure, and thermophysical and mechanical properties of new polymers prepared by the cationic copolymerization of corn oil, styrene, and divinylbenzene. J. Appl. Polym. Sci. 90, 1830–1838. https://doi.org/10.1002/app.12826

Li, F., Larock, R.C., 2003a. Synthesis, structure and properties of new tung oil - Styrene - Divinylbenzene copolymers prepared by thermal polymerization. Biomacromolecules 4, 1018–1025. https://doi.org/10.1021/bm034049j

Li, F., Larock, R.C., 2003b. New soybean oil-styrene-divinylbenzene thermosetting copolymers. VI. Time-temperature-transformation cure diagram and the effect of curing conditions on the thermoset properties. Polym. Int. 52, 126–132. https://doi.org/10.1002/pi.1060

Li, F., Larock, R.C., 2002a. New soybean oil-styrene-divinylbenzene thermosetting copolymers-IV. Good damping properties. Polym. Adv. Technol. 13, 436–449. https://doi.org/10.1002/pat.206

Li, F., Larock, R.C., 2002b. New soybean oil-styrene-divinylbenzene thermosetting copolymers. V. Shape memory effect. J. Appl. Polym. Sci. 84, 1533–1543. https://doi.org/10.1002/app.10493

Li, F., Larock, R.C., 2001a. New soybean oil-styrene-divinylbenzene thermosetting copolymers.

I. Synthesis and characterization. J. Appl. Polym. Sci. 80, 658–670. https://doi.org/10.1002/1097-4628(20010425)80:4<658::AID-APP1142>3.0.CO;2-D

Li, F., Larock, R.C., 2001b. New soybean oil-styrene-divinylbenzene thermosetting copolymers. III. Tensile Stress–Strain Behavior. J. ofPolymer Sci. Part B Polym. Phys. 39, 60–77. https://doi.org/https://doi.org/10.1002/1099-0488(20010101)39:1<60::AID-POLB60>3.0.CO;2-K

Li, F., Larock, R.C., 2000. New soybean oil-styrene-divinylbenzene thermosetting copolymers. II. Dynamic mechanical properties. J. Polym. Sci. Part B Polym. Phys. 38, 2721–2738. https://doi.org/10.1002/1099-0488(20001101)38:21<2721::AID-POLB30>3.0.CO;2-D

Li, F., Marks, D.W., Larock, R.C., Otaigbe, J.U., 2001. Soybean oil–divinylbenzene thermosetting polymers: synthesis, structure, properties and their relationships. Polymer (Guildf). 42, 1567–1579. https://doi.org/https://doi.org/10.1016/S0032-3861(00)00546-2

Li, Q., Wang, T., Ma, C., Bai, W., Bai, R., 2014. Facile and highly efficient strategy for synthesis of functional polyesters via tetramethyl guanidine promoted polyesterification at room temperature. ACS Macro Lett. 3, 1161–1164. https://doi.org/10.1021/mz5005184

Li, Y., Wang, D., Sun, X.S., 2015. Copolymers from epoxidized soybean oil and lactic acid oligomers for pressure-sensitive adhesives. RSC Adv. 5, 27256–27265. https://doi.org/10.1039/c5ra02075a

Lipshutz, B.H., Ghorai, S., 2012. "Designer"-Surfactant-Enabled Cross-Couplings in Water at Room Temperature. Aldrichimica Act 45, 3–16.

Liu, Z., Erhan, S.Z., 2010. Preparation of soybean oil polymers with high molecular weight. J. Polym. Environ. 18, 243–249. https://doi.org/10.1007/s10924-010-0179-y

Lu, Y., Larock, R.C., 2009. Novel Polymeric Materials from Vegetable Oils and Vinyl Monomers :

Preparation , Properties , and Applications. ChemSusChem 2, 136–147. https://doi.org/10.1002/cssc.200800241

Madbouly, S.A., Liu, K., Xia, Y., Kessler, M.R., 2014. Semi-interpenetrating polymer networks prepared from in situ cationic polymerization of bio-based tung oil with biodegradable polycaprolactone. RSC Adv. 4, 6710–6718. https://doi.org/10.1039/c3ra46773b

Malcolmson, S.J., Meek, S.J., Sattely, E.S., Schrock, R.R., Hoveyda, A.H., 2008. Highly efficient molybdenum-based catalysts for enantioselective alkene metathesis. Nature 456, 933–937. https://doi.org/10.1038/nature07594

Mallégol, J., Lemaire, J., Gardette, J., 2000. Drier influence on the curing of linseed oil. Prog. Org. Coatings 39, 107–113. https://doi.org/10.1016/S0300-9440(00)00126-0

Marks, D.W., Li, F., Pacha, C.M., Larock, R.C., 2001. Synthesis of thermoset plastics by Lewis acid initiated copolymerization of fish oil ethyl esters and alkenes. J. Appl. Polym. Sci. 81, 2001–2012. https://doi.org/10.1002/app.1632

Marx, V.M., Sullivan, A.H., Melaimi, M., Virgil, S.C., Keitz, B.K., Weinberger, D.S., Bertrand, G., Grubbs, R.H., 2015. Cyclic alkyl amino carbene (caac) ruthenium complexes as remarkably active catalysts for ethenolysis. Angew. Chemie - Int. Ed. 54, 1919–1923. https://doi.org/10.1002/anie.201410797

Meiorin, C., Aranguren, M.I., Mosiewicki, M.A., 2012. Smart and Structural Thermosets from the Cationic Copolymerization of a Vegetable Oil Cintia. J. Appl. Polym. Sci. 124, 5071–5078. https://doi.org/10.1002/app.35630

Miao, S., Wang, P., Su, Z., Zhang, S., 2014. Vegetable-oil-based polymers as future polymeric biomaterials. Acta Biomater. 10, 1692–1704. https://doi.org/10.1016/j.actbio.2013.08.040

Miao, X., Blokhin, A., Pasynskii, A., Nefedov, S., Osipov, S.N., Roisnel, T., Bruneau, C., Dixneuf,

P.H., 2010. Alkylidene-ruthenium-tin catalysts for the formation of fatty nitriles and esters via cross-metathesis of plant oil derivatives. Organometallics 29, 5257–5262. https://doi.org/10.1021/om100372b

Miao, X., Dixneuf, P.H., Fischmeister, C., Bruneau, C., 2011. A green route to nitrogen-containing groups: The acrylonitrile cross-metathesis and applications to plant oil derivatives. Green Chem. 13, 2258–2271. https://doi.org/10.1039/c1gc15377c

Mol, J.C., 2004. Industrial applications of olefin metathesis. J. Mol. Catal. A Chem. 213, 39–45. https://doi.org/10.1016/j.molcata.2003.10.049

Monteavaro, L.L., Da Silva, E.O., Costa, A.P.O., Samios, D., Gerbase, A.E., Petzhold, C.L., 2005. Polyurethane networks from formiated soy polyols: Synthesis and mechanical characterization. JAOCS, J. Am. Oil Chem. Soc. 82, 365–371. https://doi.org/10.1007/s11746-005-1079-0

Morrison, R.F., Lipscomb, N., Eldridge, R.B., Ginn, P., 2014. Rhenium oxide based olefin metathesis. Ind. Eng. Chem. Res. 53, 19136–19144. https://doi.org/10.1021/ie5034232

Mosiewicki, M.A., Aranguren, M.I., 2013. A short review on novel biocomposites based on plant oil precursors. Eur. Polym. J. 49, 1243–1256. https://doi.org/http://dx.doi.org/10.1016/j.eurpolymj.2013.02.034

Motasemi, F., Afzal, M.T., 2013. A review on the microwave-assisted pyrolysis technique. Renew. Sustain. Energy Rev. 28, 317–330. https://doi.org/10.1016/j.rser.2013.08.008

Mutlu, H., Meier, M.A.R., 2010. Castor oil as a renewable resource for the chemical industry. Eur. J. Lipid Sci. Technol. 112, 10–30. https://doi.org/10.1002/ejlt.200900138

Mutyala, S., Fairbridge, C., Paré, J.R.J., Bélanger, J.M.R., Ng, S., Hawkins, R., 2010. Microwave applications to oil sands and petroleum: A review. Fuel Process. Technol. 91, 127–135.

https://doi.org/10.1016/j.fuproc.2009.09.009

Ngo, H.L., Jones, K., Foglia, T.A., 2006. Metathesis of unsaturated fatty acids: Synthesis of long-chain unsaturated-α,ω-dicarboxylic acids. JAOCS, J. Am. Oil Chem. Soc. 83, 629–634. https://doi.org/10.1007/s11746-006-1249-0

Nieres, P.D., Zelin, J., Trasarti, A.F., Apesteguía, C.R., 2016. Heterogeneous catalysis for valorisation of vegetable oils via metathesis reactions : ethenolysis of methyl oleate. Catal. Sci. Technol. 6, 6561–6568. https://doi.org/10.1039/c6cy01214k

Nuyken, O., Pask, S.D., 2013. Ring-opening polymerization-An introductory review. Polymers (Basel). 5, 361–403. https://doi.org/10.3390/polym5020361

Omonov, T.S., Kharraz, E., Curtis, J.M., 2016. The epoxidation of canola oil and its derivatives. RSC Adv. 6, 92874–92886. https://doi.org/10.1039/c6ra17732h

Omonov, T.S., Kharraz, E., Foley, P., Curtis, J.M., 2014. The production of biobased nonanal by ozonolysis of fatty acids. RSC Adv. 4, 53617–53627. https://doi.org/10.1039/c4ra07917e

Patel, J., Mujcinovic, S., Jackson, W.R., Robinson, A.J., Serelis, A.K., Such, C., 2006. High conversion and productive catalyst turnovers in cross-metathesis reactions of natural oils with 2-butene. Green Chem. 8, 450–454. https://doi.org/10.1039/b600956e

Pechar, T.W., Wilkes, G.L., Zhou, B., Luo, N., 2007. Characterization of Soy-Based Polyurethane Networks Prepared with Different Diisocyanates and Their Blends with Petroleum-Based Polyols. J. Appl. Polym. Sci. 106, 2350–2362. https://doi.org/DOI 10.1002/app.26569

Pelletier, H., Belgacem, N., Gandini, A., 2006. Acrylated vegetable oils as photocrosslinkable materials. J. Appl. Polym. Sci. 99, 3218–3221. https://doi.org/10.1002/app.22322

Pradhan, R.A., Arshad, M., Ullah, A., 2020. Solvent-free rapid ethenolysis of fatty esters from spent hen and other lipidic feedstock with high turnover numbers. J. Ind. Eng. Chem. 84, 42–

45. https://doi.org/10.1016/j.jiec.2020.01.002

Rulkens, R., Koning, C., 2012. Chemistry and Technology of Polyamides, in: Matyjaszewski, K., Möller, M. (Eds.), Polymer Science: A Comprehensive Reference. Elsevier B.V., pp. 431–467. https://doi.org/10.1016/B978-0-444-53349-4.00147-3

Rüsch, M., Warwel, S., 1999. Complete and partial epoxidation of plant oils by lipase-catalyzed perhydrolysis. Ind. Crops Prod. 9, 125–132. https://doi.org/10.1016/S0926-6690(98)00023-5

Sacristán, M., Ronda, J.C., Galià, M., Cádiz, V., 2010. Rapid soybean oil copolymers synthesis by microwave-assisted cationic polymerization. Macromol. Chem. Phys. 211, 801–808. https://doi.org/10.1002/macp.200900571

Santhoshkumar, A., Thangarasu, V., Anand, R., 2019. Performance, combustion, and emission characteristics of DI diesel engine using mahua biodiesel, in: Azad, A.K., Rasul, M. (Eds.), Advanced Biofuels: Applications, Technologies and Environmental Sustainability. Elsevier Ltd, pp. 291–327. https://doi.org/10.1016/B978-0-08-102791-2.00012-X

Schrock, R.R., 2006. Multiple metal-carbon bonds for catalytic metathesis reactions (nobel lecture). Angew. Chemie - Int. Ed. 45, 3748–3759. https://doi.org/10.1002/anie.200600085

Schuchardt, U., Sercheli, R., Matheus, R., 1998. Transesterification of Vegetable Oils : a Review. J. Braz. Chem. Soc., 9, 199–210. https://doi.org/10.1590/S0103-50531998000300002

Shahbandeh, M., 2020. Vegetable oils: production worldwide 2012/13-2019/20, by type [WWW Document]. Statistica. URL https://www.statista.com/statistics/263933/production-of-vegetable-oils-worldwide-since-2000/

Sinnwell, S., Ritter, H., 2007. Recent advances in microwave-assisted polymer synthesis. Aust. J. Chem. 60, 729–743. https://doi.org/10.1071/CH07219

Song, L., Zhu, T., Yuan, L., Zhou, J., Zhang, Y., Wang, Z., Tang, C., 2019. Ultra-strong long-

chain polyamide elastomers with programmable supramolecular interactions and oriented crystalline microstructures. Nat. Commun. 10, 1–8. https://doi.org/10.1038/s41467-019-09218-6

Trnka, T.M., Grubbs, R.H., 2001. The development of L2X2RU=CHR olefin metathesis catalysts: An organometallic success story. Acc. Chem. Res. 34, 18–29. https://doi.org/10.1021/ar000114f

Türünç, O., Firdaus, M., Klein, G., Meier, M.A.R., 2012. Fatty acid derived renewable polyamides via thiol-ene additions. Green Chem. 14, 2577–2583. https://doi.org/10.1039/c2gc35982k

Ullah, A., Arshad, M., 2018. Conversion of Lipides Olefins. US Pat., US 10,138,430 B2, 2018. US 10 , 138 , 430 B2.

Ullah, A., Arshad, M., 2017. Remarkably Efficient Microwave-Assisted Cross-Metathesis of Lipids under Solvent-Free Conditions. ChemSusChem 10, 2167–2174. https://doi.org/10.1002/cssc.201601824

Valverde, M., Andjelkovic, D., Kundu, P.P., Larock, R.C., 2008. Conjugated low-saturation soybean oil thermosets: free-radical copolymerization with dicyclopentadiene and divinylbenzene. J. Appl. Polym. Sci. 107, 423–430. https://doi.org/DOI 10.1002/app.27080

Van Dam, P.B., Mittelmeijer, M.C., Boelhouwer, C., 1972. Metathesis of unsaturated fatty acid esters by a homogeneous tungsten hexachloride-tetramethyltin catalyst. J. Chem. Soc. Chem. Commun. 1221–1222. https://doi.org/10.1039/C39720001221

Wang, C.S., Li-Ting, Y., Ni, B.-L., Shi, G., 2009. Polyurethane Networks from Different Soy-Based Polyols by the Ring Opening of Epoxidized Soybean Oil with Methanol, Glycol, and 1,2-Propanediol. J. Appl. Polym. Sci. 114, 125–131. https://doi.org/10.1002/app.30493

Wang, X.Z., He, J., Weng, Y.X., Zeng, J.B., Li, Y.D., 2019. Structure-property relationship in

fully biobased epoxidized soybean oil thermosets cured by dicarboxyl terminated polyamide 1010 oligomer with different carboxyl/epoxy ratios. Polym. Test. 79, 106057 (1–7). https://doi.org/10.1016/j.polymertesting.2019.106057

Wiesbrock, F., Hoogenboom, R., Schubert, U.S., 2004. Microwave-assisted polymer synthesis: State-of-the-art and future perspectives. Macromol. Rapid Commun. 25, 1739–1764. https://doi.org/10.1002/marc.200400313

Wool, R.P., 2005. POLYMers and composite resins from plant oils, in: Bio-based polymers and composites. Elsevier Inc., pp. 56–113. https://doi.org/10.1016/B978-0-12-763952-9.50005-8

Xia, Y., Larock, R.C., 2012. Vegetable oil-based polymeric materials : synthesis , properties , and applications. Green Chem. 1893–1909. https://doi.org/10.1039/c0gc00264j

Yu, Z., Liu, L., 2005. Microwave-assisted synthesis of poly(ε-caprolactone)-poly(ethylene glycol)-poly(ε-caprolactone) tri-block co-polymers and use as matrices for sustained delivery of ibuprofen taken as model drug. J. Biomater. Sci. Polym. Ed. 16, 957–971. https://doi.org/10.1163/1568562054414667

Zelin, J., Trasarti, A.F., Apesteguía, C.R., 2013. Self-metathesis of methyl oleate on silica-supported Hoveyda-Grubbs catalysts. Catal. Commun. 42, 84–88. https://doi.org/10.1016/j.catcom.2013.08.007

Zhang, C., Garrison, T.F., Madbouly, S.A., Kessler, M.R., 2017a. Recent advances in vegetable oil-based polymers and their composites. Prog. Polym. Sci. 71, 91–143. https://doi.org/10.1016/j.progpolymsci.2016.12.009

Zhang, C., Garrison, T.F., Madbouly, S.A., Kessler, M.R., 2017b. Recent advances in vegetable oil-based polymers and their composites. Prog. Polym. Sci. 71, 91–143. https://doi.org/10.1016/j.progpolymsci.2016.12.009

Zhang, C., Liao, L., Gong, S.S., 2007. Recent developments in microwave-assisted polymerization with a focus on ring-opening polymerization. Green Chem. 9, 303–31. https://doi.org/10.1039/b608891k

Zhang, C., Xia, Y., Chen, R., Huh, S., Johnston, P.A., Kessler, M.R., 2013. Soy-castor oil based polyols prepared using a solvent-free and catalyst-free method and polyurethanes therefrom. Green Chem. 15, 1477–1484. https://doi.org/10.1039/c3gc40531a

Zhang, K., Nelson, A.M., Talley, S.J., Chen, M., Margaretta, E., Hudson, A.G., Moore, R.B., Long, T.E., 2016. Non-isocyanate poly(amide-hydroxyurethane)s from sustainable resources. Green Chem. 18, 4667–4681. https://doi.org/10.1039/c6gc01096b

CHAPTER 3: MICROWAVE-ASSISTED RAPID SYNTHESIS OF POLYETHER FROM PLANT OIL DERIVED MONOMER AND ITS OPTIMIZATION BY BOX-BEHNKEN DESIGN[1]

3. Introduction

The finite availability of petroleum resources and the destructive effect of the fossil-based products on the environment have attracted the attention of scientists, governmental and private agencies to use sustainable and environmentally friendly materials (Warwel et al., 2001); (Zhang et al., 2016). The synthesis of biopolymers from renewable resources, therefore, has been considered as a promising strategy for releasing the polymer industry from its dependence on petroleum resources (Pardal et al., 2008). An eco-friendly and sustainable alternative for the plastic materials production is the utilization of monomers from plant-derived resources (proteins, carbohydrates, lipids) as promising starting materials to replace some or all of the synthetic chemicals and polymers in many applications (Meier et al., 2007). However, biopolymers from proteins and carbohydrates are not a good choice to replace petroleum-based plastics because these are moisture sensitive, difficult to process and brittle when used without the addition of a plasticizer. In this context vegetable oils, being hydrophobic, have attracted more attention compared to other bio-based compounds (i.e., polysaccharides, or proteins) to produce biopolymers. Economic advantages and worldwide availability make vegetable oils interesting options for the industry. While diverse

---

chemistry can be applied to vegetable oils for the production of several types of monomers and polymers, only minor modification reactions are necessary in order to obtain suitable monomers for many different applications (De Espinosa and Meier, 2011).

Canola oil (Omonov and Curtis, 2014), soybean oil (Karmakar and Ghosh, 2016), castor oil (Kunduru et al., 2015), and high oleic sunflower oil (De Espinosa and Meier, 2011) are the common vegetable oils used directly for making biopolymers. Another approach, however, is to design biodegradable polymers through synthesis of monomers from plant oils and further polymerization into desired biopolymers (Roumanet et al., 2013); (Türünç et al., 2012); (Warwel et al., 2000); (Arshad et al., 2014). Among several other methods, olefin metathesis has recently emerged for the synthesis of monomers from plant oils (Chikkali and Mecking, 2012). The olefin metathesis is a potentially useful synthetic transformation tool for the chemical conversion and formation of new carbon-carbon double bonds (Takahira and Morizawa, 2015). It is generally categorized into ring-opening, ring closing, and cross-metathesis groups. Olefin cross-metathesis is a catalytic reaction between two alkene molecules that results in redistribution of alkylidene groups. The cross-metathesis of an olefinic compound could be done with ethylene or other olefins called ethenolysis and alkenolysis, respectively (Hoveyda and Zhugralin, 2007). Recently, our group has successfully reported remarkably efficient microwave-assisted ethenolysis and alkenolysis (using 1,5-hexadiene) of lipids into various monomers using 2nd generation Grubbs and Hoveyda-Grubbs catalysts (Ullah and Arshad, 2017) (Scheme 2- 16). Interestingly, the solvent free rapid conversion of the substrates resulted in high value linear α-olefin monomers like methyl 9-decenoate, and 1-decene within few minutes. The resulting monomers can be manipulated to produce different kinds of polymers like polyethers which find applications in different industries such as pharmaceutical, cosmetic, adhesive, paint, textile fiber, and ceramic (Fink, 2011); (Kline,

1962). Conventional methods have been used as the main applicable process for the synthesis of the polyethers. However, the production of polyether from vegetable oils and the manipulated monomers through conventional methods have some limitations including long reaction time, low yield, the occurrence of side reactions, and the use of a high amount of solvent. In addition, slow catalyst-monomer interaction and heating flow through conduction leading to heterogeneous reaction environment and limitations to control activation parameters in the conventional heating methods are some of the shortcomings of the conventional methods (Warwel et al., 2000); (Lidstrom et al., 2001); (Hoogenboom and Schubert, 2007); (Sinnwell and Ritter, 2007); (Zhang et al., 2004).

The use of microwave (MW) irradiation is emerging as an alternative heating technique for product development and has provided new application opportunities to overcome above-mentioned limitations of conventional heating methods (Pardal et al., 2008); (Kempe et al., 2011); (Sinnwell and Ritter, 2007), (Gawande et al., 2014). Ring-opening polymerization (ROP) of cyclic monomers such as 2-ethyl-2-oxazolines (Wiesbrock et al., 2004), ε-caprolactone (Sinnwell and Ritter, 2007), D,L-lactide (Zhang et al., 2004), and *p*-dioxanone (Li et al., 2006) in the presence of different metal catalysts and macro-initiators have also been studied under MW conditions.

The present study describes the production of a high molecular weight polyether from 1,2-epoxydecane synthesized from 1-decene using both the conventional and the MW methods. To the best of our knowledge, this is the first study reporting optimized epoxidation of 1-decane using an oxygen donor, without using catalyst, at a relatively short time with a high yield using conventional method. The epoxidation of 1-decene was also studied using the MW. The synthesized epoxy was polymerized using microwave-assisted catalytic ROP to polyether with high molecular weight in the present and absence (bulk polymerization) of solvent in just a few minutes.

3.1. **Materials and methods**

3.1.1. **Materials**

1-decene (94%), *3*-chloroperoxybenzoic acid (*m*-CPBA≤77%), modified methylaluminoxane (MMAO-12, 7 wt% Aluminum in toluene), anhydrous sodium sulfate (≥99%), dichloromethane (DCM, ≥99.5%), ethyl acetate (anhydrous, 99.8%), hexane, silica gel for chromatography (Whatman, 60 °A, 70-230 mesh), Methanol (anhydrous, 99.8%), and tetrahydrofuran (THF, ≥99%) were purchased from Sigma-Aldrich. 2,4-Pentanedione (ReagentPlus®, ≥99%) and toluene (anhydrous, 99.8%) were dried over anhydrous sodium sulfate overnight before use.

3.1.2. **Instrumentation**

A Bruker Alpha FTIR spectrophotometer (Bruker Optics, Esslingen, Germany) equipped with a single bounce diamond ATR crystal was employed to collect spectrum at a resolution of 4 cm^{-1} over the range of 410-4000 cm^{-1}. All sample spectra were recorded at 16 scans and averaged using OPUS software (Bruker version 6.5). A background spectrum of the clean ATR crystal was also collected before applying and collecting the sample spectrum. Finally, the analysis of the spectrum was done using Nicolet Omnic software (version 8).

Proton nucleic magnetic resonance (^{1}H NMR) spectra were collected in deuterated chloroform (CDCl$_3$) using a Varian Inova spectrometer (Varian, CA) at 400 MHz and 26.9 °C. The analysis of the spectrum was done using the MestReNova software (version 11.0).

X-ray Photoelectron Spectroscopy (XPS) was used to study the chemical composition of the polyether. The XPS measurements were conducted on ULTRA spectrometer (Kratos Analytical). The base pressure in the analytical chamber was lower than 3×10^{-8} Pa. The spectrometer was equipped with a monochromatic Al Kα source (hv = 1486.6 eV) operated at a power of 140 W. The spot size used was 400 × 700 μm. The resolution of the instrument is 0.55 eV for Ag 3d and

0.70 eV for Au 4f peaks. The survey scans were taken in the range of 0-1100 eV with analyzer pass energy of 160 eV and a step of 0.4 eV. For the high-resolution spectra, the pass-energy was 20 eV with a step of 0.1 eV. The sample charging if any was compensated by an electron flood gun. The data were processed using the vision-2 instrument software. The binding energy of each photopeak was referenced to the C 1s level at 284.8 eV. Compositions were calculated from the high-resolution spectra using linear background and sensitivity factors provided by the instrument database.

The molecular weight and polydispersity of the polyethers were determined using gel permeation chromatography (GPC). The GPC system was equipped with Styragel HR5E GPC column (300 × 7.8 mm^2 i.d., particle size= 5 µm, Waters Corporation). An isocratic Agilent 1100 pump (Agilent Technologies; CA) equipped with an evaporative light scattering detector (Alltech ELSD 2000, Mandel Scientific Company, Canada) was used. The THF was used as the eluent at a flow rate of 1 mL/min, sample concentrations 0.5 mg/mL, and injection volumes were 10 µL. The Agilent Polystyrene EasiVial PS-H standard kit with known molecular weight in the range of 162-7×10^6g/mol and the polydispersity ≤1 was used to generate the calibration curve by the Agilent GPC-Addon Rev. B. 01.01 Software.

The differential scanning calorimetric (DSC) analysis of all samples was carried out by a Perkin-Elmer (Pyris 1, Norwalk, CT, USA) calorimetric apparatus equipped with a cooling system in a range of -60 °C- 120 °C at a rate of 5 °C/min under a dry nitrogen gas atmosphere. The heat flow and temperature calibration of the instrument were established by a sample of pure indium. All the DSC measurements were performed following the ASTM E1356-08 (Reapproved 2014) standard procedure (ASTM 08(E1356), 2008). Thermogravimetric analysis (TGA) was performed on a Perkin-Elmer (Pyris 1, Waltham, MA, USA). Approximately 13 mg of the specimen was loaded

in the open platinum pan and scanned from 10 to 550 °C, at a heating rate of 10 °C/min under a nitrogen atmosphere with 100 mL/min purging flow following the ASTM D3850-12 (2012) standard (ASTM D 3850, 2000).

3.1.3. **Synthesis of 1,2-epoxydecane from 1-decene (Scheme 3. 1.a)**

The synthesis of 1,2-epoxydecane from 1-decene using conventional heating was carried out using reported method with some modifications (Zhang et al., 2016). Briefly, dichloromethane (10 mL) and 1-decene (7 mmol) were added into a round-bottom flask equipped with a magnetic stir bar and placed into an ice bath. The initial exothermic epoxidation reaction of 1-decene was then controlled by gradual addition and dissolution of *m*-CPBA (8.9 mmol) into the reaction mixture at 0 °C. After that, the mixture was stirred at 900 rpm for different time points (15, 30, 60, and 180 min) at room temperature to determine the best yield of 1,2-epoxydecane. The epoxy monomer was separated by silica gel column chromatography (5% of the ethyl acetate in hexane). The solvents were evaporated by rotary evaporator and resulting 1,2-epoxydecane was dried over sodium sulfate. Finally, dried 1,2-epoxydecane was purged with a nitrogen line in a glass vial equipped with a septum cap. The vial was sealed with parafilm and stored at 4 °C for further polymerization. The yield of the epoxidation reaction was calculated by the following equation:

Percent yield of product= (Actual yield/ Theoretical yield) ×100 (3. 1)

Where the actual yield is equal to the weight of the product after the reaction and theoretical yield is equal to 1.11g of 1,2-epoxdecane per 1g of 1-decene. The structure and purity of obtained 1,2-epoxydecane were confirmed using ^{1}H NMR (Figure 3. 4) and ATR-FTIR spectroscopy (Figure 3. 5).

3.1.4. **Synthesis of 1,2-epoxydecane from 1-decene using MW (Scheme 3. 1.b)**

A MW system CEM-Discover (120 V, Matthews, USA) was used as a source of microwave irradiation for performing the epoxidation reaction of 1-decene. Dichloromethane (6.5 mL) was mixed with 1-decene (3.5 mmol) in a MW reaction vessel containing a magnetic stir bar and placed into an ice bath. The *m*-CPBA (4.5 mmol) was gradually added to the mixture at 0 °C. The vessel was then placed in the MW reactor with the adjusted pressure and power (250 psi, 250 w) and reaction conducted for 5 and 6 min at 25 °C. Column chromatography, rotary evaporator and drying on the sodium sulfate steps were done same as in the conventional method to purify the resulted 1,2-epoxydecane.

3.1.5. **Ring opening polymerization of 1,2-epoxydecane (conventional method)**

The conventional ring opening polymerization of 1,2-epoxydecene was carried out using reported method with some modifications (Warwel et al., 2000). Briefly, the polymerization reaction was planned in three different steps: "in situ" catalyst preparation, polymerization, and polyether precipitation. For "in situ" catalyst preparation a 50 mL dried round bottom flask containing a magnetic stir bar was charged with dried toluene (17mL) and sealed with a rubber cap and parafilm. The oxygen in toluene and the flask was eliminated using a nitrogen line (purging toluene for 15 min and the headspace for 15 min) and then the flask was quickly sealed with parafilm again. MMAO-12 solution (215 µl) and 2,4-Pentanedione (50µl) were added stepwise into the purged flask with a purged microliter glass syringe (Hamilton Co., USA). Because of the extreme sensitivity of the catalyst to moisture and oxygen, using dried reaction flask and sealing it properly after adding each chemical is critical in these steps. The mixture was stirred for 5 min at room temperature to prepare the catalyst. For the polymerization step, the dried and purged 1,2-epoxydecane (10 mmol) was added to the catalyst mixture with a purged microliter glass syringe

and the flask was quickly sealed with parafilm again. The mixture was heated in the silicon oil bath at 100 °C for 24 hours. The catalyst was quenched with 0.5 mL methanol to stop the reaction. Polyether precipitation was performed at the last step. The quenched highly viscous mixture from the previous step was diluted with 35 mL of toluene, poured into 300 mL methanol/concentrated aqueous HCl (90/10) and stirred rapidly for 15 min. Afterward, the supernatant was decanted and the produced white to pale yellow polyether was washed twice with methanol. Finally, the resulted polyether was dried in an oven at 40 °C overnight.

3.1.6. **Ring opening polymerization of 1,2-epoxydecane (MW method)**

The same three steps used in the conventional method were applied in the MW reaction to synthesize the polyether. The yield of the reaction was optimized using three temperatures (50, 75, 100 °C), microwave irradiation time (4, 7, 10 min) and the solvent-monomer ratio or toluene-1,2-epoxydecane ratio (0:5, 3:5, 6:5 mL/mmol). For the reactions containing the solvent, the following procedure was carried out. Two dried MW tubes equipped with magnetic bars were charged with 3 and 6 mL of dried toluene and sealed with a septum cap and parafilm. The oxygen in toluene and the tube was eliminated. MMAO-12 solution (107 µl) and 2,4-Pentanedione (25µl) were added stepwise into the tube as mentioned in the conventional method. The mixture was stirred for 5 min to prepare the catalyst. 1,2-epoxydecane (5 mmol) was then added to the catalyst mixture with the purged microliter glass syringe. The sealed tube was put in the MW and run with the adjusted pressure and power (250 psi, 250 w), different temperatures (50, 75, 100 °C) and different time intervals (4, 7, 10 min). Finally, the reaction was quenched with 0.25 mL methanol and diluted with 18 mL of toluene. The polyether was precipitated with 150 mL methanol/concentrated aqueous HCl (90/10) after 15 min stirring, washed and dried as mentioned in the conventional method.

3.1.7. **Bulk ring opening polymerization of 1,2-epoxydecene (MW method)**

For bulk ROP, the catalyst was prepared without solvent in the first step. A dried MW tube equipped with a magnetic stir bar was charged with 2,4-Pentanedione (200µl), capped and sealed with parafilm tightly. The oxygen in 2,4-Pentanedione and the tube was eliminated using a nitrogen line (purging 2,4-Pentanedione for 5 min and the headspace for 15 min) and then the tube was quickly sealed with parafilm again. The purged tube was charged with the MMAO-12 solution (430 µl) and sealed as mentioned before. The mixture was stirred for 5 min to prepare the catalyst. After that, 1,2-epoxydecane (20 mmol) was added to the catalyst mixture with the purged microliter glass syringe. The rest of the process including the reaction in the MW, precipitation, washing and drying of the resulting polyether was followed as mentioned in the previous section.

3.1.8. **Experimental design for optimization of the polymerization using MW**

The response surface methodology (RSM) was employed to determine the optimum conditions for ring opening polymerization of 1,2-epoxydecane using the MW heating. RSM as an efficient multivariate technique provides a faster and more economical method allowing more than one variable to be optimized simultaneously. The experimental design and statistical analysis were performed using the Design Expert software (6.0.2, Stat-Ease Inc., USA). The experiments were performed based on the Box-Behnken Design (BBD). BBD has been frequently used as a suited design for fitting a quadratic surface and suitable chemometric tools for the process optimization. BBD reduce the number of experiments resulting in low solvent consumption and considerably less laboratory work. Moreover, BBD has a uniform precision by adequate selection of the number of center points (Kousha et al., 2012); (Iqbal et al., 2016). In the present study, the effects of the three independent variables at three levels (reaction times of 4, 7, 10 min (X_1), temperatures of 50,

75, 100 °C (X_2) and solvent-monomer ratio of 0:5, 3:5, 6:5 mL/mmol (X_3)) on the response or polymerization yield percent of the reaction (PY) were investigated.

The low, center and high factor levels were coded as −1, 0 and +1. The code with positive sign represents a synergistic effect of the variables while the negative one indicates an antagonistic effect of the variables. The variables coding was performed by the following equation (Kousha et al., 2012):

$$x_i = \frac{X_i - X_z}{\Delta X_i} \qquad 1, 2, 3, k \tag{3.2}$$

Where x_i = the dimensionless value of a process variable; X_i = the real value of an independent variable; X_z = the real value of an independent variable at the center point; and ΔX_i = the step change of the real value of the variable i corresponding to a variation of a unit for the dimensionless value of the variable i.

17 experiments were designed with five center points to allow calculations of the response function at intermediate levels and estimation of the system performance at any experimental point within the studied range. The calculation of the total number of experiments (N) was done by the following equation (Kousha et al., 2012):

$$N = K + K^2 + Cp \tag{3.3}$$

Where Cp is the replicate number of the center point and k is the factor number.

The actual design of experiments is shown in Table 3. 1.

The mathematical relationship of the response to the three significant independent variables (X_1, X_2, and X_3) can be approximated by the quadratic polynomial equation, shown as follow:

70

$$PY = \beta_0 + \beta_1 X_1 + \beta_2 X_2 + \beta_3 X_3 + \beta_{12} X_1 X_2 + \beta_{13} X_1 X_3 + \beta_{23} X_2 X_3 + \beta_{11} X_1{}^2 + \beta_{22} X_2{}^2 + \beta_{33} X_3{}^2 \qquad (3.4)$$

Where PY = predicted yield percent, β_0= the constant, β_1, β_2, and β_3= linear coefficients, β_{12}, β_{13}, and β_{23}= cross product coefficients, and β_{11}, β_{22}, and β_{33} = quadratic coefficients.

For reaching to the optimum values of the factors, the regression equation was solved; the surface of the counter response surface plot was analyzed, and the constraints for the levels of the variables were set up.

Table 3. 1) Box-Behnken design matrix of real and coded values along with experimental and predicted values of the polymerization yield (%).

	Real (coded) values			Polymerization yield (%)	
	X_1	X_2	X_3	Experimental*	Predicted
1	10 (+1)	50 (-1)	3:5 (0)	2.50	1.18
2	7 (0)	75 (0)	3:5 (0)	12.30	13.43
3	7 (0)	75 (0)	3:5 (0)	10.69	13.43
4	4 (-1)	50 (-1)	3:5 (0)	0.30	-0.08
5	7 (0)	100 (+1)	6:5 (+1)	72.56	66.62
6	7 (0)	75 (0)	3:5 (0)	14.05	13.43
7	4 (-1)	100 (+1)	3:5 (0)	21.67	25.74
8	10 (+1)	75 (0)	0:5 (-1)	3.50	3.75
9	7 (0)	100 (+1)	0:5 (-1)	40.86	37.66
10	7 (0)	50 (-1)	0:5 (-1)	0.00	0.75
11	7 (0)	75 (0)	3:5 (0)	15.35	13.43
12	4 (-1)	75 (0)	0 (-1)	0.00	-0.25
13	10 (+1)	75 (0)	6 (+1)	13.64	14.82
14	7 (0)	50 (-1)	6 (+1)	1.11	1.84
15	10 (+1)	100 (+1)	3 (0)	70.40	73.69
16	7 (0)	75 (0)	3 (0)	14.98	13.43
17	4 (-1)	75 (0)	6 (+1)	1.10	0.49

X_1: Time (min); X_2: Temperature (°C); X_3: Solvent-monomer ratio. * Average of three experiments.

3.2. **Results and discussion**

3.2.1. **Synthesis of 1,2-epoxydecane from 1-decene**

This study initially investigated the conventional and the MW methods for epoxidation of 1-decene. The epoxidation reaction was performed in the presence of *m*-CPBA as the oxidant in both methods. The percent yield of the 1,2-epoxydecane at four different time intervals using conventional heating is presented in Figure 3. 1. Higher reaction time favored the epoxidation reaction. When the reaction time increased from 15 to 60 min, the percent yield increased significantly ($p < 0.05$) from 77.56% to more than 93%. However, increasing the reaction time to more than 60 min did not further increase the product yield. Therefore, 60 min was chosen as the optimum time for the epoxidation of 1-decene using the conventional method. Epoxidation of 1-decane has been reported in the literature using different catalyst systems. Warwel *et al.* used hydrogen peroxide in ethyl acetate with Novozym 435® as a chemo-enzymatic catalyst to oxidize 1-decene (Warwel et al., 2000); (Rüsch Gen. Klaas and Warwel, 1997). The reported yield of 1,2-epoxydecane after 16 hours at 40 °C was only 85% which is lower than what was obtained in our study. Ho *et al*. reported another catalytic system for the epoxidation of 1-decene (Ho et al., 2008). They used Mn $(ClO_4)_2$ as the catalyst in acetonitrile/water with different commercial oxidants. Interestingly, when *m*-CPBA was used as the oxidant the reaction yield was only ~ 47% which is significantly lower than the yield obtained in our study. Epoxidation of 1-decene using a complex catalytic system of Na_2WO_4 dihydrate, (aminomethyl) phosphonic acid, and methyltrin-octyl ammonium hydrogen sulfate with hydrogen peroxide for 4 hours at 90 °C yielded 99% 1,2-epoxydecane which is comparable to our results (Sato et al., 1996).

An MW system (250psi pressure, 250w power) was employed to study the effect of MW irradiation on the epoxidation of 1-decene in the next step (Scheme 3. 1.b). In the course of the

study, the best result was achieved when the microwave irradiation was applied just for 5 min in the presence of *m*-CPBA with a yield of 67.13%. Although the epoxidation reaction was successful, the yield of the reaction was significantly lower than the 15 min heating in the conventional method (Figure 3. 1). When the reaction time exceeded 5 min, extra peaks were appeared in the ^{1}H NMR spectrum of the resulted product. The presence of hydroxyl peak at 3.65 ppm can be an indication of the cleavage of oxirane ring. The interference of water in the reaction mixture is potentially the reason for the observed oxirane ring break down. *m*-CPBA is the source of water in the reaction because it is not stable without water. Therefore, microwave irradiation does not appear to be a suitable method for the epoxidation of 1-decene when *m*-CPBA is used as the oxidant.
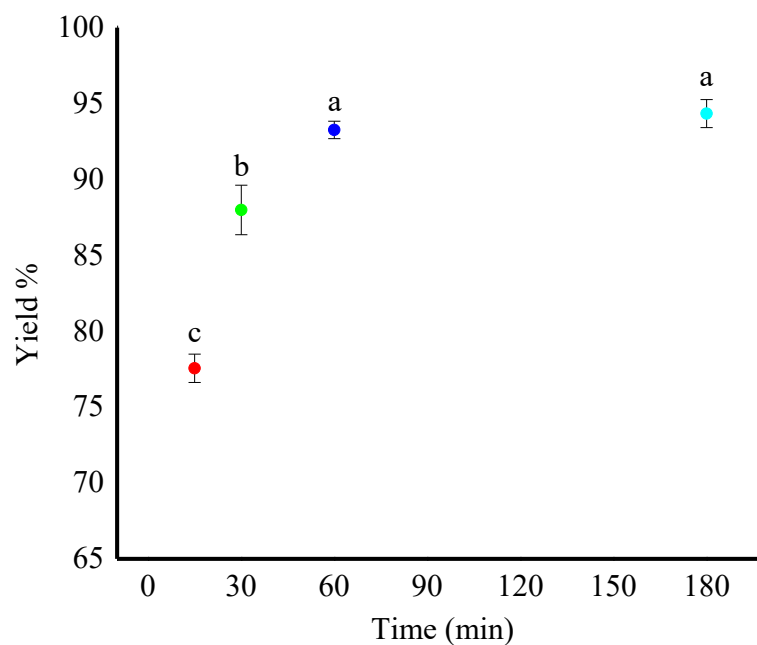
Figure 3. 1) The yield% of the produced 1,2-epoxdecae in the conventional method. Note: a, b and c are different letters representing significant differences ($p < 0.05$) between the means obtained by Duncan's test.

a)

1-decene CH_2Cl_2, t= 60 min   1,2-epoxydecane

b)

1-decene

T= 25°C
Pressure= 250 psi
Power= 250 w
t= 5 min
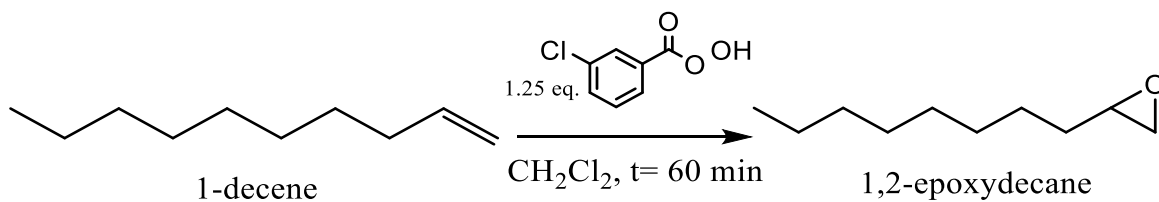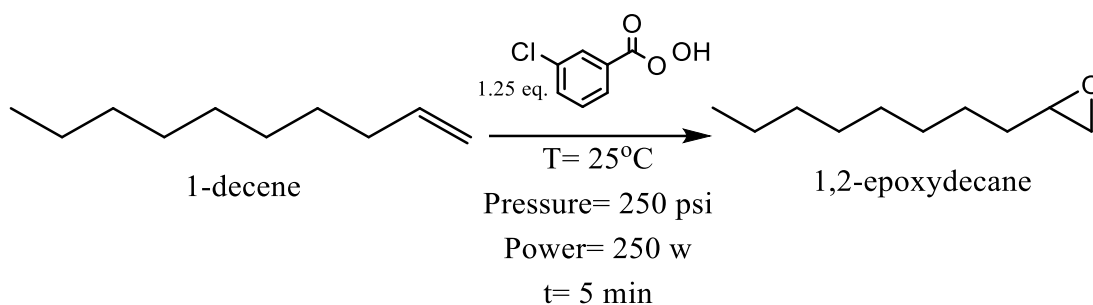
1,2-epoxydecane

Scheme 3. 1) Synthesis of 1,2-epoxydecane from 1-decene a) conventional method b) microwave irradiation method.

MMAO-12/ 2,4-pentanedione
in Toluene

Conventional method:
(T=100°C, t= 24 hr)
Microwave method:
$\begin{pmatrix} \text{T=100°C, t= 10 min} \\ \text{Pressure= 250 psi} \\ \text{Power= 250 w} \end{pmatrix}$

1,2-epoxydecane   Polyether
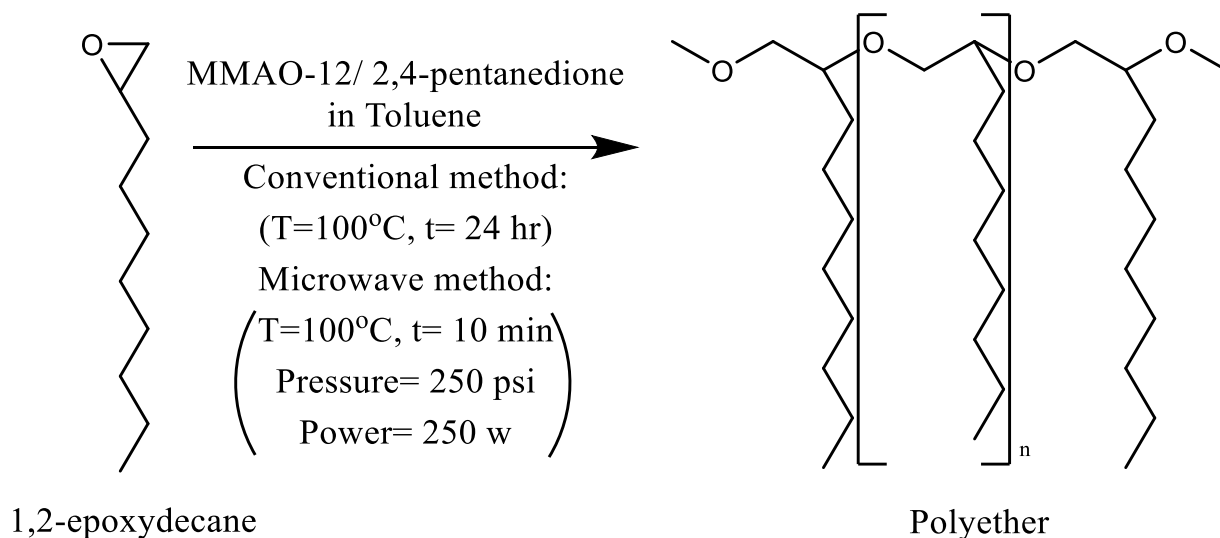
Scheme 3. 2) Synthesis of polyether from 1,2-epoxydecane.

3.2.2. **Ring opening polymerization of 1,2-epoxydecane (conventional method)**

The ring opening polymerization of 1,2-epoxydecane was carried out using previously reported procedure with some modifications (Warwel et al., 2000). Briefly, the polymerization of 1,2-

epoxydecane was performed to a quantitative conversion at 100 °C for 24 hours using the MMAO-12/ 2,4-Pentanedione as the catalyst (Scheme 3. 2). A white to pale yellow polyether was produced by its precipitation in methanol/concentrated HCL (90/10) with 74.38% yield. The obtained polyether was soluble in 1,4-dioxane at room temperature but at 50 °C in THF. The molecular weight of the polyether was determined by GPC. The molecular weight of the polyether was more than 2.4×10^6 g/mol and polydispersity 1.2.

3.2.3. Ring Opening polymerization of 1,2-epoxydecane (MW method)

BBD analysis

In accordance with our trial experiments, three independent variables that could potentially affect the yield percent of polymerization were chosen to be time, temperature and solvent-monomer ratio. In order to study the combined effects of the variables on the PY, experiments were conducted based on the different combinations of the variables using statistically designed experiments.

The observed and predicted PY results are shown in Table 3. 1. The adequacy of the model was checked based on the experimental data to ascertain whether the approximating model would provide poor or misleading results. As shown in Table 3. 2, all the linear, interactive (two factor interactions=2FI), quadratic and cubic models were fitted to the experimental data. The adequacy of these models was investigated through three different tests namely the sequential model sum of squares, lack of fit tests and model summary statistics. The results of these evaluations have been exhibited in Table 3. 2. The quadratic model was found to be the most suitable model for the optimization of polymerization reaction among four studied types of BBD because of maximum R^2, adjusted R^2, predicted R^2 and the low standard deviation. Thereafter, the analysis of variance (ANOVA) further justified the adequacy of the model (Table 3. 2).

Table 3. 2) Sequential model fitting for yield % of ring-opening polymerization of 1,2-epoxydecane through microwave method. (Underline values show the higher significance.)

Source	Sum of squares	DF	Mean square	F-value	Prob > F	Remarks
Sequential model sum of squares						
Mean	213.72	1	213.72			
Linear	77.63	3	25.88	19.81	< 0.0001	
2FI	3.18	3	1.06	0.77	0.5371	
Quadratic	<u>12.67</u>	<u>3</u>	<u>4.22</u>	<u>4.22</u>	<u>0.0004</u>	Suggested
Cubic	0.85	3	4.09	4.09	0.1035	Aliased
Residual	0.28	4	0.069	-	-	
Total	308.34	17	18.14	-	-	
Lack of fit tests						
Linear	16.70	9	1.86	26.76	0.0032	
2FI	13.52	6	2.25	32.49	0.0024	
Quadratic	0.85	<u>3</u>	<u>0.28</u>	<u>4.09</u>	<u>0.1035</u>	Suggested
Cubic	0.000	0	-	-	-	Aliased
Model summary statistics						
Source	Std. Dev.	R^2	Adjusted R^2	Predicted R^2	Press	Remarks
Linear	1.14	0.8205	0.7791	0.6297	35.04	
2FI	1.17	0.8542	0.7667	0.2730	68.78	
Quadratic	<u>0.40</u>	<u>0.9881</u>	<u>0.9727</u>	<u>0.8515</u>	<u>14.05</u>	Suggested
Cubic	0.26	0.9971	0.9883	-		Aliased

Fitting of second order polynomial equation

Based on the BBD model and the input variables, a transformed model (PY') was recommended by the Box-Cox transformation technique after performing the initial ANOVA and investigating the adequacy of the original PY data. Since the original PY data was not normally distributed and the initial approximation of the mathematical relationship of the original PY data on the independent variables had a significant lack of fit, the Box-Cox power transformation was applied on the data (Osborne, 2010). The Box-Cox power transformation was performed by adding a

constant value (k) equal to 0.784 to the original PY followed by calculating the square root of the data as shown in Eq. 3. 5. This second-order polynomial equation explained the relationship of the three variables in terms of coded factors with all terms regardless of their significance. Quadratic relationships and interaction terms are illustrated by the coefficients with higher order terms and more than one factor term, respectively. The positive sign indicates a synergistic effect whereas a negative sign indicates an antagonistic effect (Karnachi and Khan, 1996).

$$PY' = \sqrt{PY + 0.78} = 3.77 + 1.02X_1 + 2.90X_2 + 0.60X_3 - 1.04\ x_1^2 + 1.25x_2^2 - 0.70x_3^2 + 0.71X_1X_2 +$$

$$0.31X_1X_3 + 0.41X_2X_3 \tag{3. 5}$$

Statistical analysis

The ANOVA was employed to analyze the experimental data and evaluate the significance of the regression coefficients by their corresponding *p*-values presented in Table 3. 3.

p-values less than 0.0500 indicate model terms are significant or not (Azizi and Asemi, 2012). So, it could be inferred that the linear coefficients (X_1, X_2, and X_3), quadratic coefficients (x_1^2, x_2^2 and x_3^2) and interactive coefficients (X_1X_2, X_1X_3, and X_2X_3) were significant or insignificant and prove the pattern of the interactions between the variables (Azizi and Asemi, 2012). The *p*-values of model terms indicate that the linear and quadratic as well as one of the interactive coefficients (X_1X_2), were significant.

As shown in Table 3. 3, the Model *F*-value of 64.42 suggested the model is significant at $p <$ 0.0001. The lack of fit *F*-value of 4.09 and the associated *p*-value of 0.1035 was insignificant. The determination coefficient (R^2), adjusted determination coefficient (R_α^2), and predicted determination coefficient (R_p^2) were also evaluated to confirm that the model fits properly as listed in Table 3. 4. The R^2 equal to 0.9881 of the quadratic regression models indicated that the model

has a good fit and only 0.0119% of the total variations could not be explained by the model. Joglekar and May (1987) suggested R^2 should be more than 0.80 for a good fit of a model (Tian et al., 2014). The adjusted determination coefficient (R^2_α) equal to 0.9727 further confirmed the significance of the model. Moreover, the R^2 and R^2_α values are close enough to indicate a high correlation between the experimental and the predicted values (Kousha et al., 2012). In addition, the predicted determination coefficient (R^2_p) equal to 0.8515 was in a reasonable agreement with the adjusted determination coefficient (R^2_α) (Table 3. 4).

Table 3. 3) ANOVA of the regression model for the prediction of yield % of ring-opening polymerization of 1,2-epoxydecane through microwave method.

Source	Coefficient estimate	Sum of squares	Degree of freedom	Standard error	Mean square	F value	p-Value	
Model	3.77	93.49	9	0.18	10.39	64.42	< 0.0001	significant
X_1	1.01	8.16	1	0.14	8.16	50.60	0.0002	
X_2	2.88	66.57	1	0.14	66.57	412.88	< 0.0001	
X_3	0.60	2.90	1	0.14	2.90	17.99	0.0038	
X_1^2	-1.02	4.42	1	0.20	4.42	27.43	0.0012	
X_2^2	1.26	6.72	1	0.20	6.72	41.69	0.0003	
X_3^2	-0.71	2.14	1	0.20	2.14	13.25	0.0083	
X_1X_2	0.73	2.14	1	0.20	2.14	13.29	0.0082	
X_1X_3	0.31	0.38	1	0.20	0.38	2.39	0.1662	
X_2X_3	0.41	0.66	1	0.20	0.66	4.07	0.0835	
Residual		1.13	7		0.16			
Lack of fit		0.85	3		0.28	4.09	0.1035	Not Significant.
Pure error		0.28	4		0.069			
Cor Total		94.62	16					

Finally, the signal to noise ratio greater than 4 provides the adequate precision measure (Prakash Maran et al., 2013). As this ratio was 25.665, the model indicated an adequate signal, too.

Therefore, the model was authenticated based on the aforementioned result that can be used to navigate the designed space.

Table 3. 4) Summary of the regression analysis response of area ratio for fitting to the quadratic model.

R^2	Adjusted R^2	Predicted R^2	Mean ±SD	CV, %	Adequate precision
0.9881	0.9727	0.8515	3.55± 0.40	11.33	25.665

Diagnostics of model adequacy

Model adequacy was checked to diagnose if the approximating model would provide poor or misleading results. The normal probability% plot of the studentized residuals, studentized residuals versus predicted values, the influence plots outlier t versus run order and Box-Cox plot were the diagnostic plots to be checked for the model adequacy (Figure 3. 2). Figure 3. 2.a plotted the normal% probability versus the studentized residuals for the response. The resulting plot is linear indicating the normality of residuals. Figure 3. 2.b shows a reasonable random scattering of the predicted values versus studentized residuals which are necessary for an adequate model. The influence plots outlier t versus experimental run orders was also checked for influential values (Figure 3. 2.c). There were no data out of the limit lines to force a lack of fit on the model with a heavy influence on the data. Finally, Box-Cox plot was used to determine whether the power law transformation would be appropriate for the model or not. Figure 3. 2.d shows that the best results for normality were reached with Lambda values between -0.03 and 0.58 after power transformation. Although the best value is 0.31, the chosen Lambda is 0.5 (the closest whole number to 0.31) which indicates a 95% confidence interval associated with this lambda value. Therefore, the transformation was employed correctly, and the diagnostic plots illustrated the accuracy of the developed model.
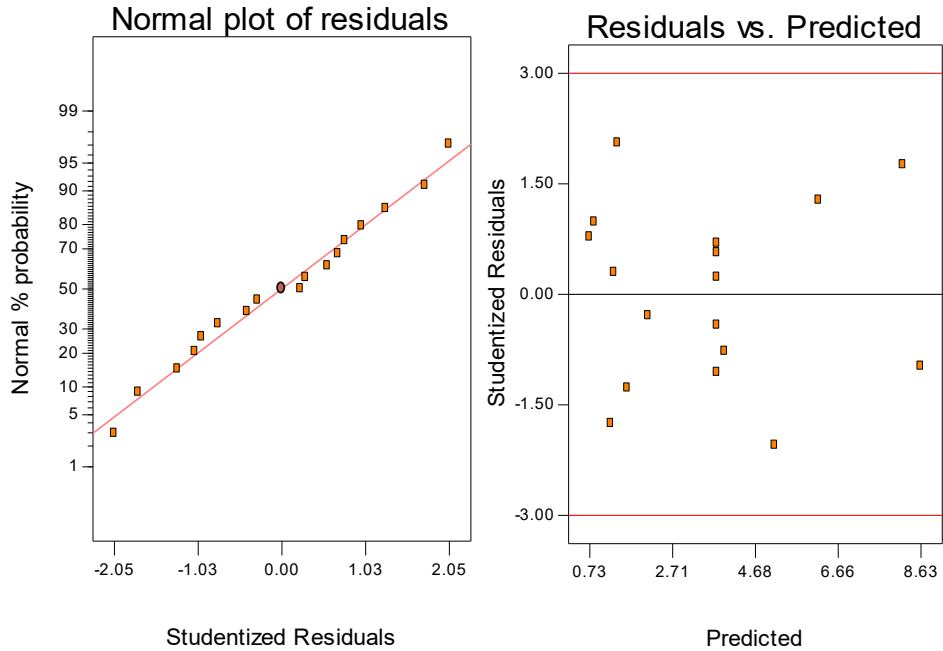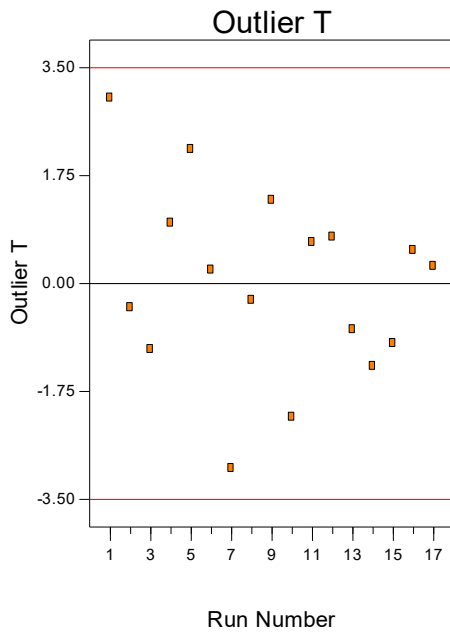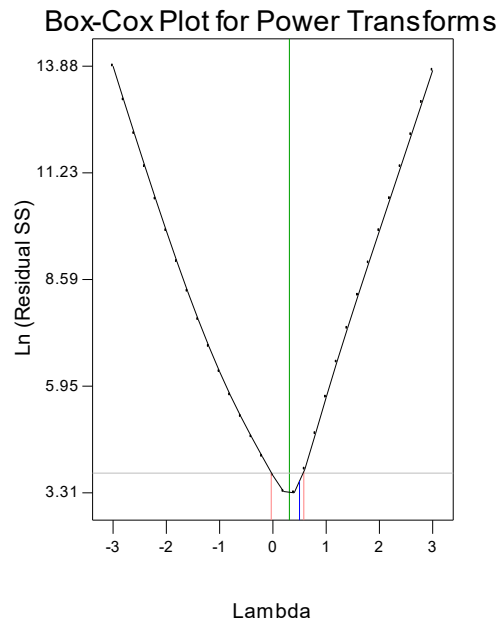
Figure 3. 2) Diagnostic plots for the model adequacy. a) Normal plot of residues, b) Predicted values versus studentized residuals, c) Influence plots outlier t versus experimental run orders, d) Box-Cox plot.
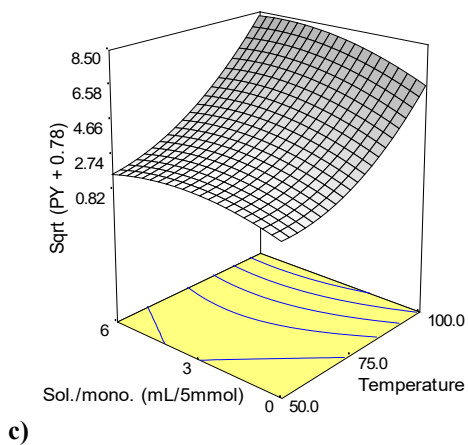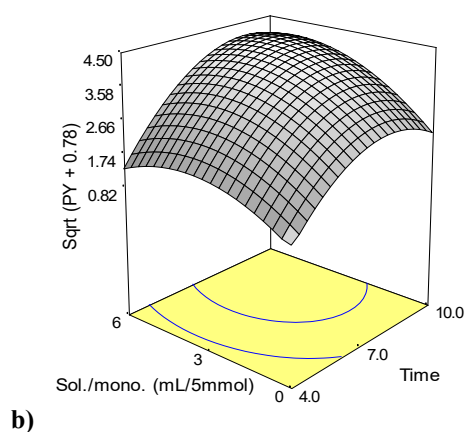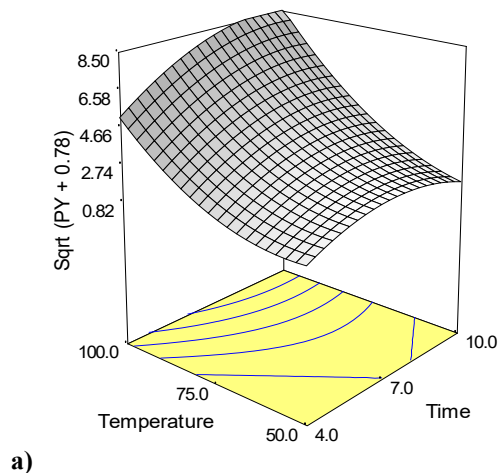
Figure 3. 3) Response surface plots showing the effect of independent variables for yield % of ring-opening polymerization of 1,2-epoxydecane through microwave method. The relationship between, a) time and temperature, b) time and solvent monomer ratio, c) temperature and solvent monomer ratio on the yield % of microwave ring-opening polymerization of 1,2-epoxydecane.

Effect of process variables on the PY

The three-dimensional (3D) response surface graphs, obtained from the developed model, were used to clarify the main and interactive effects of independent variables on the PY. These 3D graphs were drawn by keeping one factor constant (in turn at its coded zero value) and investigating the other two factors in their range. Figure 3. 3 shows that all relationship between independent variables was non-linear in accordance with the Eq. 3. 5. Figure 3. 3.a shows that although the interactive effect of the temperature and irradiation time increased the PY, the temperature has a greater effect on PY. The interactive effect of the irradiation time and the solvent-monomer ratio has been illustrated in Figure 3. 3.b. They both have a positive effect on the PY. However, the irradiation time is more effective than the solvent-monomer ratio on PY. Figure 3. 3.c which demonstrates the interactive effect of solvent-monomer ratio and the temperature on the PY indicates a more pronounced effect of temperature on the PY compared to the solvent-monomer ratio. Since toluene (dielectric constant= 2.38 and boiling point=110 °C) is a non-polar solvent and almost transparent to the MW irradiation (Lidstrom et al., 2001), it only affects the PY by providing a less viscous reaction media. The temperature, however, affects the monomer-catalyst interaction to provide the highest PY. This might be due to the significant effect of temperature on the catalytic activity of the MMAO-12/ 2,4-pentanedione in ROP of the terminal epoxide (Warwel et al., 2000).

Optimization and verification of the model

The optimum process conditions for the maximum PY were predicted using a desirability ramp in the software. The optimum conditions with a desirability value of 1 predicting 82.51% of polymerization yield were t= 9.97 min, T= 99.69 °C, and 5.27:5 for the solvent-monomer ratio. Triplet confirmatory experiments were conducted for the validation of the model. The optimum

conditions along with 2 more conditions with different solvent-monomer ratios (Table 3. 5) for maximum predicted yield were used to confirm the model and investigate the effects of solvent volume on the molecular weight of the polyether. Table 3. 5 summarizes the confirmatory conditions, the predicted and observed PY as well as the molecular weights of the obtained polymers. The observed PY has a good agreement with the predicted PY in all the selected runs. This indicates the efficiency of the Box-Behnken design incorporated with desirability function in optimizing conditions for the PY in the microwave-assisted ring-opening polymerization of 1,2-epoxydecane.

Table 3. 5) A comparison between the yield% and GPC results of the optimum microwave method, two selected conditions with the different amount of the solvent-monomer ratio resulted in highest predicted yield% and the conventional method.

Run	Time (min)	Temp. (°C)	Solvent: monomer ratio (mL:mmol)	Desirability	Predicted PY(%)	Observed*** PY(%)	Mn×10^6 (g/mol)	Mw×10^6 (g/mol)	Mw/Mn
1	9.97	99.69*	5.27:5	1	82.51	80±1.6	1.85	2.1	1.2
2	9.22	99:96*	3:5	1	73.17	74±0.62	0.40	1.6	3.9
3	9.05	100	0:5	0.75	44.08	47±3.02	0.26	1.2	4.5
4**	24hr	100	6:5	-	-	-	1.99	2.4	1.2

*The software of the microwave was just able to adjust whole numbers of temperature, so 100°C was used in these runs. Meanwhile, the maximum variance in the adjusted temperature on the machine is less than ±2 °C during hold time. ** Conventional method. *** Average of the three experiments.

3.2.4. Molecular weight of the polyether

The polymer was heated at 50 °C in THF for 5 min to be used in GPC. As shown in table 3. 5, the molecular weight of all polyethers was above one million (g/mol). Surprisingly, the molecular weight of the polyether produced with optimum conditions of the MW in less than 10 min was 2.12×10^6 (g/mol) which was comparable to that of produced by the conventional method after 24 hours (2.40×10^6 g/mol) and reported in the literature (Warwel et al., 2000). Warwel et al. referred

the remarkably slow polymerization of ω-epoxied olefins in the conventional method to the improper catalyst monomer interaction. Although they tried to solve the problem using temperatures above 100°C with the help of higher boiling solvents such as *m*-xylene, and 1,2,4-trichloro benzene (TCB), they were not successful and saw a drastic decrease in the molecular weight of polymers (Warwel et al., 2000). Therefore, our study proved that the ROP of ω-epoxied olefins with MMAO-12/2,4-pentanedione can be accelerated using MW irradiation through the improvement of the catalyst-monomer interactions.

Three different levels of solvent-monomer ratios were also investigated in the MW method. The solvent-monomer ratio has a direct effect on the molecular weight and yield of the polyether. Although the MW assisted bulk polymerization of 1,2-epoxydecane resulted in polyether of molecular weight 1.16×10^6 (g/mol) but by increasing solvent- monomer ratio from 0:5 to 5.25:5 enhanced the molecular weight of the polyether to 2.12×10^6 (g/mol). Like the conventional method, the polydispersity of the polyether synthesized using optimum microwave conditions was considerably narrow (D=1.15) (Table 3. 5). The narrow polydispersity of the polyethers produced using a higher ratio of the solvent both in MW and conventional method was probably due to the solubility of the polyethers in the solvent. However, when the solvent ratios were decreased, the polydispersity of the polyethers became considerably broad. It is possibly due to the difference in the initiation time of different changes resulting from an uncontrolled polymerization process and the decrease of the propagation rate due to increase in viscosity with time which leads to new chains with low molecular mass and high polydispersity.

3.2.5. **Confirmation of epoxidation and polymerization reactions**

The structure of the epoxidized monomer and the produced polyether was analyzed by ^{1}H NMR and ATR-FTIR. A typical ^{1}H NMR spectrum of the synthesized polyether from 1-decene is

presented in Figure 3. 4. The spectrum clearly supports the epoxidation of 1-decene and the formation of polyether from 1,2-epoxydecane. Comparison of ^{1}H NMR spectra of 1-decene and its epoxidized form demonstrated successful oxidation through the disappearance of the terminal double bond peaks at 2.04-5.82 ppm and appearance of the epoxy group peaks at 2.46-2.9 ppm (Sato et al., 1996); (Rio et al., 2010). The shift of epoxy group peaks to the δ 3.38-3.58 ppm region confirms the generation of the ether linkage after ROP.
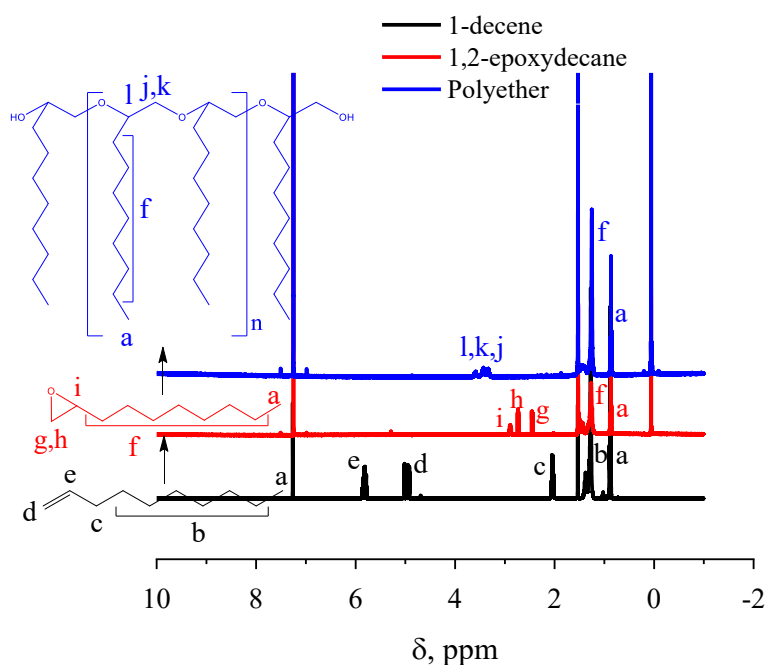
Figure 3. 4) 400 MHz ^{1}H NMR (CDCl$_3$) spectra of two steps conversion of 1-decene to 1,2-epoxydecane and then polyether.

Further confirmation of the whole process was done by the changes in the ATR-FTIR spectrum signals (Figure 3. 5). FTIR spectra of 1-decene and 1,2-epoxydecane revealed the disappearance of C=C peaks (~1640 C=C stretch, ~991, ~907, and ~634 cm^{-1} of sp^2 CH bend of alkene) and the appearance of oxirane ring peak at ~834 cm^{-1}. Two small peaks in the region between ~1130 and 1260 cm^{-1} might be related to the acyl and alkoxy groups of ethyl acetate solvent used in

column chromatography during purification. Additionally, the oxirane peak was disappeared in the polyether spectrum and a clear peak related to ether linkages appeared at ∼1101 cm^{-1}.
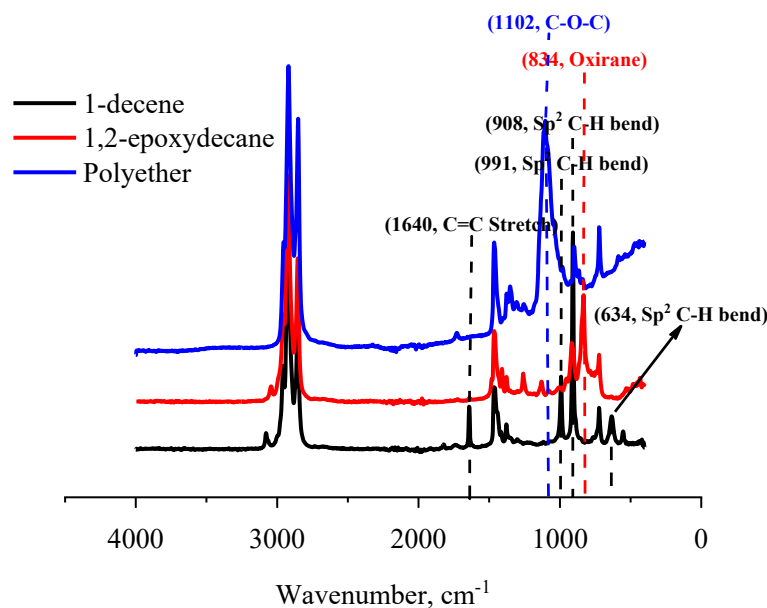
Figure 3. 5) ATR-FTIR analysis of two steps conversion of 1-decene to 1,2-epoxydecane and then polyether

According to the catalyst nature, a coordinative ring-opening polymerization mechanism can be expected for the 1,2-epoxydecane which is described in the literature. The initiation proceeds by the nucleophilic attack of the oxygen in the catalyst Al-O-Al system over the oxirane ring coordinated to a neighboring metal center. Therefore, the oxirane of the monomer opens and the monomer is inserted between the coordinated Al and the rest of the Al-O-Al bond system (Figure 3. 6.a). The propagation step happens as a coordination insertion process. The oxygen on the monomer oxirane ring is coordinated by an Al on the catalyst active site. Then, ring-opening occurs subsequently by the nucleophilic attack of the oxygen at the end of the growing chain and inserting the epoxide between that oxygen and the coordinated Al while the released Al from the end of the

growing chain and participating catalyst in reaction regenerates the bimetallic catalyst again (Figure 3. 6.b). Ideally, the growing chain moves alternatively between two vicinal Al atoms in a "flip-flop" way and leads to linear polyethers with Al-O-C bonds at both ends, and their acidic hydrolysis through the precipitation step will produce a polyetherdiol (Warwel et al., 2000); (Imada et al., 2011).

a) Initiation
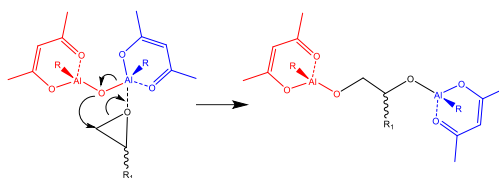
b) Propagation
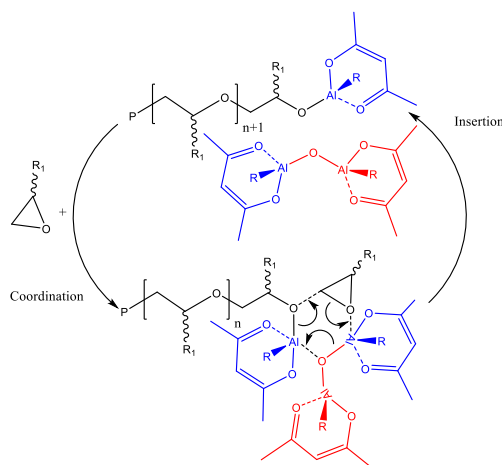
Figure 3. 6) The mechanism of the coordinative ring-opening polymerization.

3.2.6. X-ray Photoelectron Spectroscopy (XPS)

XPS was used to observe the elemental composition and functional groups of the polyether. In the literature, the peaks observed in XPS spectrum at about 101, 282 and 529 eV are due to C 1s and O 1s respectively (Gao et al., 2016). Figure 3. 7 clearly shows that the polyether is composed of carbon and oxygen only. The elemental composition of the polyether was 78% and 12% for the carbon and oxygen, respectively.
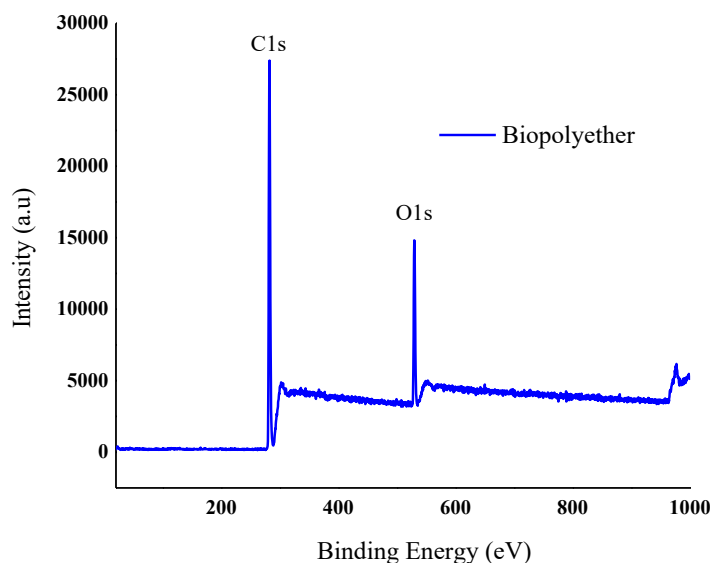
Figure 3. 7) X-ray Photoelectron Spectroscopy (XPS) survey spectra of the polyether

3.2.7. **Thermal properties of the polyether**

The thermal properties of the polyethers produced using the optimum conditions under MW irradiation and conventional method was studied using DSC and TGA. Typical DSC and TGA thermograms of the polyethers are shown in Figure 3. 8 and Figure 3. 9, respectively. DSC revealed a multiple, melting endotherms for the polyethers with a complete melting observed at 34-89 °C and 40-85 °C in the microwave and conventional method, respectively. This phenomenon has been referred to the complex structure of the polyether with the tactic and atactic regions (Warwel et al., 2000).

The polyethers exhibited a low glass transition temperature of 5 °C and -6°C in the conventional and microwave method, respectively. Generally, the presence of long dangling chains in the structure of the polyether provides a strong plasticizing effect and gives a low glass transition temperature (Gao et al., 2016). In addition, the shift of the glass transition temperature and the melting point in the polyether obtained from MW method could be due to the slight differences in

the molecular weight and different proportions of isotactic and atactic polymer chains produced in MW and conventional methods. The glass transition temperature of atactic polypropylene has been reported lower than that of isotactic (Gitsas and Floudas, 2008), therefore it is most probable that microwaves promote atacticity compared to conventional heating.
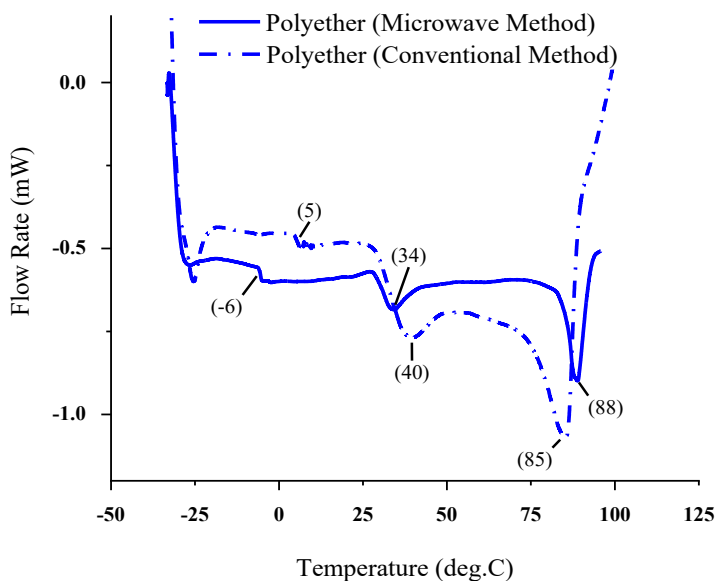
Figure 3. 8) DSC-thermogram of the polyether produced in the optimum process condition using the microwave as the heating source and conventional method.

The TGA curves illustrated a small weight loss in the range of 143- 193 °C possibly due to the presence of tiny amounts of the lower molecular weight polymers in both polyethers synthesized by conventional heating and microwaves. However, the major decomposition in the range of 325- 418 °C was observed for the polyether resulted from microwave method. Nevertheless, a contrast to one major weight loss in microwave assisted synthesized polyether, the TGA of the polyether from the conventional method showed two major weight loss zones. First major weight loss at ~200- 400 °C and second between 400 °C and 500 °C. It has also been reported that atactic polypropylene had higher thermal stability (Pasch et al., 2013). Therefore, the second weight loss

in polyether prepared by conventional heating at ~200- 400 °C could be attributed to a higher proportion of isotactic polyether and final weight loss between 400 °C and 500 °C is probably due to atactic polyether component.
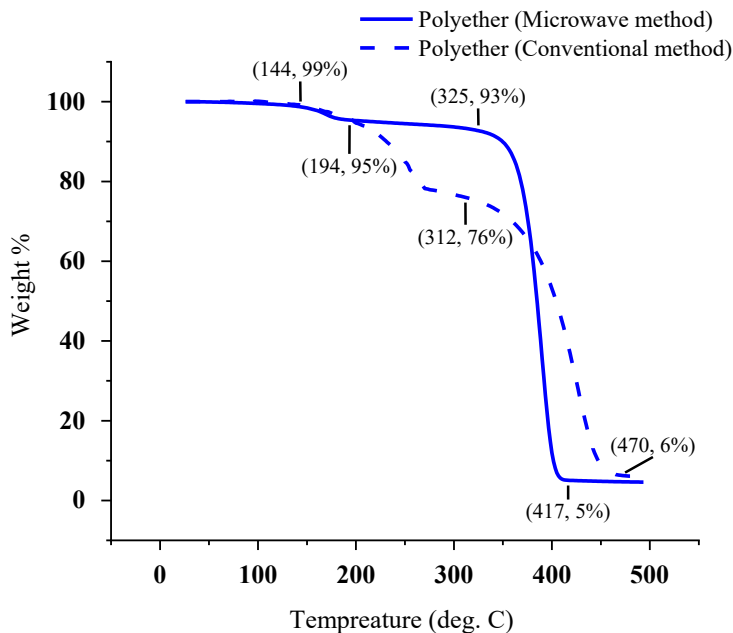
Figure 3. 9) TGA-thermogram of the polyethers produced using the optimum conditions under microwave irradiation and the conventional method.

3.3. Conclusion

This manuscript details with the production of a high molecular weight polyether from 1-decane, one of the main biorefinery products of the plant oils, through both conventional and the MW methods. The epoxidation reaction of 1-deceane was optimized and successfully completed within 1 hour, a considerably short time without using catalyst, under conventional method. MW was not found suitable for performing the epoxidation reaction of 1-decane due to epoxy ring opening by MW irradiation. Synthesized 1,2-epoxydecane was then used as the starting material to produce a high molecular weight polyether. The polymerization yield was optimized using a three-factor, three-level Box-Behnken design for the MW method. The BBD appeared to be a suitable method

for optimization of the reaction conditions to maximize the yield of the ring opening polymerization of 1,2-epoxydecane. The optimum point was identified with the graphical response surface plots. The optimum conditions for the highest polyether yield were as follow t= 9:97 min, T= 99.69 °C, and 5.27:5 solvent-monomer ratio with a desirability value of 1. The polyether produced with the optimum conditions of MW illustrated the highest yield and molecular weight in a good agreement with the results of the conventional method. This result confirmed that the MMAO-12/ 2,4-pentanedione have a good potential to use for ring-opening polymerization of the terminal olefins in the microwave method. Thermal properties study of the polyether showed a complete melting at 34-89 °C with the T_g point of -6 °C and the onset decomposition temperature of 325 °C.

References

Arshad, M., Saied, S., Ullah, A., 2014. PEG-lipid telechelics incorporating fatty acids from canola oil: Synthesis, characterization and solution self-assembly. RSC Adv. 4, 26439–26446. https://doi.org/10.1039/c4ra03583f

ASTM 08(E1356), 2008. Standard Test Method for Assignment of the Glass Transition Temperatures by Differential Scanning Calorimetry.

ASTM D 3850, 2000. Standard Test Method for Rapid Thermal Degradation of Solid Electrical Insulating Materials By Thermogravimetric Method (TGA). https://doi.org/10.1520/D3850-12.2

Azizi, S.N., Asemi, N., 2012. A Box-Behnken design for determining the optimum experimental condition of the fungicide (Vapam) sorption onto soil modified with perlite. J. Environ. Sci. Heal. - Part B Pestic. Food Contam. Agric. Wastes 47, 692–699. https://doi.org/10.1080/03601234.2012.669260

Chikkali, S., Mecking, S., 2012. Refining of plant oils to chemicals by olefin metathesis. Angew. Chemie - Int. Ed. 51, 5802–5808. https://doi.org/10.1002/anie.201107645

De Espinosa, L.M., Meier, M.A.R., 2011. Plant oils: The perfect renewable resource for polymer science?! Eur. Polym. J. 47, 837–852. https://doi.org/10.1016/j.eurpolymj.2010.11.020

Fink, J.K., 2011. Handbook of engineering and specialty thermoplastics, handbook of engineering and specialty thermoplastics. https://doi.org/10.1002/9781118087732

Gao, X., Hu, X., Guan, P., Du, C., Ding, S., Zhang, X., Li, B., Wei, X., Song, R., 2016. Synthesis of core-shell imprinting polymers with uniform thin imprinting layer: Via iniferter-induced radical polymerization for the selective recognition of thymopentin in aqueous solution. RSC Adv. 6, 110019–110031. https://doi.org/10.1039/c6ra24518h

Gawande, M.B., Shelke, S.N., Zboril, R., Varma, R.S., 2014. Microwave-assisted chemistry: Synthetic applications for rapid assembly of nanomaterials and organics. Acc. Chem. Res. 47, 1338–1348. https://doi.org/10.1021/ar400309b

Gitsas, A., Floudas, G., 2008. Pressure dependence of the glass transition in atactic and isotactic polypropylene. Macromolecules 41, 9423–9429. https://doi.org/10.1021/ma8014992

Ho, K.P., Wong, W.L., Lam, K.M., Lai, C.P., Chan, T.H., Wong, K.Y., 2008. A simple and effective catalytic system for epoxidation of aliphatic terminal alkenes with manganese(II) as the catalyst. Chem. - A Eur. J. 14, 7988–7996. https://doi.org/10.1002/chem.200800759

Hoogenboom, R., Schubert, U.S., 2007. Microwave-assisted polymer synthesis: Recent developments in a rapidly expanding field of research. Macromol. Rapid Commun. 28, 368–386. https://doi.org/10.1002/marc.200600749

Hoveyda, A.H., Zhugralin, A.R., 2007. The remarkable metal-catalysed olefin metathesis reaction. Nature 450, 243–251. https://doi.org/10.1038/nature06351

Imada, Y., Iida, H., Kitagawa, T., Naota, T., 2011. Aerobic reduction of olefins by in situ generation of diimide with synthetic flavin catalysts. Chem. - A Eur. J. 17, 5908–5920. https://doi.org/10.1002/chem.201003278

Iqbal, M., Shakeel, F., Anwer, T., 2016. Simple and sensitive UPLC-MS/MS method for high-throughput analysis of ibrutinib in rat plasma: Optimization by box-behnken experimental design. J. AOAC Int. 99, 618–625. https://doi.org/10.5740/jaoacint.15-0222

Karmakar, G., Ghosh, P., 2016. Atom transfer radical polymerization of soybean oil and its evaluation as a biodegradable multifunctional additive in the formulation of eco-friendly lubricant. ACS Sustain. Chem. Eng. 4, 775–781. https://doi.org/10.1021/acssuschemeng.5b00746

Karnachi, A.A., Khan, M.A., 1996. Box-behnken design for the optimization of formulation variables of indomethacin coprecipitates with polymer mixtures. Int. J. Pharm. 131, 9–17. https://doi.org/10.1016/0378-5173(95)04216-4

Kempe, K., Becer, C.R., Schubert, U.S., 2011. Microwave-assisted polymerizations: Recent status and future perspectives. Macromolecules 44, 5825–5842. https://doi.org/10.1021/ma2004794

Kline, G.M., 1962. High polymers. John Wiley & Sons, Inc. USA.

Kousha, M., Daneshvar, E., Dopeikar, H., Taghavi, D., Bhatnagar, A., 2012. Box-Behnken design optimization of Acid Black 1 dye biosorption by different brown macroalgae. Chem. Eng. J. 179, 158–168. https://doi.org/10.1016/j.cej.2011.10.073

Kunduru, K.R., Basu, A., Haim Zada, M., Domb, A.J., 2015. Castor oil-based biodegradable polyesters. Biomacromolecules 16, 2572–2587. https://doi.org/10.1021/acs.biomac.5b00923

Li, Y., Wang, X.L., Yang, K.K., Wang, Y.Z., 2006. A rapid synthesis of poly (p-dioxanone) by ring-opening polymerization under microwave irradiation. Polym. Bull. 57, 873–880. https://doi.org/10.1007/s00289-006-0668-2

Lidstrom, P., Tierney, J., Wathey, B., Westman Jacob, 2001. Microwave-assisted green organic synthesis-a review. Tetrahedron 57, 9225–9283.

Meier, M.A.R., Metzger, J.O., Schubert, U.S., 2007. Plant oil renewable resources as green alternatives in polymer science. Chem. Soc. Rev. 36, 1788–1802. https://doi.org/10.1039/b703294c

Omonov, T.S., Curtis, J.M., 2014. Biobased epoxy resin from canola oil. J. Appl. Polym. Sci. 131, 1–9. https://doi.org/10.1002/app.40142

Osborne, J.W., 2010. Improving your data transformations: Applying the Box-Cox transformation. Pract. Assessment, Res. Eval. 15.

Pardal, F., Salhi, S., Rousseau, B., Tessier, M., Claude, S., Fradet, A., 2008. Unsaturated polyamides from bio-based Z-octadec-9-enedioic acid. Macromol. Chem. Phys. 209, 64–74. https://doi.org/10.1002/macp.200700319

Pasch, H., Malik, M.I., Macko, T., 2013. Recent advances in high-temperature fractionation of polyolefins, in: Abe, A., Kausch, H.-H., Möller, M., Pasch, H. (Eds.), Polymer Composites -- Polyolefin Fractionation -- Polymeric Peptidomimetics -- Collagens. Springer Berlin Heidelberg, Berlin, Heidelberg, pp. 77–140. https://doi.org/10.1007/12_2012_167

Prakash Maran, J., Manikandan, S., Thirugnanasambandham, K., Vigna Nivetha, C., Dinesh, R., 2013. Box-Behnken design based statistical modeling for ultrasound-assisted extraction of corn silk polysaccharide. Carbohydr. Polym. 92, 604–611. https://doi.org/10.1016/j.carbpol.2012.09.020

Rio, E. Del, Galià, M., Cádiz, V., Lligadas, G., Ronda, J.C., 2010. Polymerization of epoxidized vegetable oil derivatives: ionic-coordinative polymerization of methylepoxyoleate. J. Polym. Sci. Part A Polym. Chem. 48, 4995–5008. https://doi.org/https://doi.org/10.1002/pola.24297

Roumanet, P.J., Laflèche, F., Jarroux, N., Raoul, Y., Claude, S., Guégan, P., 2013. Novel aliphatic polyesters from an oleic acid based monomer. Synthesis, epoxidation, cross-linking and biodegradation. Eur. Polym. J. 49, 813–822. https://doi.org/10.1016/j.eurpolymj.2012.08.002

Rüsch Gen. Klaas, M., Warwel, S., 1997. Lipase-catalyzed preparation of peroxy acids and their use for epoxidation. J. Mol. Catal. A Chem. 117, 311–319. https://doi.org/10.1016/S1381-1169(96)00264-6

Sato, K., Aoki, M., Ogawa, M., Hashimoto, T., Noyori, R., 1996. A practical method for epoxidation of terminal olefins with 30% hydrogen peroxide under halide-free conditions. J. Org. Chem. 61, 8310–8311. https://doi.org/10.1021/jo961287e

Sinnwell, S., Ritter, H., 2007. Recent advances in microwave-assisted polymer synthesis. Aust. J. Chem. 60, 729–743. https://doi.org/10.1071/CH07219

Takahira, Y., Morizawa, Y., 2015. Ruthenium-catalyzed olefin cross-metathesis with tetrafluoroethylene and analogous fluoroolefins. J. Am. Chem. Soc. 137, 7031–7034. https://doi.org/10.1021/jacs.5b03342

Tian, C., Fu, S., Chen, J., Meng, Q., Lucia, L.A., 2014. Graft polymerization of ε-caprolactone to cellulose nanocrystals and optimization of grafting conditions utilizing a response surface methodology. Nord. Pulp Pap. Res. J. https://doi.org/10.3183/npprj-2014-29-01-p058-068

Türünç, O., Firdaus, M., Klein, G., Meier, M.A.R., 2012. Fatty acid derived renewable polyamides via thiol-ene additions. Green Chem. 14, 2577–2583. https://doi.org/10.1039/c2gc35982k

Ullah, A., Arshad, M., 2017. Remarkably efficient microwave-assisted cross-metathesis of lipids under solvent-free conditions. ChemSusChem 10, 2167–2174. https://doi.org/10.1002/cssc.201601824

Warwel, S., Brüse, F., Demes, C., Kunz, M., Klaas, M.R.G., 2001. Polymers and surfactants on the basis of renewable resources. Chemosphere 43, 39–48. https://doi.org/10.1016/S0045-6535(00)00322-2

Warwel, S., Wiege, B., Fehling, E., Kunz, M., 2000. Ring-opening polymerization of oleochemical epoxides catalyzed by aluminoxane/acetyl acetone. Eur. Polym. J. 36, 2655–2663. https://doi.org/10.1016/S0014-3057(00)00046-X

Wiesbrock, F., Hoogenboom, R., Abeln, C.H., Schubert, U.S., 2004. Single-mode microwave ovens as new reaction devices: Accelerating the living polymerization of 2-ethyl-2-oxazoline. Macromol. Rapid Commun. 25, 1895–1899. https://doi.org/10.1002/marc.200400369

Zhang, C., Liao, L., Liu, L., 2004. Rapid ring-opening polymerization of D,L-lactide by microwaves. Macromol. Rapid Commun. 25, 1402–1405. https://doi.org/10.1002/marc.200400106

Zhang, K., Nelson, A.M., Talley, S.J., Chen, M., Margaretta, E., Hudson, A.G., Moore, R.B.,

Long, T.E., 2016. Non-isocyanate poly(amide-hydroxyurethane)s from sustainable resources.

Green Chem. 18, 4667–4681. https://doi.org/10.1039/c6gc01096b

CHAPTER 4: SYNTHESIS AND CHARACTERIZATION OF UNSATURATED BIOBASED-POLYAMIDES FROM PLANT OIL[2]

4. Introduction

Synthetic petrochemical-derived polymers have infiltrated into virtually all aspects of human life after their first emergence in the early 20th century (Peplow, 2016); (Nguyen et al., 2018). Polymer industry is a vital link in the sustainable growth of our modern life. Despite its undeniable role in our ever-increasing technological world, the progressively increased environmental concerns and continued depletion of fossil fuels have been a potential threat to the survival of the polymer industry. Hereupon, supplementing and/or replacing the synthetic petrochemical-derived polymers by their biobased counterparts has emerged as a promising strategy to overcome this obstacle (Nakajima et al., 2017); (Molina-Gutierrez et al., 2019); (Oliva et al., 2017). Plant oils are considered as prospective feedstocks for the polymer industry due to their worldwide availability; the annual production of major vegetable and seed oils was 773 million metric tons in 2017-2018 which increased to 804 million metric tons in 2018-2019 (Oilseeds: World Markets and Trade., 2019). Additionally, other characteristics including structural similarity to petroleum resources, economic advantages, biodegradability, renewability, sustainability, and low toxicity have made plant oils the favorable future feedstock to produce biobased polymers either in their native forms or after chemical modifications (Molina-Gutierrez et al., 2019).

Recently, our group has reported an efficient, rapid, and solvent-free method for the transformation of plant oils to high-value linear olefins such as methyl 9-decenoate, 1-decene, and dimethyl 9-

---

octadecendioate (DMOD) (Ullah and Arshad, 2017); (Ullah and Arshad, 2018) (Scheme 2. 16). The reported method is a significant step toward increasing yield and purity of the derived platform monomers from plant oils with lower production costs. These monomers have been used to produce several types of biobased polymers, including polyamide (Winkler and Meier, 2014), polyester (Jin et al., 2017), polyether (Ahmadi and Ullah, 2017), and polyurethane (Zhang et al., 2014).

Polyamides are a class of polymers with repeated amine units in their backbone. Polyamides are mainly produced through polycondensation of ω-amino carboxylic acids or dicarboxylic acids with diamines, and the ring-opening polymerization of lactams (Türünç et al., 2012). Polyamides synthesized from fossil resources have high thermal and mechanical strengths making them suitable engineering plastics used in different industrial fields such as electric and electronics, packaging, automotive, clothing, and several other areas (Jasinska et al., 2011a); (Xue et al., 2013); (Martino et al., 2014). Moreover, because of their high tensile strength and good elasticity as well as flexibility, polyamides have also been used in pharmaceutical and clinical applications to produce sutures, catheters, and dental resins. Petrochemical-based polyamides have a more severe impact on global climate change compared to other synthetic polymers, specifically in terms of carbon dioxide equivalents (Vink et al., 2003). Therefore, the synthesis of biobased polyamides from renewable resources has gained considerable attention in the scientific community in recent decades.

Most of the attempts to produce biobased polyamides have just resulted in the production of polyamides partially containing oleochemical diacid platform monomers polycondensed with petroleum-based diamines (Huf et al., 2011); (Gilbert, 2017); (Mutlu and Meier, 2009); (Stempfle et al., 2016); (Stempfle et al., 2011). Recently, biobased polyamides have been synthesized from

amine-functionalized fatty acid methyl esters using 1,5,7-triazabicyclo[4.4.0]dec-5-ene (TBD) catalyst (Türünç et al., 2012). Most of the biobased polyamides exhibit inferior physicochemical and mechanical properties compared with their petroleum-based counterparts and therefore, developing cost-effective biobased polyamides with adequate mechanical properties require further investigations.

In this study, we conceptualized condensation of different amines (a diamine and a triamine) with a canola oil-derived unsaturated diester. The key advantage of using unsaturated bio-diester in the main chain is the post-polymerization functionalization to install side chains on the polymer. We investigated the condensation of the bio-diester with one aromatic diamine and one aliphatic triamine under conventional (silicon oil bath as the heating source) and microwave heating, which has been rarely reported with other polyamide systems. The DMOD bio-diester was produced by cross-metathesis of unsaturated canola oil fatty esters with ethylene or 1,5-hexadiene under microwave irradiation. Polymerization of the DMOD bio-diester with *p*-Xylylenediamine (PXDA) and Diethylenetriamine (DETA) under conventional heating resulted in the production of two biobased polyamides (CH-PA (DMOD-PXDA) and CH-PA (DMOD-DETA)). The microwave-assisted polymerization to produce these biobased polyamides was also studied to compare the effect of the heating method on the polycondensation process. The biobased polyamides (produced under both thermal conditions) were structurally characterized by solid-state carbon nuclear magnetic resonance spectroscopy (^{13}C NMR), Fourier transform infrared spectroscopy (FTIR), and wide-angle X-ray diffraction (WAXD). Furthermore, the capability of the resulted biobased polyamides was surveyed for making thin films. Finally, the mechanical and thermomechanical properties of the generated films were examined using a universal tensile testing machine and dynamic mechanical analysis (DMA), respectively.

4.1. Materials and methods

4.1.1. Materials

Canola oil was provided by Bunge Canada, Edmonton Plant. *p*-Xylylenediamine (PXDA, 99%, CAS No. 539-48-0), Diethylenetriamine (DETA, 99%, CAS No. 111-40-0), 1,5,7-Triazabicyclo[4.4.0]dec-5-ene (TBD, 98%, CAS No. 5807-14-7), 1,1,1,3,3,3-Hexafluoro-2-propanol (HFIP, CAS No. 920-66-1), Chloroform-d (99.8 atom % D, CAS No. 865-49-6), Methanol (≥ 99.9%, CAS No. 67-56-1), and Trifluoroacetic anhydride (TFAA≥ 99%, CAS No. 407-25-0) were obtained from Sigma-Aldrich and used without further purification. Dimethyl 9-octadecenedioate (DMOD) was synthesized as reported earlier through methanolic transesterification of canola oil and cross-metathesis of the resulted unsaturated methyl esters (Ullah and Arshad, 2017), (Ullah and Arshad, 2018). Briefly, canola oil was first converted into its fatty esters using KOH. A microwave-assisted ethenolysis was then performed on the fatty esters using 2nd generation Hoveyda-Grubbs catalyst to produce a mixture of different chemical platform monomers. Finally, DMOD bio-diester was purified from the mixture using column chromatography. The final product was a colorless liquid chemical with ≥ 99% purity.

^{1}H NMR (400 MHz, CDCl$_3$, δ in ppm) δ 4.82- 5.88 (m, 2H, =CH-), 3.66- 3.71 (s, 6H, -OCH$_3$), 2.28- 2.36 (t, 4H, -CH$_2$CO-), 1.94- 2.04 (m, 4H, =CHCH$_2$-), 1.59- 1.67 (m, 4H), 1.12- 1.47 (m, 16H) (Figure 4. 1).

IR: 1736 (s, C=O), 969 (m, Trans C=C), 720 cm^{-1} (m, Cis C=C) (Figure 4. 2).

4.1.2. Synthesis of polyamides

Bulk polycondensation by conventional heating (CH)

Biobased CH-PA (DMOD-PXDA): The DMOD bio-diester (1 g, 2.94 mmol, 1 equiv.) was mixed with the PXDA diamine (1 equiv.) in a clean and dry round-bottom flask and purged with nitrogen

for 15 minutes. TBD (0.05 mol %) was added into the mixture under constant nitrogen flow and degassed for another 15min. The polymerization was performed in a silicon oil bath through a three-step heating process started at 75 ± 5°C for 1 h, continued at 100 ± 5 °C for 30 min, and completed at 205 ± 5 °C for 2 h under reduced pressure (0.7 bars). The resulted mixture was concentrated in HFIP at 60 °C. The polymer was then precipitated in cold methanol and dried at 55 °C overnight. The dried biobased CH-PA (DMOD-PXDA) was powdered and washed twice with HFIP to increase purity (Scheme 4. 1). The yield of this reaction was 86%.

Biobased CH-PA (DMOD-DETA): The DETA triamine (1 equiv.) was mixed with the degassed DMOD (1 g) under nitrogen flow for 15 min. TBD (0.05 mol %) was added to the mixture and flushed for another 15 min. The polymerization was promoted at 160 ± 2 °C under reduced pressure (0.7 bars) for 4 hours. The final product was floated in distilled water, filtered, and dried at 50 °C overnight. The resulted polymer was then frozen in liquid nitrogen, powdered, and washed twice with water and ice-cold methanol to obtain pure biobased CH-PA (DMOD-DETA) (Scheme 4. 2). The yield of this reaction was 82%.

Microwave-assisted bulk polycondensation (MH)

A single-mode microwave reactor (CEM-Discover, 120 V, Matthews, USA) equipped with an infrared temperature sensor was employed for microwave-induced polycondensation of the monomers in an open vessel mode under the maximum power of 200 W and high stirring.

Biobased MH-PA (DMOD-PXDA): The polymerization process was identical to the method used in the conventional heating polycondensation except for the heating process which was started at 75 ± 10 °C for 2 min, continued at 100 ± 5 °C for 3 min, and completed at 160 ± 2 °C for 10 min under reduced pressure (0.7 bars) excluding the heat ramping times. The same steps as in the

conventional polycondensation method were practiced to produce pure biobased MH-PA (DMOD-PXDA) (Scheme 4. 1). The yield of this reaction was 79%.

Biobased MH-PA (DMOD-DETA): The microwave-assisted polycondensation of DMOD and DETA was carried out at 160 ± 2 °C for 10 min with all the other steps being similar to the conventional method to produce this polymer (Scheme 4. 2). The yield of this reaction was 72%.

4.1.3. Film preparation and annealing conditions

The crushed polyamides (~3.0 g) were molded using a Carver press (CARVER®, INC. USA). The polymers were sandwiched between two steel plates. The molding conditions of biobased CH-PA (DMOD-PXDA) and MH-PA (DMOD-PXDA) were 200 °C for 25 min, and 160 °C for 20 min, respectively, both under compression force of 3000 pounds. Films of both biobased CH-PA (DMOD-DETA) and MH-PA (DMOD-DETA) were developed at 160 °C and 3000 pounds compression press for 20 min. The annealing of the compression molded films was done in vacuo for 12 hours at 130 °C. A stepwise cooling procedure was then applied to cool down the films from 130 °C to room temperature; the oven temperature was reduced by 30 °C in each step, and the films were allowed to equilibrate to the new temperature for 3 hours in each step.

4.1.4. Characterization

Attenuated Total Reflectance-Fourier Transform Infrared (ATR-FTIR) Analysis. FTIR experiments were performed on a Bruker Alpha FTIR spectrophotometer (Bruker Optics, Esslingen, Germany). The instrument was supplied with a single bounce diamond ATR crystal and set up to collect the spectra at a resolution of 4 cm^{-1} over the range of 410- 4000 cm^{-1}. Before applying and receiving a sample spectrum, the clean ATR crystal was scanned to correct the background signals. Each sample was then scanned 16 times to obtain an average signal using the

OPUS software (Bruker version 6.5). Finally, the resulted spectrum was analyzed using the Nicolet Omnic software (version 8).

Solid-state ^{13}C NMR. Solid-state ^{13}C NMR data were recorded on a Bruker NEO 500 NMR spectrometer equipped with a wide-bore superconducting 11.75 T magnet. Magic-angle spinning (MAS) conditions at a spinning frequency of 12-14 kHz were used for acquiring spectra using a 4 mm Bruker MAS NMR probe operating in double-resonance mode, tuned to $^1H/^{13}C$. The cross-polarization (CP) method was used to acquire MAS NMR spectra with a 4 μs ^1H $\pi/2$ pulse, ramped Hartman-Hahn match on ^1H (3 ms contact time), 2500 coadded transients with a 3 s recycle delay. All data were obtained with ^1H decoupling using the two-pulse phase-modulated decoupling scheme. ^{13}C NMR spectra were referenced with respect to tetramethylsilane ($\delta iso = 0$ ppm) by setting the high-frequency peak of adamantane to 38.56 ppm.

Differential Scanning Calorimetry (DSC) Analysis. DSC experiments were conducted using a 2920 Modulated DSC (TA Instrument, USA). Samples (4.0-6.0 mg) were heated up to 300 °C at a scan rate of 3 °C min^{-1}. Heating was started from ambient or below ambient temperatures after equilibrating at a temperature less than the melting point of the samples. Pure indium was used to calibrate the heat flow and temperature of the instrument.

Thermogravimetric Analysis (TGA). TGA was carried out with a TGA Q50 (TA Instruments, DE, USA). Each sample (13.0- 20.0 mg) was placed in a ceramic pan and heated in the instrument's furnace at a constant rate of 10 °C min^{-1} over the range of 10- 600 °C under the 60 mL min^{-1} nitrogen flow to study its weight loss or thermal behavior. Data acquisition and analysis were executed using the TA universal analysis software. Thermal decomposition temperature ($T_{d,\ 5\ wt\%}$) is considered the temperature at which 5% weight loss or degradation occurs in each sample.

Wide-Angle X-ray Diffraction (WAXD) Analysis. X-ray diffraction studies of all biobased polyamides were carried out with a diffraction unit Rigaku Ultima IV, operating at 38 kV and 38 mA. The radiation source was a Cu Kα with a wavelength (λ) of 0.154 nm. The X-ray beams at the specific angle incidences of θ on the sample. The data was recorded from 2θ values of 5 to 45° with a step size of 0.02°. The observed peak in WAXD analysis was deconvoluted using the OriginPro 2019 software.

Tensile Testing. A universal testing machine (autograph AGSX Shimadzu) was used to measure the tensile properties of the polyamide films. The rectangular film samples were inserted in the pneumatic non-shift wedge grips of the device. The film was stretched at a crosshead speed of 5 mm s^{-1} until ruptured. An average of three specimens was used for each sample to analyze data with calculated standard deviations.

Dynamic Mechanical Analysis (DMA). The viscoelastic properties of polyamide films were investigated using a DMA Q800 (TA Instruments, DE, USA), equipped with a liquid-nitrogen cooling apparatus. The measurements were done under the dry nitrogen with a 2 L min^{-1} flow. The tension mode was applied at an oscillatory frequency of 1 Hz with an applied deformation of 0.2% during heating. The temperature was programmed from -100 to +150 °C at a rate of 2 °C min^{-1}. The glass transition temperature (T_g) values were reported based on the peaks of the loss factor signal of polyamides.

4.2. Results and discussion

4.2.1. Synthesis of biobased PAs (DMOD-PXDA) and PAs (DMOD-DETA)

The prime objective of the present study was the synthesis and characterization of two different types of biobased polyamides including semi-aromatic PA (DMOD-PXDA) and aliphatic PA (DMOD-DETA) from canola oil. Microwave irradiation is considered as a highly effective heating

process to reduce reaction time and cost of the final product (Kotzebue et al., 2018). Therefore, the polycondensation reaction of monomers was studied under both conventional and microwave heating processes to compare the effect of these heating methods on the thermal and crystalline properties of the produced polyamides as well as mechanical and thermo-mechanical properties of their corresponding films.
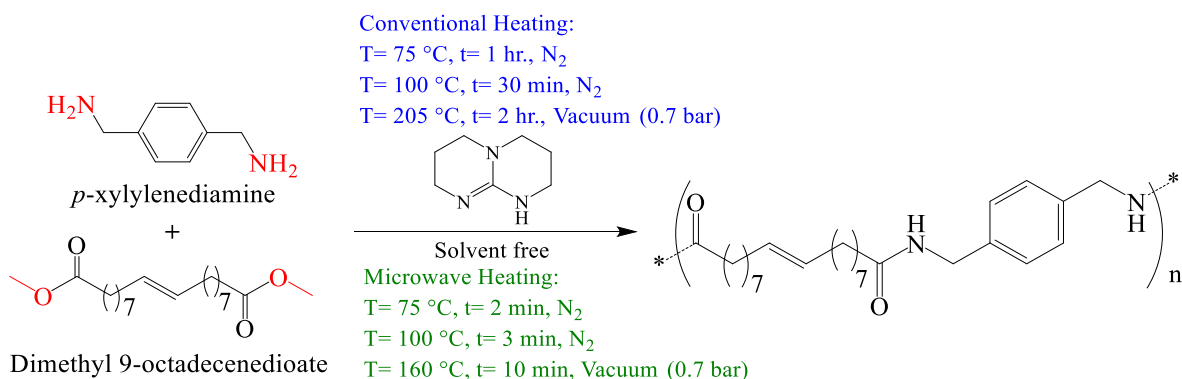
Scheme 4. 1) Synthesis of biobased CH-PA (DMOD-PXDA) and MH-PA (DMOD-PXDA).

Synthesis of biobased PAs (DMOD-PXDA): The biobased CH-PA (DMOD-PXDA) was synthesized only after the bulk polycondensation of DMOD bio-diester with PXDA diamine at the temperature as high as 205 °C (Scheme 4. 1). TBD is a an inexpensive, nontoxic, and commercially available organocatalyst used for aminolysis of esters in the presence of amines under solvent-free conditions. Indeed, TBD is able to act as a bifunctional nucleophilic catalyst to proceed the polycondensation of DMOD with amines in two sequentially-repeating steps (Scheme 4. S1). Firstly, TBD reacts on the ester groups of DMOD to create an intermediate I where a proton transfer by the protonated nitrogen creates the TBD amide II and liberates an alcohol. Secondly, the activated hydrogen bond of amines facilitate the amide formation and regeneration of TBD (Sabot et al., 2007); (Kiesewetter et al., 2009). Although TBD is a suitable catalyst for polycondensation reactions, it is a hygroscopic catalyst with high sensitivity to CO_2 and humidity

(Firdaus and Meier, 2013); (Zhang et al., 2016). Therefore, TBD needs to be carefully manipulated when used as a catalyst for polycondensation reactions. It should be noted that the stepwise conventional polycondensation heating process was chosen to accommodate a complete polymerization process through the complete melting of solid PXDA to minimize its sublimation at high temperatures. However, the melted mixture at low temperature (75 °C) was again solidified just after 30 min heating at 100 °C. This can be due to the formation of oligomers with high melting points. Hence, the temperature was gradually increased to 205 °C to melt the mixture again and complete the polymerization process. A continuous vacuum (0.7 bars) during the polymerization at high temperature was necessary to remove the generated methanol byproduct and reach the highest conversion of monomers to polymer. Interestingly, the polycondensation of DMOD and PXDA under microwave irradiation was not achievable at the same temperature required for the conventional polycondensation due to the degradation of mixture (Figure 4. S1). Heating inhomogeneity due to the less efficient stirring and the generation of hot spots in the viscous mixture created in microwave are the potential explanation for product degradation at high temperatures. The final product of both heating processes was a white to yellow powder (Figure 4. S2), non-soluble in the common solvents and even in HFIP after 24 hours heating at its boiling point (69 °C). Due to the solubility issue, size exclusion chromatography (SEC) analysis of the final polymer was not possible to perform. Therefore, structural characterization of the PAs (DMOD-PXDA) was done using ATR-FTIR and solid-state ^{13}C NMR. Since only about 35% of the produced polyamide at 8 min microwave irradiation was soluble in the mixture of THF and TFAA, overlaying ^{1}H NMR of this fraction and the monomers was used to verify the conversion of monomers to polymer during the polymerization process (Figures 4. S3 & 4. S4, Scheme 4. S2, and table 4. S1).
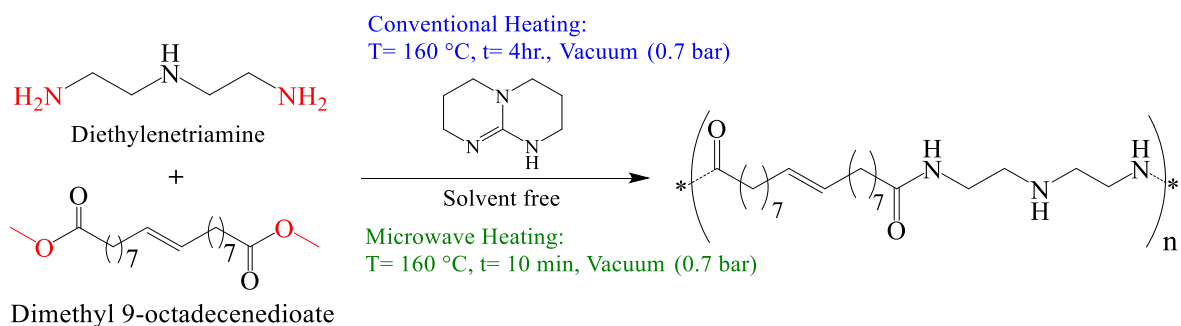
Scheme 4. 2) Synthesis of biobased CH-PA (DMOD-DETA) and MH-PA (DMOD-DETA).

Synthesis of biobased PAs (DMOD-DETA): Scheme 4. 2 shows the polymerization process of DMOD bio-diester with DETA triamine. Conventional bulk polycondensation of DMOD with DETA at 160 °C was completed in 4 hours, whereas microwave-assissted polymerization was finished in 10 minutes (Figure 4. S5). The aliphatic biobased PAs (DMOD-DETA) were rubbery with a yellow to brown color (Figure 4. S6). The conversion of monomers to the aliphatic polyamides was also confirmed by overlaying their ATR-FTIR spectra and solid-state ^{13}C NMR of polyamide. PAs (DMOD-DETA) were also not soluble in common solvents used for polymer solubilization. The heating of these polymers at the boiling points of the HFIP and TFAA for 24 hours was also not efficient for their solubilization. This can potentially be due to the presence of more hydrogen bonds in the structure of PAs (DMOD-DETA), which can also be amplified with the secondary amino groups in the middle of DETA. It is also possible that some of the secondary amine groups may participate in the cross-linking between a number of polymer chains. Therefore, we were not also able to provide the ^{1}H NMR spectrum of PAs (DMOD-DETA) in this report. PAs (DMOD-DETA) stuck hard to glassware, but these sticky viscous polymers could be easily removed from the glassware when distilled water was poured on them. These aliphatic polyamides were washed in distilled water and cold methanol to increase their purity.

4.2.2. **Characterization of the PAs (DMOD-PXDA) and PAs (DMOD-DETA)**

As the resulting polyamides were not soluble in common solvents, ATR-FTIR analyses and the solid-state ^{13}C NMR were implemented to confirm the structure of these biobased polyamides. The ATR-FTIR spectra of the monomers and polymers were used to verify the polycondensation of both PAs (DMOD-PXDA) and PAs (DMOD-DETA). Figure 4. 1 compares the spectra of PAs (DMOD-PXDA) and their monomers. The characteristic absorption bands corresponding to the primary amino group (NH stretching at 3272 and 3347 cm^{-1}) of PXDA were entirely converted to a relatively broad single band of amide at 3290 cm^{-1}. The single band at 3290 cm^{-1} is an indication of the strong hydrogen bonding between the polymer amide groups, and rather broadness of the band without any shoulder might suggest the formation of more types of hydrogen bonds with different bond lengths (Kaczmarczyk and Danuta, 1995); (Pagacz et al., 2016). The clear distinctions between the absorption bands of carbonyl groups in the bio-diester and PAs (DMOD-PXDA) can be clearly seen in their ATR-FTIR spectra. The characteristic carbonyl band of DMOD at 1738 cm^{-1} disappeared almost completely while the carbonyl bands of amide I (C=O stretch) and amide II were raised at, 1636 cm^{-1}, and 1542 cm^{-1} in the semi-aromatic polyamides' spectrum, respectively. The amide I band at 1636 cm^{-1} is also sharp, and shoulders cannot be seen, suggesting that some of the C=O amide groups are bonded by hydrogens (Kaczmarczyk and Danuta, 1995). Regarding the amide II stretching vibrations, it is reported that nearly half of them have in-plane N-H bending vibrations while just about one-third of vibrations are the C-N stretching, with the rest being C-C stretching (Coleman et al., 1986). Although the amide II band is also relatively sharp, it is smaller than the amide I band with a tiny shoulder at 1517 cm^{-1}. The shoulder is still in the region characteristic of the C=O amide II bands though (Kaczmarczyk and Danuta, 1995). A little absorption band is also seen at 1740 cm^{-1} of the semi-aromatic polyamide signal that might be due to the presence of ester terminal groups or a small amount of the remaining DMOD in the

polymer structure. A weak signal at 3720 cm^{-1} of the biobased polyamide spectrum is assigned to the N-H stretch vibrations, and amide II overtone (Pagacz et al., 2016).
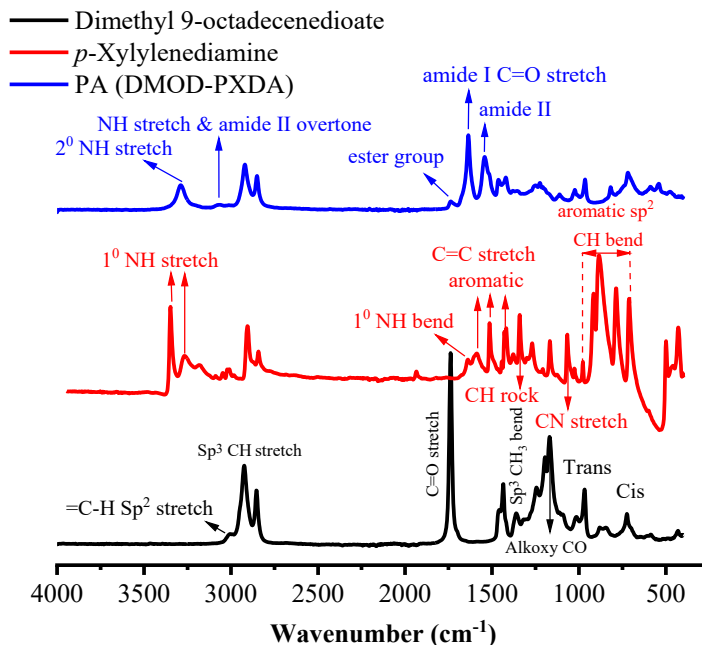
Figure 4. 1) Representative ATR-FTIR analyzes of dimethyl 9-octadecenedioate, *p*-Xylylenediamine, and biobased PA (DMOD-PXDA).

Figure 4. 2 shows the ATR-FTIR spectra of the aliphatic biobased PAs (DMOD-DETA) and their monomers. The broad triple bands of both primary and secondary amino groups of DETA (3133 to 3400 cm^{-1}) were transformed into a sharp band without any shoulders at the maximum of 3292 cm^{-1} in PAs (DMOD-DETA) spectrum. The characteristic carbonyl band of DMOD at 1738 cm^{-1} was also replaced by the carbonyl bands of amide I (1636 cm^{-1}), and amide II (1546 cm^{-1}) in PAs (DMOD-DETA) spectrum. These results support the polycondensation of the monomers into PAs (DMOD-DETA). However, the presence of a relatively strong ester band (1736 cm^{-1}) in the aliphatic polyamide signal revealed incomplete polymerization. This could be due to the high viscosity of polymer mixture at polymerization temperatures preventing the efficient mass transfer

of monomers/oligomers to the polymer chains. Ineffective washing process of the polymer due to the insolubility and stickiness of product mixture could be another explanation for the observed impurity.
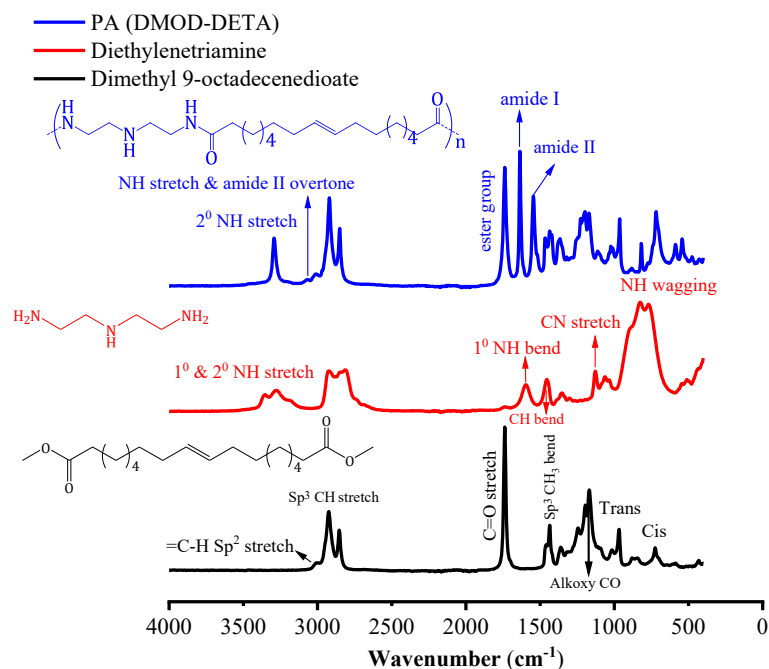
Figure 4. 2) Representative ATR-FTIR analyzes of dimethyl 9-octadecenedioate, diethylenetriamine, and biobased PA (DMOD-DETA).

Figure 4. 3 shows ^{13}C CP/MAS NMR spectra of PAs (DMOD-PXDA and DMOD-DETA). These spectra exhibit relatively well resolved peaks, although some broadening of peaks is observed. All peaks are assigned based on the published literature (Jasinska et al., 2011b); (Shah et al., 2016). The resonance peak at 174 ppm in the lowest field of ^{13}C CP/MAS NMR spectra of both polyamides is assigned to the carbon sites in carbonyl groups (C=O) not affected by different polymer structures. Linear PAs (DMOD-DETA) exhibited a relatively sharp resonance peak at 131 ppm ascribed to the carbons in double bonds of its structure. Nonlinear PAs (DMOD-PXDA) on the other hand, displayed a few peaks at 123-142 ppm attributed to aromatic carbon atoms in the phenyl rings and carbons in the double bonds of the polymer. The resonance peaks around 18-

46 ppm are assigned to the aliphatic methylene carbon atoms in the chain of both polyamides. The PAs (DMOD-PXDA) also showed another peak at 51 ppm potentially related to the carbon site between the phenyl ring and amide groups.
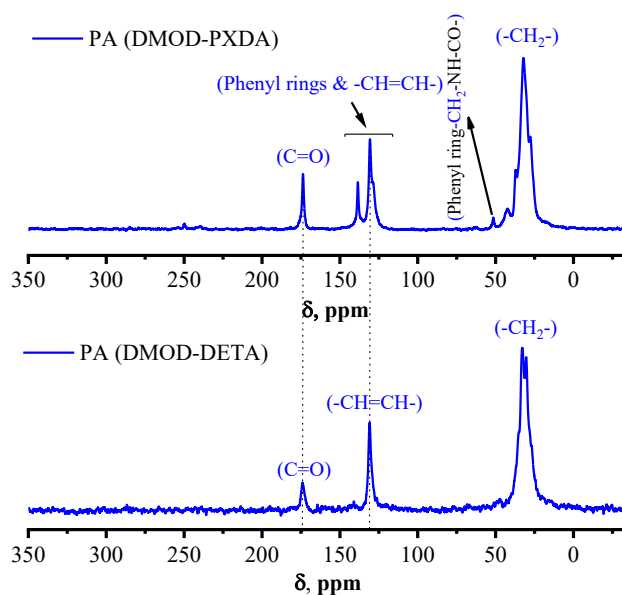
Figure 4. 3) Representative ^{13}C CP/MAS NMR spectra of the biobased PA (DMOD-PXDA) (upper trace) and PA (DMOD-DETA) (lower trace) acquired at 21 °C and 11.57 T. The MAS frequency and signal transitions were 12-14 kHz and 2500, respectively.

4.2.3. **Thermal properties of biobased PAs (DMOD-PXDA) and PAs (DMOD-DETA)**

Figure 4. 4 shows thermogravimetric analysis (TGA) of DMOD, PXDA, and the semi-aromatic biobased PAs (DMOD-PXDA) produced under conventional and microwave heating. Higher thermal stability of the products in comparison with monomers indicated the formation of semi-aromatic polyamides. Microwave heating developed MH-PA (DMOD-PXDA) with a single-stage decomposition profile, whereas CH-PA (DMOD-PXDA) produced from the conventional heating process exhibited a double-stage decomposition profile. Less polydispersity in the polymer chains developed under microwave heating due to the fast initiation of the polymerization is potentially responsible for the observed phenomenon. Interestingly, 10 minutes microwave heating at

temperatures less than the conventional heating process created MH-PA (DMOD-PXDA) with comparable thermal stability to CH-PA (DMOD-PXDA). The 5 wt% ($T_{d, 5wt\%}$) decomposition of MH-PA (DMOD-PXDA) started at 373 °C and completed at roughly 490 °C (Table 4. 1). This result is in agreement with the reported decomposition temperatures of commercial polyamides (Levchik et al., 1999). CH-PA (DMOD-PXDA) showed less stability at temperatures lower than 440 °C but was more stable at higher temperatures (Table 4. 1). Indeed, CH-PA (DMOD-PXDA) showed its first weight loss step at ~355-430 °C and the second one between ~430-526 °C with around 10% residual left.

The thermal stability of the aliphatic biobased PA (DMOD-DETA) developed under conventional and microwave heating methods is also reported in Figure 4. 4. The $T_{d, 5wt\%}$ of CH-PA (DMOD-DETA) and MH-PA (DMOD-DETA) were 176 and 124 °C, respectively, which is less than the $T_{d, 5wt\%}$ of DMOD bio-diester of 211 °C (Table 4. 1). This could be due to the presence of residual oligomers or monomers in the final products as a result of rapid increase in the viscosity of the reaction media, which was also observable in polymers' ATR-FTIR results. Moreover, the thermal stability of CH-PA (DMOD-DETA) was generally higher than MH-PA (DMOD-DETA). The more gradual increase of viscosity in the conventionally-heated polycondensation media compared to the microwave-heated one can possibly explain this difference. Indeed, conventional heating provided fairly more time for the mass transfer of monomers on polymer chains promoting higher molecular weight polymers with better thermal stability. Overall, PAs (DMOD-DETA) had promising thermal stability where more than 70% of their weights tolerated temperatures higher than 400 °C. Both conventional and microwave polycondensed aliphatic polyamides entirely decomposed at temperatures higher than 500 °C.
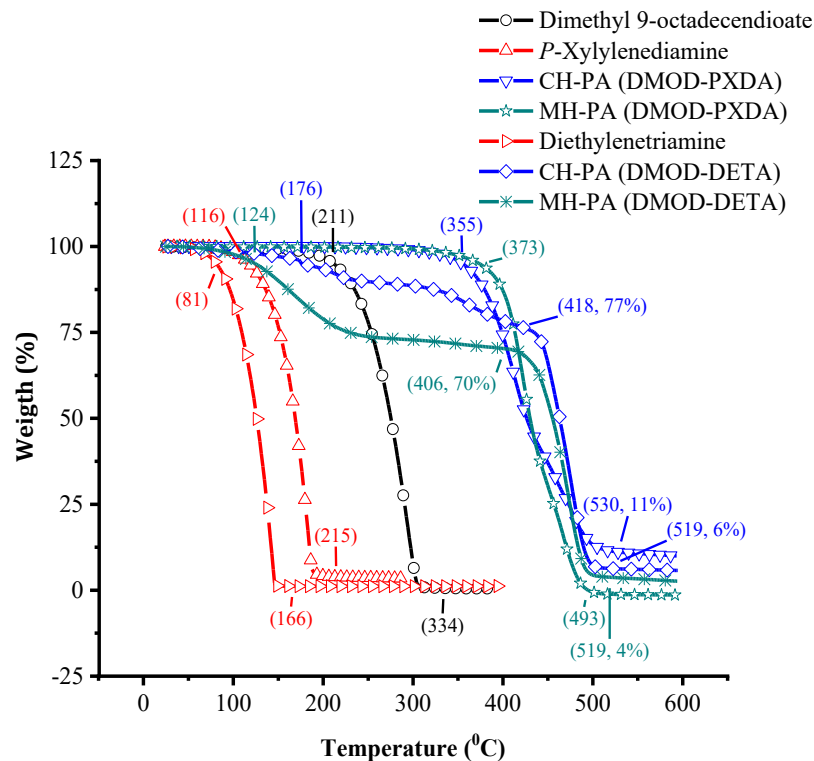
Figure 4. 4) TGA thermograms of dimethyl 9-octadecenedioate, *p*-Xylylenediamine, diethylenetriamine, biobased CH-PA (DMOD-PXDA), MH-PA (DMOD-PXDA), CH-PA (DMOD-DETA), and MH-PA (DMOD-DETA).

Thermal transitions of the biobased polyamides and monomers were also studied by DSC (Figure 4. 5). All polyamides revealed two melting points except for the aliphatic MH-PA (DMOD-DETA) (Table 4. 1). Less polydispersity in MH-PA (DMOD-DETA) compared to other polyamides may explain this phenomenon. Conventionally-heated polyamides exhibited the highest melting points as compared to the microwave-assisted polyamides. These data were in agreement with the final decomposition temperature of the polyamides measured by TGA, which could be due to the higher molecular weights of conventionally-heated polyamides as compared to their microwave-assisted counterparts.
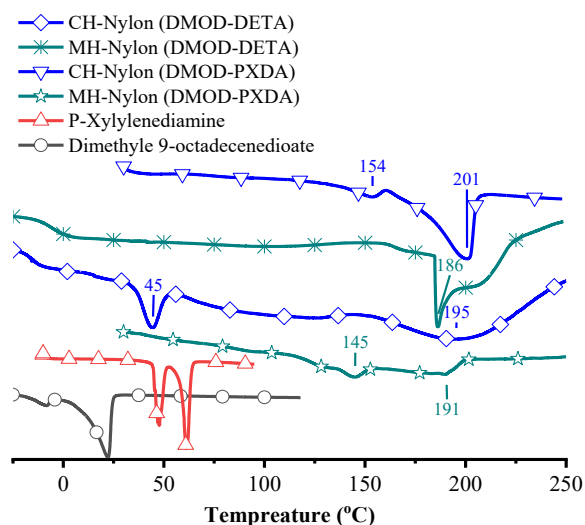
Figure 4. 5) DSC-thermograms of dimethyl 9-octadecenedioate, *p*-Xylylenediamine, biobased CH-PA (DMOD-PXDA), and MH-PA (DMOD-PXDA), CH-PA (DMOD-DETA), and MH-PA (DMOD-DETA).

4.2.4. Analysis of the crystalline structure of biobased PAs (DMOD-PXDA) and PAs (DMOD-DETA)

The WAXD analysis was performed to compare the effect of different heating processes on the crystalline structure of biobased polyamides. Figure 4. 6 represents the WAXD patterns of polyamides developed under conventional and microwave heating methods. While each of the polyamides exhibited different WAXD patterns, heating methods yielded comparable scattering patterns (Figure 4. 6).

The fitting profiles of the semi-aromatic biobased PAs (DMOD-PXDA) showed several reflections with no amorphous peaks for MH-PA (DMOD-PXDA) (Figure 4. S7 & 4. S8). The fitting profile of the semi-aromatic polyamides revealed diffraction peaks at $2\theta \sim8°$ indexed to 001, while a diffraction peak at $\sim12°$ was only observed for MH-PA (DMOD-PXDA) indexed to 002 plane (Jasinska et al., 2011a); (Pagacz et al., 2016). These somewhat broad peaks refer to the length of repeat units in the polymer (Pagacz et al., 2016). The 002 peak, which disappeared in CH-PA

(DMOD-PXDA) in favor of a broad peak at 2θ ~22° (light green peak, Figure 4. S7), represents the amorphous phase halo peak (Psarski et al., 2000). The hydrogen bonds within the 002 plane link the adjacent antiparallel chains in the α-phase crystal with a monoclinic structure and fully extended planar zigzag (Pagacz et al., 2016); (Winkler et al., 2014). Therefore, the conventional heating potentially developed CH-PA (DMOD-PXDA) without hydrogen bonds within the 002 plane (Figure 4. S7). There is another reflection located at 2θ ~22° (pink peak, Figure 4. S7) for CH-PA (DMOD-PXDA) representing the mesomorphic β-phase (Kaczmarczyk and Danuta, 1995). MH-PA (DMOD-PXDA) on the other hand, illustrates a peak located at 2θ ~21° characterizing the γ-phase (pink peak, Figure 4. S8). The hydrogen bonds in the γ-phase of polyamides are patterned between the parallel chains in a twisted conformation (Dasgupta et al., 1996); (Zhang et al., 2009). The 2θ ~21° in the XRD pattern of PA 6 is also attributed mainly to the diffraction of 001 plane while in the Kevlar 49 fiber, 2θ ~21° is assigned to the equatorial reflection of 200 plane (Holmes et al., 1955); (Arrieta et al., 2011); (Hindeleh and Abdo, 1989) . The reflection positioned at 2θ ~24° is the predominant reflection for TH-PA (DMOD-PXDA), and one of the reflections for MH-PA (DMOD-PXDA) which is assigned to α-phase (Figure 4. S7 & 4. S8) (Zhang et al., 2009); (Tao et al., 2019). This reflection has also been attributed to 002/202 and 200 reflection planes in the XRD patterns for the α-phases of PA 6 and Kevlar 49 fibers, respectively (Holmes et al., 1955); (Arrieta et al., 2011); (Hindeleh and Abdo, 1989). The peak of TH-PA (DMOD-PXDA) at 2θ ~24° is sharper and taller than the peak of MH-PA (DMOD-PXDA), indicating that the crystalline perfection of the polyamide α-phase is improved through the conventional heating (Zhang et al., 2009). The strong reflection at 2θ ~26° in fitting peaks of PAs (DMOD-PXDA) is also assigned to 060 plane. A similar result is reported for isotactic polypropylene and acrylic acid grafted isotactic polypropylene (Psarski et al., 2000). Another

broad peak, that was only observed in the XRD fitting profile of CH-PA (DMOD-PXDA) at 2θ ~49°, represented another kind of amorphous phase. The same peak is detected in the XRD pattern of PA 6,10 (Pagacz et al., 2016).
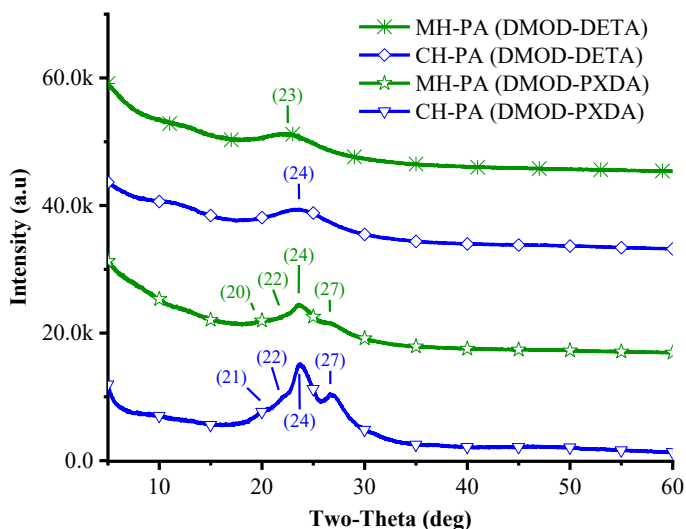
Figure 4. 6) Wide-angle X-ray diffraction patterns of biobased PAs (DMOD-PXDA) and PAs (DMOD-DETA) polymerized under conventional heating method (CH) or microwave heating method (MH).

With regard to the aliphatic biobased PAs (DMOD-DETA) fitting profiles, a strong reflection was found at 2θ ~12° for the polymers regardless of the heating method indexed to 002 (Figure 4. S9 & 4. S10) (Jasinska et al., 2011a); (Pagacz et al., 2016); (Zhang et al., 2009). CH-PA (DMOD-DETA) exhibited a characteristic peak at 2θ ~24° assigned to α-phase, whereas MH-PA (DMOD-DETA) reflected a peak at 2θ ~23° assigned to γ-phase. There is a disagreement about the 2θ ~23° characteristic peaks in literature. Although it is reported as the γ-phase reflection for PA 4.10, it is assigned to the α-phase for PA 6.6 (Jasinska et al., 2011a); (Liu et al., 2002). Finally, there is only one more peak at 2θ ~49° indicating an amorphous form in CH-PA (DMOD-DETA) (Figure 4. S9). Moreover, the apparent degree of crystallinity ($x_{c,WAXD}$) of polyamides was calculated as the

ratio of areas under the crystalline curves to the sum of the areas of both crystalline and amorphous peaks (Pagacz et al., 2016).

$$x_{c,WAXD} = \left(\frac{\Sigma A_{Crystal}}{\Sigma A_{Crystal} + \Sigma A_{Amorphous}} \right) \times 100 \qquad (3.1)$$

Polycondensation heating methods affected the apparent degree of crystallinity of the polyamides (Table 4. 1 and Figures 4. S7 to 4. S10). Interestingly, microwave irradiation led to the development of polyamides with 100% apparent degree of crystallinity whereas, conventional heating method resulted in 79.1% and 90.3% apparent degree of crystallinity in CH-PA (DMOD-PXDA) and CH-PA (DMOD-DETA), respectively.

Concluding, the polyamides in this study exhibited different crystalline structures. Overall, PAs (DMOD-PXDA) showed more diversity in the crystalline phases than PAs (DMOD-DETA). We observed that conventional heating supports the creation of more amorphous and α-crystal phases, while microwave irradiation develops more γ-crystal forms in these polyamides.

4.2.5. Thermomechanical properties of the biobased polyamide films

The films of the biobased polyamides were prepared using the compression molding method. The semi-aromatic PAs (DMOD-PXDA) were sandwiched between two steel plates covered with aluminum foil while uncovered steel plates were used to sandwich the aliphatic PAs (DMOD-DETA) due to their stickiness to the aluminum foil. Interesting, PAs (DMOD-DETA) also stuck to paper, glass, and wood but not to the latex gloves. Films were all made at 160 °C and 3000 pounds compression force, except for CH-PA (DMOD-PXDA), which required a significantly higher temperature (200 °C).
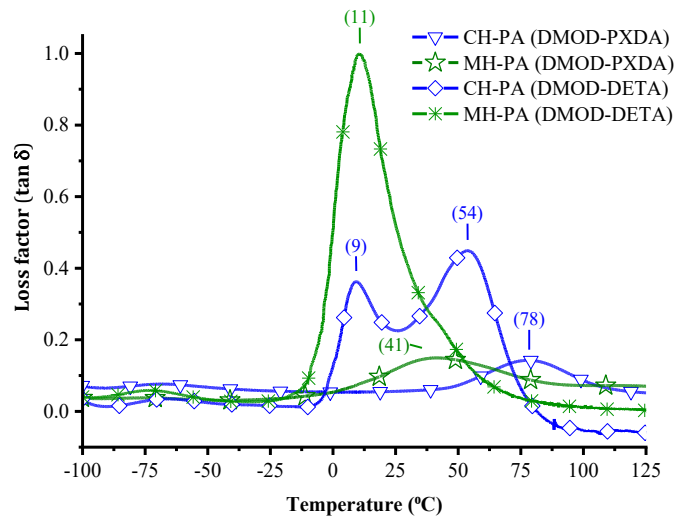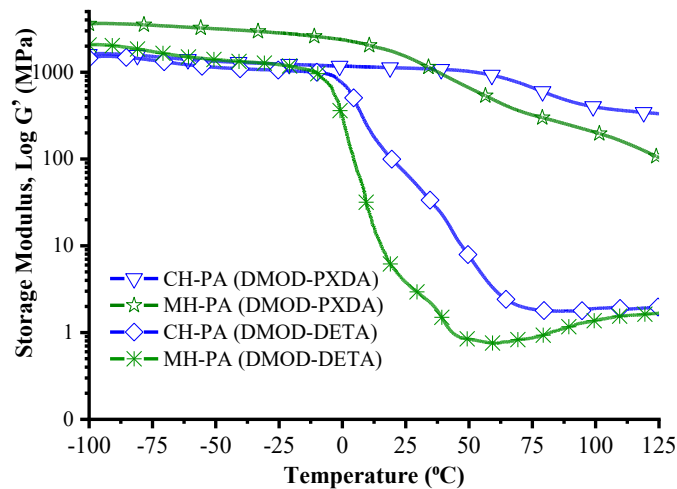
Figure 4. 7) (a) Mechanical loss factor (tan δ) and (b) Storage modulus (Log G') versus temperature of the biobased polyamide films produced under microwave and conventional heating processes.

The thermomechanical properties of the biobased polyamide films were investigated by DMA in a temperature range of -100 °C to +150 °C and frequency of 1 Hz (Figure 4. 7). There was a distinct difference in the loss factor (tan δ) and storage modulus of the compression-molded polyamide

films (Figure 4. 7.a & 4. 7.b). The smaller loss factor (peak height) of the films prepared from PAs (DMOD-PXDA) compared to the ones developed from PAs (DMOD-DETA) indicates the higher elasticity of PA (DMOD-PXDA) films (Figure 4. 7.a). This could be due to the higher molecular weights of PAs (DMOD-PXDA) compared to PAs (DMOD-DETA) as reflected in their superior thermal properties as well. The higher loss factor of the PA (DMOD-DETA) films could also be due to the plasticizing effect of the residual oligomers and monomers in the polymer structures which can increase segmental mobility (Liu et al., 2015).

The observed peaks of polyamide films in the loss factor graph also indicated the presence of β-transition and α or glass transition (T_g) in the polyamide films (Figure 4. 7.a). The β-transition occurred for all the polyamide films at around -70 °C except for MH-PA (DMOD-PXDA) film. The generation of β-transition in polyamides has been attributed to several factors including uncoordinated movement of uncrystallized diamines in rigid rod polyamides (Arnold et al., 1993), localized movement within the amide segments or the movement of very large side-chains in the polymer (Heijboer, 1977); (Morgan and Nielsen, 1974) as well as the low molecular weight chains in the bulk polyamides (Le Huy and Rault, 1994). In addition to the increase in molecular weight of polymer chains, polycondensation reactions during annealing under vacuum result in the complete disappearance of β-transitions in the polyamides (Le Huy and Rault, 1994).

The loss factor of CH-PA (DMOD-PXDA) displayed an α-transition at 78 °C nearly twice the α-transition (41 °C) of MH-PA (DMOD-PXDA) (Figure 4. 7.a & Table 4. 1). This is potentially due to the applied higher temperature (205 °C) and better homogenization of the reaction mixture in conventional heating process allowing the formation of polymer chains with higher molecular weights and T_g.

The PA (DMOD-DETA) films exhibited close α-transition temperatures (Figure 4. 7.a & Table 4. 1). CH-PA (DMOD-DETA) film showed an α-transition peak at 9 °C while this peak was observed at 11°C for MH-PA (DMOD-DETA) film. CH-PA (DMOD-DETA) film also exhibited another peak at 54 °C potentially due to the melting of low molecular weight polymer chains in its structure. The melting point of these low molecular weight polymer chains in CH-PA (DMOD-DETA) was 45 °C when measured by DSC (Figure 4. 5 & Table 4. 1).

Table 4. 1) Thermal properties of PAs (DMOD-PXDA) and PAs (DMOD-DETA) produced under conventional and microwave heating processes.

Thermal parameters	CH-PA (DMOD-PXDA)	MH-PA (DMOD-PXDA)	CH-PA (DMOD-DETA)	MH-PA (DMOD-DETA)
T_m (°C)	154-201	145-191	45-195	186
$T_{d, 5 wt\%}$ (°C)	355	373	176	124
T_g (°C, from DMA)	78	41	9	11
Degree of crystallinity	79.1%	100%	90.3%	100%

According to the storage modulus graph, the films prepared from semi-aromatic polyamides showed higher storage modulus than the ones from the linear polyamides. In fact, PA (DMOD-PXDA) films store energy more elastically compared to PA (DMOD-DETA) films. This is the classical outcome of insertion of the benzene ring into the backbone of polyamide chains (Haddou et al., 2018). Moreover, microwave heating created the biobased polyamides with different behaviors before and after their α-transition (Figure 4. 7.b). Microwave generated polyamides with higher storage modulus at temperatures below their α-transition when compared with the conventionally-heated polyamides. However, an utterly reversed behavior was observed at temperatures higher than their α-transition. This phenomenon can be related to the highly crystalline structure of the microwave-derived polyamides as supported by the WAXD and thermal data, their low polydispersity, and low molecular weight. Interestingly, the storage modulus of

MH-PA (DMOD-PXDA) film at the temperatures less than its T_g (41 °C) was also significantly higher than that for other polyamide films (Figure 4. 7.b). The highly crystalline structure and low dispersity of CH-PA (DMOD-PXDA) could explain this phenomenon.

4.2.6. **Mechanical properties of biobased PA (DMOD-PXDA) and PA (DMOD-DETA) films**

The mechanical properties of the polyamide films, including tensile strength (MPa) and percent elongation at break, are presented in Table 4. 2. The representative stress-strain graphs of the polyamide films are also illustrated in Figure 4. 8. Typical stress-strain graphs of the semi-aromatic biobased PA (DMOD-PXDA) films are the characteristics of a brittle thermoplastic polymer (Balani et al., 2014). There was not a significant difference between the tensile properties of PA (DMOD-PXDA) films created under different heating and molding conditions (Table 4. 2). CH-PA (DMOD-PXDA) film, however, displayed a significant higher percent elongation at break (22.11%) compared to MH-PA (DMOD-PXDA) film (7.99%). The presence of lower molecular weight chains and less crystallinity in CH-PA (DMOD-PXDA) could potentially explain these phenomena. The reduction in intermolecular bonds between polymer matrices as a result of the presence of low molecular weight chains and less crystallinity in bulk polymers promotes chain mobility and provides higher percent elongation at break (Liu et al., 2015).

Table 4. 2) Mechanical properties of films from the biobased PAs (DMOD-PXDA) and PAs (DMOD-DETA) produced under conventional and microwave heating processes.*

Mechanical parameters	CH-PA (DMOD-PXDA)	MH-PA (DMOD-PXDA)	CH-PA (DMOD-DETA)	MH-PA (DMOD-DETA)
Tensile strength (MPa)	18.45 ± 1.23^a	20.29 ± 3.50^a	1.85 ± 0.15^b	0.68 ± 0.08^c
Elongation at break (%)	22.11 ± 1.57^c	7.99 ± 1.55^d	71.69 ± 3.91^b	128.58 ± 4.38^a

*Means (n= 3) in same row with different letters are significantly different (p < 0.05). Data are means ± SD.

Overall, the tensile strength of PA (DMOD-PXDA) films was significantly higher than the aliphatic biobased PA (DMOD-DETA) films while the percent elongation at break of PA (DMOD-DETA) films was considerably higher than PA (DMOD-PXDA) films. The steric hindrance of rigid aromatic rings in the backbone of PAs (DMOD-PXDA) could be the contributing factor to their higher stiffness compared to PAs (DMOD-DETA) (Polk et al., 2004).

The mechanical properties of PA (DMOD-DETA) films were significantly different. CH-PA (DMOD-DETA) film showed a significantly higher tensile strength (1.85 MPa) and lower percent elongation at break (71.69%) in comparison with MH-PA (DMOD-DETA) film. The higher molecular weight of CH-PA (DMOD-DETA) compared with MH-PA (DMOD-DETA) could explain this phenomenon.
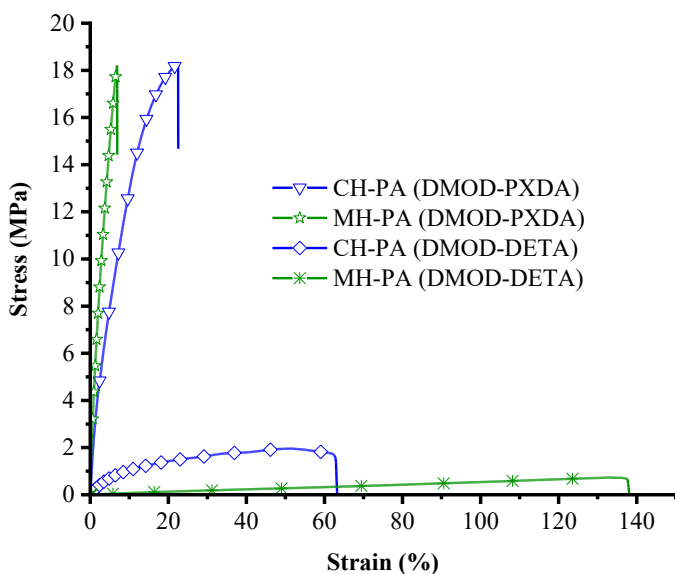
Figure 4. 8) Representative stress-strain curves of the biobased PAs (DMOD-PXDA) and PAs (DMOD-DETA) produced under conventional and microwave heating processes.

4.3. Conclusion

Two novel biobased polyamides were synthesized through the polycondensation of DMOD (a canola oil-derived diester) with a PXDA diamine and a DETA triamine under conventional and microwave heating processes. Both the heating methods and type of amines had a considerable effect on the properties of the produced biobased polyamides (PAs (DMOD-PXDA) & PAs (DMOD-DETA)). Generally, the microwave heating developed polyamides with a higher crystalline structure, lower polydispersity, but also lower melting temperature in comparison with the conventional heating. Moreover, while the microwave heating promoted less diversity in the crystalline phases of polyamides with the γ-phase as the main crystalline form, the conventional heating resulted in the formation of polyamides with more diversity in their crystalline phases. In addition, PAs (DMOD-PXDA) with the aromatic diamine (PXDA) units came out with more variability in crystalline phases compared to PAs (DMOD-DETA) with the aliphatic triamine (DETA) units in their polymer chains.

The thermomechanical analyses of the polyamide films revealed that the heating method did not substantially change the β-transition temperature and T_g of the very flexible PA (DMOD-DETA) films. Microwave heating, however, had a significant effect on the β-transition temperature and T_g of the brittle thermoplastic PA (DMOD-PXDA) films. MH-PA (DMOD-PXDA) film illustrated a T_g of almost 37 °C less than the T_g of CH-PA (DMOD-PXDA) film (78 °C) without β-transition in its polymer chains. Moreover, the storage modulus of the semi-aromatic PA (DMOD-PXDA) films was higher than the aliphatic PA (DMOD-DETA) films. Microwave heating also differentially affected the storage modulus of polyamide chains below and above their Tg: microwave polycondensed polyamides in comparison with their conventional polycondensed

counterparts exhibited higher storage modulus below their T_g and lower storage modulus above their T_g.

Concerning the mechanical properties, although the different heating methods did not result in a significant difference in the tensile strength (MPa) of PA (DMOD-PXDA) films, conventional heating significantly increased the percent elongation at break of CH-PA (DMOD-PXDA) film. All the mechanical properties of the aliphatic PA (DMOD-DETA) films, on the other hand, were significantly affected by the heating method. CH-PA (DMOD-DETA) film showed higher tensile strength but lower percent elongation at break relative to MH-PA (DMOD-DETA) film. Finally, the stirring efficacy during polymerization seems to be an important parameter in addition to the heating method, especially in the polymerization of polyamides with the aliphatic DETA triamine in their backbone.

References:

Ahmadi, R., Ullah, A., 2017. Microwave-assisted rapid synthesis of a polyether from a plant oil derived monomer and its optimization by Box-Behnken design. RSC Adv. 7, 27946–27959. https://doi.org/10.1039/c7ra03278a

Arnold, F.E., Bruno, K.R., Shen, D., Eashoo, M., Lee, C.J., Harfus, F.W., Cheng, S.D., 1993. The origin of beta relaxations in segmented rigid-rod polyimide and copolyimide films. Polym. Eng. Sci. 33, 1373–1380.

Arrieta, C., David, E., Dolez, P., Vu-Khanh, T., 2011. X-ray diffraction, raman, and differential thermal analyses of the thermal aging of a kevlar -pbi blend fabric. Polym. Compos. 32, 362–367. https://doi.org/https://doi.org/10.1002/pc.21041

Balani, K., Verma, V., Narayan, A., Roger, A., 2014. Biosurfaces: A materials science and

engineering perspective, First edit. ed. John Wiley & Sons, Inc. https://doi.org/https://doi.org/10.1002/9781118950623.app1

Coleman, M.M., Skrovanek, D.J., Painter, P.C., 1986. Hydrogen bonding in polymers : 111 further infrared temperature studies of polyamides. Makromol. Chem., Macromol. Symp 5, 21–33. https://doi.org/10.1021/ma00151a006

Dasgupta, S., Hammond, W.B., Goddard, W.A., 1996. Crystal structures and properties of nylon polymers from theory. J. Am. Chem. Soc. 118, 12291–12301. https://doi.org/10.1021/ja944125d

Firdaus, M., Meier, M.A.R., 2013. Renewable polyamides and polyurethanes derived from limonene. Green Chem. 15, 370–380. https://doi.org/10.1039/c2gc36557j

Gilbert, M., 2017. Aliphatic polyamides, in: brydson's plastics materials. Elsevier Ltd., pp. 487–511. https://doi.org/https://doi.org/10.1016/B978-0-323-35824-8.00018-9

Girardon, V., Correia, I., Tessier, M., Marchal, E., 1998. Characterization of functional aliphatic oligoamides using n-trifuoroacetylation- i. nmr aanlysis. Eur. Polym. J. 34, 363–380. https://doi.org/10.1016/S0014-3057(97)00141-9

Haddou, G., Roggero, A., Dandurand, J., Dantras, E., Ponteins, P., Lacabanne, C., 2018. Dynamic relaxations in a bio-based polyamide with enhanced mechanical modulus. J. Appl. Polym. Sci. 135, 2–7. https://doi.org/10.1002/app.46846

Heijboer, J., 1977. Secondary loss peaks in glassy amorphous polymers. Int. J. Polym. Mater. 6, 11–37. https://doi.org/10.1080/00914037708075218

Hindeleh, A.M., Abdo, S.M., 1989. Effects of annealing on the crystallinity and

microparacrystallite size of Kevlar 49 fibres. Polymer (Guildf). 30, 218–224.

Holmes, D.R., Bunn, C.W., Smith, D.J., 1955. The crystal structure of polycaproamide: Nylon 6. J. Polym. Sci. 17, 159–177. https://doi.org/10.1002/pol.1955.120178401

Huf, S., Krügener, S., Hirth, T., Rupp, S., Zibek, S., 2011. Biotechnological synthesis of long-chain dicarboxylic acids as building blocks for polymers. Eur. J. Lipid Sci. Technol. 113, 548–561. https://doi.org/10.1002/ejlt.201000112

Jasinska, L., Villani, M., Wu, J., Van Es, D., Klop, E., Rastogi, S., Koning, C.E., 2011a. Novel, fully biobased semicrystalline polyamides. Macromolecules 44, 3458–3466. https://doi.org/10.1021/ma200256v

Jasinska, L., Villani, M., Wu, J., Van Es, D., Klop, E., Rastogi, S., Koning, C.E., 2011b. Novel, fully biobased semicrystalline polyamides. Macromolecules 44, 3458–3466. https://doi.org/10.1021/ma200256v

Jin, L., Geng, K., Arshad, M., Ahmadi, R., Ullah, A., 2017. Synthesis of Fully Biobased Polyesters from Plant Oil. ACS Sustain. Chem. Eng. 5, 9793–9801. https://doi.org/10.1021/acssuschemeng.7b01668

Kaczmarczyk, B., Danuta, S., 1995. Hydrogen bonds in poly(ester amide)s and their model compounds. Polymer (Guildf). 36, 5019–5025. https://doi.org/10.1016/0032-3861(96)81631-4

Kiesewetter, M.K., Scholten, M.D., Kirn, N., Weber, R.L., Hedrick, J.L., Waymouth, R.M., 2009. Cyclic guanidine organic catalysts: What is magic about triazabicyclodecene? J. Org. Chem. 74, 9490–9496. https://doi.org/10.1021/jo902369g

Kotzebue, L.R.V., De Oliveira, J.R., Da Silva, J.B., Mazzetto, S.E., Ishida, H., Lomonaco, D., 2018. Development of fully biobased high-performance bis-benzoxazine under environmentally friendly conditions. ACS Sustain. Chem. Eng. 6, 5485–5494. https://doi.org/10.1021/acssuschemeng.8b00340

Le Huy, H.M., Rault, J., 1994. Remarks on the a and .beta. transitions in swollen polyamides. Polymer (Guildf). 35, 136–139.

Levchik, S. V, Weil, E.D., Lewin, M., 1999. Thermal decomposition of aliphatic nylons. Polym. Int. 48, 532–557. https://doi.org/10.1002/(SICI)1097-0126(199907)48:7<532::AID-PI214>3.0.CO;2-R

Liu, K., Madbouly, S.A., Schrader, J.A., Kessler, M.R., Grewell, D., Graves, W.R., 2015. Biorenewable polymer composites from tall oil-based polyamide and lignin-cellulose fiber. J. Appl. Polym. Sci. 132, 42592. https://doi.org/https://doi.org/10.1002/app.42592

Liu, X., Wu, Q., Berglund, L.A., 2002. Polymorphism in polyamide 66/clay nanocomposites. Polymer (Guildf). 43, 4967–4972. https://doi.org/10.1016/S0032-3861(02)00331-2

Martino, L., Basilissi, L., Farina, H., Ortenzi, M.A., Zini, E., Di Silvestro, G., Scandola, M., 2014. Bio-based polyamide 11: Synthesis, rheology and solid-state properties of star structures. Eur. Polym. J. 59, 69–77. https://doi.org/10.1016/j.eurpolymj.2014.07.012

Molina-Gutierrez, S., Ladmiral, V., Bongiovanni, R.M., Caillol, S., Lacroix-Desmazes, P., 2019. Radical polymerization of biobased monomers in aqueous dispersed media. Green Chem. 21, 36–53. https://doi.org/10.1039/C8GC02277A

Morgan, R.J., Nielsen, L.E., 1974. The dynamic mechanical properties of polymers at cryogenic

temperatures. J. Macromol. Sci. Part B 9, 239–253. https://doi.org/10.1080/00222347408212192

Mutlu, H., Meier, M.A.R., 2009. Unsaturated PA X,20 from renewable resources via metathesis and catalytic amidation. Macromol. Chem. Phys. 210, 1019–1025. https://doi.org/10.1002/macp.200900045

Nakajima, H., Dijkstra, P., Loos, K., 2017. The recent developments in biobased polymers toward general and engineering applications: Polymers that are upgraded from biodegradable polymers, analogous to petroleum-derived polymers, and newly developed. Polymers (Basel). 9, 1–26. https://doi.org/10.3390/polym9100523

Nguyen, H.T.H., Qi, P., Rostagno, M., Feteha, A., Miller, S.A., 2018. The quest for high glass transition temperature bioplastics. J. Mater. Chem. A 6, 9298–9331. https://doi.org/10.1039/c8ta00377g

Oilseeds: World Markets and Trade., 2019. Oilseeds: World Markets and Trade. [WWW Document]. URL https://apps.fas.usda.gov/psdonline/circulars/oilseeds.pdf) (accessed 2019-05-13

Oliva, R., Ortenzi, M.A., Salvini, A., Papacchini, A., Giomi, D., 2017. One-pot oligoamides syntheses from l-lysine and l-tartaric acid. RSC Adv. 7, 12054–12062. https://doi.org/10.1039/c7ra00676d

Pagacz, J., Raftopoulos, K.N., Leszczyńska, A., Pielichowski, K., 2016. Bio-polyamides based on renewable raw materials: Glass transition and crystallinity studies. J. Therm. Anal. Calorim. 123, 1225–1237. https://doi.org/10.1007/s10973-015-4929-x

Peplow, M., 2016. The plastics revolution: how chemists are pushing polymers to new limits. Nature 536, 266–268.

Polk, M., Vigo, T.L., Albin Turbak, F., 2004. High performance fibers. Encycl. Polym. Sci. Technol. https://doi.org/https://doi.org/10.1002/0471440264.pst523

Psarski, M., Pracella, M., Galeski, A., 2000. Crystal phase and crystallinity of polyamide 6/functionalized polyolefin blends. Polymer (Guildf). 41, 4923–4932. https://doi.org/10.1016/S0032-3861(99)00720-X

Sabot, C., Kumar, K.A., Meunier, S., Mioskowski, C., 2007. A convenient aminolysis of esters catalyzed by 1,5,7-triazabicyclo[4.4.0]dec-5-ene (TBD) under solvent-free conditions. Tetrahedron Lett. 48, 3863–3866. https://doi.org/10.1016/j.tetlet.2007.03.146

Shah, F.U., Akhtar, F., Khan, M.S.U., Akhter, Z., Antzutkin, O.N., 2016. Solid-state 13C, 15N and 29Si NMR characterization of block copolymers with CO2 capture properties. Magn. Reson. Chem. 54, 734–739. https://doi.org/10.1002/mrc.4440

Stempfle, F., Ortmann, P., Mecking, S., 2016. Long-chain aliphatic polymers to bridge the gap between semicrystalline polyolefins and traditional polycondensates. Chem. Rev. 116, 4597–4641. https://doi.org/10.1021/acs.chemrev.5b00705

Stempfle, F., Quinzler, D., Heckler, I., Mecking, S., 2011. Long-chain linear C19 and C23 monomers and polycondensates from unsaturated fatty acid esters. Macromolecules 44, 4159–4166. https://doi.org/10.1021/ma200627e

Tao, L., Liu, K., Li, T., Xiao, R., 2019. Preparation and properties of biobased polyamides based on 1,9-azelaic acid and different chain length diamines, Polymer Bulletin. Springer Berlin

Heidelberg. https://doi.org/10.1007/s00289-019-02791-2

Türünç, O., Firdaus, M., Klein, G., Meier, M.A.R., 2012. Fatty acid derived renewable polyamides via thiol-ene additions. Green Chem. 14, 2577–2583. https://doi.org/10.1039/c2gc35982k

Ullah, A., Arshad, M., 2018. Conversion of lipides olefins. US Pat., US 10,138,430 B2, 2018. US 10 , 138 , 430 B2.

Ullah, A., Arshad, M., 2017. Remarkably efficient microwave-assisted cross-metathesis of lipids under solvent-free conditions. ChemSusChem 10, 2167–2174. https://doi.org/10.1002/cssc.201601824

Vink, E.T.H., Ra'bago, K.R., Glassner, D.A., Gruber, P.R., 2003. Applications of life cycle assessment to NatureWorks TM polylactide (PLA) production 80, 403–419. https://doi.org/10.1016/S0141-3910(02)00372-5

Winkler, M., Meier, M.A.R., 2014. Olefin cross-metathesis as a valuable tool for the preparation of renewable polyesters and polyamides from unsaturated fatty acid esters and carbamates. Green Chem. 16, 3335–3340. https://doi.org/10.1039/c4gc00273c

Winkler, M., Steinbiß, M., Meier, M.A.R., 2014. A more sustainable Wohl-Ziegler bromination: Versatile derivatization of unsaturated FAMEs and synthesis of renewable polyamides. Eur. J. Lipid Sci. Technol. 116, 44–51. https://doi.org/10.1002/ejlt.201300126

Xue, X., Jia, Q.X., Zhao, G.L., 2013. Preparation and Properties of DCP-Crosslinked Biobased Polyamide. Adv. Mater. Res. 634–638, 1037–1043. https://doi.org/10.4028/www.scientific.net/AMR.634-638.1037

Zhang, C., Liu, Y., Liu, S., Li, H., Huang, K., Pan, Q., Hua, X., Hao, C., Ma, Q., Lv, C., Li, W.,

Yang, Z., Zhao, Y., Wang, D., Lai, G., Jiang, J., Xu, Y., Wu, J., 2009. Crystalline behaviors and phase transition during the manufacture of fine denier PA6 fibers. Sci. China, Ser. B Chem. 52, 1835–1842. https://doi.org/10.1007/s11426-009-0242-5

Zhang, K., Nelson, A.M., Talley, S.J., Chen, M., Margaretta, E., Hudson, A.G., Moore, R.B., Long, T.E., 2016. Non-isocyanate poly(amide-hydroxyurethane)s from sustainable resources. Green Chem. 18, 4667–4681. https://doi.org/10.1039/c6gc01096b

Zhang, L., Huang, M., Yu, R., Huang, J., Dong, X., Zhang, R., Zhu, J., 2014. Bio-based shape memory polyurethanes (Bio-SMPUs) with short side chains in the soft segment. J. Mater. Chem. A 2, 11490–11498. https://doi.org/10.1039/c4ta01640h

CHAPTER 5: ONE-POT SYNTHESIS OF A LONG-CHAIN, UNSATURATED BIOPOLYESTER FROM PLANT OIL-DERIVED MONOMERS

5. Introduction

Aliphatic polycondensates such as polyesters are a group of engineering plastics with superior properties compared to polyolefins due to their high thermal and mechanical stability, degradability, compostability, and biocompatibility (Quinzler and Mecking 2010). The high density of polar groups in polyesters, however, has a negative impact on their water resistance and processability: high processing temperatures are required for polyesters synthesis (Stempfle, Ortmann, and Mecking 2016). Long-chain aliphatic polyesters are attractive polymers having both the long aliphatic chain and functional esters groups in their structure. Long-chain aliphatic polyesters can be crystallized via van der Walls interactions between their aliphatic chains. Despite this fact, the long-chain aliphatic polyesters can still tolerate high thermal stresses and mechanical tensions due to the polar groups' presence in the structure (Song et al. 2019). Therefore, there is a growing interest in developing long-chain aliphatic polyesters, especially from renewable resources, to bridge the gap between conventional polyolefins and polycondensates and empower sustainable growth towards green bioplastics development.

Plant oils have a great potential to produce linear α, ω-difunctional monomers. Therefore, they have been considered one of the most promising feedstocks to produce long-chain monomers and polymers. Catalytic conversion of fatty acids and plant oils to long-chain α, ω-difunctional monomers require organic solvents, high catalyst loading for efficient conversions, and purified methyl esters (Marinescu et al., 2009); (Thomas et al., 2011); (van der Klis et al., 2012). Our group

has recently established an efficient, rapid, and solvent-free method for transforming plant oils into long-chain olefins such as 1-decene, methyl 9-decenoate, and dimethyl 9-octadecenedioate (DMOD) (Ullah and Arshad, 2017); (Ullah and Arshad, 2018) (Scheme 2. 16). These monomers have been used to produce several types of biobased polymers, including polyester (Jin et al., 2017), polyamide (Winkler and Meier, 2014), and polyurethane (Zhang et al., 2014). However, many polymers from α, ω-difunctional monomers still require tedious synthesis processes yet exhibit inferior physicochemical properties compared to traditionally condensate polymers. Therefore, developing long-chain aliphatic polycondensates with adequate mechanical properties requires further investigations.

In this study, we conceptualized one-pot polymerization of DMOD, its acid (9-octadecenedioic acid), and 1,2-epoxydecane as a green approach for synthesizing a long-chain, unsaturated biopolyester. DMOD and 9-octadecenedioic acid provide the unsaturated, long-chain aliphatic parts of the biopolyester. The unsaturated motifs are the key advantage for the post-polymerization functionalization of the biopolyester and the attachment of side chains to the polymer's backbone. Acid-epoxy addition of 9-octadecenedioic acid and 1,2-epoxydecane was first studied under conventional and microwave heating to synthesize a novel biodiol, (bis(2-hydroxydecyl) octadec-9-enedioate (BHOD). The biodiol's condensation with DMOD was continued by adding DMOD and catalyst to the same pot right after BHOD synthesis. The polycondensation reaction was carried out under conventional or microwave heating to generate novel long-chain, unsaturated biopolyester (BPs (DMOD-BHOD)).

The resulting biobased diol and long-chain polyester were structurally characterized by Fourier transform infrared spectroscopy (FTIR), proton nuclear magnetic spectroscopy (^{1}HNMR), and gel permeation chromatography (GPC). The thermal properties of monomers and the long-chain,

unsaturated biopolyester were also obtained using differential scanning calorimetry (DSC) and thermogravimetric analysis (TGA).

5.1. Experiment section

5.1.1. Materials

HCl (36.5-38.0%) was purchased from Fisher chemicals. Sodium hydroxide ($\geq$ 97.0%), sodium sulfate (anhydrous, $\geq$99.0), tin (II) chloride ($\geq$ 98.0%), chloroform-d (99.8 atom %), methanol ($\geq$ 99.8%), and tetrahydrofuran ($\geq$ 99.0%) were purchased from Sigma-Aldrich and used without further purification. 1,2-epoxydecane and dimethyl 9-octadecenedioate (DMOD) were produced based on our reported procedures (Ahmadi and Ullah, 2017), (Ullah and Arshad, 2017).

1,2-epoxydecane: ^{1}H NMR (400 MHz, CDCl3): δ 2.95–2.82 (m, 1H), 2.73 (dd, J = 5.0, 4.0 Hz, 1H), 2.44 (dd, J = 5.1, 2.7 Hz, 1H), 1.64-1.16 (m, 14H), 0.89 (dt, J = 9.7, 7.3 Hz, 3H). IR: 2956 cm^{-1}, 2923 cm^{-1}, 2854 cm^{-1}, 1464 cm^{-1}, 1260 cm^{-1}, 1129 cm^{-1}, 916 cm^{-1}, 833 cm^{-1} (epoxyring groups). The purity of 1,2-epoxydecane was ~94% (Figure 5. S1).

Dimethyl 9-octadecenedioate (DMOD): ^{1}H NMR (400 MHz, CDCl$_3$, δ in ppm): δ 4.82–5.88 (m, 2H, = CH−), 3.66-3.71 (s, 6H, −OCH$_3$), 2.28-2.36 (t, 4H, −CH$_2$CO−), 1.94–2.04 (m, 4H, = CHCH$_2$−), 1.59-1.67 (m, 4H), 1.12-1.47 (m, 16H). IR: 1736 (s, C=O), 969 (m, Trans C=C), and 720 cm^{-1} (m, Cis C=C). The purity of DMOD was ~91% (Figure 5. S2).

5.1.2. Synthesis of 9-octadecenedioic acid

Dimethyl 9-octadecenedioate (5.87 mmol, 2.00 g) was suspended in methanol (25 mL) and heated to 75 °C in a three-neck round bottom flask equipped with a magnetic stir bar. Sodium hydroxide (37.00 mmol, 1.48 g) was then slowly added to the solution under vigorous stirring and refluxed for 2 hours with more methanol (25 mL) addition. After adding more sodium hydroxide (32.89

mmol, 1.32 g), the mixture was refluxed overnight, and reaction completion was confirmed using TLC. A white to yellow solid material was obtained after cooling the suspension to room temperature and solvent removal in vacuo. The produced solid material was suspended in water (50 mL) and acidified to pH= 2 by adding 5 N hydrochloric acid to precipitate 9-octadecenedioic acid. Finally, the diacid was filtered, washed with water, and recrystallized from toluene to give a white solid with 87% yield (Figure 5. S3).

5.1.3. One-pot synthesis of long-chain BPs (DMOD-BHOD) under conventional heating

A mixture of 9-octadecenedioic acid (6.40 mmol, 2.00 gr) and 1,2-epoxydecane (12.80 mmol, 2.00 gr) was mixed in a round bottom flask (50 mL) with a magnetic stirrer. The sealed flask was preheated at 80 °C in a water bath while purged with nitrogen for 10 min. The flask was then immersed in a silicon oil bath at 150 °C for 3 hours to obtain the BHOD biodiol (Scheme 5. 1. a). the DMOD (5.59 mmol, 1.90 gr) and the catalyst ($SnCl_2$) (0.11 mmol, 0.021 gr) were then added to the biodiol, and the reaction was continued at the same temperature under a high vacuum (0.1 bar) for 16 hours. The obtained light brown to brown rubbery polyesters was washed with THF and dried before further analysis (Scheme 5. 2.b). The yield of the reaction was 77%.

5.1.4. One-pot synthesis of long-chain BPs (DMOD-BHOD) under microwave heating

9-octadecenedioic acid (6.40 mmol, 2.00 gr) and 1,2-epoxydecane (12.80 mmol, 2.00 gr) were put in a 10 mL microwave glass vial with a magnetic stir bar. The sealed vial was preheated at 80 °C in a water bath while purged with nitrogen for 10 min. The vial was then placed in a closed-vessel-mode microwave reactor (CEM-Discover, 120 V, Matthews, USA) equipped with an infrared temperature sensor (maximum pressure = 250 psi, maximum power = 280 W) at 150 °C for 30 min to synthesize the BHOD biodiol (Scheme 5. 1. a). The DMOD (5.59 mmol, 1.90 gr) and the catalyst ($SnCl_2$) (0.11 mmol, 0.021 gr) were mixed with the biodiol, and the polymerization was

followed using the microwave reactor in an open-vessel mode. While the temperature and power were still set up at 150 °C and 250 W, the reaction was done under a high vacuum (0.1 bar).

5.1.5. **Characterization**

Attenuated Total Reflectance-Fourier Transform Infrared (ATR-FTIR) Analysis. A Bruker Alpha FTIR spectrophotometer (Bruker Optics, Esslingen, Germany) supplied with a single bounce diamond ATR crystal was employed to perform FTIR experiments. The instrument was set up to collect the spectra at a resolution of 4 cm^{-1} over the range of 410-4000 cm^{-1}. The background signals were corrected by scanning the clean ATR crystal before applying and receiving a sample spectrum. The instrument scanned each sample 16 times to obtain an average signal using the OPUS software (Bruker version 6.5). Finally, the Nicolet Omnic software (version 8) was used to analyze the resulting spectrum.

Gel permeation chromatography (GPC). The molecular weight ($\bar{M}_w$) and polydispersity (PDI) of the BPs (DMOD-BHOD) were determined using gel permeation chromatography (GPC). The GPC system was equipped with a Phenogel^{TM} 5μm 10E4 Å GPC column (300 × 4.6 mm ID, Phenomenex Inc.). An isocratic Agilent 1100 pump (Agilent Technologies; CA) equipped with an evaporative light scattering detector (Alltech ELSD 2000, Mandel Scientific Company, Canada) was used. Samples were dissolved in toluene at the concentration of 0.5 mg mL^{-1}, the toluene flow rate was 0.35 mL min^{-1}, and the injection volume was 10 mL. Calibration was done against polystyrene standards.

Nuclear Magnetic Resonance (NMR). A Varian Inova spectrometer (Varian, CA) was used to collect the ^{1}HNMR spectra of samples at 400 MHz and 25.9 °C. All samples were dissolved in

chloroform-d (CDCl₃) before obtaining their ^{1}HNMR spectrum except for the biopolyester, which was dissolved in Toluene-d8.

Differential Scanning Calorimetry (DSC) Analysis. DSC experiments were conducted using a 2920 Modulated DSC (TA Instrument, USA). Samples (4.0- 6.0 mg) were first equilibrated at a temperature less than their melting point and then heated at a scan rate of 3 °C min^{-1} starting from the equilibrated temperature. The heat flow and instrument temperature were calibrated using pure indium. DSC profiles of the 2nd heating cycle were selected to eliminate the material's thermal history.

Thermogravimetric Analysis (TGA). Samples' decomposition was analyzed using a TGA Q50 instrument (TA Instruments, DE, USA). Weight loss/thermal behavior of samples (13.0-20.0 mg) was analyzed over the range of 10- 600 °C, at a constant heating rate of 10 °C min^{-1} under 60 mL min^{-1} nitrogen flow. Data acquisition and analysis were executed using the TA universal analysis software. The temperature at which 5% weight loss or degradation occurred in each sample ($T_{d,5wt\%}$) was considered the initial decomposition temperature of that particular sample.

5.2. Results and discussion

5.2.1. Synthesis of BPs (DMOD-BHOD)

The study's prime objective was to synthesize and characterize a biopolyester from two different canola oil-derived monomers, DMOD and 1-decene. To reach this goal, we first converted 1-decene to 1,2-epoxydecane based on our previous study (Ahmadi and Ullah, 2017). Briefly, 1-decene was epoxidized using *m*-chloroperbenzoic acid at room temperature in toluene for 1 hour. Second, conversion of DMOD to 9-octadecenoic acid was carried out according to the reported method for converting fatty acid methyl esters to their fatty acids with some modifications (Stempfle et al., 2011). DMOD was first converted to its salt using NaOH in methanol, followed

by dissolving the salt in water and then its acidification by 5 N hydrochloric acid. The filtered and dried 9-octadecenoic acid was a white to yellow solid with about 87% yield (Figure 5. S3). Synthesis of the biopolyester was followed by a one-pot reaction of 1,2-epoxydecene, 9-octadecenedioic acid, and DMOD using $SnCl_2$ as the catalyst. This reaction was studied under both microwave irradiation, as an alternative heating source, and conventional heating to compare the heating method's effects on the synthesis process and the resulting products.

a)
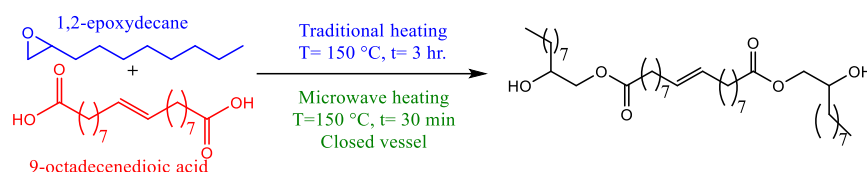
b)
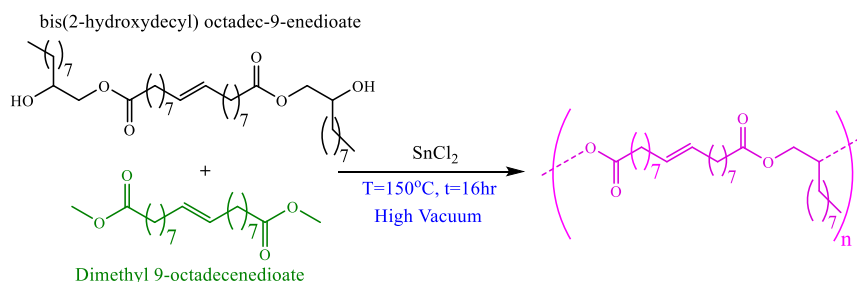
Scheme 5. 1) a) Synthesis of biodiol ((bis(2-hydroxydecyl) octadec-9-enedioate or BHOD) under conventional and microwave heating. b) Synthesis of long-chain, unsaturated biopolyester (BPs (DMBO) under conventional heating.

5.2.2. **One-pot synthesis of long-chain BPs (DMOD-BHOD) under conventional heating**

The one-pot polymerization of 1,2-epoxydecene, 9-octadecenedioic acid, and DMOD was performed in a two-step sequencing process. The first step was acid-epoxy addition started by melting 9-octadecenedioic acid at 85 °C and mixing with 1,2-epoxydecene under nitrogen flow. The acid-epoxy addition occurred naturally at 150 °C with the aliphatic carboxylic acid working both as a catalyst and a comonomer (Scheme 5. 1.a) (Nameer and Johansson, 2017). The acid-

epoxy addition is rather a complex reaction due to the possibility of side reactions. The main reported acid-epoxy reactions are (1st) carboxylic acid group addition on an epoxy ring yielding β-hydroxy esters; (2nd) hydroxyl group addition on an epoxy ring yielding ethers; (3rd) Fischer esterification of the hydroxyl groups by carboxylic acids (Nameer and Johansson, 2017), (Capelot et al., 2012), (Hoppe et al., 2005). Due to the molecular structures of DMOD and 1,2-epoxydecane, their reaction can lead to a diol's production with any of the above-mentioned acid-epoxy reactions occur. However, in this study, we optimized the reaction conditions to the minimum required time for consuming 9-octadecenedioic acid in the reaction media and producing bis(2-hydroxydecyl) octadec-9-enedioate (BHOD) as the main product. An ATR-FTIR was used to monitor the reaction process and BHOD synthesis. Both ATR-FTIR and ^{1}H NMR confirmed the elimination of 9-octadecenedioic acid and the acid-epoxy addition after 3 hr at 150 °C, resulting in BHOD production. In the second step, DMOD and SnCl$_2$ were introduced to the flask to proceed with the polycondensation of DMOD and BHOD at the same temperature. Since the elimination of methanol, as the polycondensation by-product, was necessary to obtain a high molecular weight polymer, a high vacuum was applied to the flask. The reaction was continued at the same temperature for 16 hours to increase the system's viscosity. After cooling to room temperature, the crude product was washed with THF and dried to reach a light brown to brown rubbery biopolyester (BPs (DMOD-BHOD)) (Figure 5. S4). The resulting biopolyester was not soluble in a variety of solvents with a wide range of polarities (methanol, diethyl ether, THF, DMF, TFAA, and HFIP), even after several hours of heating at the boiling point of solvents. However, after heating the biopolyester in toluene at 100 °C for 72 hours, we were able to dissolve 34% of the biopolyester. The average molecular weight ($\overline{M}_w$) of the soluble part of the biopolyester analyzed

by GPC was 1.64×10^4 g.mol^{-1}, while its average molecular number ($\bar{M}_n$) was 1.23×10^4 g.mol^{-1} with a polydispersity index (PD) of 1.32 (Fig. 5. 1).
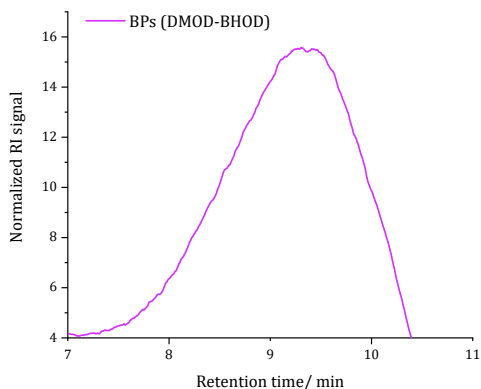
Figure 5. 1) Size exclusion chromatogram of BPs (DMOD-BHOD) traces (34%) dissolved in toluene after heating at 100 °C for 72 hours.

5.2.3. One-pot synthesis of long-chain BPs (DMOD-BHOD) under microwave heating

Microwave irradiation (wavelengths between infrared and radio) has been widely used as an efficient technique for the acceleration of various organic reactions since the late 20th century (Gedye et al., 1986); (Lidstrom et al., 2001). However, microwave-assisted acid-epoxy addition has rarely been investigated to the best of our knowledge. Therefore, the microwave-assisted acid-epoxy addition reaction was also optimized as the first step of the one-pot polymerization. The microwave-assisted acid-epoxy addition of 9-octadecenedioic acid and 1,2-epoxydecane was carried out in a single-mode microwave reactor (CEM-Discover, 120 V, Matthews, USA) equipped with an infrared temperature sensor. The preheating of monomers was identical to the traditional heating for melting 9-octadecenedioic acid. The microwave-assisted acid-epoxy addition was studied at different times from 5 to 30 min with 5 min intervals to find the minimum time required for acid addition to epoxy rings. The microwave reactor was set at a maximum of

280 W power under closed vessel mode for all reactions. Interestingly, acid addition to epoxy was done in less than 30 min at 150 °C under microwave irradiation.

In the polymerization step, the reactor's mode was first converted to an open vessel mode to conduct the polycondensation step. Then, the DMOD and catalyst were added into the microwave vial, and a high vacuum (~0.1 bar) was applied on it. However, the blue plasma occurred to the catalyst and the starting materials were charred after a few seconds of microwave irradiation (Figure 5. S5). Since the reduction of the vacuum has been suggested to prevent plasma occurrence (Jin et al., 2017), we tried to perform the polycondensation reaction under low vacuum pressure (0.7 bar) at 150 °C for more than 1 hour. This attempt also failed because the catalyst did not melt and mix with monomers. Moreover, methanol, the undesirable byproduct of the reaction, was also condensed on the microwave vial's wall at its headspace and turned backed into the reaction media due to the low and inefficient applied vacuum.

5.2.4. Characterization

Characterization of the bis(2-hydroxydecyl) octadec-9-enedioate (BHOD) synthesized under both heating methods

While the ATR-FTIR spectroscopy was implemented to optimize the conventional and microwave acid-epoxy addition of 9-octadecenedioic acid and 1,2-epoxydecane, it was also used to verify the final product's structure (BHOD). The characteristic absorption bands corresponding to the oxirane ring of 1,2-epoxydecane (834 cm^{-1}) and the acid groups of DMOD (O-H bend at 914 cm^{-1} and O-H stretch, a prominent shoulder from 2463 to 3326 cm^{-1} beside the CH stretch bands) were eliminated in the BHOD's spectrum after 3 hours in conventional heating (Figure 5. 2.a) and 30 min in microwave heating (Figure 5. 2.b). Moreover, the single band at 1687 cm^{-1} corresponding to the diacid's carbonyl groups (C=O stretch) moved to the higher wavelength of 1736 cm^{-1}

corresponding to the BHOD's ester groups. During the acid-epoxy reaction, a new peak at 1171 cm^{-1} was gradually raised in the BHOD spectrum related to BHOD's alkoxy group (CO stretch). The emergence of a broad peak at 3495 cm^{-1} was also an indication for the alcohol OH stretch of BHOD. These results support the occurrence of acid-epoxy addition and BHOD synthesis within 3 hours under conventional heating and 30 min under microwave irradiation.
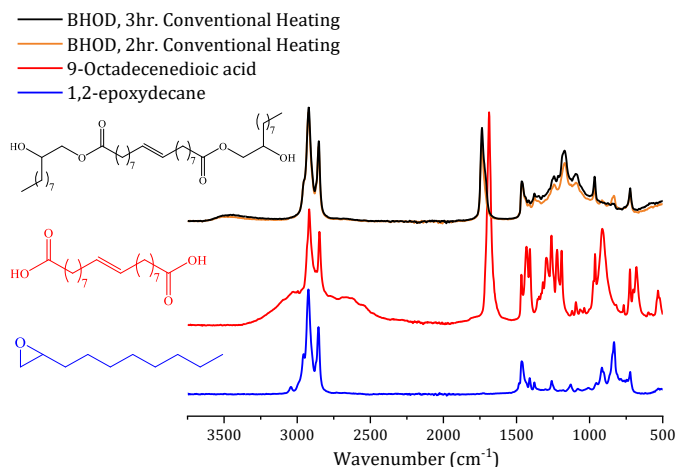
a)
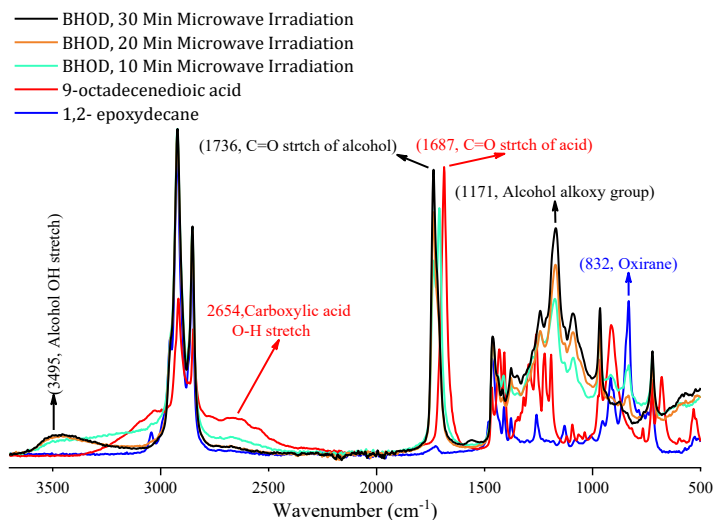
b)

Figure 5. 2) ATR-FTIR spectrum of the acid-epoxy addition of 9-octadecenedioic acid and 1,2-epoxydecene a) under conventional heating, b) under microwave heating at different time intervals.

BHOD structure was also confirmed by ^{1}HNMR spectroscopy (Figure 5. 3). All peaks associated with different protons in the monomers and BHOD have been clearly labeled in Figure 5. 3 and Figure 5. S6. The peaks regarding the aliphatic chains of monomers are identical in the biodiol spectrum. However, the peaks associated with the epoxy ring of 1,2-epoxydecane (m, n, and l) and the acid hydroxyl groups (g) are entirely disappeared in the BHOD's spectrum. On the other hand, three peaks related to the acid addition on the epoxy ring raised in the BHOD's spectrum. Two peaks (labeled with p and q) are related to the ring-opening of epoxy monomer and acid addition, while the third one (r) corresponds to the hydroxyl group creating BHOD. Besides, some small peaks in the BHOD spectrum could potentially stem from the side reactions of acid-epoxy addition (Nameer and Johansson, 2017); (Capelot et al., 2012). In total, the comparison of the monomers' and BHOD's ^{1}HNMR spectrum indicated the successful production of the novel BHOD biodiol.
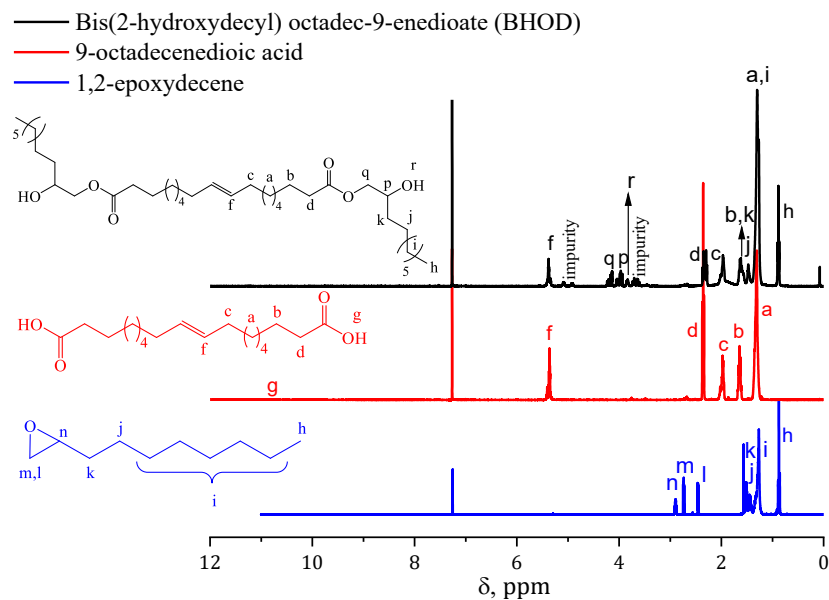
Figure 5. 3) ^{1}H NMR spectrum of 1,2-epoxydecane, 9-octadecenedioic acid, and diol (BHOD), the acid-epoxy addition product.

5.2.5. **Characterization of long-chain BPs (DMOD-BHOD)**

In the acid-epoxy addition step, 9-octadecenedioate acid (the acid of DMOD) was positioned between 1,2-epoxydecane monomers to synthesize BHOD (Scheme 5. 1.a). Polycondensation of BHOD and DMOD resulted in the production of BPs (DMBO) with the same structure as BHOD, with the hydroxyl group (OH) of BHOD being eliminated (Scheme 5. 1.b). The comparison of ATR-FTIR spectra of the biodiol (BHOD), diester (DMOD), and biopolyester confirmed occurrence of polycondensation reaction and BPs (DMOD-BHOD) structure (Figure 5. 4). The monomers (BHOD) and BPs (DMOD-BHOD) showed similar spectra except for the BHOD having an absorption band at 3489 cm^{-1} corresponding to its OH groups. Consequently, the absence of this absorption band in the biopolyester's spectrum verified successful polycondensation and creation of long-chain BPs (DMOD-BHOD).
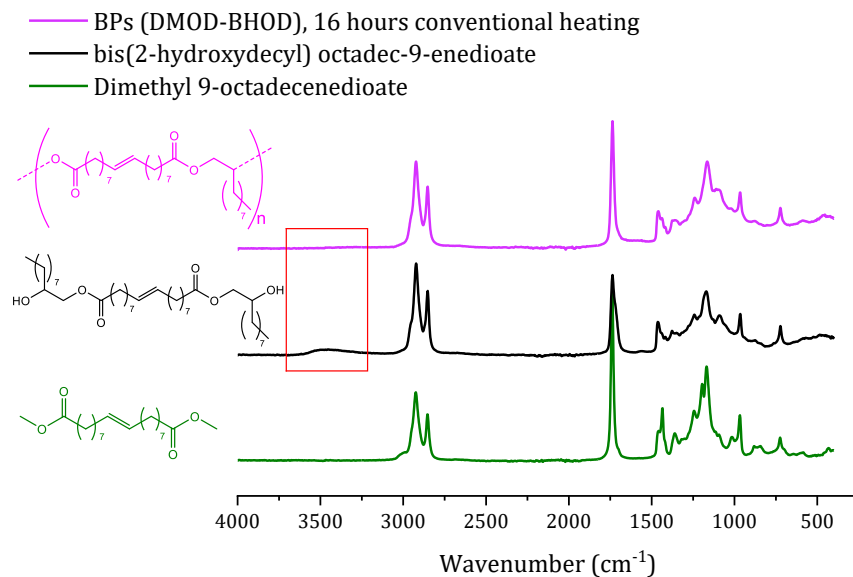
Figure 5. 4) ATR-FTIR spectrum of the BHOD, DMOD, and the long-chain, unsaturated biopolyester BPs (DMOD-BHOD).

145

To obtain the ^{1}H NMR analysis of the biopolyester, we managed to dissolve about 30% of the BPs (DMOD-BHOD) in toluene-d8 after heating at 100 °C for more than 72 hours. The ^{1}H NMR spectra of DMOD, BHOD, and BPs (DMOD-BHOD) were then leveled off and compared to verify monomers' polymerization and confirm the biopolyester's structure (Figure 5. 5 & Figure 5. S6). The characteristic signal of DMOD biodiester was identified at 3.68 ppm corresponding to the protons of its methyl end-groups (e), whereas, the characteristic signal of BHOD biodiol was identified at 3.83 ppm corresponding to protons of its hydroxyl end-groups (r). Disappearance of these two signals in the BPs (DMOD-BHOD) spectrum, therefore, verified the monomers' reaction through external groups and polymer synthesis.

Biopolyester production caused changes in the chemical shift of protons on the carbons near the ester and alcohol groups of the BHOD biodiol (Figure 5. 5). The proton signals of two carbons at 1.30 ppm (i) in biodiol were shifted to the downfield ~1.54 ppm (i") of biopolyester spectrum while the rest stayed at the same position. The proton signals at 1.47 ppm (j) in biodiol were also shifted to the downfield of biopolyester at 1.54 ppm (j'), making one peak with (i") signal. Moreover, the proton signals of carbon (b) in the biodiol spectrum at 1.62 ppm were shifted to the biopolyester spectrum's downfield joining the proton signal of carbon (c) at 2.02 ppm. Finally, both proton signals of carbon (d) at 2.30 ppm and carbon (k) at 1.61 ppm in the biodiol spectrum were shifted to the biopolyester spectrum's downfield at 2.85 ppm (d') and 3.36 ppm (k'), respectively. The rest of proton signals in the biopolyester and monomers spectra stayed almost at the same ^{1}H NMR field. A little shift towards downfield observed for these signals in the biopolyester spectrum can potentially be due to the different solvent (toluene-d8 instead of chloroform-d) used for dissolving the biopolyester.
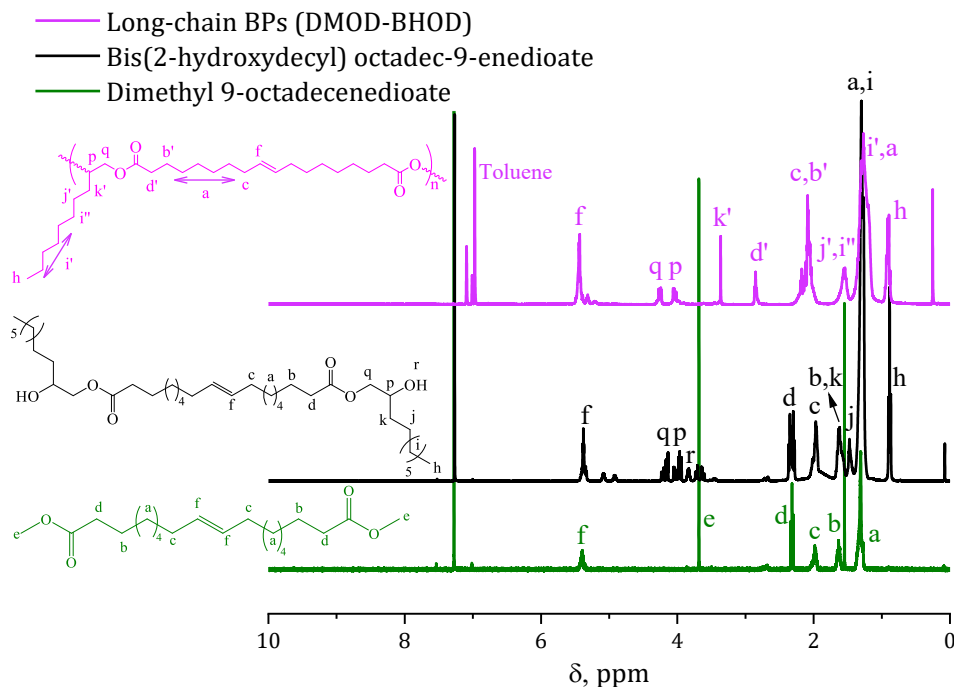
Figure 5. 5) ¹HNMR of DMOD, BHOD, and the soluble part of BPs (DMOD-BHOD) in Toluene-d8.

5.3. **Thermal properties of long-chain BPs (DMOD-BHOD)**

The thermogravimetric analysis (TGA) of DMOD, 9-octadecenedioic acid, 1,2-epoxydecane, and the long-chain BPs (DMOD-BHOD) was performed in the range of 25 °C to 600 °C (Figure 5. 6). The formation of the long-chain biopolyester can be verified through distinct differences between the higher thermal stability of the biopolyester compared to monomers. The one-pot polymerization process developed a biopolyester with a two-stage decomposition profile. The 5 wt. % ($T_{d,5wt\%}$) decomposition of the biopolyester started at 329 °C and completed roughly at 500 °C. These thermal properties are comparable to that of commercial thermoplastic polyesters such as poly(ethylene terephthalate) (PET) and poly(1,4-butylene terephthalate) (PBT) with a decomposition temperature around 400 °C (Levchik and Weil, 2004); (Qu et al., 2014); (Silva et al., 2018). The BPs (DMOD-BHOD) was less stable at temperatures lower than 430 °C, where the first mass loss of about 70% was observed at ~329- 430 °C. BPs (DMOD-BHOD) exhibited more

stability at higher temperatures; the second mass loss of about 20% occurred between ~430- 500

°C while the remaining ~10% was decomposed when the temperature elevated to 600 °C.
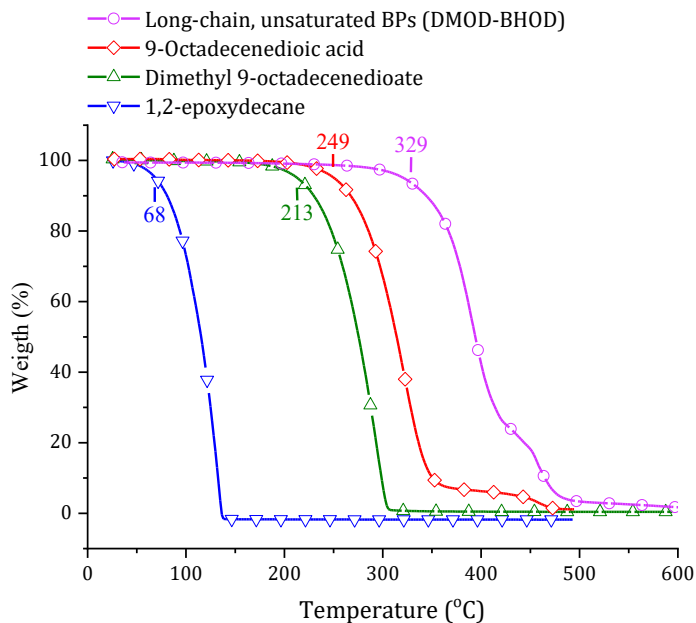
Figure 5. 6) TGA thermograms of 1,2-epoxydecane, dimethyl 9-octadecenedioate, 9-octadecenedioic acid, and long-chain, unsaturated biopolyester (BPs (DMOD-BHOD)).

Figure 5. 7 shows the monomers' and biopolyester's thermal transition obtained by the DSC. Both

monomers and produced polymer showed two melting points. The BPs (DMOD-BHOD) exhibited

a quite distinct higher melting point than the monomers verifying the formation of the BPs

(DMOD-BHOD). The highest melting point among monomers was between 40-89 °C for 9-

octadecenedioic acid, which was improved to 276-304 °C for BPs (DMOD-BHOD). These results

indicated the creation of a high heat resistance biopolyester with comparable melting points to

those of commercially available thermoplastic polyesters such as PET and PBT. The T_g point of

the biopolyester was not observable in its DSC thermogram.
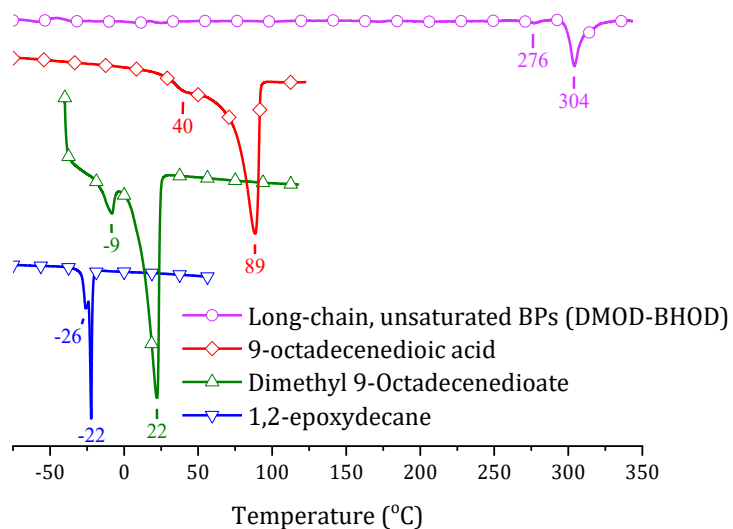
Figure 5. 7) DSC thermograms of 1,2-epoxydecane, dimethyl 9-octadecenedioate, 9-octadecenedioic acid, and long-chain, unsaturated biopolyester (BPs (DMOD-BHOD)).

5.4. Conclusions

A novel long-chain, unsaturated biopolyester (BPs (DMOD-BHOD)) was synthesized through the one-pot reaction of 9-octadecenedioic acid, 1,2-epoxydecane, and dimethyl 9-octadecenedioate (DMOD). This process had two sequential steps: 1) acid-epoxy addition of 9-octadecenedioic acid and 1,2-epoxydecane to produce BHOD and 2) polycondensation of BHOD and DMOD with 2% SnCl$_2$ catalyst under high vacuum. Both conventional and microwave heating methods successfully added the diacid on the epoxy ring of 1,2-epoxydecane. The synthesis of BHOD under microwave irradiation was more efficient by decreasing the acid-epoxy addition time from 3 hours to less than 30 min. The long-chain BPs (DMOD-BHOD) was only achievable under conventional heating at 150 °C for 16 hours and a high vacuum. The BHOD's polycondensation with DMOD under microwave heating was not successful due to several reasons, including the catalyst's blue plasma occurrence under high vacuum and methanol condensation on the microwave vial's wall

149

as well as incomplete catalyst melting under lower vacuums in the microwave. The biopolyester's thermal analysis confirmed the synthesis of a thermally stable long-chain polymer with a decomposition temperature of more than 329 °C and a melting point of more than 276 °C. The thermal properties of BPs (DMOD-BHOD) were comparable with commercial polyesters such as PET and PBT. Overall, the reported process is a green approach to synthesizing a thermally stable biopolyester with long-chain and unsaturated motifs. The properties of the resulted biopolyester being comparable to some commercial polyesters makes it attractive not only from academic but also from industrial point of view.

References

Ahmadi, R., Ullah, A., 2017. Microwave-assisted rapid synthesis of a polyether from a plant oil derived monomer and its optimization by Box-Behnken design. RSC Adv. 7, 27946–27959. https://doi.org/10.1039/c7ra03278a

Capelot, M., Montarnal, D., Tournilhac, F., Leibler, L., 2012. Metal-catalyzed transesterification for healing and assembling of thermosets. J. Am. Chem. Soc. 134, 7664–7667. https://doi.org/10.1021/ja302894k

Gedye, R., Smith, F., Westaway, K., Ali, H., Baldisera, L., Laberge, L., Rousell, J., 1986. The use of microwave ovens for rapid organic synthesis. Tetrahedron Lett. 27, 279–282. https://doi.org/10.1016/S0040-4039(00)83996-9

Hoppe, C.E., Galante, M.J., Oyanguren, P.A., Williams, R.J.J., 2005. Epoxies modified by palmitic acid: From hot-melt adhesives to plasticized networks. Macromol. Mater. Eng. 290, 456–462. https://doi.org/10.1002/mame.200400348

Jin, L., Geng, K., Arshad, M., Ahmadi, R., Ullah, A., 2017. Synthesis of fully biobased polyesters from plant oil. ACS Sustain. Chem. Eng. 5, 9793–9801. https://doi.org/10.1021/acssuschemeng.7b01668

Levchik, S. V., Weil, E.D., 2004. A review on thermal decomposition and combustion of thermoplastic polyesters. Polym. Adv. Technol. 15, 691–700. https://doi.org/10.1002/pat.526

Lidstrom, P., Tierney, J., Wathey, B., Westman Jacob, 2001. Microwave-assisted green organic synthesis-a review. Tetrahedron 57, 9225–9283.

Marinescu, S.C., Schrock, R.R., Müller, P., Hoveyda, A.H., 2009. Ethenolysis reactions catalyzed by imido alkylidene monoaryloxide monopyrrolide (MAP) complexes of molybdenum. J. Am. Chem. Soc. 131, 10840–10841. https://doi.org/10.1021/ja904786y

Nameer, S., Johansson, M., 2017. Fully bio-based aliphatic thermoset polyesters via self-catalyzed self-condensation of multifunctional epoxy monomers directly extracted from natural sources. J. Coatings Technol. Res. 14, 757–765. https://doi.org/10.1007/s11998-017-9920-y

Qu, H., Liu, X., Xu, J., Ma, H., Jiao, Y., Xie, J., 2014. Investigation on thermal degradation of poly(1,4-butylene terephthalate) filled with aluminum hypophosphite and trimer by thermogravimetric analysis-fourier transform infrared spectroscopy and thermogravimetric analysis-mass spectrometry. Ind. Eng. Chem. Res. 53, 8476–8483. https://doi.org/10.1021/ie404297r

Silva, C.V.G., da Silva Filho, E.A., Uliana, F., de Jesus, L.F.R., de Melo, C.V.P., Barthus, R.C., Rodrigues, J.G.A., Vanini, G., 2018. PET glycolysis optimization using ionic liquid [Bmin]ZnCl 3 as catalyst and kinetic evaluation. Polimeros 28, 450–459.

https://doi.org/10.1590/0104-1428.00418

Stempfle, F., Quinzler, D., Heckler, I., Mecking, S., 2011. Long-chain linear C19 and C23 monomers and polycondensates from unsaturated fatty acid esters. Macromolecules 44, 4159–4166. https://doi.org/10.1021/ma200627e

Thomas, R.M., Keitz, B.K., Champagne, T.M., Grubbs, R.H., 2011. Highly selective ruthenium metathesis catalysts for ethenolysis. J. Am. Chem. Soc. 133, 7490–7496. https://doi.org/10.1021/ja200246e

Ullah, A., Arshad, M., 2018. Conversion of lipides olefins. US Pat., US 10,138,430 B2, 2018. US 10 , 138 , 430 B2.

Ullah, A., Arshad, M., 2017. Remarkably efficient microwave-assisted cross-metathesis of lipids under solvent-free conditions. ChemSusChem 10, 2167–2174. https://doi.org/10.1002/cssc.201601824

van der Klis, F., Le Nôtre, J., Blaauw, R., van Haveren, J., van Es, D.S., 2012. Renewable linear alpha olefins by selective ethenolysis of decarboxylated unsaturated fatty acids. Eur. J. Lipid Sci. Technol. 114, 911–918. https://doi.org/10.1002/ejlt.201200024

Winkler, M., Meier, M.A.R., 2014. Olefin cross-metathesis as a valuable tool for the preparation of renewable polyesters and polyamides from unsaturated fatty acid esters and carbamates. Green Chem. 16, 3335–3340. https://doi.org/10.1039/c4gc00273c

Zhang, L., Huang, M., Yu, R., Huang, J., Dong, X., Zhang, R., Zhu, J., 2014. Bio-based shape memory polyurethanes (Bio-SMPUs) with short side chains in the soft segment. J. Mater. Chem. A 2, 11490–11498. https://doi.org/10.1039/c4ta01640h

CHAPTER 6: GENERAL DISCUSSION AND FUTURE DIRECTIONS

6. Key findings of the present research

In this thesis, the primary purpose was to investigate the reactivity of different monomers synthesized through the metathesis reaction of canola oil's fatty methyl esters. Therefore, it was essential to study synthesized monomers/biochemical reactivity in both functionalization/modification and polymerization reactions. The effect of microwave irradiation on the efficiency of modification/functionalization and polymerization reactions compared to the traditional heating was investigated to evaluate the microwave's suitability as an alternative greener synthesis method and microwave's synthesis potential under reduced solvent or solvent-free conditions. We fulfilled these purposes by reducing or eliminating the required solvents from reactions, avoiding catalysts, and cutting the reaction steps. The outcomes of this research are attractive from both academic and industrial points of view. The key findings of the research are outlined in the following section.

6.1. 1-decene, a canola oil-derived monomer, is desirable for epoxidation and then polymerization to a high molecular weight biopolyether under both conventional and microwave heating methods

The study in chapter 3 (published in *RSC Adv.*,2017, 7, 27946-27959) was essential to evaluate: 1) the epoxidation of 1-decene in the absence of a catalyst; 2) the ring-opening polymerization of epoxidized 1-decene to a high molecular weight biopolyether; 3) the effect of microwave irradiation compared to conventional heating on, a) the epoxidation reaction of 1-decene and ring-

opening polymerization of 1,2-epoxydecane and b) the structural and thermal properties of the resulting polyethers.

The epoxidation reaction of 1-decene was optimized and completed within 1 hour, a considerably short time, and using 3-choloroperoxybenzoic acid as an oxidizing agent under the conventional method. Microwave irradiation was not suitable for the epoxidation reaction of 1-decane using the oxidant. Oxirane rings were cleaved at the irradiation times > 5 min in microwave. The water interference in the reaction mixture, originating from 3-choloroperoxybenzoic acid, was potentially the reason for the observed oxirane ring break down. Therefore, microwave irradiation is not a suitable method for oxidizing 1-decene using 3-choloroperoxybenzoic acid.

Conventional ring-opening polymerization of 1,2-epoxydecane was done using an "*in situ*" prepared catalyst from MMAO-12 and 2,4-pentanedione in toluene and yielded a biopolyether with high molecular weight ($>2 \times 10^6$ g.mol^{-1}) and narrow polydispersity (1.2). The microwave-assisted ring-opening polymerization of 1,2-epoxydecane was also optimized using a three-factor, three-level Box-Behnken design. Microwave irradiation substantially reduced polymerization time from 24 hours to less than 10 min and increased polymerization yield with a lower amount of solvent compared to conventional polymerization. The molecular weight and polydispersity of biopolyether synthesized under microwave condition was comparable to the biopolyether synthesized under conventional heating. Nevertheless, the biopolyether produced under the microwave-assisted ring-opening polymerization was less thermally stable than the biopolyether produced under the conventional heating method. The observed differences in thermal stability were potentially due to the slight differences between polymers' molecular weight and tacticity. Microwave irradiation produced polyether chains with a higher atactic portion than isotactic

compared to the conventional heating method, which resulted in the production of biopolyethers with less thermal stability.

6.2. Canola oil-derived dimethyl 9-octadecenedioate (DMOD) is a reactive monomer in polycondensation with amine monomers under both microwave and conventional heating methods

The study in chapter 4 (published in *ACS Sustainable Chem. Eng. 2020, 8, 8049−8058*) was essential to evaluate: 1) the reactivity of biodiester (dimethyl 9-octadecenedioate, DMOD) in polycondensation with the aromatic diamine of *p*-xylylenediamine (PXDA), 2) the reactivity of dimethyl 9-octadecenedioate in polycondensation with the linear triamine of diethylenetriamine (DETA), 3) the polycondensation capability of selected monomers to high molecular weight polyamides, 4) the effect of different heating methods on the polycondensation of monomers and synthesized polyamides from dimethyl 9-octadecenedioate, 5) the effect of microwave-assisted polycondensation on the resulting polyamides' crystalline structure, 6) the capability of the biobased polyamides for making thin films without using any additives like plasticizers, and 7) mechanical and thermomechanical properties of the generated polyamide films.

6.3. The semi-aromatic PA (DMOD-PXDA)'s synthesis through polycondensation of DMOD with PXDA

The conventional polycondensation of DMOD with PXDA was followed through a stepwise heating process: 75 °C for 1 hour under nitrogen gas, 100 °C for 30 min, and 200 °C for 2 hours under a low vacuum (0.7 bar). The polymerization process was successful in a solvent-free media using the organic TBD catalyst. The stepwise heating process was employed to accommodate the melting of the solid PXDA and minimize its sublimation at high temperatures for a complete polymerization process. The microwave-assisted polycondensation of monomers was achievable in less than 15 min through a similar stepwise heating approach except for the final temperature of

160 °C. Applying higher temperatures to the reaction media for microwave polycondensation degraded the monomers. The monomer degradation could be potentially due to hot spots' formation in the viscous reaction mixture and less efficient stirring under microwave irradiation. The final product of both heating processes was a white to yellow powder insoluble in common solvents and even HFIP after 24 h heating at its boiling point (69 °C).

The thermal analysis of PAs (DMOD-PXDA) indicated two melting points for the polyamides synthesized under both heating processes. The traditional heating produced semi-aromatic PA (DMOD-PXDA) with a higher melting points (145-210 °C) compared to the microwave heating. On the other hand, conventional polycondensation resulted in polyamide with higher decomposition temperatures and lower uniformity. Consequently, conventional polycondensation created PA (DMOD-PXDA) chains with higher polydispersity and molecular weight as well as higher thermal stability than microwave heating. Conventional polycondensation also resulted in the formation of semi-aromatic polyamides with a lower crystalline structure but more diversity in their crystalline phases based on the Wide-angle X-ray diffraction analysis.

Thin films from semi-aromatic polyamides produced under both microwave and conventional heating were molded and annealed to analyze their thermomechanical and mechanical properties. PA (DMOD-PXDA) films were a kind of brittle, thermoplastic polymer. DMA analyses revealed that microwave heating affected the β-transition temperature and α or glass transition (T_g) of the polyamides. Indeed, microwave irradiation created a PA (DMOD-PXDA) film with lower T_g and without β-transition in the polymer chains. The applied higher temperatures and better homogenization of the reaction mixture in conventional heating allowed the formation of polymer chains with higher molecular weights and T_g. While the tensile strength of the films made from PA (DMOD-PXDA) under both heating methods was comparable, the percent elongation at break

of the film from the polyamide prepared by conventional heating was significantly higher than the one made by microwave irradiation. The less crystallinity and presence of lower molecular weight chains in the bulk CH-PA (DMOD-PXDA) could potentially explain these phenomena. The polymer's intermolecular bonds were reduced by the presence of oligomers and low crystallinity in the polymer network. Consequently, the higher chain mobility promoted from less intermolecular bonds caused a higher percent elongation at the polymer break.

6.3.1. The linear PA (DMOD-DETA)'s synthesis through polycondensation of DMOD with DETA

PA (DMOD-DETA) was produced as an aliphatic biobased polyamide from the polycondensation of DMOD and DETA at 160 °C (under nitrogen) in a solvent-free media with TBD catalyst. Microwave-assisted synthesis reduced the time of polycondensation from 4 hours to less than 10 min. The aliphatic biobased PA (DMOD-DETA) was rubbery with a yellow to brown color and not soluble in common solvents used for polymer solubilization. The polymer heating at the boiling points of the HFIP and TFAA for 24 hours was also not efficient for their solubilization. The presence of multiple hydrogen bonds in PA (DMOD-DETA) structure amplified by the secondary amino groups in the middle of DETA was potentially responsible for the polymer's insolubility. The potential participation of some secondary amine groups in the cross-linking between polymer chains was also considered to be another reason.

The ATR-FTIR results verified the incomplete polycondensation of DMOD and DETA under microwave irradiation and revealed monomer traces in the polymer structure. The inefficient mass transfer of monomers/oligomers to the polymer chains due to the polymer mixture's high viscosity caused an incomplete polycondensation. The product mixture's solubility and stickiness preventing the polymer's effective washing was the reason for the observed impurity.

157

The thermomechanical and mechanical properties of the PA (DMOD-DETA) films were also examined. Based on the DMA analysis, the PA (DMOD-DETA) films, especially the one with the polymer prepared under microwave irradiation, showed a high loss factor. This phenomenon could be due to residual oligomers and monomers' plasticizing effect in the polymer structures, which increases segmental mobility. PA (DMOD-DETA) films displayed both the presence of β-transition and α transition (T_g) regardless of the heating method, while their T_g were close together at around 10 °C. Conventional polycondensation yielded PA (DMOD-DETA) film with higher tensile strength but lower percent elongation at break relative to the films made from microwave polycondensed polyamides.

6.3.2. The overall outcome of polycondensation of DMOD with different amines under conventional and microwave heating methods

Generally, microwave irradiation developed polyamides with higher crystalline structures, lower melting points, and lower initial decomposition temperatures compared to traditional heating. Microwave heating also promoted less diversity in the crystalline phases of polyamides with the γ-phase as the main crystalline form. Variability in crystalline phases of polyamides was more evident when aromatic monomer (PXDA) was used in polyamide structure compared to the liner triamine (DETA).

The smaller loss factor of the films prepared from PAs (DMOD-PXDA) compared to the ones developed from PAs (DMOD-DETA) indicates the higher elasticity of PA (DMOD-PXDA) films. The semi-aromatic polyamide films (PAs (DMOD-PXDA)) also showed higher storage modulus, an indication of storing energy more elastically in them compared to PA (DMOD-DETA) films. This phenomenon is the classical outcome of the benzene ring insertion into the backbone of polyamide chains.

6.4. **Bio-derived monomers of dimethyl 9-octadecenedioate (DMOD) and 1,2-epoxydecane can make a long-chain unsaturated biopolyester**

The study in chapter 5 was essential to evaluate: 1) the conversion of dimethyl 9-octadecenedioate (DMOD) to its acid (9-octadecenedioic acid); 2) acid-epoxy addition of DMOD on the epoxy ring of 1,2-epoxydecane and making a novel biodiol ((bis(2-hydroxydecyl) octadec-9-enedioate (BHOD); 3) one-pot polymerization of 9-octadecenedioic acid with DMOD and 1,2-epoxydecane as a green polymerization process for the production of a novel, long-chain, unsaturated biopolyester (BPs (DMOD-BMOD)); 4) microwave effect on BHOD production; and 5) microwave effect on the polycondensation of DMOD and BHOD.

In this study, 1-decene and DMOD were first converted to 1,2-epoxydecane and 9-octadecenedioic acid, respectively. Then, the one-pot polymerization of 1,2-epoxydecane, 9-octadecenedioic acid, and DMOD was carried out using a two-step procedure. First, a novel biodiol (BHOD) was synthesized from the acid-epoxy addition of 9-octadecenedioic acid and 1,2-epoxydecane in a solvent- and catalyst-free reaction media at 150 °C. Then, DMOD and $SnCl_2$ were added to the mixture, and the novel biopolyester was produced at the same temperature after 16 hours under a high vacuum with a quantitative yield of 77%. Acid-epoxy addition reaction was completed after 3 hours, as confirmed with ATR-FTIR. Importantly, microwave heating reduced this step to less than 30 min. The second step, on the other hand, was only achievable by the conventional polycondensation after 16 hours. Applying a high vacuum under microwave irradiation led to a blue plasma occurrence for the catalyst ($SnCl_2$). Changing the experimental parameters of applied vacuum, temperature, and time of microwave irradiation were not effective in the successful production of the biopolyester. The polycondensation reaction did not work under a low vacuum due to the incomplete melting of the catalyst, which has a high melting point, as well as inactivation

of the reaction because of methanol condensation (the unsuitable byproduct of polycondensation) and turning back into the reaction media.

The produced biopolyester was a light brown to brown rubbery biopolyester, insoluble in a variety of solvents with a wide range of polarities. We managed to dissolve 34% of this biopolyester in toluene (at 100 °C and 72 hours) for the GPC analysis. The soluble fraction of the biopolyester showed an average molecular weight ($\bar{M}_w$) of 1.64×10^4 g mol^{-1}, an average molecular number ($\bar{M}_n$) of 1.23×10^4 g.mol^{-1}, and a polydispersity index (PD) of 1.32.

Thermal analysis (DSC and TGA) of the BPs (DMOD-BMOD) confirmed the production of a highly thermal stable biopolyester exhibiting a melting point of > 267 °C and decomposition temperature of around 400 °C. Interestingly, the thermal properties of BPs (DMOD-BMOD) was comparable to those of commercial thermoplastic polyesters such as poly(ethylene terephthalate) (PET) and poly(1,4-butylene terephthalate) (PBT).

6.5. Overall Conclusion

The reported studies in this thesis revealed the potential of canola oil-derived monomers including 1-decene and dimethyl 9-octadecenedioate for chemical modification and polymerization. 1-decene was suitable to produce high molecular weight polyether and polyester. Dimethyl 9-octadecenedioate, on the other hand, exhibited attractive potential for synthesizing different long-chain aliphatic polyesters and polyamides to bridge the gap between conventional polyolefins and polycondensates, empowering sustainable growth towards green bioplastics development. The resulted polyamides and polyesters exhibited thermal stability comparable to commercial ones.

This thesis also evaluated the potential of microwave irradiation on chemical reactions and polymerization processes. Acid-epoxy addition reactions can be performed under microwave

irradiation in a solvent- and catalyst-free media and in a short span of time compared to the conventional method. Microwave-assisted epoxidation reactions, on the other hand, are hampered due to the destructive effect of water on the epoxidation process. Therefore, water needs to be avoided in the epoxidation reactions under microwave irradiation. Regarding polymerization reactions, microwave irradiation can substitute conventional heating methods for inherently fast polymerization reactions such as ring-opening polymerization. Whereas, slow polymerization reactions such as polycondensation in which the polymerization process is stepwise, are not easily and rapidly developed under microwave irradiation. When employing microwave irradiation for polymerization reactions, one should also consider the compatibility between the catalyst, reaction media, and applied atmospheric conditions under microwave irradiation. While both organic and metallic catalysts can work properly under microwave irradiation in an inert atmosphere or a low vacuum condition, metallic catalysts cannot be used in microwave-assisted polycondensation reactions under high vacuum due to the occurrence of blue plasma phenomenon.

Another important aspect of the current research was elucidating the potential effect of microwave irradiation on polymers characteristics as compared to the traditional heating methods. Table 6.1 compares the characteristics of the polymers synthesized under conventional and microwave irradiation. Given that microwave irradiation changes thermal stability, decomposition uniformity, crystallinity, tacticity, and mechanical properties of polymers, they can fulfill different expectations in terms of applicability as compared to the polymers produced under conventional heating methods.

In conclusion, microwave irradiation has great potential to replace conventional heating methods for chemical reactions and polymerization processes and has economic advantages due to shorter

reaction times. The efficacy of microwave radiations for chemical modifications and polymerization reactions, however, needs to be determined for different kinds of polymers.

Table 6. 1) Characteristics of biobased polymers synthesized under different heating processes.

Polymer and Their Characteristics			Conventional Heating	Microwave Irradiation
Biopolyether		Molecular weight	✓	
		Initial melting point	✓	
		Final melting point		✓
		Glass transition temperature	✓	
		Initial decomposition temperature		✓
		Final decomposition temperature	✓	
		Decomposition uniformity		✓
		Tacticity	✓	
PA (DMOD-PXDA)	**Crude polymer**	Initial melting point	✓	
		Final melting point	✓	
		Initial decomposition temperature		✓
		Final decomposition temperature	✓	
		Decomposition uniformity		✓
		Degree of crystallinity		✓
	Film	Glass transition temperature	✓	
		Tensile strength	NS	NS
		Elongation at break	✓	
PA (DMOD-DETA)	**Crude polymer**	Initial melting point		✓
		Final melting point	✓	
		Initial decomposition temperature	✓	
		Final decomposition temperature	✓	
		Decomposition uniformity		✓
		Degree of crystallinity		✓
	Film	Glass transition temperature		✓
		Tensile strength	✓	
		Elongation at break		✓

The checked symbol indicates higher property in the respective method. NS means non-significant. The biopolyester excluded from the table because its microwave polycondensation was not successful.

6.6. Recommendations for future research

Based on the research outcomes in this thesis, the recommended future experiments and studies from different perspectives are as follow:

6.6.1. Recommendations regarding the biopolyethers synthesized from 1,2-epoxydecane:

1) The biodegradability of the biopolyethers should be investigated.

2) The biopolyethers' film should be made, and its thermomechanical and mechanical properties be investigated using DMA and universal testing machine.

3) The capability of biopolyethers' film as an adhesive should be examined, too.

6.6.2. Recommendations regarding biobased polyamides PA (DMOD-PXDA)

1) Since stirring has an essential effect in producing high molecular weight polymers, polymerization of DMOD with PXDA should be studied using a reactor equipped with a mechanical stirrer to mix viscous reaction media at high temperatures.

2) The biodegradability of the biobased polyamides PA (DMOD-PXDA) should be studied.

3) The polyamide films' capability for use in different industries, such as the paint industry, should be investigated.

4) Post-polymerization modification of the polyamides for making a robust thermoset polyamide should be examined, too.

6.6.3. Recommendations regarding biobased polyamides PA (DMOD-DETA)

1) The polymerization of DMOD with DETA should be studied using a reactor equipped with a mechanical stirrer to improve the mixing of viscous media reactions and completing the polymerization.

2) Since the polymerization media of DMOD and DETA got highly viscous even at the initial polymerization steps, monomers' polymerization can be studied in solvent for a complete polycondensation reaction to reach high molecular weight polymers.

3) Biodegradability of the biobased polyamides PA (DMOD-DETA) should be studied.

4) As the resulted polymers was highly sticky to different materials, the polyamide films' capability for use as an adhesive should be investigated.

5) Post-polymerization of the PAs (DMOD-DETA) for making a thermoset polyamide should be examined, too.

6.6.4. **Recommendations regarding the long-chain unsaturated biopolyester (BPs (DMOD-BHOD))**

1) The BPs (DMOD-BHOD)'s biodegradability should be investigated.

2) The BPs (DMOD-BHOD)'s film should be made and its thermomechanical and mechanical properties should be investigated.

3) Polymerization of the novel biodiol (BHOD) with other diesters or diamines to produce other polyesters and polyamides can be studied.

4) The production of the other biodiol from the reaction of DMOD with other epoxy monomers need to be studied and the resulted biodiols can use to produce the other polyesters.

5) The polycondensation step of DMOD and biodiol (BHOD) should be studied using other catalysts.

Bibliography

Adekunle, K.F., 2015. A review of vegetable oil-based polymers: synthesis and applications. Open J. Polym. Chem. 05, 34–40. https://doi.org/10.4236/ojpchem.2015.53004

Ahmadi, R., Ullah, A., 2017. Microwave-assisted rapid synthesis of a polyether from a plant oil derived monomer and its optimization by Box-Behnken design. RSC Adv. 7, 27946–27959. https://doi.org/10.1039/c7ra03278a

Alperowicz, N., 2002. PCS studies propylene expansion using olefin conversion process. Chem. Week, Mar 6 164, 16.

Andjelkovic, D.D., Valverde, M., Henna, P., Li, F., Larock, R.C., 2005. Novel thermosets prepared by cationic copolymerization of various vegetable oils - Synthesis and their structure-property relationships. Polymer (Guildf). 46, 9674–9685. https://doi.org/10.1016/j.polymer.2005.08.022

Anneken, D.J., Both, S., Christoph, R., Fieg, G., Steinberner, U., Westfechtel, A., 2012. Fatty Acids. Ullmann's Encycl. Ind. Chem. https://doi.org/10.1002/14356007.a10

Arnold, F.E., Bruno, K.R., Shen, D., Eashoo, M., Lee, C.J., Harfus, F.W., Cheng, S.D., 1993. The origin of beta relaxations in segmented rigid-rod polyimide and copolyimide films. Polym. Eng. Sci. 33, 1373–1380.

Arrieta, C., David, E., Dolez, P., Vu-Khanh, T., 2011. X-ray diffraction, raman, and differential thermal analyses of the thermal aging of a Kevlar -PBI blend fabric. Polym. Compos. 32, 362–367. https://doi.org/https://doi.org/10.1002/pc.21041

Arshad, M., Saied, S., Ullah, A., 2014. PEG-lipid telechelics incorporating fatty acids from canola

oil: Synthesis, characterization and solution self-assembly. RSC Adv. 4, 26439–26446. https://doi.org/10.1039/c4ra03583f

ASTM 08(E1356), 2008. Standard test method for assignment of the glass transition temperatures by differential scanning calorimetry.

ASTM D 3850, 2000. Standard test method for rapid thermal degradation of solid electrical insulating materials by thermogravimetric method (TGA). https://doi.org/10.1520/D3850-12.2

Auclai, N., Kaboorani, A., Riedl, B., Landry, V., 2016. Acrylated betulin as a comonomer for bio-based coatings. Part II: Mechanical and optical properties. Ind. Crops Prod. 82, 118–126. https://doi.org/10.1016/j.indcrop.2015.11.081

Auclair, N., Kaboorani, A., Riedl, B., Landry, V., 2015. Acrylated betulin as a comonomer for bio-based coatings. Part I: Characterization, photo-polymerization behavior and thermal stability. Ind. Crops Prod. 76, 530–537. https://doi.org/10.1016/j.indcrop.2015.07.020

Awang, N.W., Tsutsumi, K., Huštáková, B., Yusoff, S.F.M., Nomura, K., Yamin, B.M., 2016. Cross metathesis of methyl oleate (MO) with terminal, internal olefins by ruthenium catalysts: Factors affecting the efficient MO conversion and the selectivity. RSC Adv. 6, 100925–100930. https://doi.org/10.1039/c6ra24200f

Azizi, S.N., Asemi, N., 2012. A Box-Behnken design for determining the optimum experimental condition of the fungicide (Vapam) sorption onto soil modified with perlite. J. Environ. Sci. Heal. - Part B Pestic. Food Contam. Agric. Wastes 47, 692–699. https://doi.org/10.1080/03601234.2012.669260

Balani, K., Verma, V., Narayan, A., Roger, A., 2014. Biosurfaces: a materials science and engineering perspective, First edit. ed. John Wiley & Sons, Inc. https://doi.org/https://doi.org/10.1002/9781118950623.app1

Behr, A., Krema, S., Kampar, A., 2012. Ethenolysis of ricinoleic acid methyl ester – an efficient way to the oleochemical key substance methyl dec-9-enoate. RSC Adv. 2, 12775–12781. https://doi.org/10.1039/c2ra22499b

Biermann, U., Bornscheuer, U., Meier, M.A.R., Metzger, J.O., Schäfer, H.J., 2011. Oils and fats as renewable raw materials in chemistry. Angew. Chemie - Int. Ed. 50, 3854–3871. https://doi.org/10.1002/anie.201002767

Bogdal, D., Penczek, P., Pielichowski, J., Prociak, A., 2003. Microwave assisted synthesis, crosslinking, and processing of polymeric materials. Adv. Polym. Sci. 163, 193–263. https://doi.org/10.1007/b11051

Braun, D., Cherdron, H., Rehahn, M., Ritter, H., Brigitte, V., 2013. Polymer synthesis: theory and practice, 5th ed, Trabajo Infantil. Springer-Verlag Berlin Heidelberg. https://doi.org/10.1017/CBO9781107415324.004

Bujok, S., Konefał, M., Abbrent, S., Pavlova, E., Svoboda, J., Trhlíková, O., Walterová, Z., Beneš, H., 2020. Ionic liquid-functionalized LDH as catalytic-initiating nanoparticles for microwave-activated ring opening polymerization of ε-caprolactone. React. Chem. Eng. 5, 506–518. https://doi.org/10.1039/c9re00399a

Çakmakli, B., Hazer, B., Tekin, I.Ö., Cömert, F.B., 2005. Synthesis and characterization of polymeric soybean oil-g-methyl methacrylate (and n-butyl methacrylate) graft copolymers:

Biocompatibility and bacterial adhesion. Biomacromolecules 6, 1750–1758. https://doi.org/10.1021/bm050063f

Cakmakli, B., Hazer, B., Tekin, I.O., Kizgut, S., Koksal, M., Menceloglu, Y., 2004. Synthesis and characterization of polymeric linseed oil grafted methyl methacrylate or styrene. Macromol. Biosci. 4, 649–655. https://doi.org/10.1002/mabi.200300117

Cama, G., Mogosanu, D.E., Houben, A., Dubruel, P., 2017. Synthetic biodegradable medical polyesters: poly-ε-caprolactone, in: Zhang, X. (Ed.), science and principles of biodegradable and bioresorbable medical polymers. Elsevier Ltd. https://doi.org/https://doi.org/10.1016/B978-0-08-100372-5.00003-9

Capelot, M., Montarnal, D., Tournilhac, F., Leibler, L., 2012. Metal-catalyzed transesterification for healing and assembling of thermosets. J. Am. Chem. Soc. 134, 7664–7667. https://doi.org/10.1021/ja302894k

Chauvin, Y., 2006. Olefin metathesis: The early days (nobel lecture). Angew. Chemie - Int. Ed. 45, 3740–3747. https://doi.org/10.1002/anie.200601234

Chia, L.H.L., Boey, F.Y.C., Jacob, J., 1995. Review Thermal and non-thermal interaction of microwave radiation with materials. J. Mater. Sci. 30, 5321–5327.

Chikkali, S., Mecking, S., 2012a. Refining of plant oils to chemicals by olefin metathesis. Angew. Chemie - Int. Ed. 51, 5802–5808. https://doi.org/10.1002/anie.201107645

Chikkali, S., Mecking, S., 2012b. Refining of plant oils to chemicals by olefin metathesis. Angew. Chemie - Int. Ed. 51, 5802–5808. https://doi.org/10.1002/anie.201107645

Coleman, M.M., Skrovanek, D.J., Painter, P.C., 1986. hydrogen bonding in polymers : 111 further

infrared temperature studies of polyamides. Makromol. Chem., Macromol. Symp 5, 21–33.

Dai, H., Yang, L., Lin, B., Wang, C., Shi, G., 2009. Synthesis and characterization of the different soy-based polyols by ring opening of epoxidized soybean oil with methanol, 1,2-ethanediol and 1,2-propanediol. JAOCS, J. Am. Oil Chem. Soc. 86, 261–267. https://doi.org/10.1007/s11746-008-1342-7

Dam, V.P.B., Mittelmeijer, C., M., C., B., 1974. Homogeneous catalytic metathesis of unsaturated fatty esters: New synthetic method for preparation of unsaturated mono-and dicarboxylic acids. J. Am. Oil Chem. Soc. 51, 389–392. https://doi.org/10.1007/BF02635013

Dasgupta, S., Hammond, W.B., Goddard, W.A., 1996. Crystal structures and properties of nylon polymers from theory. J. Am. Chem. Soc. 118, 12291–12301. https://doi.org/10.1021/ja944125d

De Espinosa, L.M., Meier, M.A.R., 2011. Plant oils: The perfect renewable resource for polymer science?! Eur. Polym. J. 47, 837–852. https://doi.org/10.1016/j.eurpolymj.2010.11.020

De la Hoz, A., Díaz-Ortiz, A., Moreno, A., 2007. Review on non-thermal effects of microwave irradiation in organic synthesis. J. Microw. Power Electromagn. Energy 41, 44–64. https://doi.org/10.1080/08327823.2006.11688549

Deb, P.K., Kokaz, S.F., Abed, S.N., Paradkar, A., Tekade, R.K., 2018. Pharmaceutical and biomedical applications of polymers, in: Basic fundamentals of drug delivery. pp. 203–267. https://doi.org/10.1016/B978-0-12-817909-3.00006-6

Du, Y., Shen, S.Z., Cai, K., Casey, P.S., 2012. Research progress on polymer-inorganic thermoelectric nanocomposite materials. Prog. Polym. Sci. 37, 820–841.

https://doi.org/10.1016/j.progpolymsci.2011.11.003

Dynamic growth: global production capacities of bioplastics 2019-2024 Bioplastics [WWW Document], 2019. . Eur. Bioplastics. URL https://www.european-bioplastics.org/wp-content/uploads/2019/11/Report_Bioplastics-Market-Data_2019_short_version.pdf

Enferadi Kerenkan, A., Béland, F., Do, T.O., 2016. Chemically catalyzed oxidative cleavage of unsaturated fatty acids and their derivatives into valuable products for industrial applications: A review and perspective. Catal. Sci. Technol. 6, 971–987. https://doi.org/10.1039/c5cy01118c

Falciglia, P.P., Roccaro, P., Bonanno, L., De Guidi, G., Vagliasindi, F.G.A., Romano, S., 2018. A review on the microwave heating as a sustainable technique for environmental remediation/detoxification applications. Renew. Sustain. Energy Rev. 95, 147–170. https://doi.org/10.1016/j.rser.2018.07.031

Fink, J.K., 2011. Handbook of engineering and specialty thermoplastics, handbook of engineering and specialty thermoplastics. https://doi.org/10.1002/9781118087732

Firdaus, M., Meier, M.A.R., 2013. Renewable polyamides and polyurethanes derived from limonene. Green Chem. 15, 370–380. https://doi.org/10.1039/c2gc36557j

Gandini, A., Lacerda, T.M., 2019. Polymers from plant oils, 2nd ed. John Wiley & Sons, Inc.

Gao, X., Hu, X., Guan, P., Du, C., Ding, S., Zhang, X., Li, B., Wei, X., Song, R., 2016. Synthesis of core-shell imprinting polymers with uniform thin imprinting layer: Via iniferter-induced radical polymerization for the selective recognition of thymopentin in aqueous solution. RSC Adv. 6, 110019–110031. https://doi.org/10.1039/c6ra24518h

Garside, M., 2020. Global plastic production 1950-2018 [WWW Document]. Statistica. URL https://www.statista.com/statistics/282732/global-production-of-plastics-since-1950/

Gawande, M.B., Shelke, S.N., Zboril, R., Varma, R.S., 2014. Microwave-assisted chemistry: Synthetic applications for rapid assembly of nanomaterials and organics. Acc. Chem. Res. 47, 1338–1348. https://doi.org/10.1021/ar400309b

Gedye, R., Smith, F., Westaway, K., Ali, H., Baldisera, L., Laberge, L., Rousell, J., 1986. The use of microwave ovens for rapid organic synthesis. Tetrahedron Lett. 27, 279–282. https://doi.org/10.1016/S0040-4039(00)83996-9

Giguere, R.J., Bray, T.L., Duncan, S.M., Majetich, G., 1986. Application of commercial microwave ovens to organic synthesis. Tetrahedron Lett. 27, 4945–4948. https://doi.org/10.1016/S0040-4039(00)85103-5

Gilbert, M., 2017. Aliphatic polyamides, in: brydson's plastics materials. Elsevier Ltd., pp. 487–511. https://doi.org/https://doi.org/10.1016/B978-0-323-35824-8.00018-9

Girardon, V., Correia, I., Tessier, M., Marchal, E., 1998. characterization of functional aliphatic oligoamides using N-trifuoroacetylation- I. NMR aanlysis. Eur. Polym. J. 34, 363–380. https://doi.org/10.1016/S0014-3057(97)00141-9

Gitsas, A., Floudas, G., 2008. Pressure dependence of the glass transition in atactic and isotactic polypropylene. Macromolecules 41, 9423–9429. https://doi.org/10.1021/ma8014992

Grubbs, R.H., 2006. Olefin-metathesis catalysts for the preparation of molecules and materials (Nobel lecture). Angew. Chemie - Int. Ed. 45, 3760–3765. https://doi.org/10.1002/anie.200600680

Guo, B., Glavas, L., Albertsson, A.C., 2013. Biodegradable and electrically conducting polymers for biomedical applications. Prog. Polym. Sci. 38, 1263–1286. https://doi.org/10.1016/j.progpolymsci.2013.06.003

Haddou, G., Roggero, A., Dandurand, J., Dantras, E., Ponteins, P., Lacabanne, C., 2018. Dynamic relaxations in a bio-based polyamide with enhanced mechanical modulus. J. Appl. Polym. Sci. 135, 2–7. https://doi.org/10.1002/app.46846

Heijboer, J., 1977. Secondary loss peaks in glassy amorphous polymers. Int. J. Polym. Mater. 6, 11–37. https://doi.org/10.1080/00914037708075218

Henna, P.H., Andjelkovic, D.D., Kundu, P.P., Larock, R.C., 2007. Biobased thermosets from the free-radical copolymerization of conjugated linseed oil phillip. J. Appl. Polym. Sci. 104, 979–985.

Herrán, R., Amalvy, J.I., Chiacchiarelli, L.M., 2019. Highly functional lactic acid ring-opened soybean polyols applied to rigid polyurethane foams. J. Appl. Polym. Sci. 136, 47959 (1–13). https://doi.org/10.1002/app.47959

Hindeleh, A.M., Abdo, S.M., 1989. Effects of annealing on the crystallinity and microparacrystallite size of Kevlar 49 fibres. Polymer (Guildf). 30, 218–224.

Ho, K.P., Wong, W.L., Lam, K.M., Lai, C.P., Chan, T.H., Wong, K.Y., 2008. A simple and effective catalytic system for epoxidation of aliphatic terminal alkenes with manganese(II) as the catalyst. Chem. - A Eur. J. 14, 7988–7996. https://doi.org/10.1002/chem.200800759

Holmes, D.R., Bunn, C.W., Smith, D.J., 1955. The crystal structure of polycaproamide: Nylon 6. J. Polym. Sci. 17, 159–177. https://doi.org/10.1002/pol.1955.120178401

Hoogenboom, R., Schubert, U.S., 2007. Microwave-assisted polymer synthesis: Recent developments in a rapidly expanding field of research. Macromol. Rapid Commun. 28, 368–386. https://doi.org/10.1002/marc.200600749

Hoppe, C.E., Galante, M.J., Oyanguren, P.A., Williams, R.J.J., 2005. Epoxies modified by palmitic acid: From hot-melt adhesives to plasticized networks. Macromol. Mater. Eng. 290, 456–462. https://doi.org/10.1002/mame.200400348

Hoveyda, A.H., Zhugralin, A.R., 2007. The remarkable metal-catalysed olefin metathesis reaction. Nature 450, 243–251. https://doi.org/10.1038/nature06351

Huf, S., Krügener, S., Hirth, T., Rupp, S., Zibek, S., 2011. Biotechnological synthesis of long-chain dicarboxylic acids as building blocks for polymers. Eur. J. Lipid Sci. Technol. 113, 548–561. https://doi.org/10.1002/ejlt.201000112

Imada, Y., Iida, H., Kitagawa, T., Naota, T., 2011. Aerobic reduction of olefins by in situ generation of diimide with synthetic flavin catalysts. Chem. - A Eur. J. 17, 5908–5920. https://doi.org/10.1002/chem.201003278

Ionescu, M., Petrović, Z.S., Wan, X., 2008. Primary hydroxyl content of soybean polyols. J. Am. Oil Chem. Soc. 85, 465–473. https://doi.org/10.1007/s11746-008-1210-5

Iqbal, M., Shakeel, F., Anwer, T., 2016. Simple and sensitive UPLC-MS/MS method for high-throughput analysis of ibrutinib in rat plasma: Optimization by box-behnken experimental design. J. AOAC Int. 99, 618–625. https://doi.org/10.5740/jaoacint.15-0222

Jambeck, J., Geyer, R., Wilcox, C., Siegler, T.R., Perryman, M., Andrady, A., Narayan, R., Law, K.L., 2015. Plastic waste inputs from land into the ocean 347, 3–6.

https://doi.org/10.1126/science.1260352

Jasinska, L., Villani, M., Wu, J., Van Es, D., Klop, E., Rastogi, S., Koning, C.E., 2011a. Novel, fully biobased semicrystalline polyamides. Macromolecules 44, 3458–3466. https://doi.org/10.1021/ma200256v

Jasinska, L., Villani, M., Wu, J., Van Es, D., Klop, E., Rastogi, S., Koning, C.E., 2011b. Novel, fully biobased semicrystalline polyamides. Macromolecules 44, 3458–3466. https://doi.org/10.1021/ma200256v

Jin, L., Geng, K., Arshad, M., Ahmadi, R., Ullah, A., 2017. Synthesis of Fully Biobased Polyesters from Plant Oil. ACS Sustain. Chem. Eng. 5, 9793–9801. https://doi.org/10.1021/acssuschemeng.7b01668

Kaczmarczyk, B., Danuta, S., 1995. Hydrogen bonds in poly(ester amide)s and their model compounds. Polymer (Guildf). 36, 5019–5025. https://doi.org/10.1016/0032-3861(96)81631-4

Karmakar, G., Ghosh, P., 2016. Atom transfer radical polymerization of soybean oil and its evaluation as a biodegradable multifunctional additive in the formulation of eco-friendly lubricant. ACS Sustain. Chem. Eng. 4, 775–781. https://doi.org/10.1021/acssuschemeng.5b00746

Karnachi, A.A., Khan, M.A., 1996. Box-behnken design for the optimization of formulation variables of indomethacin coprecipitates with polymer mixtures. Int. J. Pharm. 131, 9–17. https://doi.org/10.1016/0378-5173(95)04216-4

Kempe, K., Becer, C.R., Schubert, U.S., 2011. Microwave-assisted polymerizations: Recent status

and future perspectives. Macromolecules 44, 5825–5842. https://doi.org/10.1021/ma2004794

Kennedy, J.P., Marechal, E., 1982. Carbocationic Polymerization. John Wiley & Sons, New York.

Kerep, P., Ritter, H., 2006. Influence of microwave irradiation on the lipase-catalyzed ring-opening polymerization of e-caprolactone. Macromol. Rapid Commun. 27, 707–710. https://doi.org/10.1002/marc.200500781

Kiesewetter, M.K., Scholten, M.D., Kirn, N., Weber, R.L., Hedrick, J.L., Waymouth, R.M., 2009. Cyclic guanidine organic catalysts: What is magic about triazabicyclodecene? J. Org. Chem. 74, 9490–9496. https://doi.org/10.1021/jo902369g

Kline, G.M., 1962. High polymers. John Wiley & Sons, Inc. USA.

Kollbe Ahn, B., Wang, H., Robinson, S., Shrestha, T.B., Troyer, D.L., Bossmann, S.H., Sun, X.S., 2012. Ring opening of epoxidized methyl oleate using a novel acid-functionalized iron nanoparticle catalyst. Green Chem. 14, 136–142. https://doi.org/10.1039/c1gc16043e

Kollbe Ahn, B.J., Kraft, S., Sun, X.S., 2011. Chemical pathways of epoxidized and hydroxylated fatty acid methyl esters and triglycerides with phosphoric acid. J. Mater. Chem. 21, 9498–9505. https://doi.org/10.1039/c1jm10921a

Komorowska-Durka, M., Dimitrakis, G., Bogdał, D., Stankiewicz, A.I., Stefanidis, G.D., 2015. A concise review on microwave-assisted polycondensation reactions and curing of polycondensation polymers with focus on the effect of process conditions. Chem. Eng. J. 264, 633–644. https://doi.org/10.1016/j.cej.2014.11.087

Kotzebue, L.R.V., De Oliveira, J.R., Da Silva, J.B., Mazzetto, S.E., Ishida, H., Lomonaco, D., 2018. Development of fully biobased high-performance bis-benzoxazine under

environmentally friendly conditions. ACS Sustain. Chem. Eng. 6, 5485–5494. https://doi.org/10.1021/acssuschemeng.8b00340

Kousha, M., Daneshvar, E., Dopeikar, H., Taghavi, D., Bhatnagar, A., 2012. Box-Behnken design optimization of Acid Black 1 dye biosorption by different brown macroalgae. Chem. Eng. J. 179, 158–168. https://doi.org/10.1016/j.cej.2011.10.073

Kovács, E., Turczel, G., Szabó, L., Varga, R., Tóth, I., Anastas, P.T., Tuba, R., 2017. Synthesis of 1,6-Hexandiol, polyurethane monomer derivatives via isomerization metathesis of methyl linolenate. ACS Sustain. Chem. Eng. 5, 11215–11220. https://doi.org/10.1021/acssuschemeng.7b03309

Kumar, A., Kuang, Y., Liang, Z., Sun, X., 2020. Microwave chemistry, recent advancements, and eco-friendly microwave-assisted synthesis of nanoarchitectures and their applications: a review. Mater. Today Nano 11, 100076. https://doi.org/10.1016/j.mtnano.2020.100076

Kundu, P.P., Larock, R.C., 2005. Novel conjugated linseed oil-styrene-divinylbenzene copolymers prepared by thermal polymerization. 1. Effect of monomer concentration on the structure and properties. Biomacromolecules 6, 797–806. https://doi.org/10.1021/bm049429z

Kunduru, K.R., Basu, A., Haim Zada, M., Domb, A.J., 2015. Castor oil-based biodegradable polyesters. Biomacromolecules 16, 2572–2587. https://doi.org/10.1021/acs.biomac.5b00923

Larock, R.C., Dong, X., Chung, S., Reddy, C.K., Ehlers, L.E., 2001. Preparation of conjugated soybean oil and other natural oils and fatty acids by homogeneous transition metal catalysis. JAOCS, J. Am. Oil Chem. Soc. 78, 447–453. https://doi.org/10.1007/s11746-001-0284-1

Le, D., Samart, C., Tsutsumi, K., Nomura, K., Kongparakul, S., 2018. Efficient conversion of

renewable unsaturated fatty acid methyl esters by cross-metathesis with eugenol. ACS Omega 3, 11041–11049. https://doi.org/10.1021/acsomega.8b01695

Le Huy, H.M., Rault, J., 1994. Remarks on the a and .beta. transitions in swollen polyamides. Polymer (Guildf). 35, 136–139.

Levchik, S. V., Weil, E.D., 2004. A review on thermal decomposition and combustion of thermoplastic polyesters. Polym. Adv. Technol. 15, 691–700. https://doi.org/10.1002/pat.526

Levchik, S. V, Weil, E.D., Lewin, M., 1999. Thermal decomposition of aliphatic nylons. Polym. Int. 48, 532–557. https://doi.org/10.1002/(SICI)1097-0126(199907)48:7<532::AID-PI214>3.0.CO;2-R

Li, F., Hasjim, J., Larock, R.C., 2003. Synthesis, structure, and thermophysical and mechanical properties of new polymers prepared by the cationic copolymerization of corn oil, styrene, and divinylbenzene. J. Appl. Polym. Sci. 90, 1830–1838. https://doi.org/10.1002/app.12826

Li, F., Larock, R.C., 2003a. Synthesis, structure and properties of new tung oil - Styrene - Divinylbenzene copolymers prepared by thermal polymerization. Biomacromolecules 4, 1018–1025. https://doi.org/10.1021/bm034049j

Li, F., Larock, R.C., 2003b. New soybean oil-styrene-divinylbenzene thermosetting copolymers. VI. Time-temperature-transformation cure diagram and the effect of curing conditions on the thermoset properties. Polym. Int. 52, 126–132. https://doi.org/10.1002/pi.1060

Li, F., Larock, R.C., 2002a. New soybean oil-styrene-divinylbenzene thermosetting copolymers-IV. Good damping properties. Polym. Adv. Technol. 13, 436–449. https://doi.org/10.1002/pat.206

178

Li, F., Larock, R.C., 2002b. New soybean oil-styrene-divinylbenzene thermosetting copolymers. V. Shape memory effect. J. Appl. Polym. Sci. 84, 1533–1543. https://doi.org/10.1002/app.10493

Li, F., Larock, R.C., 2001a. New soybean oil-styrene-divinylbenzene thermosetting copolymers. I. Synthesis and characterization. J. Appl. Polym. Sci. 80, 658–670. https://doi.org/10.1002/1097-4628(20010425)80:4<658::AID-APP1142>3.0.CO;2-D

Li, F., Larock, R.C., 2001b. New soybean oil-styrene-divinylbenzene thermosetting copolymers. III. Tensile Stress–Strain Behavior. J. of Polymer Sci. Part B Polym. Phys. 39, 60–77. https://doi.org/https://doi.org/10.1002/1099-0488(20010101)39:1<60::AID-POLB60>3.0.CO;2-K

Li, F., Larock, R.C., 2000. New soybean oil-styrene-divinylbenzene thermosetting copolymers. II. Dynamic mechanical properties. J. Polym. Sci. Part B Polym. Phys. 38, 2721–2738. https://doi.org/10.1002/1099-0488(20001101)38:21<2721::AID-POLB30>3.0.CO;2-D

Li, F., Marks, D.W., Larock, R.C., Otaigbe, J.U., 2001. Soybean oil–divinylbenzene thermosetting polymers: synthesis, structure, properties and their relationships. Polymer (Guildf). 42, 1567–1579. https://doi.org/https://doi.org/10.1016/S0032-3861(00)00546-2

Li, Q., Wang, T., Ma, C., Bai, W., Bai, R., 2014. Facile and highly efficient strategy for synthesis of functional polyesters via tetramethyl guanidine promoted polyesterification at room temperature. ACS Macro Lett. 3, 1161–1164. https://doi.org/10.1021/mz5005184

Li, Y., Wang, D., Sun, X.S., 2015. Copolymers from epoxidized soybean oil and lactic acid oligomers for pressure-sensitive adhesives. RSC Adv. 5, 27256–27265.

https://doi.org/10.1039/c5ra02075a

Li, Y., Wang, X.L., Yang, K.K., Wang, Y.Z., 2006. A rapid synthesis of poly (p-dioxanone) by ring-opening polymerization under microwave irradiation. Polym. Bull. 57, 873–880. https://doi.org/10.1007/s00289-006-0668-2

Lidstrom, P., Tierney, J., Wathey, B., Westman Jacob, 2001. Microwave-assisted green organic synthesis-a review. Tetrahedron 57, 9225–9283.

Lim, L.T., Auras, R., Rubino, M., 2008. Processing technologies for poly(lactic acid). Prog. Polym. Sci. 33, 820–852. https://doi.org/10.1016/j.progpolymsci.2008.05.004

Lipshutz, B.H., Ghorai, S., 2012. "Designer"-Surfactant-Enabled Cross-Couplings in Water at Room Temperature. Aldrichimica Act 45, 3–16.

Liu, K., Madbouly, S.A., Schrader, J.A., Kessler, M.R., Grewell, D., Graves, W.R., 2015. Biorenewable polymer composites from tall oil-based polyamide and lignin-cellulose fiber. J. Appl. Polym. Sci. 132, 42592. https://doi.org/https://doi.org/10.1002/app.42592

Liu, X., Wu, Q., Berglund, L.A., 2002. Polymorphism in polyamide 66/clay nanocomposites. Polymer (Guildf). 43, 4967–4972. https://doi.org/10.1016/S0032-3861(02)00331-2

Liu, Z., Erhan, S.Z., 2010. Preparation of soybean oil polymers with high molecular weight. J. Polym. Environ. 18, 243–249. https://doi.org/10.1007/s10924-010-0179-y

Lligadas, G., Ronda, J.C., Galià, M., Cádiz, V., 2013. Renewable polymeric materials from vegetable oils: A perspective. Mater. Today 16, 337–343. https://doi.org/10.1016/j.mattod.2013.08.016

Lu, Y., Larock, R.C., 2009. Novel polymeric materials from vegetable oils and vinyl monomers : preparation , properties , and applications. ChemSusChem 2, 136–147. https://doi.org/10.1002/cssc.200800241

Madbouly, S.A., Liu, K., Xia, Y., Kessler, M.R., 2014. Semi-interpenetrating polymer networks prepared from in situ cationic polymerization of bio-based tung oil with biodegradable polycaprolactone. RSC Adv. 4, 6710–6718. https://doi.org/10.1039/c3ra46773b

Malcolmson, S.J., Meek, S.J., Sattely, E.S., Schrock, R.R., Hoveyda, A.H., 2008. Highly efficient molybdenum-based catalysts for enantioselective alkene metathesis. Nature 456, 933–937. https://doi.org/10.1038/nature07594

Mallégol, J., Lemaire, J., Gardette, J., 2000. Drier influence on the curing of linseed oil. Prog. Org. Coatings 39, 107–113. https://doi.org/10.1016/S0300-9440(00)00126-0

Marinescu, S.C., Schrock, R.R., Müller, P., Hoveyda, A.H., 2009. Ethenolysis reactions catalyzed by imido alkylidene monoaryloxide monopyrrolide (MAP) complexes of molybdenum. J. Am. Chem. Soc. 131, 10840–10841. https://doi.org/10.1021/ja904786y

Marks, D.W., Li, F., Pacha, C.M., Larock, R.C., 2001. Synthesis of thermoset plastics by Lewis acid initiated copolymerization of fish oil ethyl esters and alkenes. J. Appl. Polym. Sci. 81, 2001–2012. https://doi.org/10.1002/app.1632

Martino, L., Basilissi, L., Farina, H., Ortenzi, M.A., Zini, E., Di Silvestro, G., Scandola, M., 2014. Bio-based polyamide 11: Synthesis, rheology and solid-state properties of star structures. Eur. Polym. J. 59, 69–77. https://doi.org/10.1016/j.eurpolymj.2014.07.012

Marx, V.M., Sullivan, A.H., Melaimi, M., Virgil, S.C., Keitz, B.K., Weinberger, D.S., Bertrand,

G., Grubbs, R.H., 2015. Cyclic alkyl amino carbene (caac) ruthenium complexes as remarkably active catalysts for ethenolysis. Angew. Chemie - Int. Ed. 54, 1919–1923. https://doi.org/10.1002/anie.201410797

Meier, M.A.R., Metzger, J.O., Schubert, U.S., 2007. Plant oil renewable resources as green alternatives in polymer science. Chem. Soc. Rev. 36, 1788–1802. https://doi.org/10.1039/b703294c

Meiorin, C., Aranguren, M.I., Mosiewicki, M.A., 2012. Smart and structural thermosets from the cationic copolymerization of a vegetable oil cintia. J. Appl. Polym. Sci. 124, 5071–5078. https://doi.org/10.1002/app.35630

Miao, S., Wang, P., Su, Z., Zhang, S., 2014. Vegetable-oil-based polymers as future polymeric biomaterials. Acta Biomater. 10, 1692–1704. https://doi.org/10.1016/j.actbio.2013.08.040

Miao, X., Blokhin, A., Pasynskii, A., Nefedov, S., Osipov, S.N., Roisnel, T., Bruneau, C., Dixneuf, P.H., 2010. Alkylidene-ruthenium-tin catalysts for the formation of fatty nitriles and esters via cross-metathesis of plant oil derivatives. Organometallics 29, 5257–5262. https://doi.org/10.1021/om100372b

Miao, X., Dixneuf, P.H., Fischmeister, C., Bruneau, C., 2011. A green route to nitrogen-containing groups: The acrylonitrile cross-metathesis and applications to plant oil derivatives. Green Chem. 13, 2258–2271. https://doi.org/10.1039/c1gc15377c

Mol, J.C., 2004. Industrial applications of olefin metathesis. J. Mol. Catal. A Chem. 213, 39–45. https://doi.org/10.1016/j.molcata.2003.10.049

Molina-Gutierrez, S., Ladmiral, V., Bongiovanni, R.M., Caillol, S., Lacroix-Desmazes, P., 2019.

Radical polymerization of biobased monomers in aqueous dispersed media. Green Chem. 21, 36–53. https://doi.org/10.1039/C8GC02277A

Monteavaro, L.L., Da Silva, E.O., Costa, A.P.O., Samios, D., Gerbase, A.E., Petzhold, C.L., 2005. Polyurethane networks from formiated soy polyols: Synthesis and mechanical characterization. JAOCS, J. Am. Oil Chem. Soc. 82, 365–371. https://doi.org/10.1007/s11746-005-1079-0

Morgan, R.J., Nielsen, L.E., 1974. The dynamic mechanical properties of polymers at cryogenic temperatures. J. Macromol. Sci. Part B 9, 239–253. https://doi.org/10.1080/00222347408212192

Morrison, R.F., Lipscomb, N., Eldridge, R.B., Ginn, P., 2014. Rhenium oxide based olefin metathesis. Ind. Eng. Chem. Res. 53, 19136–19144. https://doi.org/10.1021/ie5034232

Mosiewicki, M.A., Aranguren, M.I., 2013. A short review on novel biocomposites based on plant oil precursors. Eur. Polym. J. 49, 1243–1256. https://doi.org/http://dx.doi.org/10.1016/j.eurpolymj.2013.02.034

Motasemi, F., Afzal, M.T., 2013. A review on the microwave-assisted pyrolysis technique. Renew. Sustain. Energy Rev. 28, 317–330. https://doi.org/10.1016/j.rser.2013.08.008

Mutlu, H., Meier, M.A.R., 2010. Castor oil as a renewable resource for the chemical industry. Eur. J. Lipid Sci. Technol. 112, 10–30. https://doi.org/10.1002/ejlt.200900138

Mutlu, H., Meier, M.A.R., 2009. Unsaturated PA X,20 from renewable resources via metathesis and catalytic amidation. Macromol. Chem. Phys. 210, 1019–1025. https://doi.org/10.1002/macp.200900045

Mutyala, S., Fairbridge, C., Paré, J.R.J., Bélanger, J.M.R., Ng, S., Hawkins, R., 2010. Microwave applications to oil sands and petroleum: A review. Fuel Process. Technol. 91, 127–135. https://doi.org/10.1016/j.fuproc.2009.09.009

Nagahata, R., Nakamura, T., Takeuchi, K., 2018. Microwave-assisted rapid synthesis of poly(butylene succinate): Principal effect of microwave irradiation of accelerating the polycondensation reaction. Polym. J. 50, 347–354. https://doi.org/10.1038/s41428-018-0024-z

Nagahata, R., Sano, D., Suzuki, H., Takeuchi, K., 2007. Microwave-assisted single-step synthesis of poly(lactic acid) by direct polycondensation of lactic acid. Macromol. Rapid Commun. 28, 437–442. https://doi.org/10.1002/marc.200600715

Nakajima, H., Dijkstra, P., Loos, K., 2017. The recent developments in biobased polymers toward general and engineering applications: Polymers that are upgraded from biodegradable polymers, analogous to petroleum-derived polymers, and newly developed. Polymers (Basel). 9, 1–26. https://doi.org/10.3390/polym9100523

Nameer, S., Johansson, M., 2017. Fully bio-based aliphatic thermoset polyesters via self-catalyzed self-condensation of multifunctional epoxy monomers directly extracted from natural sources. J. Coatings Technol. Res. 14, 757–765. https://doi.org/10.1007/s11998-017-9920-y

Nayak, P.L., 2000. Natural oil-based polymers: Opportunities and challenges. J. Macromol. Sci. - Polym. Rev. 40, 1–21. https://doi.org/10.1081/MC-100100576

Ngo, H.L., Jones, K., Foglia, T.A., 2006. Metathesis of unsaturated fatty acids: Synthesis of long-chain unsaturated-α,ω-dicarboxylic acids. JAOCS, J. Am. Oil Chem. Soc. 83, 629–634.

https://doi.org/10.1007/s11746-006-1249-0

Nguyen, H.T.H., Qi, P., Rostagno, M., Feteha, A., Miller, S.A., 2018. The quest for high glass transition temperature bioplastics. J. Mater. Chem. A 6, 9298–9331. https://doi.org/10.1039/c8ta00377g

Nieres, P.D., Zelin, J., Trasarti, A.F., Apesteguía, C.R., 2016. Heterogeneous catalysis for valorisation of vegetable oils via metathesis reactions : ethenolysis of methyl oleate. Catal. Sci. Technol. 6, 6561–6568. https://doi.org/10.1039/c6cy01214k

Nuyken, O., Pask, S.D., 2013. Ring-opening polymerization-An introductory review. Polymers (Basel). 5, 361–403. https://doi.org/10.3390/polym5020361

Oilseeds: World Markets and Trade., 2019. Oilseeds: World markets and trade. [WWW Document]. URL https://apps.fas.usda.gov/psdonline/circulars/oilseeds.pdf) (accessed 2019-05-13

Oliva, R., Ortenzi, M.A., Salvini, A., Papacchini, A., Giomi, D., 2017. One-pot oligoamides syntheses from l-lysine and l-tartaric acid. RSC Adv. 7, 12054–12062. https://doi.org/10.1039/c7ra00676d

Omonov, T.S., Curtis, J.M., 2014. Biobased epoxy resin from canola oil. J. Appl. Polym. Sci. 131, 1–9. https://doi.org/10.1002/app.40142

Omonov, T.S., Kharraz, E., Curtis, J.M., 2016. The epoxidation of canola oil and its derivatives. RSC Adv. 6, 92874–92886. https://doi.org/10.1039/c6ra17732h

Omonov, T.S., Kharraz, E., Foley, P., Curtis, J.M., 2014. The production of biobased nonanal by ozonolysis of fatty acids. RSC Adv. 4, 53617–53627. https://doi.org/10.1039/c4ra07917e
185

Osborne, J.W., 2010. Improving your data transformations: Applying the Box-Cox transformation. Pract. Assessment, Res. Eval. 15.

Pagacz, J., Raftopoulos, K.N., Leszczyńska, A., Pielichowski, K., 2016. Bio-polyamides based on renewable raw materials: Glass transition and crystallinity studies. J. Therm. Anal. Calorim. 123, 1225–1237. https://doi.org/10.1007/s10973-015-4929-x

Pardal, F., Salhi, S., Rousseau, B., Tessier, M., Claude, S., Fradet, A., 2008. Unsaturated polyamides from bio-based Z-octadec-9-enedioic acid. Macromol. Chem. Phys. 209, 64–74. https://doi.org/10.1002/macp.200700319

Pasch, H., Malik, M.I., Macko, T., 2013. Recent advances in high-temperature fractionation of polyolefins, in: Abe, A., Kausch, H.-H., Möller, M., Pasch, H. (Eds.), Polymer Composites - - Polyolefin Fractionation -- Polymeric Peptidomimetics -- Collagens. Springer Berlin Heidelberg, Berlin, Heidelberg, pp. 77–140. https://doi.org/10.1007/12_2012_167

Patel, J., Mujcinovic, S., Jackson, W.R., Robinson, A.J., Serelis, A.K., Such, C., 2006. High conversion and productive catalyst turnovers in cross-metathesis reactions of natural oils with 2-butene. Green Chem. 8, 450–454. https://doi.org/10.1039/b600956e

Pechar, T.W., Wilkes, G.L., Zhou, B., Luo, N., 2007. Characterization of soy-based polyurethane networks prepared with different diisocyanates and their blends with petroleum-based polyols. J. Appl. Polym. Sci. 106, 2350–2362. https://doi.org/DOI 10.1002/app.26569

Pelletier, H., Belgacem, N., Gandini, A., 2006. Acrylated vegetable oils as photocrosslinkable materials. J. Appl. Polym. Sci. 99, 3218–3221. https://doi.org/10.1002/app.22322

Peplow, M., 2016. The plastics revolution: how chemists are pushing polymers to new limits.

Nature 536, 266–268.

Polk, M., Vigo, T.L., Albin Turbak, F., 2004. High performance fibers. Encycl. Polym. Sci. Technol. https://doi.org/https://doi.org/10.1002/0471440264.pst523

Pradhan, R.A., Arshad, M., Ullah, A., 2020. Solvent-free rapid ethenolysis of fatty esters from spent hen and other lipidic feedstock with high turnover numbers. J. Ind. Eng. Chem. 84, 42–45. https://doi.org/10.1016/j.jiec.2020.01.002

Prakash Maran, J., Manikandan, S., Thirugnanasambandham, K., Vigna Nivetha, C., Dinesh, R., 2013. Box-Behnken design based statistical modeling for ultrasound-assisted extraction of corn silk polysaccharide. Carbohydr. Polym. 92, 604–611. https://doi.org/10.1016/j.carbpol.2012.09.020

Psarski, M., Pracella, M., Galeski, A., 2000. Crystal phase and crystallinity of polyamide 6/functionalized polyolefin blends. Polymer (Guildf). 41, 4923–4932. https://doi.org/10.1016/S0032-3861(99)00720-X

Qu, H., Liu, X., Xu, J., Ma, H., Jiao, Y., Xie, J., 2014. Investigation on thermal degradation of poly(1,4-butylene terephthalate) filled with aluminum hypophosphite and trimer by thermogravimetric analysis-fourier transform infrared spectroscopy and thermogravimetric analysis-mass spectrometry. Ind. Eng. Chem. Res. 53, 8476–8483. https://doi.org/10.1021/ie404297r

Rio, E. Del, Galià, M., Cádiz, V., Lligadas, G., Ronda, J.C., 2010. Polymerization of epoxidized vegetable oil derivatives: ionic-coordinative polymerization of methylepoxyoleate. J. Polym. Sci. Part A Polym. Chem. 48, 4995–5008. https://doi.org/https://doi.org/10.1002/pola.24297

Roumanet, P.J., Laflèche, F., Jarroux, N., Raoul, Y., Claude, S., Guégan, P., 2013. Novel aliphatic polyesters from an oleic acid based monomer. Synthesis, epoxidation, cross-linking and biodegradation. Eur. Polym. J. 49, 813–822. https://doi.org/10.1016/j.eurpolymj.2012.08.002

Rulkens, R., Koning, C., 2012. Chemistry and Technology of Polyamides, in: Matyjaszewski, K., Möller, M. (Eds.), Polymer Science: A Comprehensive Reference. Elsevier B.V., pp. 431–467. https://doi.org/10.1016/B978-0-444-53349-4.00147-3

Rüsch Gen. Klaas, M., Warwel, S., 1997. Lipase-catalyzed preparation of peroxy acids and their use for epoxidation. J. Mol. Catal. A Chem. 117, 311–319. https://doi.org/10.1016/S1381-1169(96)00264-6

Rüsch, M., Warwel, S., 1999. Complete and partial epoxidation of plant oils by lipase-catalyzed perhydrolysis. Ind. Crops Prod. 9, 125–132. https://doi.org/10.1016/S0926-6690(98)00023-5

Sabot, C., Kumar, K.A., Meunier, S., Mioskowski, C., 2007. A convenient aminolysis of esters catalyzed by 1,5,7-triazabicyclo[4.4.0]dec-5-ene (TBD) under solvent-free conditions. Tetrahedron Lett. 48, 3863–3866. https://doi.org/10.1016/j.tetlet.2007.03.146

Sacristán, M., Ronda, J.C., Galià, M., Cádiz, V., 2010. Rapid soybean oil copolymers synthesis by microwave-assisted cationic polymerization. Macromol. Chem. Phys. 211, 801–808. https://doi.org/10.1002/macp.200900571

Santhoshkumar, A., Thangarasu, V., Anand, R., 2019. Performance, combustion, and emission characteristics of DI diesel engine using mahua biodiesel, in: Azad, A.K., Rasul, M. (Eds.), Advanced Biofuels: Applications, Technologies and Environmental Sustainability. Elsevier Ltd, pp. 291–327. https://doi.org/10.1016/B978-0-08-102791-2.00012-X

Sato, K., Aoki, M., Ogawa, M., Hashimoto, T., Noyori, R., 1996. A practical method for epoxidation of terminal olefins with 30% hydrogen peroxide under halide-free conditions. J. Org. Chem. 61, 8310–8311. https://doi.org/10.1021/jo961287e

Schrock, R.R., 2006. Multiple metal-carbon bonds for catalytic metathesis reactions (nobel lecture). Angew. Chemie - Int. Ed. 45, 3748–3759. https://doi.org/10.1002/anie.200600085

Schuchardt, U., Sercheli, R., Matheus, R., 1998. Transesterification of vegetable oils : a review. J. Braz. Chem. Soc., 9, 199–210. https://doi.org/10.1590/S0103-50531998000300002

Shah, F.U., Akhtar, F., Khan, M.S.U., Akhter, Z., Antzutkin, O.N., 2016. Solid-state 13C, 15N and 29Si NMR characterization of block copolymers with CO2 capture properties. Magn. Reson. Chem. 54, 734–739. https://doi.org/10.1002/mrc.4440

Shahbandeh, M., 2020. Vegetable oils: production worldwide 2012/13-2019/20, by type [WWW Document]. Statistica. URL https://www.statista.com/statistics/263933/production-of-vegetable-oils-worldwide-since-2000/

Silva, C.V.G., da Silva Filho, E.A., Uliana, F., de Jesus, L.F.R., de Melo, C.V.P., Barthus, R.C., Rodrigues, J.G.A., Vanini, G., 2018. PET glycolysis optimization using ionic liquid [Bmin]ZnCl 3 as catalyst and kinetic evaluation. Polimeros 28, 450–459. https://doi.org/10.1590/0104-1428.00418

Sinnwell, S., Ritter, H., 2007. Recent advances in microwave-assisted polymer synthesis. Aust. J. Chem. 60, 729–743. https://doi.org/10.1071/CH07219

Song, L., Zhu, T., Yuan, L., Zhou, J., Zhang, Y., Wang, Z., Tang, C., 2019. Ultra-strong long-chain polyamide elastomers with programmable supramolecular interactions and oriented

crystalline microstructures. Nat. Commun. 10, 1–8. https://doi.org/10.1038/s41467-019-09218-6

Stempfle, F., Ortmann, P., Mecking, S., 2016. Long-chain aliphatic polymers to bridge the gap between semicrystalline polyolefins and traditional polycondensates. Chem. Rev. 116, 4597–4641. https://doi.org/10.1021/acs.chemrev.5b00705

Stempfle, F., Quinzler, D., Heckler, I., Mecking, S., 2011. Long-chain linear C19 and C23 monomers and polycondensates from unsaturated fatty acid esters. Macromolecules 44, 4159–4166. https://doi.org/10.1021/ma200627e

Takahira, Y., Morizawa, Y., 2015. Ruthenium-catalyzed olefin cross-metathesis with tetrafluoroethylene and analogous fluoroolefins. J. Am. Chem. Soc. 137, 7031–7034. https://doi.org/10.1021/jacs.5b03342

Tao, L., Liu, K., Li, T., Xiao, R., 2019. Preparation and properties of biobased polyamides based on 1,9-azelaic acid and different chain length diamines, Polymer Bulletin. Springer Berlin Heidelberg. https://doi.org/10.1007/s00289-019-02791-2

Temur Ergan, B., Bayramoğlu, M., 2018. Poly (l-lactic acid) synthesis using continuous microwave irradiation–simultaneous cooling method. Chem. Eng. Commun. 205, 1665–1677. https://doi.org/10.1080/00986445.2018.1464446

Thomas, R.M., Keitz, B.K., Champagne, T.M., Grubbs, R.H., 2011. Highly selective ruthenium metathesis catalysts for ethenolysis. J. Am. Chem. Soc. 133, 7490–7496. https://doi.org/10.1021/ja200246e

Tian, C., Fu, S., Chen, J., Meng, Q., Lucia, L.A., 2014. Graft polymerization of ε-caprolactone to

cellulose nanocrystals and optimization of grafting conditions utilizing a response surface methodology. Nord. Pulp Pap. Res. J. https://doi.org/10.3183/npprj-2014-29-01-p058-068

Trnka, T.M., Grubbs, R.H., 2001. The development of L2X2RU=CHR olefin metathesis catalysts: An organometallic success story. Acc. Chem. Res. 34, 18–29. https://doi.org/10.1021/ar000114f

Türünç, O., Firdaus, M., Klein, G., Meier, M.A.R., 2012. Fatty acid derived renewable polyamides via thiol-ene additions. Green Chem. 14, 2577–2583. https://doi.org/10.1039/c2gc35982k

Ullah, A., Arshad, M., 2018. Conversion of lipides olefins. US Pat., US 10,138,430 B2, 2018. US 10 , 138 , 430 B2.

Ullah, A., Arshad, M., 2017a. Remarkably efficient microwave-assisted cross-metathesis of lipids under solvent-free conditions. ChemSusChem 10, 2167–2174. https://doi.org/10.1002/cssc.201601824

Ullah, A., Arshad, M., 2017b. Remarkably efficient microwave-assisted cross-metathesis of lipids under solvent-free conditions. ChemSusChem 10, 2167–2174. https://doi.org/10.1002/cssc.201601824

Valverde, M., Andjelkovic, D., Kundu, P.P., Larock, R.C., 2008. Conjugated low-saturation soybean oil thermosets: free-radical copolymerization with Dicyclopentadiene and Divinylbenzene. J. Appl. Polym. Sci. 107, 423–430. https://doi.org/DOI 10.1002/app.27080

Van Dam, P.B., Mittelmeijer, M.C., Boelhouwer, C., 1972. Metathesis of unsaturated fatty acid esters by a homogeneous tungsten hexachloride-tetramethyltin catalyst. J. Chem. Soc. Chem. Commun. 1221–1222. https://doi.org/10.1039/C39720001221

Van der Klis, F., Le Nôtre, J., Blaauw, R., van Haveren, J., van Es, D.S., 2012. Renewable linear alpha olefins by selective ethenolysis of decarboxylated unsaturated fatty acids. Eur. J. Lipid Sci. Technol. 114, 911–918. https://doi.org/10.1002/ejlt.201200024

Van Der Ploeg, F., 2011. Natural resources: Curse or blessing? J. Econ. Lit. 49, 366–420. https://doi.org/10.1257/jel.49.2.366

Vink, E.T.H., Ra'bago, K.R., Glassner, D.A., Gruber, P.R., 2003. Applications of life cycle assessment to nature works TM polylactide (PLA) production 80, 403–419. https://doi.org/10.1016/S0141-3910(02)00372-5

Wang, C.S., Li-Ting, Y., Ni, B.-L., Shi, G., 2009. Polyurethane networks from different soy-based polyols by the ring opening of epoxidized soybean oil with methanol, glycol, and 1,2-propanediol. J. Appl. Polym. Sci. 114, 125–131. https://doi.org/10.1002/app.30493

Wang, X.Z., He, J., Weng, Y.X., Zeng, J.B., Li, Y.D., 2019. Structure-property relationship in fully biobased epoxidized soybean oil thermosets cured by dicarboxyl terminated polyamide 1010 oligomer with different carboxyl/epoxy ratios. Polym. Test. 79, 106057 (1–7). https://doi.org/10.1016/j.polymertesting.2019.106057

Warwel, S., Brüse, F., Demes, C., Kunz, M., Klaas, M.R.G., 2001. Polymers and surfactants on the basis of renewable resources. Chemosphere 43, 39–48. https://doi.org/10.1016/S0045-6535(00)00322-2

Warwel, S., Wiege, B., Fehling, E., Kunz, M., 2000. Ring-opening polymerization of oleochemical epoxides catalyzed by aluminoxane/acetyl acetone. Eur. Polym. J. 36, 2655–2663. https://doi.org/10.1016/S0014-3057(00)00046-X

Wiesbrock, F., Hoogenboom, R., Abeln, C.H., Schubert, U.S., 2004a. Single-mode microwave ovens as new reaction devices: Accelerating the living polymerization of 2-ethyl-2-oxazoline. Macromol. Rapid Commun. 25, 1895–1899. https://doi.org/10.1002/marc.200400369

Wiesbrock, F., Hoogenboom, R., Schubert, U.S., 2004b. Microwave-assisted polymer synthesis: State-of-the-art and future perspectives. Macromol. Rapid Commun. 25, 1739–1764. https://doi.org/10.1002/marc.200400313

Winkler, M., Meier, M.A.R., 2014. Olefin cross-metathesis as a valuable tool for the preparation of renewable polyesters and polyamides from unsaturated fatty acid esters and carbamates. Green Chem. 16, 3335–3340. https://doi.org/10.1039/c4gc00273c

Winkler, M., Steinbiß, M., Meier, M.A.R., 2014. A more sustainable Wohl-Ziegler bromination: Versatile derivatization of unsaturated FAMEs and synthesis of renewable polyamides. Eur. J. Lipid Sci. Technol. 116, 44–51. https://doi.org/10.1002/ejlt.201300126

Wool, R.P., 2005. Polymers and composite resins from plant oils, in: Bio-based polymers and composites. Elsevier Inc., pp. 56–113. https://doi.org/10.1016/B978-0-12-763952-9.50005-8

Xia, Y., Larock, R.C., 2012. Vegetable oil-based polymeric materials : synthesis , properties , and applications. Green Chem. 1893–1909. https://doi.org/10.1039/c0gc00264j

Xue, X., Jia, Q.X., Zhao, G.L., 2013. Preparation and Properties of DCP-Crosslinked Biobased Polyamide. Adv. Mater. Res. 634–638, 1037–1043. https://doi.org/10.4028/www.scientific.net/AMR.634-638.1037

Yu, Z., Liu, L., 2005. Microwave-assisted synthesis of poly(ε-caprolactone)-poly(ethylene glycol)-poly(ε-caprolactone) tri-block co-polymers and use as matrices for sustained delivery

of ibuprofen taken as model drug. J. Biomater. Sci. Polym. Ed. 16, 957–971. https://doi.org/10.1163/1568562054414667

Zelin, J., Trasarti, A.F., Apesteguía, C.R., 2013. Self-metathesis of methyl oleate on silica-supported Hoveyda-Grubbs catalysts. Catal. Commun. 42, 84–88. https://doi.org/10.1016/j.catcom.2013.08.007

Zhang, C., Garrison, T.F., Madbouly, S.A., Kessler, M.R., 2017a. Recent advances in vegetable oil-based polymers and their composites. Prog. Polym. Sci. 71, 91–143. https://doi.org/10.1016/j.progpolymsci.2016.12.009

Zhang, C., Garrison, T.F., Madbouly, S.A., Kessler, M.R., 2017b. Recent advances in vegetable oil-based polymers and their composites. Prog. Polym. Sci. 71, 91–143. https://doi.org/10.1016/j.progpolymsci.2016.12.009

Zhang, C., Liao, L., Gong, S.S., 2007. Recent developments in microwave-assisted polymerization with a focus on ring-opening polymerization. Green Chem. 9, 303–31. https://doi.org/10.1039/b608891k

Zhang, C., Liao, L., Liu, L., 2004. Rapid ring-opening polymerization of D,L-lactide by microwaves. Macromol. Rapid Commun. 25, 1402–1405. https://doi.org/10.1002/marc.200400106

Zhang, C., Liu, Y., Liu, S., Li, H., Huang, K., Pan, Q., Hua, X., Hao, C., Ma, Q., Lv, C., Li, W., Yang, Z., Zhao, Y., Wang, D., Lai, G., Jiang, J., Xu, Y., Wu, J., 2009. Crystalline behaviors and phase transition during the manufacture of fine denier PA6 fibers. Sci. China, Ser. B Chem. 52, 1835–1842. https://doi.org/10.1007/s11426-009-0242-5

Zhang, C., Xia, Y., Chen, R., Huh, S., Johnston, P.A., Kessler, M.R., 2013. Soy-castor oil based polyols prepared using a solvent-free and catalyst-free method and polyurethanes therefrom. Green Chem. 15, 1477–1484. https://doi.org/10.1039/c3gc40531a

Zhang, K., Nelson, A.M., Talley, S.J., Chen, M., Margaretta, E., Hudson, A.G., Moore, R.B., Long, T.E., 2016. Non-isocyanate poly(amide-hydroxyurethane)s from sustainable resources. Green Chem. 18, 4667–4681. https://doi.org/10.1039/c6gc01096b

Zhang, L., Huang, M., Yu, R., Huang, J., Dong, X., Zhang, R., Zhu, J., 2014. Bio-based shape memory polyurethanes (Bio-SMPUs) with short side chains in the soft segment. J. Mater. Chem. A 2, 11490–11498. https://doi.org/10.1039/c4ta01640h

Zhu, Y., Romain, C., Williams, C.K., 2016. Sustainable polymers from renewable resources. Nature 540, 354–362. https://doi.org/10.1038/nature21001

Appendix A: Supplementary Information of Chapter 4
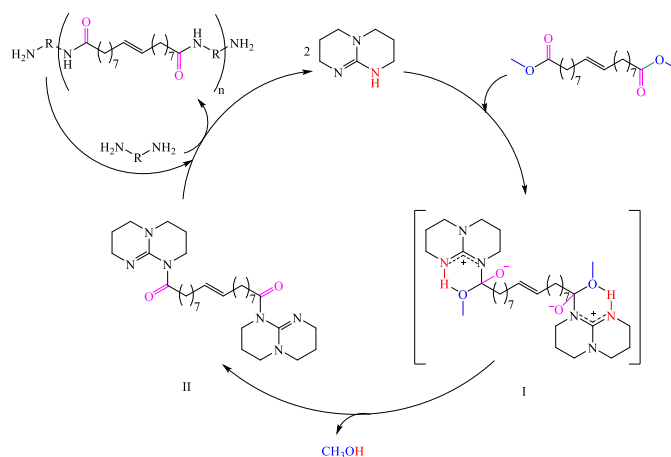
Scheme 4. S1) Polycondensation mechanism of biobased diester (DMOD) with amines (PXDA or DETA) by TBD catalyst.
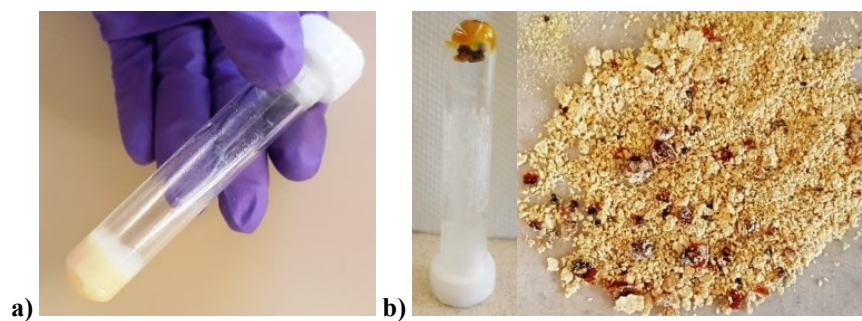
Figure 4. S1) Polycondensation of PA (DMOD-PXDA) under microwave irradiation. the representatives of a) a successful reaction and b) an unsuccessful reaction.
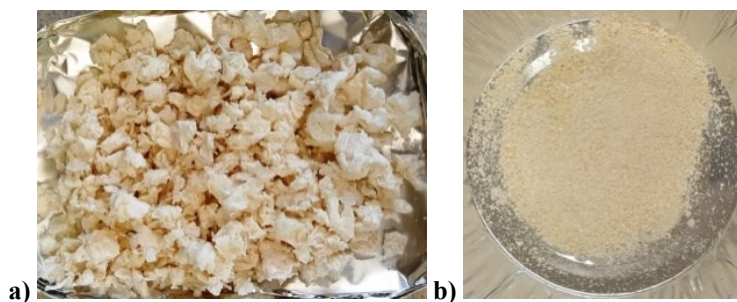
Figure 4. S2) Representative semi-aromatic biobased PAs (DMOD-PXDA), (a) after precipitation in cold methanol and, (b) after crushing and washing.

Nuclear Magnetic Resonance (NMR) Analysis. A Varian Inova spectrometer (Varian, CA) was used to collect the ^{1}H NMR spectra of sample at 400 MHz and 25.9 °C. Almost 35% of the polyamide resulted from DMOD and PXDA after 8 min microwave irradiation was dissolved in deuterated chloroform ($CDCl_3$) with the help of TFAA.
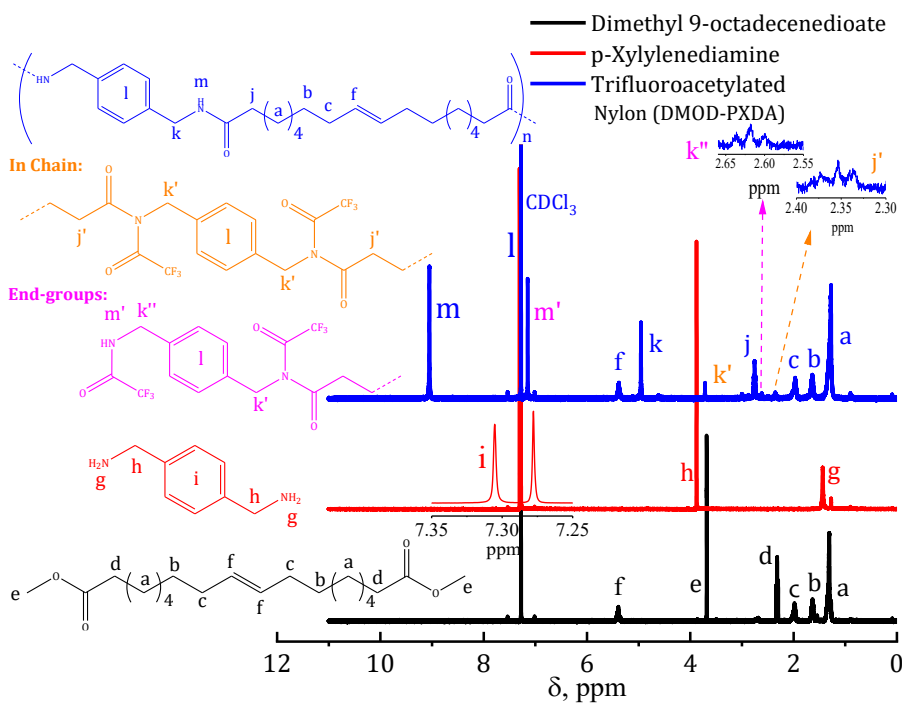
Figure 4. S3) Representative ^{1}H NMR spectra of dimethyl 9-octadecenedioate, *p*-Xylylenediamine, and the 35% dissolvable polyamide resulted from microwave irradiation of DMOD and PXDA for 8 min.
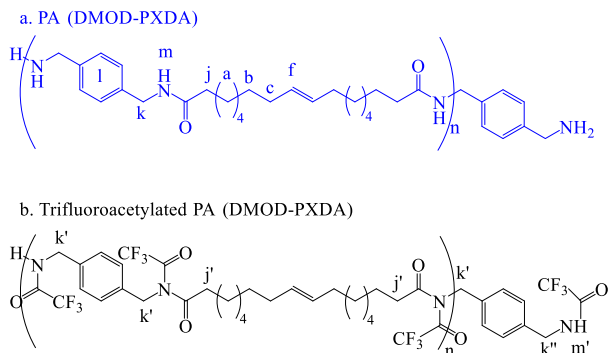
Scheme 4. S2) a) The suggested structure and b) trifluoroacetylated structure of the 35% dissolvable polyamide resulted from microwave irradiation of DMOD and PXDA.
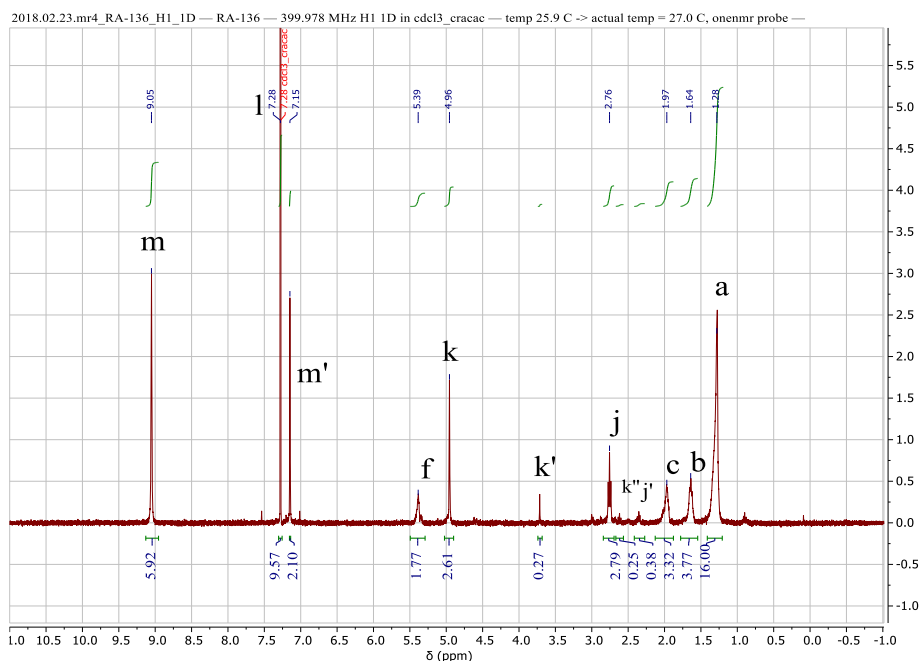
Figure 4. S4) Representative ^{1}H NMR spectra of the 35% dissolvable polyamide resulted from microwave irradiation of DMOD and PXDA for 8 min.

Table 4. S1) The resulted table from the ^{1}H NMR of the 35% dissolvable polyamide resulted from microwave irradiation of DMOD and PXDA for 8 min.

Peak	ppm	Intensity	Width	Area
m	9.05	3.0	4.60	272.13
l	7.28	20.7	0.51	216.65
3	7.28	18.2	0.58	243.80
m'	7.15	2.8	2.05	117.93
f	5.39	0.3	12.90	90.36
k	4.96	1.7	3.30	114.70
k'	3.72	0.3	1.98	14.64
j	2.76	0.8	3.52	60.60
k''	2.62	0.1	2.93	3.94
j'	2.35	0.1	2.35	4.64
c	1.97	0.4	18.85	178.97
b	1.64	0.5	19.11	175.55
a	1.28	2.3	9.73	438.64

The ^{1}H NMR studies of the 35% dissolvable polyamide resulted from microwave irradiation of DMOD and PXDA for 8 min were conducted in the CDCl$_3$/TFAA solvent mixture. TFAA reacts with the amide and amino end-groups leadings to their N-acylation which consequently, breaks hydrogen bonds between polymer chains leading to finally solubilization of the polyamide.(Firdaus and Meier, 2013) Typical ^{1}H NMR spectra of trifluoroacetylated MH-PA (DMOD-PXDA) and their monomers are presented in Figure 4. S3, where peak assignments were based on the literature data (Firdaus and Meier, 2013); (Girardon et al., 1998). The characteristic signals of DMOD bio-diester were identified at 3.68 ppm and 5.39 ppm, corresponding to the protons of the methyl end-groups (e) and the double bond (f) of the bio-diester, respectively. PXDA also exhibited clear signals at 1.44 ppm and 7.31 ppm matching its primary amino end-groups (g) and phenol group (i), respectively. The signal for the phenolic protons at 7.31 ppm (i) in the spectrum of PXDA appeared close to that of the solvent CDCl$_3$ at 7.28 ppm. The signals of the diester's methyl groups at 3.68 (e) and diamine's amino end-groups at 1.44 ppm (g) were disappeared in MH-PA (DMOD-PXDA) spectra with the appearance of a signal at 9.05 ppm related to amide groups (m). Furthermore, the peak related to the methylene groups in α position to the carbonyl groups of bio-diester (d) experienced two shifts towards the down-field in the ^{1}H NMR spectrum of the partly trifluoroacetylated biobased polyamides; the first shift from 2.32 ppm (d) to 2.76 ppm (j) and the second shift to 2.35 ppm (j') due to the formation of trifluoroacetylated amide linkages. The peak of phenolic protons was also shifted from 7.31 ppm (i) to 7.28 ppm (l) in the spectrum of MH-PA (DMOD-PXDA). Additionally, the signal corresponding to the methylene group of PXDA at 3.88 ppm (h) experienced different shifts due to shielding effects in the structure of trifluoroacetylated semi-aromatic polyamides. This signal was moved towards down-field region at 4.96 ppm (K), while its counterparts beside the trifluoroacetylated amide

group inside the polymer chain and amino end-groups of polymer were shielded more and appeared at 3.72 ppm (K') and 2.62 ppm (k''), respectively. The trifluoroacetylated amino end-groups of the semi-aromatic polyamides were also identified at 7.15 ppm (m').
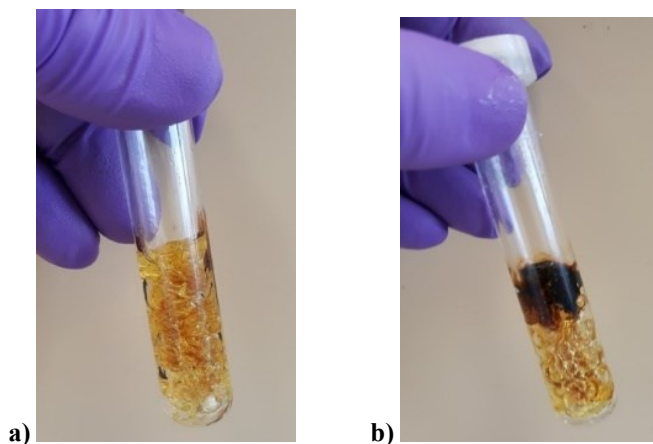
Figure 4. S5) Polycondensation of PA (DMOD-DETA) under microwave irradiation. The representatives of a) a successful reaction and b) an unsuccessful reaction.
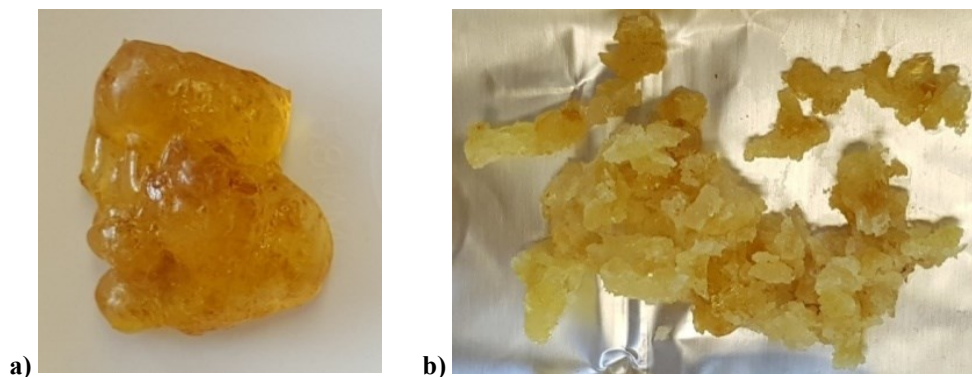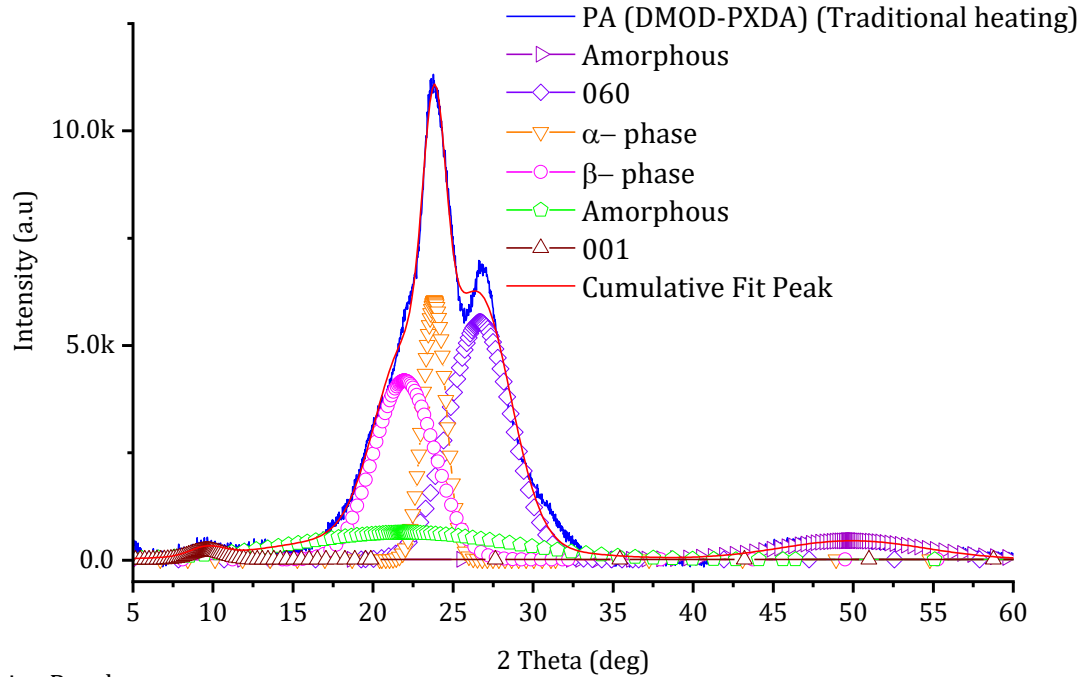

Figure 4. S6) Representative aliphatic biobased PAs (DMOD-DETA) before (a) and after (b) washing.

Analysis of the crystalline structure of biobased PAs (DMOD-PXDA) and PAs (DMOD-DETA):

Peak Analysis

Data Set:[X12813]X12813!PXDA"PXDA"	Date:2020-02-13
BaseLine:ExpDec2	
Chi^2=2.13690E+004 Adj. R-Square=9.94861E-001 # of Data Points=4245.	
SS=9.03054E+007 Degree of Freedom=4226.	

Fitting Results

Peak Index	Peak Type	Area Intg	FWHM	Max Height	Center Grvty	Area IntgP
1.	Gaussian	4994.7648	10.71546	437.89721	49.93452	6.77829
2.	Gaussian	26901.40939	4.57263	5526.84058	26.68334	36.50736
3.	Gaussian	10971.82876	1.70913	6030.75155	23.83485	14.88965
4.	Gaussian	19863.15351	4.47748	4167.56142	21.9586	26.95588
5.	Gaussian	10416.95465	15.74133	625.16481	21.95686	14.13664
6.	Gaussian	539.53094	2.45969	206.06583	9.62754	0.73219

Figure 4. S7) The profile fittings of biobased TH-PA (DMOD-PXDA).

Peaks:

1-Amorphous, 2-060, 3- α-phase, 4- β-phase, 5- Amorphous, 6- 001

$$x_{c,WAXD} = \left(\frac{\sum A_{Crystal}}{\sum A_{Crystal} + \sum A_{Amorphous}}\right) \times 100 = \left(\frac{58257.8}{73687.5}\right) \times 100 = 79.1\%$$

Peak Analysis

Fitting Results

Peak Index	Peak Type	Area Intg	FWHM	Max Height	Center Grvty	Area IntgP
1.	Gaussian	4195.46548	1.83246	2150.86111	23.73322	14.88414
2.	Gaussian	15516.22319	5.75777	2531.62733	25.78768	55.04649
3.	Gaussian	83.5105	0.87839	89.31421	12.88573	0.29627
4.	Gaussian	63.08515	0.35295	167.91327	8.34221	0.22381
5.	Gaussian	8329.20403	4.59603	1702.5057	21.46735	29.54929

Figure 4. S8) The profile fittings of biobased MH-PA (DMOD-PXDA).
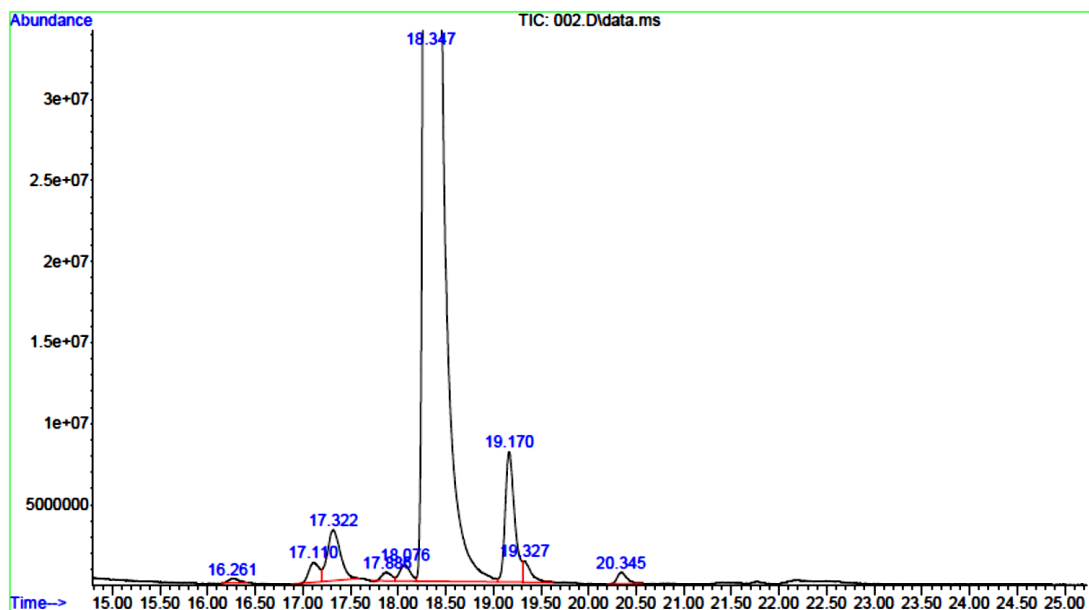
Peaks:

1- α-phase, 2-060, 3- 002, 4-001, 5- γ-phase

$$x_{c,WAXD} = \left(\frac{\sum A_{Crystal}}{\sum A_{Crystal} + \sum A_{Amorphous}} \right) \times 100 = 100\%$$

Peak Analysis

Fitting Results

Peak Index	Peak Type	Area Intg	FWHM	Max Height	Center Grvty	Area IntgP
1.	Gaussian	2642.01018	10.96213	226.41606	49.29837	9.67525
2.	Gaussian	21454.18072	6.39315	3152.57162	23.97197	78.56687
3.	Gaussian	3210.71296	3.5206	856.7527	11.51345	11.75788

Figure 4. S9) The profile fittings of biobased TH-PA (DMOD-DETA).

Peaks:

1- Amorphous, 2- α-phase, 3- 002,

$$x_{c,WAXD} = \left(\frac{\sum A_{Crystal}}{\sum A_{Crystal} + \sum A_{Amorphous}} \right) \times 100 = \left(\frac{24664.9}{27306.9} \right) \times 100 = 90.3 \%$$

Peak Analysis
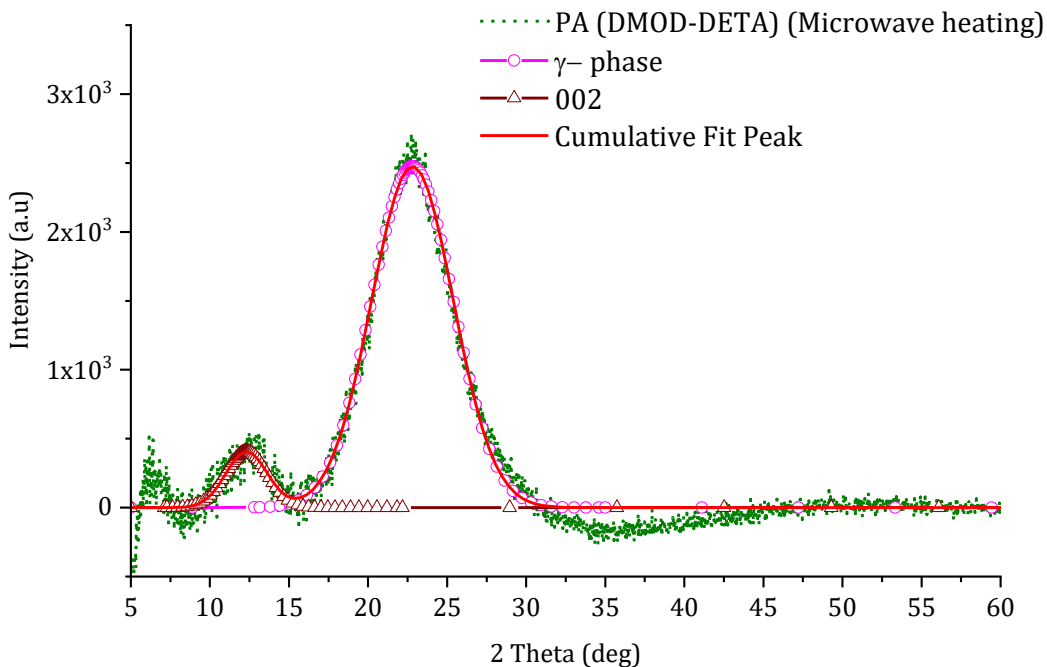
Fitting Results

Peak Index	Peak Type	Area Intg	FWHM	Max Height	Center Grvty	Area IntgP
1.	Gaussian	16061.9149	6.09403	2476.0582	22.80854	92.33336
2.	Gaussian	1333.6558	3.07819	407.02079	12.31296	7.66664

Figure 4. S10) The profile fittings of biobased MH-PA (DMOD-DETA).

Peaks:

1- γ-phase 2- 002,

$$x_{c,WAXD} = \left(\frac{\sum A_{Crystal}}{\sum A_{Crystal} + \sum A_{Amorphous}} \right) \times 100 = 100 \, \%$$

References:

(1)   Firdaus, M.; Meier, M. A. R. *Green Chem*. 2013, 15, 370-380.
https://doi.org/10.1039/C2GC36557J
(2)   Girardon, V.; Correia, I.; Tessier, M.; Marchal, E. Eur. *Polym. J*. 1998, 34, 363-380.
https://doi.org/10.1016/S0014-3057(97)00141-9

Appendix B: Supplementary Information of Chapter 5


```
peak   R.T.  first  max last   PK   peak      corr.      corr.    % of
 #     min   scan scan scan    TY   height     area      % max.   total
---   -----  ----- ---- ----   ---  -------   -------    ------   -------
 1   16.261   399  419  450    M10   271966   21171646    0.10%   0.099%
 2   17.110   537  583  600  BV 4  1225103    88225181    0.44%   0.413%
 3   17.322   600  624  675  VV 5  3140948   300682405    1.49%   1.407%
 4   17.886   698  732  747  BV 6   536024    35650341    0.18%   0.167%
 5   18.076   747  769  790  VV 3  1000152    77103578    0.38%   0.361%

 6   18.347   790  821  954  VV 3  248362278 20168962387 100.00%  94.383%
 7   19.170   954  980 1007  VV 4  8031756   550842412    2.73%   2.578%
 8   19.327  1007 1010 1069  VB 5  1293855    78605228    0.39%   0.368%
 9   20.345  1176 1206 1251  BB 8   705646    48132407    0.24%   0.225%
```

Figure 5. S1) Gas chromatography-mass spectrometry of 1,2-epoxydecane. Peak # 6 is associated with 1,2-epoxydecane.
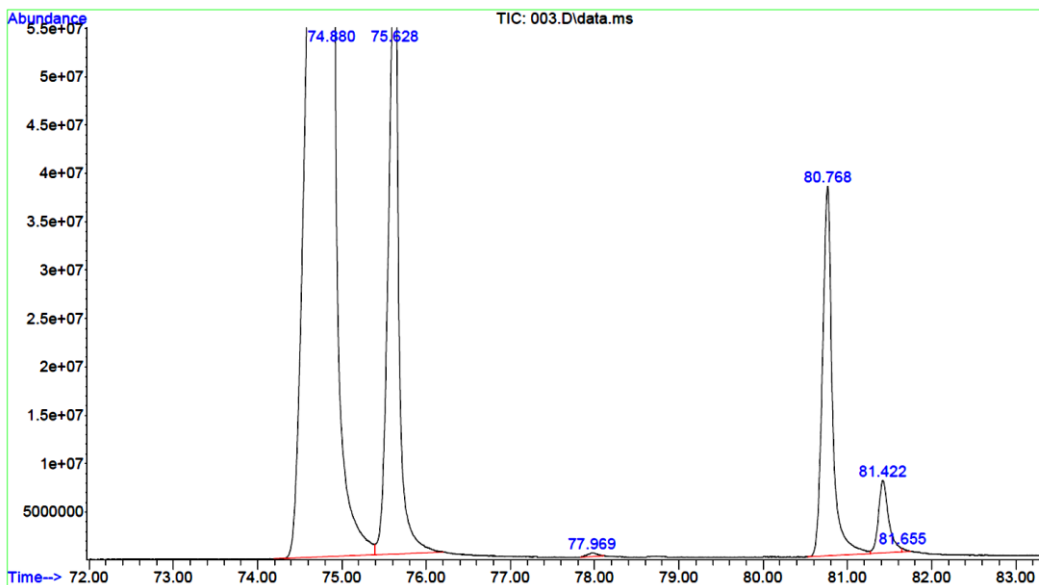
```
peak   R.T.  first max  last  PK    peak        corr.      corr.     % of
 #     min   scan scan scan   TY   height        area      % max.    total
---   -----  ----- ---- ---- ---   -------      -------    ------    -------
 1   74.880  11583 11717 11815 BV 7 229608892 33936980235 100.00%   78.313%
 2   75.628  11815 11861 11972 VV 2  68052112  5579328775  16.44%   12.875%
 3   77.969  12285 12312 12340    M2   377605    30869059   0.09%    0.071%
 4   80.768  12805 12851 12948 BV 5  38181843  3145325717   9.27%    7.258%
 5   81.422  12948 12977 13021 VV 6   7497921   631610941   1.86%    1.457%

 6   81.655  13021 13022 13041 VB 6    374711    11129053   0.03%    0.026%
```

Figure 5. S2) Gas chromatography-mass spectrometry of dimethyl 9-octadecenedioate (DMOD).
Peak # 1 & 2 are associated with DMOD.

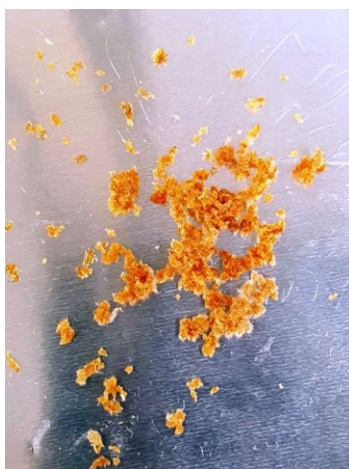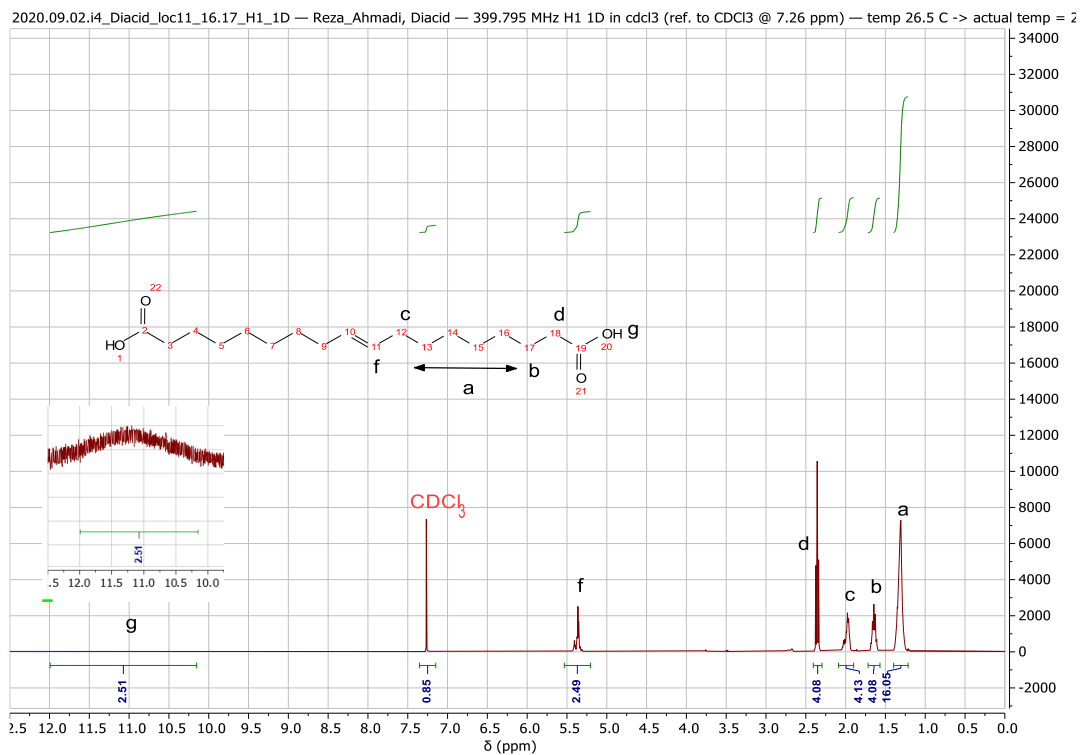Figure 5. S3) ^{1}H NMR spectrum of 9-octadecenedioic acid.

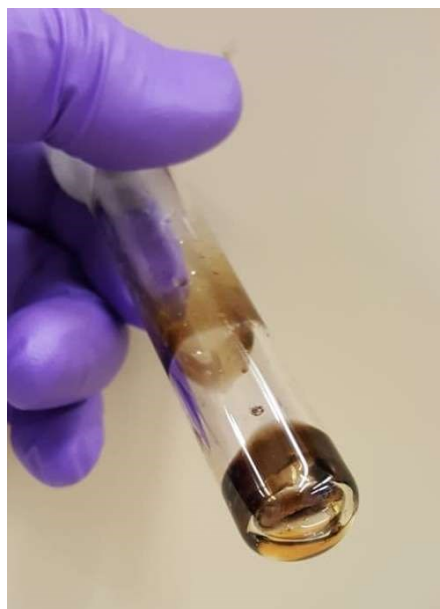
Figure 5. S4) Long-chain, unsaturated BPs (DMOD-BHOD).

Figure 5. S5) The blue plasma of the catalyst and charring the monomers.
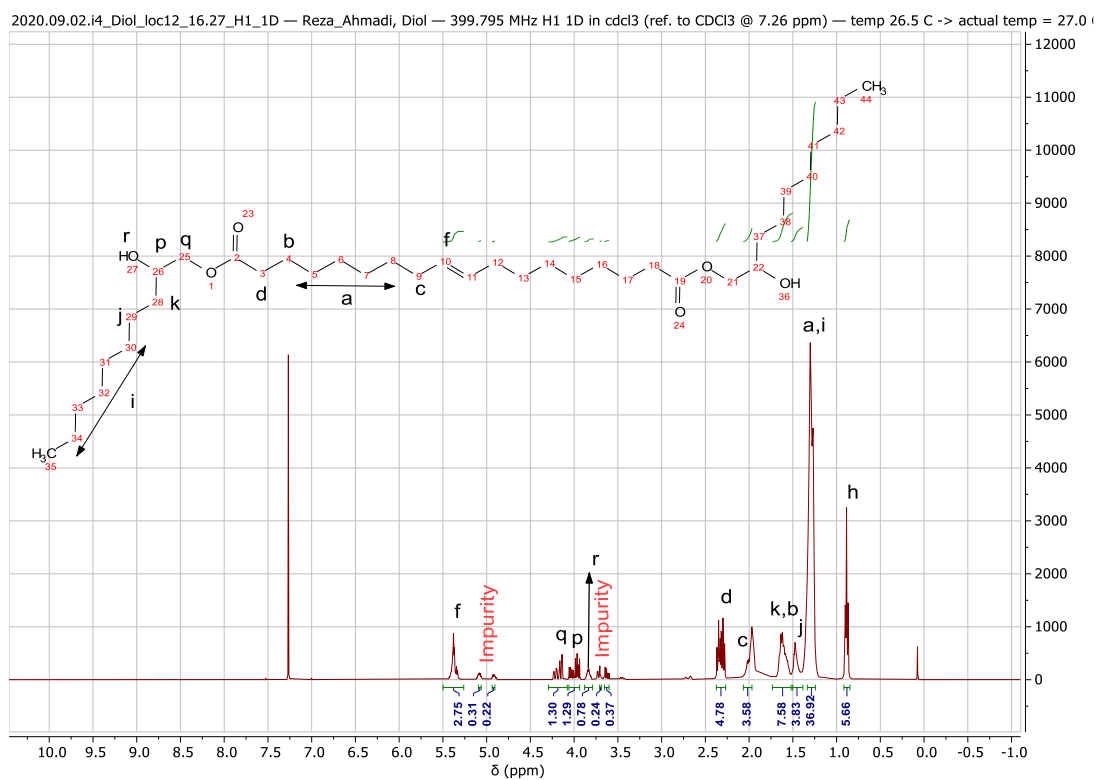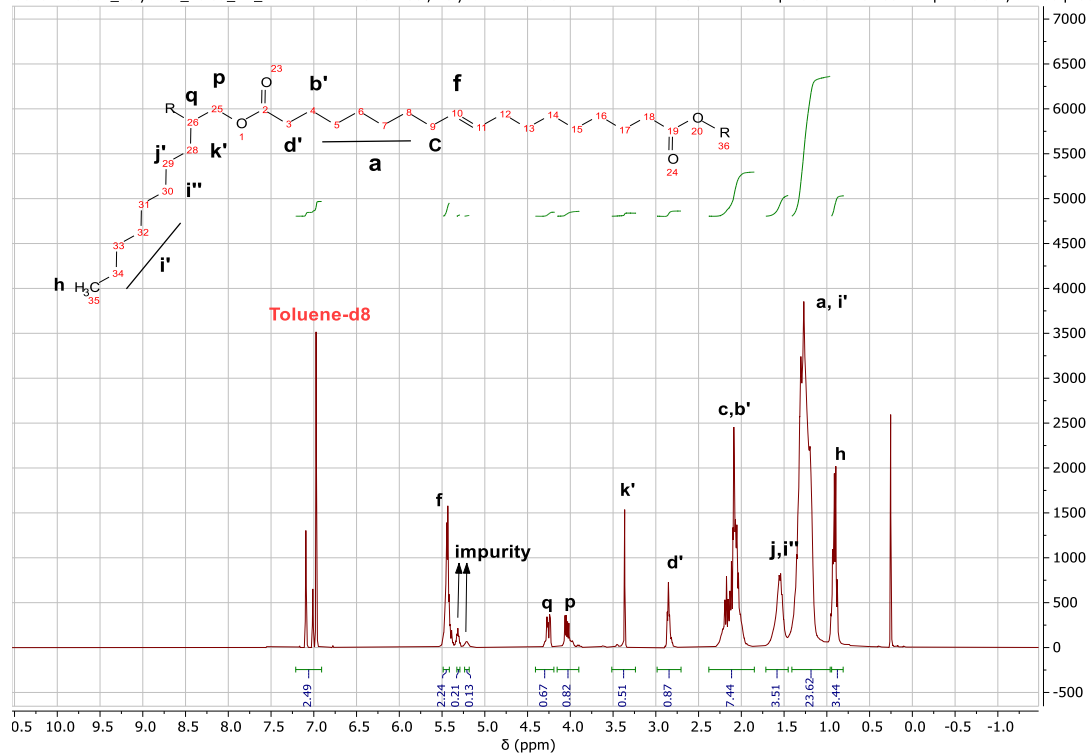

Figure 5. S6) ¹HNMR spectrum of 9-octadecenedioic acid.

Figure 5. S6) ^{1}HNMR spectrum of long-chain BPs (DMOD-BHOD).